Regulation of skeletal muscle oxidative phenotype by hypoxia - implications for COPD

Regulation of skeletal muscle oxidative phenotype by hypoxia – implications for COPD

Cover design	I.G.M. Slot
Layout	I.G.M. Slot
Printed by	CPI - Koninklijke Wöhrmann, Zutphen
ISBN	978-94-6203-878-3

The study presented in this thesis was performed within NUTRIM School of Nutrition and Translational Research in Metabolism which participates in the Graduate School VLAG (Food Technology, Agrobiotechnology, Nutrition and Health Sciences), accredited by the Royal Netherlands Academy of Arts and Sciences (KNAW).

The studies described in this thesis were supported by research grants from the Lung Foundation (Longfonds; project number NAF #3.2.05.038) and from the Translational University Limburg (tUL), and were performed within the framework of the Dutch Top Institute Pharma, project "Transition of systemic inflammation into multiorgan pathology, T1-201". Partners in this project are Maastricht University Medical Center+, University Medical Center Groningen, University Medical Center Utrecht, GlaxoSmithKline, AstraZeneca Nederland BV, Danone Research, and Nycomed (now Takeda).

Regulation of skeletal muscle oxidative phenotype by hypoxia – implications for COPD

Proefschrift

ter verkrijging van de graad van doctor aan de Universiteit Maastricht,
op gezag van de Rector Magnificus, Prof. Dr. L.L.G. Soete,
volgens het besluit van het College van Decanen,
in het openbaar te verdedigen
op donderdag 8 oktober 2015 om 14.00 uur

door

Ilse Geertruida Mathilda Slot

Geboren op 1 maart 1985 te Utrecht

PROMOTOR

Prof. dr. A.M.W.J. Schols

COPROMOTOR

Dr. H.R. Gosker

BEOORDELINGSCOMMISSIE

Prof. dr. J.P. Kooman (voorzitter)
Prof. dr. M.K.C. Hesselink
Dr. P.R. Kemp (Imperial College London, United Kingdom)
Prof. dr. ir. A.H. Kersten (Wageningen University)
Prof. dr. L.J. de Windt

TABLE OF CONTENTS

Chapter 1

General introduction

INTRODUCTION

Definition of Chronic Obstructive Pulmonary Disease (COPD)

According to the Global Initiative for Chronic Obstructive Lung Disease (GOLD) COPD, a common preventable and treatable disease, is characterized by persistent airflow limitation that is usually progressive and associated with an enhanced chronic inflammatory response in the airways and the lung to noxious particles or gases (1). Exacerbations and comorbidities contribute to the overall severity in individual patients. Estimates by the World Health Organization indicate that approximately 65 million people worldwide are affected (201). The prevalence of COPD is even increasing, and the 'global burden of disease' study (BOLD) indicates that in 2020 COPD will be the third leading cause of death (131) and the fifth leading cause of years lost through early mortality or handicap (73). In Maastricht (The Netherlands) the overall prevalence of COPD in people aged ≥40 years is 24% (192).

The primary risk factor for development of COPD is active smoking, which supposedly causes ~90% of COPD deaths (189). However, studies from the last decade increasingly suggest that cigarette smoking is a cause in only 50% of the cases of COPD, and that non-smoking COPD contributes more than previously assumed (168). Contributors to non-smoking COPD include second-hand smoke, frequent lower respiratory infections, untreated asthma, dust, chemical fumes, and air pollution in the workplace or the environment (202). In addition, genetic disorders can predispose to develop COPD (188). Although development of COPD can begin early in life, it is frequently undiagnosed before age 40 (203).

Skeletal muscle dysfunction in COPD

An important and often investigated systemic manifestation of COPD is skeletal muscle dysfunction, which seriously affects disease burden (112). Loss of skeletal muscle mass due to muscle fiber atrophy results in reduced muscular strength and predicts morbidity and mortality independently from lung function impairment measured as forced expiratory volume in 1 s (FEV_1) (116, 183), hypoxia or hypercapnia (172). Furthermore, a reduced proportion of oxidative muscle fiber types and mitochondrial capacity (*i.e.* loss of oxidative phenotype; Oxphen) in the lower limb muscle is associated with increased muscular fatigability and reduced exercise capacity (6, 52, 83, 113, 164, 208). As COPD is more prevalent in the older population and COPD patients suffer from labored breathing, patients adapt to a sedentary lifestyle, which further worsens muscle function (148). Nevertheless, exercise training is currently the only evidence-based intervention to improve skeletal muscle function in COPD (112).

Patients with COPD often suffer from comorbidities such as metabolic syndrome, cardiovascular disease, gastro-esophageal reflux, osteoporosis, lung cancer, diabetes mellitus, psychological disorders, and anemia (26, 44, 127, 132, 162). Comorbidities are associated with increased risk of hospitalization both for respiratory (114) and non-respiratory causes (115). Moreover, patients with COPD and comorbidities are more dyspneic and have reduced exercise capacity compared to patients without comorbidities (125).

Loss of skeletal muscle mass and Oxphen has been associated with some of the above-mentioned comorbidities. For example, osteoporosis risk is increased in patients

with low muscle mass (55) and in skeletal muscle of patients with type II diabetes, a shift in fiber-type composition from slow to fast has been linked to increased insulin resistance (101, 140, 177). Moreover, patients with chronic heart failure have been shown to exhibit a similar loss of skeletal muscle Oxphen as patients with COPD (51). Interestingly, loss of Oxphen has been proposed to accelerate muscle wasting in COPD (158) and to be a driver of cardiovascular and metabolic risk in COPD (190). The potentially extensive consequences of loss of Oxphen make delaying or even reversing loss of Oxphen a promising approach in modifying COPD progression, increasing quality of life and decreasing health care costs by reducing the amount of hospital admissions.

Skeletal muscle oxidative phenotype

Muscle function and fiber type

Skeletal muscle is vital for posture, movement, energy storage and consumption, as well as whole-body metabolism. Muscles are composed of bundles of muscle fibers that based on their type have specialized functions and are plastic in response to triggers such as contractile activity, nutrient availability, and hormones (16). Human skeletal muscle is made up of three different pure fiber types and two hybrid intermediary types: type I – I/IIA – IIA – IIA/IIX – IIX (170). The fiber types have specific biochemical, physiological, structural and metabolic characteristics, which determine function, size, metabolism and fatigability (170). The specific combination of fiber types that makes up a muscle determine the functional properties of that muscle (170). Roughly, the fibers are classified based on their contractile properties as slow-twitch type I or fast-twitch type II (171). The fiber types are further divided based on the metabolic properties into oxidative type I, oxidative-glycolytic type IIA and glycolytic type IIX, where the name is based on the expressed isoform of the myosin heavy chain protein (178). Rodent muscle has 4 different pure and three mixed fiber types (I – I/IIa – IIa – IIa/IIx – IIx – IIx/IIb – IIb), but in contrast to human fiber types the most glycolytic fiber type in rodents is type IIb, whereas type IIx has an intermediary metabolism (53). Oxidative fibers have a high mitochondrial content, use mainly oxidative metabolism for energy production, and are important for endurance. Glycolytic fibers are more dependent on glycolytic metabolism, important for strength and speed, but fatigue quickly (170).

Energy metabolism

The main energy source in the muscle is adenosine triphosphate (ATP), which can be generated from the substrates glucose, fat and protein through multiple converging pathways. Glucose can be converted to ATP through glycolysis. Glucose is internalized through either diffusion or active transport by glucose transporters (GLUT-1, -2, -3, -4, -5). In addition, glucose may be derived from intracellular glycogen after phosphorylation by glycogen phosphorylase. Glucose internalization by GLUT transporters can be modulated by stimuli including exercise, hypoxia and insulin stimulation. Once glucose is in the cell, it is retained through phosphorylation by hexokinase (HK). Phosphorylated glucose enters the glycolytic pathway where it is converted to fructose-6-phosphate. Based on the cells' energy requirements, phosphofructokinase (PFK) phosphorylates fructose-6-phosphate to yield fructose-1,6-biphosphate. PFK is the key regulatory and rate-limiting enzyme in glycolysis. Fructose-1,6-biphosphate is further converted to two molecules of glyceraldehyde-3-phosphate. Up to this point, glycolysis has cost 2 ATP

molecules. Both glyceraldehyde-3-phosphate molecules are then converted to pyruvate with the concomitant release of 4 ATP and 2 nicotinamide adenine dinucleotide (NADH) molecules. Up to this stage, no oxygen is required, but energy yield from glycolysis is low. This pathway can operate both under aerobic and under anaerobic or hypoxic conditions. Aerobic glycolysis involves pyruvate entering the mitochondrion where it is converted to acetyl-coenzyme A (acetyl-CoA), yielding 1 NADH, and further metabolized in the tricarboxylic acid (TCA) cycle. During anaerobic glycolysis pyruvate is reduced to lactate in order to regenerate NAD^+ from accumulating NADH; lactate acidifies the cytoplasm if it is not shuttled out of the cell.

In the mitochondrial matrix, acetyl-CoA is converted to citrate by citrate synthase (CS), the rate-limiting enzyme of the TCA cycle. Further metabolization yields 1 ATP, 1 flavin adenine dinucleotide ($FADH_2$) and 3 NADH molecules. The electron carriers NADH and $FADH_2$ are used by the electron transport chain (ETC) to produce ATP by the process of oxidative phosphorylation (OXPHOS). The NADH molecules are oxidized at complex I (NADH dehydrogenase) of the ETC and $FADH_2$ enters the ETC at complex II (succinate dehydrogenase). By the process of oxidative phosphorylation, further electron shuttling through complex III (cytochrome *c* reductase) and complex IV (cytochrome *c* oxidase; COX) creates a proton motive force over the inner mitochondrial membrane, which is used by complex V (ATP synthase) to convert adenosine diphosphate (ADP) to ATP. One molecule of glucose can yield 36 ATPs when all three metabolic pathways are used.

In addition to glucose, free fatty acids and protein can also be converted to ATP. Fatty acids are oxidized through the β-oxidation pathway in the mitochondrial matrix, each cycle yielding 1 acetyl-CoA molecule that enters the TCA cycle, and 1 NADH and 1 $FADH_2$, which are used by the ETC. The third step of β-oxidation is catalyzed by 3-hydroxyacyl-CoA dehydrogenase (HADH). Hydrolysis of proteins produces glucogenic amino acids that are converted to pyruvate or other intermediates of the TCA cycle, and ketogenic amino acids that are degraded to acetyl-CoA. Pyruvate, TCA cycle intermediates and acetyl-CoA then enter the TCA cycle or ETC to produce ATP.

In times of low effort, excess ATP can be used to produce phosphocreatine (PCr) to create a high-energy phosphate reserve. In the first 10 seconds of high-intensity exercise, the muscle can use this reserve to replenish ATP by transfer of inorganic phosphate from PCr to ADP. This is the fastest method for ATP generation and does not require oxygen and is therefore also called alactic anaerobic metabolism. In the next two minutes of high-intensity exercise, glucose is derived from anaerobic glycolysis. Build-up of lactate results in muscle burn and fatigue and high-intensity exercise can no longer be maintained when the blood lactate threshold is reached. With increased breathing frequency and heart rate there is more oxygen available that can be used in aerobic metabolism. Therefore, after approximately five minutes, the muscle mainly derives its energy from fatty acid metabolism. Due to the need of oxygen, this is the slowest method of ATP generation because it relies on the circulatory system for oxygen transport to the muscle, but due to the high amount of energy stores well-suited for longer duration of exercise at a modest intensity.

The total mitochondrial content, the surface of the inner mitochondrial membrane and the activity of the ETC complexes determine the oxidative capacity of the muscle cell. In turn, oxidative capacity of the lower limb muscles is a major determinant of aerobic exercise capacity (20, 68).

Regulation of oxidative metabolism

Oxidative metabolism is regulated by stimuli such as physical (in)activity and inflammation (56, 157). A simplified signaling scheme is presented in Figure 1. The mitochondrial content is tightly regulated to meet cellular metabolic demand, but at the same time to avoid excessive mitochondrial capacity (4, 37, 138, 149). Nuclear DNA (nDNA) encodes genes for all non-OXPHOS mitochondrial proteins, most of the OXPHOS complex subunits, as well as OXPHOS-related genes involved in OXPHOS assembly, mitochondrial nucleotide balance, and mitochondrial DNA (mtDNA) replication, maintenance, transcription and translation. However, 13 OXPHOS complex subunits that are critical for ETC function are encoded by the mtDNA. The coordinated expression of OXPHOS complex subunits from the nuclear and mitochondrial genomes is under tight regulation. Whereas expression of nuclear OXPHOS subunits is determined by transcriptional regulation and mRNA level, expression of mitochondrially encoded OXPHOS subunits is largely determined by mtDNA content (200).

Peroxisome proliferator-activated receptor coactivator-1α

One of the most studied regulators of mitochondrial metabolism and biogenesis is peroxisome proliferator-activated receptor co-activator 1α (PGC-1α). It is controlled by many cellular stresses and when activated co-activates a plethora of transcription factors influencing amongst others mitochondrial biogenesis and metabolism, and expression of structural proteins related to a slow-twitch fiber type (102). Originally, PGC-1α was discovered as a binding partner of peroxisome proliferator-activated receptor γ (PPARγ) in brown fat cells (154). PGC-1α was shown to confer a brown adipocyte-like phenotype to the white adipocytes upon overexpression, including increased mitochondrial biogenesis and thermogenic uncoupling (154). Further research in muscle showed that PGC-1α and its later discovered homologs PGC-1β and PGC-1-related coactivator (PRC) co-activate many more transcription factors, among which are nuclear respiratory factors (NRF)-1 and -2 as well as nuclear receptors (NRs) such as estrogen-related receptors (ERRs), PPARs and thyroid hormone receptor (TR) (9, 74, 95, 102, 103, 128, 173, 206, 214). Although PGC-1 coactivators are necessary for the oxidative and mitochondrial programs of skeletal muscle, they are dispensable for fundamental fiber type determination and insulin sensitivity (210).

Docking of PGC-1α to these transcription factors induces a conformational change in PGC-1α which enables binding of histone acetyltransferases (HATs) such as steroid receptor coactivator–1 (SRC-1) and CREB binding protein (CBP)/p300 (152). Acetylation of histones modifies chromatin structure to become less compact and permit binding of transcription factors and transcriptional activation. Deacetylation of histones by histone deacetylases (HDACs) induces a compact chromatin environment, which results in transcriptional repression.

PGC-1α activity is post-translationally regulated by phosphorylation, acetylation, methylation and ubiquitylation (42). With metabolic stress, the adenosine monophosphate (AMP)/ATP ratio is increased and the AMP-activated protein kinase (AMPK) is activated (59). AMPK phosphorylates PGC-1α to increase its activity (78), but also stimulates its expression (182). Other kinases that positively influence PGC-1α stability and transactivation capacity include p38 mitogen-activated protein kinase (MAPK) (40, 153) and protein kinase A (PKA) (25). p38 MAPK also promotes PGC-1α gene

expression (3). Phosphorylation by glycogen-synthase kinase (GSK) 3β stimulates PGC-1α intranuclear proteasomal degradation (8). Acetylation of PGC-1α is regulated based on cellular energy status: an increase in the NAD^+/NADH ratio activates silent information regulator 1 (SIRT1), which stimulates PGC-1α transcriptional activation by deacetylation (23, 48, 163). High energy status on the other hand activates general control non-derepressible (GCN) 5 and steroid receptor coactivator (SRC) 3 which repress PGC-1α activity (29, 88, 99). Methylation of PGC-1α by protein arginine N-methyltransferase 1 (PRMT1) enhances PGC-1α-mediated transcription (185), and ubiquitylation of PGC-1α by the E3 ligase Skp1, Cullin/Cdc53, and the F-box protein Cdc4 (SCF^{Cdc4}) complex increases ubiquitin-mediated proteolysis (142).

The pathways that regulate PGC-1α are also intertwined, as AMPK increases fatty acid oxidation, which results in increased NAD^+ and SIRT1 activation to stimulate PGC-1α deacetylation and activation (23). Moreover, AMPK-mediated phosphorylation of PGC-1α is required for SIRT1-mediated deacetylation (23).

Nuclear respiratory factors

PGC-1α regulates expression of and coactivates NRF-1 and -2 (206). The NRFs in turn regulate transcription of mitochondrial transcription factor A (Tfam), a transcription factor involved in OXPHOS protein expression and mitochondrial DNA replication (39, 194). mtDNA transcription by Tfam is markedly enhanced by the mitochondrial transcription specificity factors TFB1M and TFB2M (49). Expression of both is regulated by the NRFs in conjunction with PGC-1α and PRC (49). The nuclear expression of these mitochondrial transcription factors makes them crucial in the synergistic regulation of mitochondrial protein expression from the nuclear and mitochondrial genome (87). Furthermore, PGC-1α has been shown to also be active in the mitochondria where it functions as a transcriptional co-activator of Tfam (166).

Peroxisome proliferator-activated receptors

Some of the NRs that are coactivated by PGC-1α function as metabolic sensors because their ligands consist of substrates and end-product molecules of metabolic pathways. The PPARs for example bind to and are activated by free fatty acids, especially poly-unsaturated fatty acids (96). When no ligand is bound by the PPARs, corepressors and HDACs are recruited. Ligand binding changes PPAR conformation thereby dissociating repressors and recruiting protein complexes with histone acetyltransferase (HAT) activity to allow gene transcription. PGC-1α coactivates PPARα to regulate expression of genes involved in mitochondrial fatty acid import and β-oxidation (98, 193). PPARδ is coactivated by PGC-1α to stimulate expression of genes involved in fatty acid metabolism (92). Furthermore, overexpression of an activated form of PPARδ increased mitochondrial

Figure 1 | Pathways regulating muscle oxidative phenotype. AMP, adenosine monophosphate; AMPK, AMP-activated protein kinase; ATF2, activating transcription factor 2; ATP, adenosine triphosphate; CaMKs, Ca_2+/calmodulin-dependent protein kinases; Cn, calcineurin; ERRs, estrogen-related receptors; FFA, free fatty acids; HIF-1, hypoxia-inducible factor; MEF2, myocyte enhancer factor-2; mtDNA, mitochondrial DNA; NAD, nicotinamide adenine dinucleotide; nDNA, nuclear DNA; NFAT, nuclear factor of activated T-cells; NRFs, nuclear respiratory factors; OXPHOS, oxidative phosphorylation; PGC-1α, peroxisome proliferator-activated receptor γ, coactivator 1 α; PHDs, prolyl hydroxylase domain enzymes; PPARs, peroxisome proliferator-activated receptors; ROS, reactive oxygen species; SIRT1, sirtuin 1; Tfam, mitochondrial transcription factor A.

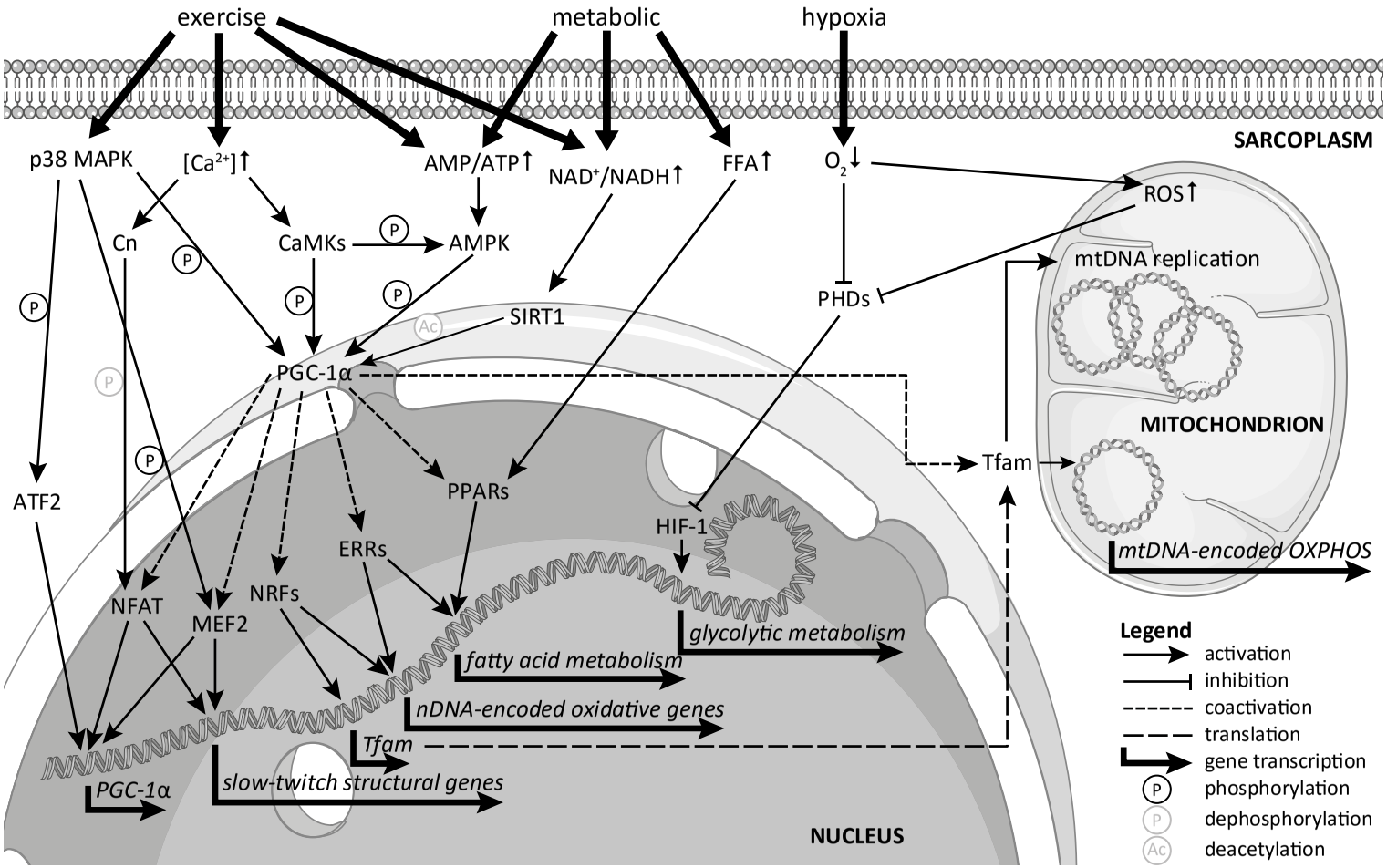
exercise
metabolic
hypoxia
SARCOPLASM
p38 MAPK
[Ca2+]↑
AMP/ATP↑
NAD+/NADH↑
FFA↑
O2↓
ROS↑
Cn
CaMKs
AMPK
mtDNA replication
PHDs
SIRT1
PGC-1α
MITOCHONDRION
Tfam
ATF2
PPARs
HIF-1
ERRs
mtDNA-encoded OXPHOS
NFAT
MEF2
NRFs
glycolytic metabolism
fatty acid metabolism
nDNA-encoded oxidative genes
Tfam
PGC-1α
slow-twitch structural genes
NUCLEUS
Legend
activation
inhibition
coactivation
translation
gene transcription
phosphorylation
dephosphorylation
deacetylation

biogenesis (197). Moreover, PGC-1α induces PPARδ expression and coativates PPARδ to induce its own expression (65).

Estrogen-related receptors

Although the natural ligands of estrogen-related receptors have yet to be discovered, it is known that PGC-1 coactivators can serve as protein ligands for the ERRs (36). Coactivation of ERRα by PGC-1α stimulates expression of OXPHOS genes and mitochondrial biogenesis (173), whereas ERRγ activates angiogenesis and promotes oxidative metabolism and type I fibers independent of PGC-1α in muscle-specific ERRγ overexpression mice via activation of 5'-adenosine monophosphate-activated protein kinase (AMPK) (134). The role of ERRβ in metabolism is unknown, although it is known that ERRβ is expressed in skeletal muscle in an oscillating manner (209). Due to the light/dark-dependent oscillating expression of ERR isoforms it has been suggested that ERRs act as molecular links between the circadian clock and energy metabolism (209).

Regulation of fiber type

Calcium signaling

Multiple signaling pathways are involved in regulation of muscle fiber type. The Ras/mitogen-activated protein kinase (MAPK) pathway couples excitation and transcriptional regulation to promote the slow program in regenerating muscle (130). The calcium/calmodulin-activated phosphatase calcineurin (Cn) dephosphorylates the transcription factor NFAT in response to nerve activity, which results in nuclear translocation of NFAT and activation of the slow-type muscle program in cooperation with among others the myocyte enhancer factor 2 (MEF2) proteins (28, 136, 176). Slow motor neuron activity also stimulates activity of calcium-dependent calcium/calmodulin-dependent protein kinase IV (CaMKIV) to promote MEF2 transactivator function and to stimulate mitochondrial biogenesis (204). Moreover, MEF2 directly interacts with PGC-1α to synergistically activate transcription of slow-twitch muscle genes and stimulate calcineurin signaling (104, 205). Overexpression of PGC-1α in skeletal muscle drives a fiber-type shift with increased proportion of type I fibers (104). Also, muscle-specific overexpression of activated PPARδ has been shown to result in a so-called 'endurance phenotype' with an increased proportion of slow-twitch fibers in addition to increases of oxidative enzymes and mitochondrial biogenesis (197).

MyomiR network

In the last decade it has become increasingly clear that muscle-specific microRNAs (miRNAs) play a significant role in muscle development and repair. miRNAs were discovered as small non-coding RNAs that regulate cytoplasmic mRNA stability and translation via partial base-pairing with the target mRNA sequence in RNA-induced silencing complexes (RISC). mRNA is then either cleaved by the slicing-competent argonaute protein Ago2 in the core of RISC and degraded, or is modified by deadenylating and decapping enzymes that are recruited by the Ago partner GW182. This permits exonucleases to cut unprotected mRNA and it interferes with binding of cap-binding protein eIF4E and ribosome scanning (30). One single mRNA can be targeted by multiple miRNAs and one individual miRNA can target mRNAs in multiple signaling pathways, thereby ensuring pleotropic regulation, or it can target multiple mRNAs with products in

the same pathway to amplify its effect. miRNAs that are specifically expressed in muscle cells have been named myomiRs.

In addition to their cytoplasmic localization, miRNAs have also been detected in secreted vesicles (213) and in mitochondria (13, 15, 19, 31, 94, 179). Interestingly, in the mitochondria the cardiac and skeletal muscle-specific miRNA miR-1 has been shown to stimulate mitochondrial translation of multiple mtDNA-encoded mRNAs, while inhibiting nDNA-encoded target mRNAs (212). This function has been shown to occur during myogenic differentiation and enables increased expression of mitochondrial proteins without significantly increasing mtDNA copy number or transcription (212).

miR-1 is expressed from a bicistronic cluster with miR-133a, but these miRNAs have opposing functions: whereas miR-1 targets HDAC4 (27), a transcriptional repressor of myogenic gene expression via MEF2 (107), miR-133a targets serum response factor (SRF) to enhance myoblast proliferation (27). Another pair of skeletal-muscle specific miRNAs that is bicistronically transcribed is miR-133b and miR-206. miR-133b is highly homologous to miR-133a, while miR-206 shares similarity to miR-1 and has similar target mRNAs (27, 122). miR-206 shows sequence similarity with miR-1 and stimulates differentiation via indirect upregulation of MyoD (90). Expression of miR-1 and miR-133 family members is regulated by myogenic regulators including MEF2, MyoD and myogenin (106, 156).

Other muscle-specific miRNAs include miR-208b, miR-486 and miR-499. miR-208b and miR-499 are encoded in the introns of the mouse slow type I β-MHC (Myh7) gene and slow type I MHC7b (My7b) gene, respectively, and functionally redundant (191). They promote a slow-twitch gene program by targeting transcription factors that regulate a fast-twitch gene program, such as Sox6, Purβ, Sp3, HP-1β and Thrap1 (18, 123, 191) and have been shown to be regulated by ERRγ (46). miR-486 is a target of myostatin signaling and stimulates the IGF-1/Akt/mTOR pathway to regulate muscle size (64).

Regulation by exercise

Endurance training has been shown to stimulate expression of mitochondrial enzymes (24), whereas detraining results in decreased mitochondrial capacity (61). An increased proportion of oxidative fibers make the muscle more resistant to fatigue, but disuse can reduce the proportion of oxidative fibers in muscle (72). In response to exercise, expression of Oxphen regulators including PGC-1α, PPAR-α and -δ, and Tfam is induced (111, 146). Upon nerve stimulation, calcium signaling is activated by activation of CaMKIV and calcineurin A (CnA), which in turn activate MEF2C and MEF2D that drive PGC-1α transcription (58). MEF2C and MEF2D expression is regulated by PGC-1α, which creates a positive feedback loop (104, 124). Furthermore, CaMKIV activates cAMP response element (CRE)-binding protein (CREB), which is another transcription factor that regulates PGC-1α expression (58, 204). Calcineurin dephosphorylates NFAT, which then translocates to the nucleus to activate transcription of a slow-twitch gene program (28, 33). Phosphorylation of NFAT by GSK-3β or casein kinase 1 or 2 results in export out of the nucleus (17, 137, 141, 216). Treatment of rats with the calcineurin inhibitor cyclosporin A (CsA) induces a fiber-type shift from slow to fast (28, 176). On the other hand, calcineurin-overexpressing mice display an increased proportion of slow fibers in skeletal muscle (28, 184). Exercise also activates p38 MAPK and AMPK (3, 84). p38 MAPK can activate both MEF2 (215) and activating transcription factor 2 (ATF2) to induce

PGC-1α expression (3). Effects of AMPK on mitochondrial biogenesis and function are mediated by PGC-1α, but how exactly AMPK stimulates PGC-1α expression is unknown (78).

It has been shown that the exercise intensity is related to the induction of PGC-1α mRNA expression (139): low-intensity exercise stimulates phosphorylation of p38 MAPK but does not affect PGC-1α gene expression (35). High-intensity exercise on the other hand increases phosphorylation of AMPK, CaMKII and p38 MAPK and induces mRNA expression of PGC-1α (35). Moreover, it has been suggested that PGC-1α expression is induced by exercise only if the intensity is high enough to exceed the lactate threshold (186).

It is known from mouse studies that 90 min of exhaustive endurance exercise decreased expression of miR-23, which correlated with increased PGC-1α expression (165), a predicted target of miR-23 (199). Furthermore, four weeks of threadmill endurance training resulted in decreased miR-696 expression, which correlated with increased PGC-1α protein levels in mice (11). miR-696 has been shown *in vitro* to negatively affect PGC-1α protein but not mRNA expression (11). Expression of miR-696 or its regulation of PGC-1α translation has not yet been verified in human skeletal muscle.

Hypoxia

Cellular signaling

Glycolytic metabolism is associated with with reduced oxygen availability, or hypoxia (198). Oxygen can be sensed by all nucleated cells in the human body. The hypoxia inducible factor (HIF) plays a critical role in the transcriptional regulation of angiogenesis and hypoxic adaptation (63, 91) and is also expressed in skeletal muscle (181). HIF is a heterodimeric protein that belongs to the basic helix-loop-helix-PAS family of transcription factors (195). It is composed of a regulatory alpha subunit and a constitutively expressed beta subunit (196). The alpha subunit has a short half-life of approximately 5 minutes and is highly sensitive to oxygen (167). Three different HIF alpha isoforms have been described: HIF-1α is ubiquitously expressed and the most characterized form. HIF-2α and HIF-3α expression is generally restricted to certain cell types (e.g. endothelial, epithelial, neuronal, fibroblast and macrophage cells). Whereas HIF-2α has a structure and function similar to HIF-1α, HIF-3α function is still incompletely understood but probably related to inhibition of HIF-1α and HIF-2α (60). The only beta isoform, HIF-1β (also known as ARNT: aryl hydrocarbon nuclear receptor) is insensitive to oxygen levels.

Under normoxic conditions, HIF-1α is continuously degraded. Oxygen permits activity of prolyl hydroxylases (PHDs), which tag HIF-1α in its oxygen-dependent degradation domain (ODDD) for ubiquitylation and proteasomal degradation via the E3 ligase von Hippel-Lindau (VHL) protein (85, 119). In addition, hydroxylation of HIF-1α in its transactivation domain by the factor inhibiting HIF-1 (FIH-1) protein inhibits transcriptional activity of HIF-1α (97). Under hypoxic conditions, PHD and FIH activities and subsequent hydroxylation of HIF-1α are inhibited (41). The result is stabilized HIF-1α protein and HIF-1α accumulation, which can then bind to HIF-1β and recognize hypoxia-responsive elements (HRE) in target genes to trigger transcription (175). One hour of systemic hypoxia is sufficient to increase HIF-1α expression in skeletal muscle (108). Target genes of HIF-1α include genes related to erythropoiesis and iron metabolism (e.g.

erythropoietin and transferrin), angiogenesis (e.g. vascular endothelial growth factor, heme oxygenase-1), glucose metabolism (e.g. glucose transporter-1, hexokinase) and genes related to cell proliferation and survival, including growth factors (e.g. insulin-like growth factor-2, IGF binding protein, transforming growth factor-α) (86).

In skeletal muscle of sedentary humans and mice, HIF-1α is activated in response to a single bout of endurance exercise (7, 117, 118). However, after a period of training, the response of HIF-1 to an exercise bout is blunted (109, 161) and therefore negative regulation of HIF has been suggested to contribute to skeletal muscle adaptations to training (105).

Regulation of Oxphen by hypoxia

In response to hypoxia, cells shift their metabolism from oxidative phosphorylation to anaerobic glycolysis. Because glycolysis is less efficient than oxidative phosphorylation to produce ATP, activity of the glycolytic enzymes is stimulated to maintain production of the necessary amount of ATP (174). HIF-1 diverts pyruvate flux from the mitochondria through increased expression of PDK-1 and inactivation of the pyruvate dehydrogenase complex (PDC) (91, 144).

In murine skeletal muscle, HIF-1α expression is fiber-type dependent with higher expression in glycolytic than in oxidative muscles (147). Muscle-specific knockout of HIF-1α in mice results in a metabolic shift characterized by decreased activity of the glycolytic pathway and increased citric acid cycle activity and fatty acid oxidation (117). The HIF-1α knockout mice display improved running endurance, but repeated exercise results in extensive muscle damage which harms endurance in the long term (117). Whereas HIF-1α knockout promotes oxidative phenotype, hypoxia has been shown to stimulate muscle glycolytic capacity over oxidative capacity (76, 117).

In humans, HIF-1α is highly expressed even in normoxic conditions and might be involved in muscle homeostasis even in normoxia (108). The effects of hypoxic exposure on human muscle are often studied during mountaineering expeditions. Hypoxia has been shown to decrease activities of mitochondrial enzymes (21, 70) and to reduce mitochondrial volume (reviewed in (69)). Also, mass-specific maximal oxidative phosphorylation capacity has been shown to slightly decrease after 9-11 days of high-altitude exposure (77). However, mountaineering expeditions are heavily confounded by strenuous physical activity (66, 67, 70). In a hypobaric chamber, wherein confounders related to these expeditions, such as low temperature, dietary imbalance and extreme exercise can be controlled, hypoxia has been shown to repress enzyme activities of citrate synthase, succinate dehydrogenase and hexokinase with no change of other glycolytic enzymes or fiber-type distribution (57). The role of HIF in determining muscle phenotype and metabolism can be investigated in humans by studying patients with Chuvash polycythemia (CP), which involves a homozygous germline mutation in the VHL gene (10). This mutation results in impaired binding of VHL protein to hydroxylated HIF-α, increased HIF-α stabilization and expression of HIF-target genes in lymphocytes and plasma under normoxic conditions (10, 22). However, CP patients do not have a significantly different distribution of muscle fiber types (43). In response to exercise these patients experience increased lactate accumulation, reduced muscle pH, lower maximum exercise capacities and faster depletion of PCr than healthy controls (43). Interestingly, expression of VHL was found to be increased in skeletal muscle of patients

with COPD and has been suggested to impair capillarization and hypoxic signaling to VEGF (82). Overall, hypoxia modulates multiple pathways in addition to the HIF pathway, so these results related to VHL should be interpreted cautiously when inferring to hypoxic conditions.

HIF regulates metabolism via different routes. It transcriptionally regulates genes that encode enzymes of the glycolytic pathway (71). By inducing expression/activity of pyruvate dehydrogenase kinase (PDK), the mitochondrial pyruvate dehydrogenase complex (PDC) is inhibited from converting pyruvate to acetyl-CoA and mitochondrial oxygen consumption is downregulated (12, 91, 144). Furthermore, HIF stimulates differential expression of cytochrome *c* oxidase (COX) subunit 4 isoform to improve respiration efficiency at lower oxygen tension (45). Interestingly, two papers report that COX activity is increased in skeletal muscle of patients with COPD, and that higher COX activity is associated with lower arterial oxygen pressure (PaO_2) (150, 169). Other papers however report reduced COX activity in COPD muscle (52, 133). Lastly, in *in vitro* experiments increased HIF-1 activity has been shown to be associated with increased autophagy of mitochondria (211). However, mitochondrial content of HIF-1α knockout mice is not different from that of wild-type mice (117).

OXPHEN regulation in COPD

The loss of oxidative capacity in skeletal muscle of patients with COPD has been suggested to be related to amongst others reduced mitochondrial content and biogenesis (50) and increased oxidative stress (151). In skeletal muscle of patients with severe COPD, decreased expression of PGC-1α, Tfam, and PPARδ has been shown (160). Also several microRNAs that are expressed in skeletal muscle have been shown to be differentially expressed in COPD patients compared to healthy controls: Lewis *et al.* showed downregulation of SRF and miR-1 in quadriceps of COPD patients and an association of miR-1 with type I fiber proportion (100). However, miR-1 abundance was increased in the blood of COPD patients, which is suggested to be related to increased muscle turnover (34). Reduced expression of miR-1 in the muscle was accompanied by increased HDAC4 protein content, which potentially causes decreased type I fiber proportion because HDAC4 inhibits MEF2-regulated expression of amongst others type I myosin heavy chain (100).

Skeletal muscle of patients with COPD is exposed to an array of deleterious factors that may be implicated in the loss of skeletal muscle Oxphen, including low-grade systemic inflammation, oxidative stress, systemic corticosteroid medication, malnutrition, physical inactivity, and hypoxia (207). Previously, inflammation has been shown to negatively affect muscle Oxphen (157) and to be associated with loss of Oxphen in patients with COPD (159). Likewise, oxidative stress in COPD has been associated with loss of Oxphen (120, 121, 151). Furthermore, chronic corticosteroid medication has been shown to cause mitochondrial dysfunction and reduce oxidative capacity (93, 126), although this has not yet been proven in the context of COPD. Malnutrition has been shown to depress activities of mitochondrial complexes (110) and is suggested to be associated with reduced glycolytic and oxidative capacity in both type I and type II fibers in COPD (5). Although exercise is an important physiological booster of Oxphen (75), a link between physical inactivity and loss of Oxphen has not been convincingly shown in patients with COPD (54, 135). There are however indications that loss of muscle

Oxphen in COPD could be related to hypoxia: Jakobsson *et al.* showed that low type I fiber proportion is associated with PaO_2 in patients with respiratory failure (RF) (80). Moreover, Wuyam *et al.* showed that patients with RF have impaired muscle oxidative capacity (208), whereas Jakobsson *et al.* described that decreased oxidative enzyme activities in quadriceps muscle of patients with advanced COPD (81) could be partly restored by long-term oxygen therapy (79). More research into the role of hypoxia in loss of skeletal muscle Oxphen is warranted, since it is rather unexplored in the context of COPD.

Hypoxia in COPD

In light of the ventilatory limitations, decreased oxygenation is not a rare symptom in patients with COPD (89). Even so, the role of decreased oxygenation in the loss of muscle Oxphen has not yet been conclusively established. The nature of hypoxia exposure in muscle of COPD patients can be both acute and chronic. Acute hypoxia may occur as a consequence of exertional or nocturnal oxygen desaturation (89), where nocturnal desaturation has been shown to occur more often than exertional desaturation in patients with COPD (129). Since there is no uniform definition of exertional oxygen desaturation and type of activity influences whether desaturation occurs, there are no definite numbers on the prevalence of oxygen desaturation in patients with COPD (47, 143). A study by Stolz showed that exertional desaturation is common in stable moderate to very severe COPD patients, with a prevalence of 29.1% (180). Short-term hypoxia may happen during acute exacerbations of COPD (14). In addition, patients may be chronically hypoxic in resting conditions due to progressive airflow limitation and emphysematous destruction of the lung (89). Moreover, patients may have mild or moderate hypoxemia, but not severe enough for physicians to prescribe oxygen therapy (resting $PaO_2 < 7.3$ kPa) (2, 155).

Hypoxia has been shown to reduce exercise capacity . Studies in hypoxemic patients with COPD have shown that impaired exercise capacity can only be partially restored by supplementing oxygen during exercise (145). This implies that the working muscle in COPD patients could have a disability with regard to the extraction or utilization of oxygen, which can be restored by oxygen supplementation. However, exercise capacity is not fully restored to levels similar to those in healthy controls (145), which implies that structural muscle changes have occurred in the COPD patient, possibly under influence of chronic hypoxemia. This is supported by a study by Jakobsson and colleagues who found that 6-9 months of long-term oxygen therapy (LTOT) improved oxidative phosphorylation function reflected by high-energy phosphate metabolism (79). Another study by Hildebrand and colleagues showed that hemodilution in COPD patients with polycythemia resulted in improved arterial oxygen tension and decreased the proportion of type II muscle fibers, which were significantly higher in the patients than in healthy controls (62). Moreover, the proportion of type II fibers inversely correlated with PaO_2 and SaO_2 (62), which is in line with the positive correlation of PaO_2 and type I fiber proportion reported by Jakobsson *et al.* (80).

Signs that muscle abnormalities in COPD are likely caused by hypoxia are also obtained from systems biology approaches. Turan *et al.* showed that in response to exercise skeletal muscle of COPD patients fail to activate expression of several tissue remodeling and bioenergetics pathways that are potentially regulated by histone

modifiers (187). Expression of these histone modifiers correlated with VO_2max in the patients and is also altered in mice exposed to 2 weeks of hypoxia, which implies a potential role of hypoxia in skeletal muscle abnormalities in COPD (187). Another recent systems biology analysis of guinea pigs exposed to cigarette smoke and/or chronic hypoxia revealed that muscle alterations in these animals were very reminiscent of those in patients with COPD (32). Interestingly, significant inverse correlations of serum protein levels of CXCL9 and CXCL10 with skeletal muscle expression of aerobic energy metabolism genes were found in the COPD patients, whereas expression of both chemokines appeared to be induced by exposure to chronic hypoxia in guinea pigs (32).

Further indications of a role for hypoxia in limitation of exercise capacity in COPD comes from findings of a disturbed muscle-to-capillary interface in muscle of COPD patients and a positive correlation between exercise capacity and degree of muscle capillarization (38). Skeletal muscle of patients with mild and moderate COPD has been shown to have elevated expression of von Hippel-Lindau protein, which has been hypothesized to negatively affect tissue capillarization by limiting angiogenic potential (82). Moreover, skeletal muscle of COPD patients has been reported to have significantly decreased capillarization (83).

OBJECTIVE, AIMS AND OUTLINE OF THE THESIS

The overall objective of the work described in this thesis is to characterize the role of hypoxia in the loss of peripheral skeletal muscle oxidative phenotype (Oxphen) in COPD and to explore the underlying molecular mechanisms.

In **Chapter 2**, we investigated our hypothesis that chronic hypoxia *per se* reduces markers of Oxphen in an *in vitro* model of myofibers. Furthermore, we modulated the PPAR regulators and HIF-1α to prove their involvement in the underlying mechanism. In **Chapter 3**, we aimed to translate the *in vitro* findings to the *in vivo* situation of young, adult and aged mice exposed to 8% oxygen for 3 weeks. We chose to include three age groups, because animal studies are often performed in young animals. However, COPD patients are middle-aged to aged when diagnosed and aged mice might therefore present a more appropriate model. We hypothesized that hypoxia would reduce expression of markers and regulators of Oxphen, and that this effect would be stronger in the aged mice.

Although loss of Oxphen has previously been shown in patients with advanced COPD (GOLD stages 3 and 4), no data are available in less advanced disease. In **Chapter 4**, muscle function and fiber phenotype were therefore assessed in a cohort of mild to moderate COPD patients. We hypothesized that loss of Oxphen in the quadriceps is already present in this stage of the disease and that it is associated with decreased quadriceps endurance. In **Chapter 5** we investigated in these patients the response of markers of Oxphen and oxidative stress to a maximal exercise bout and studied the effect of intermittent hypoxia in the form of exercise-induced oxygen desaturation on the early gene-regulatory exercise response. We hypothesized that Oxphen response would be blunted in patients who desaturate during exercise due to an inhibitory effect of muscle hypoxia on the expression of Oxphen regulators. Furthermore, we expected that oxidative stress would be increased in the desaturating patients, because hypoxia has been shown to increase production of reactive oxygen species. Finally, in **Chapter 6** the implications of the experimental findings of the studies described in this thesis for COPD management and directions for future research are discussed.

REFERENCES

1. Global Initiative for Chronic Obstructive Lung Disease www.goldcopd.org. [1 Feb, 2015].
2. Richtlijn Diagnostiek en behandeling van COPD, 2010. Nederlandse Vereniging van Artsen voor Longziekten en Tuberculose. http://www.nvalt.nl/uploads/Mn/U9/MnU99pqRBYK7a_zStHhumA/Richtlijn-Diagnostiek-en-behandeling-van-COPD-maart-2010.pdf. [1 Feb, 2015].
3. Akimoto T, Pohnert SC, Li P, Zhang M, Gumbs C, Rosenberg PB, Williams RS, and Yan Z. Exercise stimulates PGC-1alpha transcription in skeletal muscle through activation of the p38 MAPK pathway. J Biol Chem 280: 19587-19593, 2005.
4. Akimoto T, Ribar TJ, Williams RS, and Yan Z. Skeletal muscle adaptation in response to voluntary running in Ca2+/calmodulin-dependent protein kinase IV-deficient mice. Am J Physiol Cell Physiol 287: C1311-1319, 2004.
5. Alcolea Batres S, Villamor Leon J, and Alvarez-Sala R. [Nutritional Status in COPD]. Arch Bronconeumol 43: 283-288, 2007.
6. Allaire J, Maltais F, Doyon JF, Noel M, LeBlanc P, Carrier G, Simard C, and Jobin J. Peripheral muscle endurance and the oxidative profile of the quadriceps in patients with COPD. Thorax 59: 673-678, 2004.
7. Ameln H, Gustafsson T, Sundberg CJ, Okamoto K, Jansson E, Poellinger L, and Makino Y. Physiological activation of hypoxia inducible factor-1 in human skeletal muscle. FASEB J 19: 1009-1011, 2005.
8. Anderson RM, Barger JL, Edwards MG, Braun KH, O'Connor CE, Prolla TA, and Weindruch R. Dynamic regulation of PGC-1alpha localization and turnover implicates mitochondrial adaptation in calorie restriction and the stress response. Aging Cell 7: 101-111, 2008.
9. Andersson U, and Scarpulla RC. PGC-1-related coactivator, a novel, serum-inducible coactivator of nuclear respiratory factor 1-dependent transcription in mammalian cells. Mol Cell Biol 21: 3738-3749, 2001.
10. Ang SO, Chen H, Hirota K, Gordeuk VR, Jelinek J, Guan Y, Liu E, Sergueeva AI, Miasnikova GY, Mole D, Maxwell PH, Stockton DW, Semenza GL, and Prchal JT. Disruption of oxygen homeostasis underlies congenital Chuvash polycythemia. Nat Genet 32: 614-621, 2002.
11. Aoi W, Naito Y, Mizushima K, Takanami Y, Kawai Y, Ichikawa H, and Yoshikawa T. The microRNA miR-696 regulates PGC-1{alpha} in mouse skeletal muscle in response to physical activity. Am J Physiol Endocrinol Metab 298: E799-806, 2010.
12. Aragones J, Schneider M, Van Geyte K, Fraisl P, Dresselaers T, Mazzone M, Dirkx R, Zacchigna S, Lemieux H, Jeoung NH, Lambrechts D, Bishop T, Lafuste P, Diez-Juan A, Harten SK, Van Noten P, De Bock K, Willam C, Tjwa M, Grosfeld A, Navet R, Moons L, Vandendriessche T, Deroose C, Wijeyekoon B, Nuyts J, Jordan B, Silasi-Mansat R, Lupu F, Dewerchin M, Pugh C, Salmon P, Mortelmans L, Gallez B, Gorus F, Buyse J, Sluse F, Harris RA, Gnaiger E, Hespel P, Van Hecke P, Schuit F, Van Veldhoven P, Ratcliffe P, Baes M, Maxwell P, and Carmeliet P. Deficiency or inhibition of oxygen sensor Phd1 induces hypoxia tolerance by reprogramming basal metabolism. Nat Genet 40: 170-180, 2008.
13. Bandiera S, Ruberg S, Girard M, Cagnard N, Hanein S, Chretien D, Munnich A, Lyonnet S, and Henrion-Caude A. Nuclear outsourcing of RNA interference components to human mitochondria. PLoS One 6: e20746, 2011.
14. Barbera JA, Roca J, Ferrer A, Felez MA, Diaz O, Roger N, and Rodriguez-Roisin R. Mechanisms of worsening gas exchange during acute exacerbations of chronic obstructive pulmonary disease. Eur Respir J 10: 1285-1291, 1997.
15. Barrey E, Saint-Auret G, Bonnamy B, Damas D, Boyer O, and Gidrol X. Pre-microRNA and mature microRNA in human mitochondria. PLoS One 6: e20220, 2011.
16. Bassel-Duby R, and Olson EN. Signaling pathways in skeletal muscle remodeling. Annu Rev Biochem 75: 19-37, 2006.
17. Beals CR, Sheridan CM, Turck CW, Gardner P, and Crabtree GR. Nuclear export of NF-ATc enhanced by glycogen synthase kinase-3. Science 275: 1930-1934, 1997.
18. Bell ML, Buvoli M, and Leinwand LA. Uncoupling of expression of an intronic microRNA and its myosin host gene by exon skipping. Mol Cell Biol 30: 1937-1945, 2010.
19. Bian Z, Li LM, Tang R, Hou DX, Chen X, Zhang CY, and Zen K. Identification of mouse liver mitochondria-associated miRNAs and their potential biological functions. Cell Res 20: 1076-1078, 2010.
20. Booth FW, and Narahara KA. Vastus lateralis cytochrome oxidase activity and its relationship to maximal oxygen consumption in man. Pflugers Arch 349: 319-324, 1974.
21. Boutellier U, Howald H, di Prampero PE, Giezendanner D, and Cerretelli P. Human muscle adaptations to chronic hypoxia. Prog Clin Biol Res 136: 273-285, 1983.
22. Bushuev VI, Miasnikova GY, Sergueeva AI, Polyakova LA, Okhotin D, Gaskin PR, Debebe Z, Nekhai S, Castro OL, Prchal JT, and Gordeuk VR. Endothelin-1, vascular endothelial growth factor and systolic pulmonary artery pressure in patients with Chuvash polycythemia. Haematologica 91: 744-749, 2006.
23. Canto C, Gerhart-Hines Z, Feige JN, Lagouge M, Noriega L, Milne JC, Elliott PJ, Puigserver P, and Auwerx J. AMPK regulates energy expenditure by modulating NAD+ metabolism and SIRT1 activity. Nature 458: 1056-1060, 2009.
24. Carter SL, Rennie CD, Hamilton SJ, and Tarnopolsky. Changes in skeletal muscle in males and females following endurance training. Can J Physiol Pharmacol 79: 386-392, 2001.
25. Chang JS, Huypens P, Zhang Y, Black C, Kralli A, and Gettys TW. Regulation of NT-PGC-1alpha subcellular localization and function by protein kinase A-dependent modulation of nuclear export by CRM1. J Biol Chem 285: 18039-18050, 2010.
26. Chatila WM, Thomashow BM, Minai OA, Criner GJ, and Make BJ. Comorbidities in chronic obstructive pulmonary disease. Proc Am Thorac Soc 5: 549-555, 2008.
27. Chen JF, Mandel EM, Thomson JM, Wu Q, Callis TE, Hammond SM, Conlon FL, and Wang DZ. The role of microRNA-1 and microRNA-133 in skeletal muscle proliferation and differentiation. Nat Genet 38: 228-233, 2006.
28. Chin ER, Olson EN, Richardson JA, Yang Q, Humphries C, Shelton JM, Wu H, Zhu W, Bassel-Duby R, and Williams RS. A

calcineurin-dependent transcriptional pathway controls skeletal muscle fiber type. Genes Dev 12: 2499-2509, 1998.
29. Coste A, Louet JF, Lagouge M, Lerin C, Antal MC, Meziane H, Schoonjans K, Puigserver P, O'Malley BW, and Auwerx J. The genetic ablation of SRC-3 protects against obesity and improves insulin sensitivity by reducing the acetylation of PGC-1{alpha}. Proc Natl Acad Sci U S A 105: 17187-17192, 2008.
30. Czech B, and Hannon GJ. Small RNA sorting: matchmaking for Argonautes. Nat Rev Genet 12: 19-31, 2011.
31. Das S, Ferlito M, Kent OA, Fox-Talbot K, Wang R, Liu D, Raghavachari N, Yang Y, Wheelan SJ, Murphy E, and Steenbergen C. Nuclear miRNA regulates the mitochondrial genome in the heart. Circ Res 110: 1596-1603, 2012.
32. Davidsen PK, Herbert JM, Antczak P, Clarke K, Ferrer E, Peinado VI, Gonzalez C, Roca J, Egginton S, Barbera JA, and Falciani F. A systems biology approach reveals a link between systemic cytokines and skeletal muscle energy metabolism in a rodent smoking model and human COPD. Genome Med 6: 59, 2014.
33. Delling U, Tureckova J, Lim HW, De Windt LJ, Rotwein P, and Molkentin JD. A calcineurin-NFATc3-dependent pathway regulates skeletal muscle differentiation and slow myosin heavy-chain expression. Mol Cell Biol 20: 6600-6611, 2000.
34. Donaldson A, Natanek SA, Lewis A, Man WD, Hopkinson NS, Polkey MI, and Kemp PR. Increased skeletal muscle-specific microRNA in the blood of patients with COPD. Thorax 68: 1140-1149, 2013.
35. Egan B, Carson BP, Garcia-Roves PM, Chibalin AV, Sarsfield FM, Barron N, McCaffrey N, Moyna NM, Zierath JR, and O'Gorman DJ. Exercise intensity-dependent regulation of peroxisome proliferator-activated receptor coactivator-1 mRNA abundance is associated with differential activation of upstream signalling kinases in human skeletal muscle. J Physiol 588: 1779-1790, 2010.
36. Eichner LJ, and Giguere V. Estrogen related receptors (ERRs): a new dawn in transcriptional control of mitochondrial gene networks. Mitochondrion 11: 544-552, 2011.
37. Eisenberg HA, and Hood DA. Blood flow, mitochondria, and performance in skeletal muscle after denervation and reinnervation. J Appl Physiol (1985) 76: 859-866, 1994.
38. Eliason G, Abdel-Halim SM, Piehl-Aulin K, and Kadi F. Alterations in the muscle-to-capillary interface in patients with different degrees of chronic obstructive pulmonary disease. Respir Res 11: 97, 2010.
39. Evans MJ, and Scarpulla RC. NRF-1: a trans-activator of nuclear-encoded respiratory genes in animal cells. Genes Dev 4: 1023-1034, 1990.
40. Fan M, Rhee J, St-Pierre J, Handschin C, Puigserver P, Lin J, Jaeger S, Erdjument-Bromage H, Tempst P, and Spiegelman BM. Suppression of mitochondrial respiration through recruitment of p160 myb binding protein to PGC-1alpha: modulation by p38 MAPK. Genes Dev 18: 278-289, 2004.
41. Fandrey J, Gorr TA, and Gassmann M. Regulating cellular oxygen sensing by hydroxylation. Cardiovasc Res 71: 642-651, 2006.
42. Fernandez-Marcos PJ, and Auwerx J. Regulation of PGC-1alpha, a nodal regulator of mitochondrial biogenesis. Am J Clin Nutr 93: 884S-890, 2011.
43. Formenti F, Constantin-Teodosiu D, Emmanuel Y, Cheeseman J, Dorrington KL, Edwards LM, Humphreys SM, Lappin TR, McMullin MF, McNamara CJ, Mills W, Murphy JA, O'Connor DF, Percy MJ, Ratcliffe PJ, Smith TG, Treacy M, Frayn KN, Greenhaff PL, Karpe F, Clarke K, and Robbins PA. Regulation of human metabolism by hypoxia-inducible factor. Proc Natl Acad Sci U S A 107: 12722-12727, 2010.
44. Franssen FM, and Rochester CL. Comorbidities in patients with COPD and pulmonary rehabilitation: do they matter? Eur Respir Rev 23: 131-141, 2014.
45. Fukuda R, Zhang H, Kim JW, Shimoda L, Dang CV, and Semenza GL. HIF-1 regulates cytochrome oxidase subunits to optimize efficiency of respiration in hypoxic cells. Cell 129: 111-122, 2007.
46. Gan Z, Rumsey J, Hazen BC, Lai L, Leone TC, Vega RB, Xie H, Conley KE, Auwerx J, Smith SR, Olson EN, Kralli A, and Kelly DP. Nuclear receptor/microRNA circuitry links muscle fiber type to energy metabolism. J Clin Invest 123: 2564-2575, 2013.
47. Garvey C, Tiep B, Carter R, Barnett M, Hart M, and Casaburi R. Severe exercise-induced hypoxemia. Respir Care 57: 1154-1160, 2012.
48. Gerhart-Hines Z, Rodgers JT, Bare O, Lerin C, Kim S-H, Mostoslavsky R, Alt FW, Wu Z, and Puigserver P. Metabolic control of muscle mitochondrial function and fatty acid oxidation through SIRT1/PGC-1α. EMBO J 26: 1913-1923, 2007.
49. Gleyzer N, Vercauteren K, and Scarpulla RC. Control of mitochondrial transcription specificity factors (TFB1M and TFB2M) by nuclear respiratory factors (NRF-1 and NRF-2) and PGC-1 family coactivators. Mol Cell Biol 25: 1354-1366, 2005.
50. Gosker HR, Hesselink MK, Duimel H, Ward KA, and Schols AM. Reduced mitochondrial density in the vastus lateralis muscle of patients with COPD. Eur Respir J 30: 73-79, 2007.
51. Gosker HR, Lencer NH, Franssen FM, van der Vusse GJ, Wouters EF, and Schols AM. Striking similarities in systemic factors contributing to decreased exercise capacity in patients with severe chronic heart failure or COPD. Chest 123: 1416-1424, 2003.
52. Gosker HR, van Mameren H, van Dijk PJ, Engelen MP, van der Vusse GJ, Wouters EF, and Schols AM. Skeletal muscle fibre-type shifting and metabolic profile in patients with chronic obstructive pulmonary disease. Eur Respir J 19: 617-625, 2002.
53. Gouspillou G, Sgarioto N, Norris B, Barbat-Artigas S, Aubertin-Leheudre M, Morais JA, Burelle Y, Taivassalo T, and Hepple RT. The relationship between muscle fiber type-specific PGC-1alpha content and mitochondrial content varies between rodent models and humans. PLoS One 9: e103044, 2014.
54. Gouzi F, Maury J, Molinari N, Pomies P, Mercier J, Prefaut C, and Hayot M. Reference values for vastus lateralis fiber size and type in healthy subjects over 40 years old: a systematic review and metaanalysis. J Appl Physiol (1985) 115: 346-354, 2013.
55. Graat-Verboom L, Wouters EF, Smeenk FW, van den Borne BE, Lunde R, and Spruit MA. Current status of research on

osteoporosis in COPD: a systematic review. Eur Respir J 34: 209-218, 2009.
56. Gram M, Dahl R, and Dela F. Physical inactivity and muscle oxidative capacity in humans. European journal of sport science 14: 376-383, 2014.
57. Green HJ, Sutton JR, Cymerman A, Young PM, and Houston CS. Operation Everest II: adaptations in human skeletal muscle. J Appl Physiol (1985) 66: 2454-2461, 1989.
58. Handschin C, Rhee J, Lin J, Tarr PT, and Spiegelman BM. An autoregulatory loop controls peroxisome proliferator-activated receptor gamma coactivator 1alpha expression in muscle. Proc Natl Acad Sci U S A 100: 7111-7116, 2003.
59. Hardie DG. AMP-activated protein kinase: an energy sensor that regulates all aspects of cell function. Genes Dev 25: 1895-1908, 2011.
60. Heikkila M, Pasanen A, Kivirikko KI, and Myllyharju J. Roles of the human hypoxia-inducible factor (HIF)-3alpha variants in the hypoxia response. Cell Mol Life Sci 68: 3885-3901, 2011.
61. Henriksson J, and Reitman JS. Time course of changes in human skeletal muscle succinate dehydrogenase and cytochrome oxidase activities and maximal oxygen uptake with physical activity and inactivity. Acta Physiol Scand 99: 91-97, 1977.
62. Hildebrand IL, Sylven C, Esbjornsson M, Hellstrom K, and Jansson E. Does chronic hypoxaemia induce transformations of fibre types? Acta Physiol Scand 141: 435-439, 1991.
63. Hirota K, and Semenza GL. Regulation of angiogenesis by hypoxia-inducible factor 1. Crit Rev Oncol Hematol 59: 15-26, 2006.
64. Hitachi K, Nakatani M, and Tsuchida K. Myostatin signaling regulates Akt activity via the regulation of miR-486 expression. Int J Biochem Cell Biol 47: 93-103, 2014.
65. Hondares E, Pineda-Torra I, Iglesias R, Staels B, Villarroya F, and Giralt M. PPARdelta, but not PPARalpha, activates PGC-1alpha gene transcription in muscle. Biochem Biophys Res Commun 354: 1021-1027, 2007.
66. Hoppeler H, and Desplanches D. Muscle structural modifications in hypoxia. Int J Sports Med 13 Suppl 1: S166-168, 1992.
67. Hoppeler H, Kleinert E, Schlegel C, Claassen H, Howald H, Kayar SR, and Cerretelli P. Morphological adaptations of human skeletal muscle to chronic hypoxia. Int J Sports Med 11 Suppl 1: S3-9, 1990.
68. Hoppeler H, Luthi P, Claassen H, Weibel ER, and Howald H. The ultrastructure of the normal human skeletal muscle. A morphometric analysis on untrained men, women and well-trained orienteers. Pflugers Arch 344: 217-232, 1973.
69. Hoppeler H, Vogt M, Weibel ER, and Fluck M. Response of skeletal muscle mitochondria to hypoxia. Exp Physiol 88: 109-119, 2003.
70. Howald H, Pette D, Simoneau JA, Uber A, Hoppeler H, and Cerretelli P. Effect of chronic hypoxia on muscle enzyme activities. Int J Sports Med 11 Suppl 1: S10-14, 1990.
71. Hu CJ, Wang LY, Chodosh LA, Keith B, and Simon MC. Differential roles of hypoxia-inducible factor 1alpha (HIF-1alpha) and HIF-2alpha in hypoxic gene regulation. Mol Cell Biol 23: 9361-9374, 2003.
72. Huey KA, Roy RR, Baldwin KM, and Edgerton VR. Temporal effects of inactivty on myosin heavy chain gene expression in rat slow muscle. Muscle Nerve 24: 517-526, 2001.
73. Hurd S. The impact of COPD on lung health worldwide: epidemiology and incidence. Chest 117: 1S-4S, 2000.
74. Huss JM, Torra IP, Staels B, Giguere V, and Kelly DP. Estrogen-related receptor alpha directs peroxisome proliferator-activated receptor alpha signaling in the transcriptional control of energy metabolism in cardiac and skeletal muscle. Mol Cell Biol 24: 9079-9091, 2004.
75. Irrcher I, Adhihetty PJ, Joseph AM, Ljubicic V, and Hood DA. Regulation of mitochondrial biogenesis in muscle by endurance exercise. Sports Med 33: 783-793, 2003.
76. Itoh K, Itoh M, Ishihara A, Hirofuji C, and Hayashi H. Influence of 12 weeks of hypobaric hypoxia on fibre type composition of the rat soleus muscle. Acta Physiol Scand 154: 417-418, 1995.
77. Jacobs RA, Boushel R, Wright-Paradis C, Calbet JA, Robach P, Gnaiger E, and Lundby C. Mitochondrial function in human skeletal muscle following high-altitude exposure. Exp Physiol 98: 245-255, 2013.
78. Jager S, Handschin C, St-Pierre J, and Spiegelman BM. AMP-activated protein kinase (AMPK) action in skeletal muscle via direct phosphorylation of PGC-1alpha. Proc Natl Acad Sci U S A 104: 12017-12022, 2007.
79. Jakobsson P, and Jorfeldt L. Long-term oxygen therapy may improve skeletal muscle metabolism in advanced chronic obstructive pulmonary disease patients with chronic hypoxaemia. Respir Med 89: 471-476, 1995.
80. Jakobsson P, Jorfeldt L, and Brundin A. Skeletal muscle metabolites and fibre types in patients with advanced chronic obstructive pulmonary disease (COPD), with and without chronic respiratory failure. Eur Respir J 3: 192-196, 1990.
81. Jakobsson P, Jorfeldt L, and Henriksson J. Metabolic enzyme activity in the quadriceps femoris muscle in patients with severe chronic obstructive pulmonary disease. Am J Respir Crit Care Med 151: 374-377, 1995.
82. Jatta K, Eliason G, Portela-Gomes GM, Grimelius L, Caro O, Nilholm L, Sirjso A, Piehl-Aulin K, and Abdel-Halim SM. Overexpression of von Hippel-Lindau protein in skeletal muscles of patients with chronic obstructive pulmonary disease. J Clin Pathol 62: 70-76, 2009.
83. Jobin J, Maltais F, Doyon JF, LeBlanc P, Simard PM, Simard AA, and Simard C. Chronic obstructive pulmonary disease: capillarity and fiber-type characteristics of skeletal muscle. J Cardiopulm Rehabil 18: 432-437, 1998.
84. Jorgensen SB, Wojtaszewski JF, Viollet B, Andreelli F, Birk JB, Hellsten Y, Schjerling P, Vaulont S, Neufer PD, Richter EA, and Pilegaard H. Effects of alpha-AMPK knockout on exercise-induced gene activation in mouse skeletal muscle. FASEB J 19: 1146-1148, 2005.
85. Kaelin WG, Jr., and Ratcliffe PJ. Oxygen sensing by metazoans: the central role of the HIF hydroxylase pathway. Mol Cell 30: 393-402, 2008.
86. Ke Q, and Costa M. Hypoxia-inducible factor-1 (HIF-1). Mol Pharmacol 70: 1469-1480, 2006.

87. Kelly DP, and Scarpulla RC. Transcriptional regulatory circuits controlling mitochondrial biogenesis and function. Genes Dev 18: 357-368, 2004.
88. Kelly TJ, Lerin C, Haas W, Gygi SP, and Puigserver P. GCN5-mediated transcriptional control of the metabolic coactivator PGC-1beta through lysine acetylation. J Biol Chem 284: 19945-19952, 2009.
89. Kent BD, Mitchell PD, and McNicholas WT. Hypoxemia in patients with COPD: cause, effects, and disease progression. Int J Chron Obstruct Pulmon Dis 6: 199-208, 2011.
90. Kim HK, Lee YS, Sivaprasad U, Malhotra A, and Dutta A. Muscle-specific microRNA miR-206 promotes muscle differentiation. J Cell Biol 174: 677-687, 2006.
91. Kim JW, Tchernyshyov I, Semenza GL, and Dang CV. HIF-1-mediated expression of pyruvate dehydrogenase kinase: a metabolic switch required for cellular adaptation to hypoxia. Cell metabolism 3: 177-185, 2006.
92. Kleiner S, Nguyen-Tran V, Bare O, Huang X, Spiegelman B, and Wu Z. PPAR{delta} agonism activates fatty acid oxidation via PGC-1{alpha} but does not increase mitochondrial gene expression and function. J Biol Chem 284: 18624-18633, 2009.
93. Koski CL, Rifenberick DH, and Max SR. Oxidative metabolism of skeletal muscle in steroid atrophy. Arch Neurol 31: 407-410, 1974.
94. Kren BT, Wong PY, Sarver A, Zhang X, Zeng Y, and Steer CJ. MicroRNAs identified in highly purified liver-derived mitochondria may play a role in apoptosis. RNA Biol 6: 65-72, 2009.
95. Kressler D, Schreiber SN, Knutti D, and Kralli A. The PGC-1-related protein PERC is a selective coactivator of estrogen receptor alpha. J Biol Chem 277: 13918-13925, 2002.
96. Krey G, Braissant O, L'Horset F, Kalkhoven E, Perroud M, Parker MG, and Wahli W. Fatty acids, eicosanoids, and hypolipidemic agents identified as ligands of peroxisome proliferator-activated receptors by coactivator-dependent receptor ligand assay. Mol Endocrinol 11: 779-791, 1997.
97. Lando D, Peet DJ, Gorman JJ, Whelan DA, Whitelaw ML, and Bruick RK. FIH-1 is an asparaginyl hydroxylase enzyme that regulates the transcriptional activity of hypoxia-inducible factor. Genes Dev 16: 1466-1471, 2002.
98. Lee WJ, Kim M, Park HS, Kim HS, Jeon MJ, Oh KS, Koh EH, Won JC, Kim MS, Oh GT, Yoon M, Lee KU, and Park JY. AMPK activation increases fatty acid oxidation in skeletal muscle by activating PPARalpha and PGC-1. Biochem Biophys Res Commun 340: 291-295, 2006.
99. Lerin C, Rodgers JT, Kalume DE, Kim SH, Pandey A, and Puigserver P. GCN5 acetyltransferase complex controls glucose metabolism through transcriptional repression of PGC-1alpha. Cell metabolism 3: 429-438, 2006.
100. Lewis A, Riddoch-Contreras J, Natanek SA, Donaldson A, Man WD, Moxham J, Hopkinson NS, Polkey MI, and Kemp PR. Downregulation of the serum response factor/miR-1 axis in the quadriceps of patients with COPD. Thorax 67: 26-34, 2012.
101. Lillioja S, Young AA, Culter CL, Ivy JL, Abbott WG, Zawadzki JK, Yki-Jarvinen H, Christin L, Secomb TW, and Bogardus C. Skeletal muscle capillary density and fiber type are possible determinants of in vivo insulin resistance in man. J Clin Invest 80: 415-424, 1987.
102. Lin J, Handschin C, and Spiegelman BM. Metabolic control through the PGC-1 family of transcription coactivators. Cell metabolism 1: 361-370, 2005.
103. Lin J, Puigserver P, Donovan J, Tarr P, and Spiegelman BM. Peroxisome proliferator-activated receptor gamma coactivator 1beta (PGC-1beta), a novel PGC-1-related transcription coactivator associated with host cell factor. J Biol Chem 277: 1645-1648, 2002.
104. Lin J, Wu H, Tarr PT, Zhang CY, Wu Z, Boss O, Michael LF, Puigserver P, Isotani E, Olson EN, Lowell BB, Bassel-Duby R, and Spiegelman BM. Transcriptional co-activator PGC-1 alpha drives the formation of slow-twitch muscle fibres. Nature 418: 797-801, 2002.
105. Lindholm ME, Fischer H, Poellinger L, Johnson RS, Gustafsson T, Sundberg CJ, and Rundqvist H. Negative regulation of HIF in skeletal muscle of elite endurance athletes: a tentative mechanism promoting oxidative metabolism. Am J Physiol Regul Integr Comp Physiol 307: R248-255, 2014.
106. Liu N, Williams AH, Kim Y, McAnally J, Bezprozvannaya S, Sutherland LB, Richardson JA, Bassel-Duby R, and Olson EN. An intragenic MEF2-dependent enhancer directs muscle-specific expression of microRNAs 1 and 133. Proc Natl Acad Sci U S A 104: 20844-20849, 2007.
107. Lu J, McKinsey TA, Zhang CL, and Olson EN. Regulation of skeletal myogenesis by association of the MEF2 transcription factor with class II histone deacetylases. Mol Cell 6: 233-244, 2000.
108. Lundby C, Calbet JA, and Robach P. The response of human skeletal muscle tissue to hypoxia. Cell Mol Life Sci 66: 3615-3623, 2009.
109. Lundby C, Gassmann M, and Pilegaard H. Regular endurance training reduces the exercise induced HIF-1alpha and HIF-2alpha mRNA expression in human skeletal muscle in normoxic conditions. Eur J Appl Physiol 96: 363-369, 2006.
110. Madapallimattam AG, Law L, and Jeejeebhoy KN. Effect of hypoenergetic feeding on muscle oxidative phosphorylation and mitochondrial complex I-IV activities in rats. Am J Clin Nutr 76: 1031-1039, 2002.
111. Mahoney DJ, Parise G, Melov S, Safdar A, and Tarnopolsky MA. Analysis of global mRNA expression in human skeletal muscle during recovery from endurance exercise. FASEB J 19: 1498-1500, 2005.
112. Maltais F, Decramer M, Casaburi R, Barreiro E, Burelle Y, Debigare R, Dekhuijzen PN, Franssen F, Gayan-Ramirez G, Gea J, Gosker HR, Gosselink R, Hayot M, Hussain SN, Janssens W, Polkey MI, Roca J, Saey D, Schols AM, Spruit MA, Steiner M, Taivassalo T, Troosters T, Vogiatzis I, Wagner PD, and COPD AEAHCoLMDi. An official American Thoracic Society/European Respiratory Society statement: update on limb muscle dysfunction in chronic obstructive pulmonary disease. Am J Respir Crit Care Med 189: e15-62, 2014.

113. Maltais F, LeBlanc P, Whittom F, Simard C, Marquis K, Belanger M, Breton MJ, and Jobin J. Oxidative enzyme activities of the vastus lateralis muscle and the functional status in patients with COPD. Thorax 55: 848-853, 2000.
114. Mannino DM, Thorn D, Swensen A, and Holguin F. Prevalence and outcomes of diabetes, hypertension and cardiovascular disease in COPD. Eur Respir J 32: 962-969, 2008.
115. Mannino DM, Watt G, Hole D, Gillis C, Hart C, McConnachie A, Davey Smith G, Upton M, Hawthorne V, Sin DD, Man SF, Van Eeden S, Mapel DW, and Vestbo J. The natural history of chronic obstructive pulmonary disease. Eur Respir J 27: 627-643, 2006.
116. Marquis K, Debigare R, Lacasse Y, LeBlanc P, Jobin J, Carrier G, and Maltais F. Midthigh muscle cross-sectional area is a better predictor of mortality than body mass index in patients with chronic obstructive pulmonary disease. Am J Respir Crit Care Med 166: 809-813, 2002.
117. Mason SD, Howlett RA, Kim MJ, Olfert IM, Hogan MC, McNulty W, Hickey RP, Wagner PD, Kahn CR, Giordano FJ, and Johnson RS. Loss of skeletal muscle HIF-1alpha results in altered exercise endurance. PLoS Biol 2: e288, 2004.
118. Mason SD, Rundqvist H, Papandreou I, Duh R, McNulty WJ, Howlett RA, Olfert IM, Sundberg CJ, Denko NC, Poellinger L, and Johnson RS. HIF-1alpha in endurance training: suppression of oxidative metabolism. Am J Physiol Regul Integr Comp Physiol 293: R2059-2069, 2007.
119. Masson N, Willam C, Maxwell PH, Pugh CW, and Ratcliffe PJ. Independent function of two destruction domains in hypoxia-inducible factor-alpha chains activated by prolyl hydroxylation. EMBO J 20: 5197-5206, 2001.
120. Mattson JP, and Poole DC. Pulmonary emphysema decreases hamster skeletal muscle oxidative enzyme capacity. J Appl Physiol (1985) 85: 210-214, 1998.
121. Mattson JP, Sun J, Murray DM, and Poole DC. Lipid peroxidation in the skeletal muscle of hamsters with emphysema. Pathophysiology 8: 215-221, 2002.
122. McCarthy JJ. MicroRNA-206: the skeletal muscle-specific myomiR. Biochim Biophys Acta 1779: 682-691, 2008.
123. McCarthy JJ, Esser KA, Peterson CA, and Dupont-Versteegden EE. Evidence of MyomiR network regulation of beta-myosin heavy chain gene expression during skeletal muscle atrophy. Physiol Genomics 39: 219-226, 2009.
124. Michael LF, Wu Z, Cheatham RB, Puigserver P, Adelmant G, Lehman JJ, Kelly DP, and Spiegelman BM. Restoration of insulin-sensitive glucose transporter (GLUT4) gene expression in muscle cells by the transcriptional coactivator PGC-1. Proc Natl Acad Sci U S A 98: 3820-3825, 2001.
125. Miller J, Edwards LD, Agusti A, Bakke P, Calverley PM, Celli B, Coxson HO, Crim C, Lomas DA, Miller BE, Rennard S, Silverman EK, Tal-Singer R, Vestbo J, Wouters E, Yates JC, Macnee W, and Evaluation of CLtIPSEI. Comorbidity, systemic inflammation and outcomes in the ECLIPSE cohort. Respir Med 107: 1376-1384, 2013.
126. Mitsui T, Azuma H, Nagasawa M, Iuchi T, Akaike M, Odomi M, and Matsumoto T. Chronic corticosteroid administration causes mitochondrial dysfunction in skeletal muscle. J Neurol 249: 1004-1009, 2002.
127. Mokhlesi B, Morris AL, Huang CF, Curcio AJ, Barrett TA, and Kamp DW. Increased prevalence of gastroesophageal reflux symptoms in patients with COPD. Chest 119: 1043-1048, 2001.
128. Mootha VK, Handschin C, Arlow D, Xie X, St Pierre J, Sihag S, Yang W, Altshuler D, Puigserver P, Patterson N, Willy PJ, Schulman IG, Heyman RA, Lander ES, and Spiegelman BM. Erralpha and Gabpa/b specify PGC-1alpha-dependent oxidative phosphorylation gene expression that is altered in diabetic muscle. Proc Natl Acad Sci U S A 101: 6570-6575, 2004.
129. Mulloy E, Fitzpatrick M, Bourke S, O'Regan A, and McNicholas WT. Oxygen desaturation during sleep and exercise in patients with severe chronic obstructive pulmonary disease. Respir Med 89: 193-198, 1995.
130. Murgia M, Serrano AL, Calabria E, Pallafacchina G, Lomo T, and Schiaffino S. Ras is involved in nerve-activity-dependent regulation of muscle genes. Nat Cell Biol 2: 142-147, 2000.
131. Murray CJ, and Lopez AD. Mortality by cause for eight regions of the world: Global Burden of Disease Study. Lancet 349: 1269-1276, 1997.
132. Naik D, Joshi A, Paul TV, and Thomas N. Chronic obstructive pulmonary disease and the metabolic syndrome: Consequences of a dual threat. Indian J Endocrinol Metab 18: 608-616, 2014.
133. Naimi AI, Bourbeau J, Perrault H, Baril J, Wright-Paradis C, Rossi A, Taivassalo T, Sheel AW, Rabol R, Dela F, and Boushel R. Altered mitochondrial regulation in quadriceps muscles of patients with COPD. Clin Physiol Funct Imaging 31: 124-131, 2011.
134. Narkar VA, Fan W, Downes M, Yu RT, Jonker JW, Alaynick WA, Banayo E, Karunasiri MS, Lorca S, and Evans RM. Exercise and PGC-1alpha-independent synchronization of type I muscle metabolism and vasculature by ERRgamma. Cell metabolism 13: 283-293, 2011.
135. Natanek SA, Gosker HR, Slot IG, Marsh GS, Hopkinson NS, Man WD, Tal-Singer R, Moxham J, Kemp PR, Schols AM, and Polkey MI. Heterogeneity of quadriceps muscle phenotype in chronic obstructive pulmonary disease (Copd); implications for stratified medicine? Muscle Nerve 48: 488-497, 2013.
136. Naya FJ, Mercer B, Shelton J, Richardson JA, Williams RS, and Olson EN. Stimulation of slow skeletal muscle fiber gene expression by calcineurin in vivo. J Biol Chem 275: 4545-4548, 2000.
137. Neal JW, and Clipstone NA. Glycogen synthase kinase-3 inhibits the DNA binding activity of NFATc. J Biol Chem 276: 3666-3673, 2001.
138. Nielsen J, Suetta C, Hvid LG, Schroder HD, Aagaard P, and Ortenblad N. Subcellular localization-dependent decrements in skeletal muscle glycogen and mitochondria content following short-term disuse in young and old men. Am J Physiol Endocrinol Metab 299: E1053-1060, 2010.
139. Nordsborg NB, Lundby C, Leick L, and Pilegaard H. Relative workload determines exercise-induced increases in PGC-1alpha mRNA. Med Sci Sports Exerc 42: 1477-1484, 2010.

140. Oberbach A, Bossenz Y, Lehmann S, Niebauer J, Adams V, Paschke R, Schon MR, Bluher M, and Punkt K. Altered fiber distribution and fiber-specific glycolytic and oxidative enzyme activity in skeletal muscle of patients with type 2 diabetes. Diabetes Care 29: 895-900, 2006.
141. Okamura H, Garcia-Rodriguez C, Martinson H, Qin J, Virshup DM, and Rao A. A conserved docking motif for CK1 binding controls the nuclear localization of NFAT1. Mol Cell Biol 24: 4184-4195, 2004.
142. Olson BL, Hock MB, Ekholm-Reed S, Wohlschlegel JA, Dev KK, Kralli A, and Reed SI. SCFCdc4 acts antagonistically to the PGC-1alpha transcriptional coactivator by targeting it for ubiquitin-mediated proteolysis. Genes Dev 22: 252-264, 2008.
143. Panos RJ, and Eschenbacher W. Exertional desaturation in patients with chronic obstructive pulmonary disease. Copd 6: 478-487, 2009.
144. Papandreou I, Cairns RA, Fontana L, Lim AL, and Denko NC. HIF-1 mediates adaptation to hypoxia by actively downregulating mitochondrial oxygen consumption. Cell metabolism 3: 187-197, 2006.
145. Payen JF, Wuyam B, Levy P, Reutenauer H, Stieglitz P, Paramelle B, and Le Bas JF. Muscular metabolism during oxygen supplementation in patients with chronic hypoxemia. Am Rev Respir Dis 147: 592-598, 1993.
146. Pilegaard H, Saltin B, and Neufer PD. Exercise induces transient transcriptional activation of the PGC-1alpha gene in human skeletal muscle. J Physiol 546: 851-858, 2003.
147. Pisani DF, and Dechesne CA. Skeletal muscle HIF-1alpha expression is dependent on muscle fiber type. J Gen Physiol 126: 173-178, 2005.
148. Pitta F, Troosters T, Spruit MA, Probst VS, Decramer M, and Gosselink R. Characteristics of physical activities in daily life in chronic obstructive pulmonary disease. Am J Respir Crit Care Med 171: 972-977, 2005.
149. Pogozelski AR, Geng T, Li P, Yin X, Lira VA, Zhang M, Chi JT, and Yan Z. p38gamma mitogen-activated protein kinase is a key regulator in skeletal muscle metabolic adaptation in mice. PLoS One 4: e7934, 2009.
150. Puente-Maestu L, Perez-Parra J, Godoy R, Moreno N, Tejedor A, Gonzalez-Aragoneses F, Bravo JL, Alvarez FV, Camano S, and Agusti A. Abnormal mitochondrial function in locomotor and respiratory muscles of COPD patients. Eur Respir J 33: 1045-1052, 2009.
151. Puente-Maestu L, Tejedor A, Lazaro A, de Miguel J, Alvarez-Sala L, Gonzalez-Aragoneses F, Simon C, and Agusti A. Site of mitochondrial reactive oxygen species production in skeletal muscle of chronic obstructive pulmonary disease and its relationship with exercise oxidative stress. Am J Respir Cell Mol Biol 47: 358-362, 2012.
152. Puigserver P, Adelmant G, Wu Z, Fan M, Xu J, O'Malley B, and Spiegelman BM. Activation of PPARgamma coactivator-1 through transcription factor docking. Science 286: 1368-1371, 1999.
153. Puigserver P, Rhee J, Lin J, Wu Z, Yoon JC, Zhang CY, Krauss S, Mootha VK, Lowell BB, and Spiegelman BM. Cytokine stimulation of energy expenditure through p38 MAP kinase activation of PPARgamma coactivator-1. Mol Cell 8: 971-982, 2001.
154. Puigserver P, Wu Z, Park CW, Graves R, Wright M, and Spiegelman BM. A cold-inducible coactivator of nuclear receptors linked to adaptive thermogenesis. Cell 92: 829-839, 1998.
155. Qaseem A, Wilt TJ, Weinberger SE, Hanania NA, Criner G, van der Molen T, Marciniuk DD, Denberg T, Schunemann H, Wedzicha W, MacDonald R, Shekelle P, American College of P, American College of Chest P, American Thoracic S, and European Respiratory S. Diagnosis and management of stable chronic obstructive pulmonary disease: a clinical practice guideline update from the American College of Physicians, American College of Chest Physicians, American Thoracic Society, and European Respiratory Society. Ann Intern Med 155: 179-191, 2011.
156. Rao PK, Kumar RM, Farkhondeh M, Baskerville S, and Lodish HF. Myogenic factors that regulate expression of muscle-specific microRNAs. Proc Natl Acad Sci U S A 103: 8721-8726, 2006.
157. Remels AH, Gosker HR, Bakker J, Guttridge DC, Schols AM, and Langen RC. Regulation of skeletal muscle oxidative phenotype by classical NF-kappaB signalling. Biochim Biophys Acta 1832: 1313-1325, 2013.
158. Remels AH, Gosker HR, Langen RC, and Schols AM. The mechanisms of cachexia underlying muscle dysfunction in COPD. J Appl Physiol (1985) 114: 1253-1262, 2013.
159. Remels AH, Gosker HR, Schrauwen P, Hommelberg PP, Sliwinski P, Polkey M, Galdiz J, Wouters EF, Langen RC, and Schols AM. TNF-alpha impairs regulation of muscle oxidative phenotype: implications for cachexia? FASEB J 24: 5052-5062, 2010.
160. Remels AH, Schrauwen P, Broekhuizen R, Willems J, Kersten S, Gosker HR, and Schols AM. Peroxisome proliferator-activated receptor expression is reduced in skeletal muscle in COPD. Eur Respir J 30: 245-252, 2007.
161. Richardson RS, Wagner H, Mudaliar SR, Saucedo E, Henry R, and Wagner PD. Exercise adaptation attenuates VEGF gene expression in human skeletal muscle. Am J Physiol Heart Circ Physiol 279: H772-778, 2000.
162. Roca M, Roca IC, and Mihaescu T. Lung cancer - a comorbidity in chronic obstructive pulmonary disease. Rev Med Chir Soc Med Nat Iasi 116: 1055-1062, 2012.
163. Rodgers JT, Lerin C, Haas W, Gygi SP, Spiegelman BM, and Puigserver P. Nutrient control of glucose homeostasis through a complex of PGC-1alpha and SIRT1. Nature 434: 113-118, 2005.
164. Saey D, Michaud A, Couillard A, Cote CH, Mador MJ, LeBlanc P, Jobin J, and Maltais F. Contractile fatigue, muscle morphometry, and blood lactate in chronic obstructive pulmonary disease. Am J Respir Crit Care Med 171: 1109-1115, 2005.
165. Safdar A, Abadi A, Akhtar M, Hettinga BP, and Tarnopolsky MA. miRNA in the regulation of skeletal muscle adaptation to acute endurance exercise in C57Bl/6J male mice. PLoS One 4: e5610, 2009.
166. Safdar A, Little JP, Stokl AJ, Hettinga BP, Akhtar M, and Tarnopolsky MA. Exercise increases mitochondrial PGC-1alpha content and promotes nuclear-mitochondrial cross-talk to coordinate mitochondrial biogenesis. J Biol Chem 286: 10605-

10617, 2011.
167. Salceda S, and Caro J. Hypoxia-inducible factor 1alpha (HIF-1alpha) protein is rapidly degraded by the ubiquitin-proteasome system under normoxic conditions. Its stabilization by hypoxia depends on redox-induced changes. J Biol Chem 272: 22642-22647, 1997.
168. Salvi SS, and Barnes PJ. Chronic obstructive pulmonary disease in non-smokers. Lancet 374: 733-743, 2009.
169. Sauleda J, Garcia-Palmer F, Wiesner RJ, Tarraga S, Harting I, Tomas P, Gomez C, Saus C, Palou A, and Agusti AG. Cytochrome oxidase activity and mitochondrial gene expression in skeletal muscle of patients with chronic obstructive pulmonary disease. Am J Respir Crit Care Med 157: 1413-1417, 1998.
170. Schiaffino S. Fibre types in skeletal muscle: a personal account. Acta Physiol (Oxf) 199: 451-463, 2010.
171. Schiaffino S, and Reggiani C. Molecular diversity of myofibrillar proteins: gene regulation and functional significance. Physiol Rev 76: 371-423, 1996.
172. Schols AM, Broekhuizen R, Weling-Scheepers CA, and Wouters EF. Body composition and mortality in chronic obstructive pulmonary disease. Am J Clin Nutr 82: 53-59, 2005.
173. Schreiber SN, Emter R, Hock MB, Knutti D, Cardenas J, Podvinec M, Oakeley EJ, and Kralli A. The estrogen-related receptor alpha (ERRalpha) functions in PPARgamma coactivator 1alpha (PGC-1alpha)-induced mitochondrial biogenesis. Proc Natl Acad Sci U S A 101: 6472-6477, 2004.
174. Seagroves TN, Ryan HE, Lu H, Wouters BG, Knapp M, Thibault P, Laderoute K, and Johnson RS. Transcription factor HIF-1 is a necessary mediator of the pasteur effect in mammalian cells. Mol Cell Biol 21: 3436-3444, 2001.
175. Semenza GL, Jiang BH, Leung SW, Passantino R, Concordet JP, Maire P, and Giallongo A. Hypoxia response elements in the aldolase A, enolase 1, and lactate dehydrogenase A gene promoters contain essential binding sites for hypoxia-inducible factor 1. J Biol Chem 271: 32529-32537, 1996.
176. Serrano AL, Murgia M, Pallafacchina G, Calabria E, Coniglio P, Lomo T, and Schiaffino S. Calcineurin controls nerve activity-dependent specification of slow skeletal muscle fibers but not muscle growth. Proc Natl Acad Sci U S A 98: 13108-13113, 2001.
177. Simoneau JA, and Kelley DE. Altered glycolytic and oxidative capacities of skeletal muscle contribute to insulin resistance in NIDDM. J Appl Physiol (1985) 83: 166-171, 1997.
178. Smerdu V, Karsch-Mizrachi I, Campione M, Leinwand L, and Schiaffino S. Type IIx myosin heavy chain transcripts are expressed in type IIb fibers of human skeletal muscle. Am J Physiol 267: C1723-1728, 1994.
179. Sripada L, Tomar D, Prajapati P, Singh R, Singh AK, and Singh R. Systematic analysis of small RNAs associated with human mitochondria by deep sequencing: detailed analysis of mitochondrial associated miRNA. PLoS One 7: e44873, 2012.
180. Stolz D, Boersma W, Blasi F, Louis R, Milenkovic B, Kostikas K, Aerts JG, Rohde G, Lacoma A, Rakic J, Boeck L, Castellotti P, Scherr A, Marin A, Hertel S, Giersdorf S, Torres A, Welte T, and Tamm M. Exertional hypoxemia in stable COPD is common and predicted by circulating proadrenomedullin. Chest 146: 328-338, 2014.
181. Stroka DM, Burkhardt T, Desbaillets I, Wenger RH, Neil DA, Bauer C, Gassmann M, and Candinas D. HIF-1 is expressed in normoxic tissue and displays an organ-specific regulation under systemic hypoxia. FASEB J 15: 2445-2453, 2001.
182. Suwa M, Nakano H, and Kumagai S. Effects of chronic AICAR treatment on fiber composition, enzyme activity, UCP3, and PGC-1 in rat muscles. J Appl Physiol (1985) 95: 960-968, 2003.
183. Swallow EB, Reyes D, Hopkinson NS, Man WD, Porcher R, Cetti EJ, Moore AJ, Moxham J, and Polkey MI. Quadriceps strength predicts mortality in patients with moderate to severe chronic obstructive pulmonary disease. Thorax 62: 115-120, 2007.
184. Talmadge RJ, Otis JS, Rittler MR, Garcia ND, Spencer SR, Lees SJ, and Naya FJ. Calcineurin activation influences muscle phenotype in a muscle-specific fashion. BMC Cell Biol 5: 28, 2004.
185. Teyssier C, Ma H, Emter R, Kralli A, and Stallcup MR. Activation of nuclear receptor coactivator PGC-1alpha by arginine methylation. Genes Dev 19: 1466-1473, 2005.
186. Tobina T, Yoshioka K, Hirata A, Mori S, Kiyonaga A, and Tanaka H. Peroxisomal proliferator-activated receptor gamma co-activator-1 alpha gene expression increases above the lactate threshold in human skeletal muscle. J Sports Med Phys Fitness 51: 683-688, 2011.
187. Turan N, Kalko S, Stincone A, Clarke K, Sabah A, Howlett K, Curnow SJ, Rodriguez DA, Cascante M, O'Neill L, Egginton S, Roca J, and Falciani F. A systems biology approach identifies molecular networks defining skeletal muscle abnormalities in chronic obstructive pulmonary disease. PLoS Comput Biol 7: e1002129, 2011.
188. U.S. Department of Health and Human Services. The Health Consequences of Smoking—50 Years of Progress: A Report of the Surgeon General Atlanta, GA: U.S. Department of Health and Human Services, Centers for Disease Control and Prevention, National Center for Chronic Disease Prevention and Health Promotion, Office on Smoking and Health, 2014.
189. U.S. Department of Health and Human Services. Surgeon General's Report—The Health Consequences of Smoking Atlanta, GA: U.S. Department of Health and Human Services, Centers for Disease Control and Prevention, National Center for Chronic Disease Prevention and Health Promotion, Office on Smoking and Health, 2004.
190. van den Borst B, Gosker HR, and Schols AM. Central fat and peripheral muscle: partners in crime in chronic obstructive pulmonary disease. Am J Respir Crit Care Med 187: 8-13, 2013.
191. van Rooij E, Quiat D, Johnson BA, Sutherland LB, Qi X, Richardson JA, Kelm RJ, Jr., and Olson EN. A family of microRNAs encoded by myosin genes governs myosin expression and muscle performance. Dev Cell 17: 662-673, 2009.
192. Vanfleteren LE, Franssen FM, Wesseling G, and Wouters EF. The prevalence of chronic obstructive pulmonary disease in Maastricht, the Netherlands. Respir Med 106: 871-874, 2012.
193. Vega RB, Huss JM, and Kelly DP. The coactivator PGC-1 cooperates with peroxisome proliferator-activated receptor alpha

in transcriptional control of nuclear genes encoding mitochondrial fatty acid oxidation enzymes. Mol Cell Biol 20: 1868-1876, 2000.
194. Virbasius JV, and Scarpulla RC. Activation of the human mitochondrial transcription factor A gene by nuclear respiratory factors: a potential regulatory link between nuclear and mitochondrial gene expression in organelle biogenesis. Proc Natl Acad Sci U S A 91: 1309-1313, 1994.
195. Wang GL, Jiang BH, Rue EA, and Semenza GL. Hypoxia-inducible factor 1 is a basic-helix-loop-helix-PAS heterodimer regulated by cellular O2 tension. Proc Natl Acad Sci U S A 92: 5510-5514, 1995.
196. Wang GL, and Semenza GL. Purification and characterization of hypoxia-inducible factor 1. J Biol Chem 270: 1230-1237, 1995.
197. Wang YX, Zhang CL, Yu RT, Cho HK, Nelson MC, Bayuga-Ocampo CR, Ham J, Kang H, and Evans RM. Regulation of muscle fiber type and running endurance by PPARdelta. PLoS Biol 2: e294, 2004.
198. Wheaton WW, and Chandel NS. Hypoxia. 2. Hypoxia regulates cellular metabolism. Am J Physiol Cell Physiol 300: C385-393, 2011.
199. Wilfred BR, Wang WX, and Nelson PT. Energizing miRNA research: a review of the role of miRNAs in lipid metabolism, with a prediction that miR-103/107 regulates human metabolic pathways. Mol Genet Metab 91: 209-217, 2007.
200. Williams RS. Mitochondrial gene expression in mammalian striated muscle. Evidence that variation in gene dosage is the major regulatory event. J Biol Chem 261: 12390-12394, 1986.
201. World Health Organization. Burden of COPD http://www.who.int/respiratory/copd/burden/en/. [14 July, 2014].
202. World Health Organization. Causes of COPD http://www.who.int/respiratory/copd/causes/en/. [14 July, 2014].
203. World Health Organization. Diagnosis of COPD http://www.who.int/respiratory/copd/diagnosis/en/. [14 July, 2014].
204. Wu H, Kanatous SB, Thurmond FA, Gallardo T, Isotani E, Bassel-Duby R, and Williams RS. Regulation of mitochondrial biogenesis in skeletal muscle by CaMK. Science 296: 349-352, 2002.
205. Wu H, Rothermel B, Kanatous S, Rosenberg P, Naya FJ, Shelton JM, Hutcheson KA, DiMaio JM, Olson EN, Bassel-Duby R, and Williams RS. Activation of MEF2 by muscle activity is mediated through a calcineurin-dependent pathway. EMBO J 20: 6414-6423, 2001.
206. Wu Z, Puigserver P, Andersson U, Zhang C, Adelmant G, Mootha V, Troy A, Cinti S, Lowell B, Scarpulla RC, and Spiegelman BM. Mechanisms controlling mitochondrial biogenesis and respiration through the thermogenic coactivator PGC-1. Cell 98: 115-124, 1999.
207. Wust RC, and Degens H. Factors contributing to muscle wasting and dysfunction in COPD patients. Int J Chron Obstruct Pulmon Dis 2: 289-300, 2007.
208. Wuyam B, Payen JF, Levy P, Bensaidane H, Reutenauer H, Le Bas JF, and Benabid AL. Metabolism and aerobic capacity of skeletal muscle in chronic respiratory failure related to chronic obstructive pulmonary disease. Eur Respir J 5: 157-162, 1992.
209. Yang X, Downes M, Yu RT, Bookout AL, He W, Straume M, Mangelsdorf DJ, and Evans RM. Nuclear receptor expression links the circadian clock to metabolism. Cell 126: 801-810, 2006.
210. Zechner C, Lai L, Zechner JF, Geng T, Yan Z, Rumsey JW, Collia D, Chen Z, Wozniak DF, Leone TC, and Kelly DP. Total skeletal muscle PGC-1 deficiency uncouples mitochondrial derangements from fiber type determination and insulin sensitivity. Cell metabolism 12: 633-642, 2010.
211. Zhang H, Bosch-Marce M, Shimoda LA, Tan YS, Baek JH, Wesley JB, Gonzalez FJ, and Semenza GL. Mitochondrial autophagy is an HIF-1-dependent adaptive metabolic response to hypoxia. J Biol Chem 283: 10892-10903, 2008.
212. Zhang X, Zuo X, Yang B, Li Z, Xue Y, Zhou Y, Huang J, Zhao X, Zhou J, Yan Y, Zhang H, Guo P, Sun H, Guo L, Zhang Y, and Fu XD. MicroRNA directly enhances mitochondrial translation during muscle differentiation. Cell 158: 607-619, 2014.
213. Zhang Y, Liu D, Chen X, Li J, Li L, Bian Z, Sun F, Lu J, Yin Y, Cai X, Sun Q, Wang K, Ba Y, Wang Q, Wang D, Yang J, Liu P, Xu T, Yan Q, Zhang J, Zen K, and Zhang CY. Secreted monocytic miR-150 enhances targeted endothelial cell migration. Mol Cell 39: 133-144, 2010.
214. Zhang Y, Ma K, Song S, Elam MB, Cook GA, and Park EA. Peroxisomal proliferator-activated receptor-gamma coactivator-1 alpha (PGC-1 alpha) enhances the thyroid hormone induction of carnitine palmitoyltransferase I (CPT-I alpha). J Biol Chem 279: 53963-53971, 2004.
215. Zhao M, New L, Kravchenko VV, Kato Y, Gram H, di Padova F, Olson EN, Ulevitch RJ, and Han J. Regulation of the MEF2 family of transcription factors by p38. Mol Cell Biol 19: 21-30, 1999.
216. Zhu J, Shibasaki F, Price R, Guillemot JC, Yano T, Dotsch V, Wagner G, Ferrara P, and McKeon F. Intramolecular masking of nuclear import signal on NF-AT4 by casein kinase I and MEKK1. Cell 93: 851-861, 1998.

Chapter 2

Hypoxia differentially regulates muscle oxidative fiber type and metabolism in a HIF-1α-dependent manner

Ilse G.M. Slot, Annemie M.W.J. Schols, Bettine A.H. Vosse, Marco C.J.M. Kelders, Harry R. Gosker

Cellular Signalling, 2014. 26(9): p. 1837-45

ABSTRACT

Loss of skeletal muscle oxidative fiber types and mitochondrial capacity is a hallmark of chronic obstructive pulmonary disease and chronic heart failure. Based on *in vivo* human and animal studies, tissue hypoxia has been hypothesized as determinant, but the direct effect of hypoxia on muscle oxidative phenotype remains to be established. Hence, we determined the effect of hypoxia on *in vitro* cultured muscle cells, including gene and protein expression levels of mitochondrial components, myosin isoforms (reflecting slow-oxidative *versus* fast-glycolytic fibers), and the involvement of the regulatory PPAR/PGC-1α pathway. We found that hypoxia inhibits the PPAR/PGC-1α pathway and the expression of mitochondrial components through HIF-1α. However, in contrast to our hypothesis, hypoxia stimulated the expression of slow-oxidative type I myosin via HIF-1α. Collectively, this study shows that hypoxia differentially regulates contractile and metabolic components of muscle oxidative phenotype in a HIF-1α-dependent manner.

INTRODUCTION

Hypoxia has been implicated in skeletal muscle metabolic impairments in chronic diseases such as chronic obstructive pulmonary disease (COPD) and chronic heart failure (CHF) (9, 13, 21, 43). Although it is generally known that hypoxia is involved in the stimulation of glycolytic metabolism through among others the hypoxia-inducible factor 1 (HIF-1) (48), a direct role for hypoxia in the downregulation of oxidative metabolism is less firmly established. Skeletal muscle of patients with COPD or CHF is characterized by an impaired oxidative phenotype, including reduced oxidative enzyme activities and a shift from oxidative to glycolytic fiber types (13) and (12). Hypoxia has been suggested to be involved in this downregulation of muscle oxidative phenotype (13). However, studies involving humans as well as experimental animal models resulted in inconsistent findings; *i.e.* loss of, unchanged or even improved muscle oxidative phenotype has been shown (1, 4, 5, 8, 10, 14, 18, 20, 40-42). These inconsistencies are inherent to the *in vivo* nature of these studies in which any direct effect of hypoxia probably was confounded by indirect effects, such as hypoxia-induced changes in food intake, physical activity or circulating hormone levels. Moreover, mountain expeditions were frequently seized to study muscular adaptations to hypoxia in humans, thereby however certainly introducing strenuous exercise as a confounding factor, as well as disturbance of the sleep cycle, cold temperatures and the anorexic effect of altitude (16-18).

In response to cellular hypoxia, cells are forced to limit oxygen consumption and to shift from mitochondrial respiration to glycolysis for ATP production (29). Hypoxia-inducible factor (HIF) protein, the master regulator of the hypoxic response, is stabilized under hypoxic conditions and directly involved in the upregulation of several glycolytic enzymes to stimulate glycolytic metabolism (22). Also, overexpression of HIF-1α has been linked to a fast muscle fiber type (26). It is however unclear whether hypoxia can reciprocally inhibit oxidative phenotype in muscle, although it has been shown that HIF-1α knockout mice indeed demonstrate a modestly improved activity of oxidative enzymes (27).

Master regulators of oxidative phenotype are the peroxisome proliferator-activated receptors (PPARs) and specifically the PPARγ coactivator-1 family (PGC-1s) (3, 49). PGC-1s coactivate not only PPARs, but also estrogen-related receptors (ERRs) and nuclear respiratory factors (NRFs), to stimulate mitochondrial biogenesis and oxidative capacity (28, 36). Decreased expression levels of PPARs and PGC-1α have indeed been shown in skeletal muscle of COPD patients (34) and rats with CHF (46), suggesting potential involvement of these factors in the loss of oxidative capacity.

In this study, we investigated the direct effect of hypoxia on oxidative phenotype in an *in vitro* model of muscle fibers (myotubes) and the role of HIF-1α herein. We hypothesized that hypoxia impairs muscle oxidative phenotype in a HIF-1α-dependent manner by downregulating the PPAR/PGC-1α pathway, either through direct targeting of the PPARs or by influencing expression or activity of PPAR co-regulators.

MATERIALS AND METHODS

Chemicals, reagents and materials

All reagents used were analytical grade. Tricine, glycine, sodium chloride (NaCl), potassium chloride (KCl), disodium hydrogen phosphate (Na_2HPO_4), monopotassium phosphate (KH_2PO_4), magnesium sulfate ($MgSO_4$), magnesium carbonate ($[MgCO_3]_4Mg[OH]_2 \bullet 5H_2O$) and cobalt chloride ($CoCl_2$) were obtained from Merck (Roden, The Netherlands). Tris, methanol, ethylenediaminetetraacetic acid (EDTA), sodium dodecyl sulfate (SDS), glycerol, nonidet P40, sodium orthovanadate (Na_3VO_4), dithiothreitol (DTT), phenylmethylsulfonyl fluoride (PMSF), leupeptin, aprotinin, bromophenol blue, coenzyme A, dimethyl sulfoxide (DMSO), and bovine serum albumin (BSA) were from Sigma (Zwijndrecht, The Netherlands). ATP was purchased from Roche (Woerden, The Netherlands) and GW-501516 from Alexis Biochemicals (Lausen, Switzerland).

Cell culture flasks and stripettes were from Corning Life Sciences BV (Schiphol-Rijk, The Netherlands) and culture dishes from BD Falcon (Breda, The Netherlands). Fetal bovine serum (FBS), penicillin/streptomycin and Hank's Buffered Salt Solution (HBSS; calcium-, magnesium- and phenol red-free) were from PAA Laboratories (Pasching, Germany). Dulbecco's Modified Eagle's Medium (DMEM) was purchased from Invitrogen (Breda, The Netherlands) and Matrigel from BD Biosciences (San Jose, CA, USA). TNF-α was obtained from Calbiochem (Nottingham, United Kingdom) and dissolved in 0.1% BSA. Reporter Lysis 5× Buffer and beetle luciferin potassium salt for luciferase reporter assays were from Promega (Leiden, The Netherlands).

Cell culture

The *in vitro* model for assessing the effect of hypoxia on muscle consisted of myotubes that were exposed for some hours up to several days to hypoxic conditions. Murine skeletal muscle C2C12 cells were obtained from the American Tissue Culture Collection (ATCC, no. CRL-1772; Manassas, VA, USA). Myocytes were cultured in growth medium consisting of low glucose DMEM, 9% (v/v) FBS, 45 U/ml penicillin and 45 µg/ml streptomycin in a 37 °C incubator with 5% CO_2. Cells were seeded on Matrigel-coated 35-mm dishes at a density of $4 \cdot 10^4$ cells/cm^2 and grown to ± 80% confluency after which differentiation was induced by two washes with HBSS and addition of differentiation medium (DMEM, 1% [v/v] heat-inactivated FBS [30 min at 56 °C], 50 U/ml penicillin and 50 µg/ml streptomycin). After 5 days myotubes were fully differentiated and used for the actual experiments. For hypoxic conditions, myotubes were placed in a hypoxic incubator with 4% O_2, 5% CO_2 and 91% N_2 for 24 h up to 3 days, depending on the type of experiment.

Luciferase reporter assays

To assess the effect of hypoxia on the transcriptional activity of HIF, PPAR and NF-κB transcription factors, C2C12 cells were stably transfected with luciferase reporter plasmids sensitive to HIF (HIF reporter), PPAR (PPAR reporter) or NF-κB (NF-κB reporter), respectively. The HIF reporter expresses the luciferase gene controlled by a promoter bearing five consecutive hypoxia-inducible factor (HIF) responsive elements (HREs) from the human vascular endothelial growth factor A (VEGFA) promoter (5HRE/hCMVmp-luc (39)) and was kindly provided by Dr. Twan van den Beucken (Maastricht University, The

Netherlands). As a positive control, HIF-1α was stabilized under normoxic conditions by adding $CoCl_2$ to a final concentration of 150 µM. The PPAR reporter promoter contains the peroxisome proliferator-activated receptor (PPAR)-responsive element from the human carnitine palmitoyltransferase 1B promoter (MCPT.Luc.1025 (6)) and was a gift from Dr. Marc van Bilsen (Maastricht University). The NF-κB reporter plasmid holds three repeats of the human immunodeficiency virus type 1 (HIV-1) tandem NF-κB sites in front of a minimal thymidine kinase (TK) promoter (6× κB-tk Luc (35)) and was kindly provided by Dr. Patrick Baeuerle (Micromet, Germany). As a positive control, NF-κB transcriptional activity was stimulated by adding TNF-α to selected dishes at 10 ng/ml. BSA was added to dishes to a final concentration of 0.005% as a vehicle control for the TNF-α treated dishes.

To assess treatment-associated expression of luciferase, myotubes were harvested by washing twice with cold phosphate-buffered saline (PBS; 137 mM NaCl, 2.7 mM KCl, 10.1 mM Na_2HPO_4, 1.8 mM KH_2PO_4, pH 7.4) and lysis in Reporter Lysis 5× Buffer by scraping with a rubber policeman and freezing at −80 °C. After thawing, insoluble material was spun down in 2 min at 20000 × *g* and the soluble fraction was used for luciferase activity assay. Samples were analyzed on a single-tube luminometer with injector (LB9507, Berthold Technologies, Bad Wildbad, Germany) to add Luciferase Assay Reagent (20 mM Tricine, 1.07 mM $[(MgCO_3)_4Mg(OH)_2 \bullet 5H_2O]$, 2.67 mM $MgSO_4$, 0.1 mM EDTA, 33.3 mM DTT, 270 µM coenzyme A, 470 µM beetle luciferin potassium salt and 580 µM ATP, pH 7.8) to the sample. Luciferase activities were expressed relative to protein concentration in the soluble fraction as measured by Bio-Rad Protein Assay (Bio-Rad, Veenendaal, The Netherlands) in a microtiter plate according to the manufacturer's protocol.

RNA extraction and qRT-PCR analysis

RNA was extracted using the RNeasy Plus Mini Kit (Qiagen, Venlo, The Netherlands) with gDNA eliminator spin columns to remove genomic DNA according to the manufacturer's protocol. After elution, RNA concentration was determined using a spectrophotometer (NanoDrop ND-1000, Isogen Lifescience, IJsselstein, The Netherlands) and integrity verified for a selection of samples by gel electrophoresis.

400 ng RNA was reverse transcribed to cDNA with a mix of anchored oligo(dT) and random hexamer primers according to the supplier's protocol (Transcriptor First Strand cDNA Synthesis kit, Roche Diagnostics, Woerden, The Netherlands). Quantitative reverse-transcription PCR (qRT-PCR) primers were based on Ensembl (11) transcript sequences and designed intron-spanning if possible. Primers were ordered from Sigma Genosys (Zwijndrecht, The Netherlands) (Table 1 and Table 2). For relative quantification, standard curves were prepared from pooled neat cDNA aliquots of all samples by five serial five-fold dilutions. cDNA samples were diluted 1/50 and for both standards and samples, 5 µl diluted cDNA was loaded in a Hard-Shell Full-Height 96-Well Semi-Skirted PCR Plate (Bio-Rad) covered with Microseal 'B' adhesive seals (Bio-Rad). cDNA was amplified with SensiMix SYBR & Fluorescein Kit (Quantace-Bioline, London, UK) supplemented with 300 nM primers on a Bio-Rad MyiQ thermocycler (Bio-Rad). Two-step PCR was performed with the following cycling conditions: 10 min at 95 °C, 40 cycles of 10 s at 95 °C and 15 s at 60 °C and then 30 s at 95 °C and 30 s at 60 °C, followed by a melting curve (heating from 60 °C to 95 °C with 10 s per 0.5 °C increase). Standard curves and melt curves were

analyzed to verify efficiency and specificity of amplification. Five reference genes (*Axin1*, *B2m*, *Canx*, *Ppia* and *Rplp0*) were measured and stability of expression was assessed by visual inspection of expression differences between the study conditions and a stability assessment by geNorm (45). Stable genes were included to calculate a normalization factor to normalize expression levels of the other measured target genes.

Western blot analysis

Cells were washed twice with ice-cold PBS followed by 10 min incubation in lysis buffer (20 mM Tris, 150 mM NaCl, 1% (v/v) nonidet P40, 1 mM DTT, 1 mM Na_3VO_4, 1 mM PMSF, 10 µg/ml leupeptin, 1% (v/v) aprotinin, pH 7.4) on ice. Cells were scraped with rubber policemen and lysates were incubated for 30 min on a rotating wheel at 4 °C. Insoluble contents were precipitated during 30 min centrifugation at 20000 × *g* at 4 °C. A small volume of soluble fraction was kept for protein assay and the rest diluted in 4× sample buffer (0.25 M Tris, 8% (w/v) SDS, 40% glycerol, 0.4 M DTT, 0.02% bromophenol blue, pH 6.8) and boiled for 5 min at 95 °C. Per sample, 20 µg protein was separated on gel (4–12% Bis-Tris XT gel, Criterion, Bio-Rad) with XT MOPS running buffer (Bio-Rad). Proteins were transferred to a 0.45 µm nitrocellulose membrane (Protran, Schleicher and Schuell, 's-Hertogenbosch, The Netherlands) in transfer buffer (25 mM Tris, 192 mM glycine, 20% (v/v) methanol) by electrophoresis for 3 h at 30 mA and 4 °C. After transfer, membranes were blocked from nonspecific protein binding with 5% non-fat dry milk (Campina, Eindhoven, The Netherlands) in Tris-buffered saline (TBS; 25 mM Tris, 137 mM NaCl, 2.7 mM KCl, pH 7.4) with 0.05% Tween 20 (TBST) in 1 h at room temperature, followed by incubation in primary antibody overnight at 4 °C (mouse anti-myosin slow (M8421, Sigma), mouse anti-myosin fast (M4276, Sigma), mouse anti-Total OXPHOS Rodent WB Antibody Cocktail (MS604-300, MitoSciences, Eugene, OR, USA), rabbit anti-GAPDH (#2118, Cell Signaling Technology, Beverly, MA, USA), or mouse anti-α-tubulin (T6074, Sigma) diluted in 5% BSA (Sigma) in TBST). Membranes were incubated in secondary antibody solutions (peroxidase-labeled horse anti-mouse IgG [Vector Laboratories, Burlingame, CA, USA] in 5% non-fat dry milk in TBST) during 3 h at room temperature before incubation with enhanced chemiluminescence substrate (Pierce SuperSignal West PICO Chemiluminescent Substrate; Thermo Fisher Scientific, Breda, The Netherlands). Protein bands were detected using Super RX films (Fujifilm, Düsseldorf, Germany) and scanned on a GS-800 densitometer (Bio-Rad). Bands were quantified using Quantity One software (v4.6.2, Bio-Rad), with GAPDH or α-tubulin as loading control. Equal GAPDH or α-tubulin content in normoxic compared to hypoxic samples was verified before correction of the other protein targets.

Transient knockdown of HIF-1α gene expression

To study the role of HIF-1α in the response of oxidative capacity to hypoxia, the gene expression of HIF-1α was knocked down by RNA interference. Four-day old myotubes were transfected with Stealth RNAi siRNA for HIF-1α (MSS205126, Invitrogen) or Stealth RNAi Negative Control LO GC (Invitrogen) using Lipofectamine™ RNAiMAX (Invitrogen) and returned to the normoxic incubator. The next day, myotubes were exposed to hypoxia, or kept in normoxia. Medium was replaced 48 h after transfection and cells were harvested 24 h later.

Table 1 | qRT-PCR primer details for reference genes

Symbol	Name	Ensembl ID	Forward primer (5'→3')	Reverse primer (5'→3')	Amplicon size (bp)
Axin1	Axin 1	ENSMUSG00000024182	AGTGGATCATTGAGGGAGAGA	GCCCCAGGACGCTCGAT	124
B2m	Beta-2-microglobulin	ENSMUSG00000060802	CTTTCTGGTGCTTGTCTCACTGA	GTATGTTCGGCTTCCCATTCTC	104
Canx	Calnexin	ENSMUSG00000020368	GCAGCGACCTATGATTGACAACC	GCTCCAAACCAATAGCACTGAAAGG	170
Ppia	Peptidyl-prolyl cis–trans isomerase A; Cyclophilin A	ENSMUSG00000071866	TTCCTCCTTTCACAGAATTATTCCA	CCGCCAGTGCCATTATGG	75
Rplp0	Large ribosomal protein P0	ENSMUSG00000067274	GGACCCGAGAAGACCTCCTT	GCACATCACTCAGAATTTCAATGG	85

Transient overexpression of PPAR/PGC-1α protein

To disentangle through which molecule hypoxia exerts its effect on PPAR transcriptional activity, myoblasts were transiently transfected with expression plasmids encoding PPARα, PPARδ and PGC-1α protein, which were kindly provided by Dr. Marc van Bilsen (Maastricht University). Stimulation of PPAR transcriptional activity by these expression plasmids has previously been shown in C2C12 myoblasts (32). Myoblasts were plated at a density of 30% and allowed to attach overnight. The next day, the cells were transfected with plasmids encoding murine PPARα (mPPARα), PGC-1α (mPGC1α) or rat PPARδ (rPPARδ) or empty vector (pcDNA3.1+, Invitrogen) combined with a vector expressing β-gal using PfU Nanofectin (PAA Laboratories). For luciferase assays, the PPAR reporter plasmid was cotransfected. After a two-hour incubation period, growth medium was replaced and dishes were replaced to the hypoxic incubator or kept in normoxia. Cells were harvested 24 h later. Luciferase activities were corrected for β-gal activity to control for differences in transfection efficiencies.

Statistical analyses

Data were analyzed using IBM SPSS Statistics 21.0 (IBM Corp., Armonk, NY). Differences between samples exposed to hypoxia or $CoCl_2$ and those exposed to normoxia were tested using the Mann–Whitney test. Data are presented by mean + SD. A two-tailed *p*-value < 0.05 was considered statistically significant.

Table 2 | qRT-PCR primer details for genes of interest

Symbol	Name	Ensembl ID	Forward primer (5'→3')	Reverse primer (5'→3')	Amplicon size (bp)
Cox5a	Cytochrome c oxidase subunit Va	ENSMUSG00000000088	TGCGAGCATGTAGACCGTTAAAT	GAGGTCCTGCTTTGTCCTTAACA	77
Cyc1	Cytochrome c-1	ENSMUSG00000022551	GCATTCGGAGGGGTTTCCAG	CCGCATGAACATCTCCCCA	176
Esrra	Estrogen-related receptor alpha	ENSMUSG00000024955	GGCGGACGGCAGAAGTACAAA	GCGACACCAGAGCGTTCAC	130
Gabpa	GA binding protein alpha; nuclear respiratory factor 2 alpha	ENSMUSG00000008976	TGCTGCACTGGAAGGCTACA	TTACCCAAACCACCCAATGC	104
HIF-1a	Hypoxia inducible factor 1 alpha	ENSMUSG00000021109	AATGAAGTGCACCCTAACAAGCCG	TGGCCCGTGCAGTGAAGC	81
Hk2	Hexokinase II	ENSMUSG00000000628	AACCTCAAAGTGACGGTGGGC	AAGGACACGTCACATTTCGGAGC	113
Hmox1	Heme oxygenase 1	ENSMUSG00000005413	AAGCCGAGAATGCTGAGTTCATGA	GGCCGTGTAGATATGGTACAAGGAAG	101
Myh1	Myosin heavy chain 1 (type IIx isoform)	ENSMUSG00000056328	GACAAACTGCAATCAAAGG	TTGGTCACTTTCCTGCACTT	231
Myh2	Myosin heavy chain 2 (type IIa isoform)	ENSMUSG00000033196	CGATGATCTTGCCAGTAATG	ATAACTGAGATACCAGCG	221
Myh4	Myosin heavy chain 4 (type IIb isoform)	ENSMUSG00000057003	AGGGCGGCGGTGGAA	TGGGAATGAGGCATCTGACAA	141
Myh7	Myosin heavy chain 7 (type I isoform)	ENSMUSG00000053093	CAGATCGGGAGAATCAGTCCAT	AGCAAAATATTGGATGACCCTCTTA	89
Ndufb5	NADH dehydrogenase (ubiquinone) 1 beta subcomplex 5	ENSMUSG00000027673	CATCCCTGAACACTGGGAGTA	CCTTTAACCGTAACTCAGCCTTT	143
Nrf1	Nuclear respiratory factor 1	ENSMUSG00000058440	AGCCACATTGGCTGATGCTT	GGTCATTTCACCGCCCTGTA	124

Table 2 (continued) | qRT-PCR primer details for genes of interest

Symbol	Name	Ensembl ID	Forward primer (5'→3')	Reverse primer (5'→3')	Amplicon size (bp)
Ppara	Peroxisome proliferator-activated receptor alpha	ENSMUSG00000022383	ACTACGGAGTTCACGCATGTG	TTGTCGTACACCAGCTTCAGC	76
Ppard	Peroxisome proliferator-activated receptor delta	ENSMUSG00000002250	AGGCCCGGAGCATCCTCA	TGGATGACAAAGGGTGCGTTG	55
Ppargc1a	Peroxisome proliferator-activated receptor gamma coactivator 1 alpha	ENSMUSG00000029167	CAACAATGAGCCTGCGAACA	CTTCATCCACGGGGAGACTG	104
Ppargc1b	Peroxisome proliferator-activated receptor gamma coactivator 1 beta	ENSMUSG00000033871	ACCCTGAGAAAGCGCAATGA	CCCAGATGAGGGAAGGGACT	120
Sdhb	Succinate dehydrogenase complex, subunit B	ENSMUSG00000009863	AATTTGCCATTTACCGATGGGA	AGCATCCAACACCATAGGTCC	104
Slc2a1	Glucose transporter (GLUT) 1	ENSMUSG00000028645	TGACCATCGCCCTGGCCT	GGACCAGGGCCTACTTCAAAGAAG	103
Tfam	Mitochondrial transcription factor A	ENSMUSG00000003923	CCGGCAGAGACGGTTAAAAA	TCATCCTTTGCCTCCTGGAA	129
Vegfa	Vascular endothelial growth factor A	ENSMUSG00000023951	CTGTACCTCCACCATGCCAAGT	TCGCTGGTAGACATCCATGAACT	99

RESULTS

Hypoxia impairs muscle oxidative capacity and the regulatory PPAR/PGC-1α pathway

To study the effect of hypoxia on the markers of oxidative capacity, myotubes were exposed to hypoxia (4% O_2) for three days. This resulted in significantly decreased protein content of the oxidative phosphorylation (OXPHOS) complex III and V subunits (Figure 1A). Reduced OXPHOS protein content was associated with lower gene expression levels of OXPHOS subunits from complexes I to IV (Figure 1B). At the same time, gene expression of the glycolytic enzyme hexokinase-II was significantly increased by hypoxia.

To investigate how regulators of mitochondrial biogenesis and oxidative phenotype are affected by hypoxia, we measured the gene expression levels of PPARα, PPARδ, PGC-1α, PGC-1β, Tfam, ERRα, NRF-1 and NRF-2α. In response to hypoxia, the gene expression levels of PPARα, PPARδ, PGC-1α, PGC-1β and ERRα were markedly decreased. Levels of NRF-1 and NRF-2α were increased, whereas Tfam expression levels were unchanged (Figure 1C). It is worth mentioning that the expression of Tfam was significantly decreased after 24 h exposure to hypoxia, indicating that hypoxia reduced Tfam gene expression in a more transient fashion. As a functional signaling outcome measure, we assessed PPAR transcriptional activity using the PPAR luciferase reporter cell line and found it to be substantially decreased by hypoxia (Figure 1D). Hypoxia-induced increased PPARγ expression (data not shown) suggests that the reduced PPAR transcriptional activity probably reflects decreased PPARα or PPARδ activity.

Hypoxia shifts muscle towards oxidative fiber-type I profile

To assess whether exposure to hypoxia induces a shift from oxidative towards a more glycolytic fiber-type profile, we determined the protein content and mRNA levels of the respective myosin heavy chain (MyHC) isoforms in myotubes exposed to 4% oxygen for three days. Protein content of the slow oxidative type I MyHC isoform was markedly increased, while content of fast isoforms was reduced under hypoxic conditions (Figure 2A). mRNA levels of oxidative type I and type IIa MyHC were significantly increased, which was associated with a reduction of MyHC type IIx and IIb mRNA levels (Figure 2B).

Hypoxia induces HIF-1α transcriptional activity and stimulates glycolytic metabolism in muscle

HIF transcriptional activity was measured in C2C12 cells that were transfected with a plasmid carrying a luciferase gene under control of HIF-responsive elements. Myoblasts transiently transfected with the HIF reporter plasmid were exposed to 1%, 2%, 4% and 21% oxygen for 24 h. HIF luciferase reporter activity was strongly induced by lower oxygen concentrations (Figure 3A). At 4% O_2 HIF activation was still evident. This oxygen level also has negligible effects on myotube morphology and viability, indicating that this condition was most suitable for our experiments. To validate whether the hypoxic response was physiologically intact, we determined the mRNA expression levels of HIF-regulated genes in myotubes after three days of 4% oxygen exposure. Levels of VEGF-A, GLUT1 and HO-1 were significantly increased in the hypoxic myotubes (Figure 3B).

In addition to HIF-1α, two other HIFα isoforms, HIF-2α and HIF-3α, have been described to mediate the hypoxic response. To confirm that the HIF luciferase reporter

mainly reflects HIF-1α transcriptional activity, myotubes stably carrying the HIF luciferase reporter were transiently transfected with siRNA targeting HIF-1α. The HIF-1α siRNA reduced the expression of the HIF-1α gene by 60–80% (Figure 3C) and more importantly, it completely abrogated the hypoxia-induced increase of HIF luciferase reporter activity (Figure 3D).

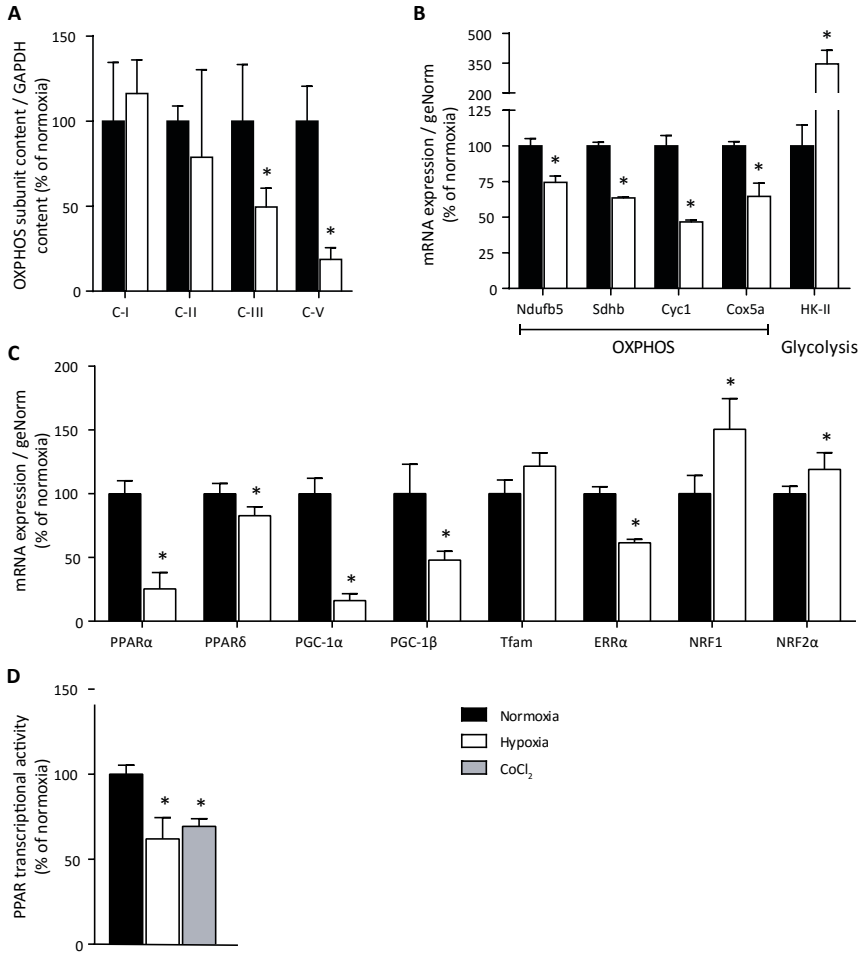

Figure 1 | Three days of hypoxia (4% O_2) attenuates content and activity of several components and regulators of oxidative capacity. A, protein content of labile subunits of the oxidative phosphorylation (OXPHOS) complexes; **B**, gene expression levels of nuclear-encoded OXPHOS subunits of complexes I–IV and the glycolytic gene hexokinase-II; **C**, gene expression levels of several regulators of mitochondrial biogenesis and oxidative capacity, and **D**, PPAR transcriptional activity by luciferase reporter assay. $CoCl_2$ was added to additional normoxic dishes as a hypoxia mimetic. Mean + SD; expression levels were normalized with geNorm to RPLP0, B2M, PPIA and Axin1; Ndufb5, complex I; Sdhb, complex II; Cyc1, complex III; Cox5a, complex IV; HKII, hexokinase-II; PPAR, peroxisome proliferator-activated receptor; PGC-1, PPAR gamma coactivator 1; Tfam, mitochondrial transcription factor A; ERRα, estrogen-related receptor α; NRF, nuclear respiratory factor. Experiments were performed in triplicate; $^{*}p < 0.05$ compared to normoxic control.

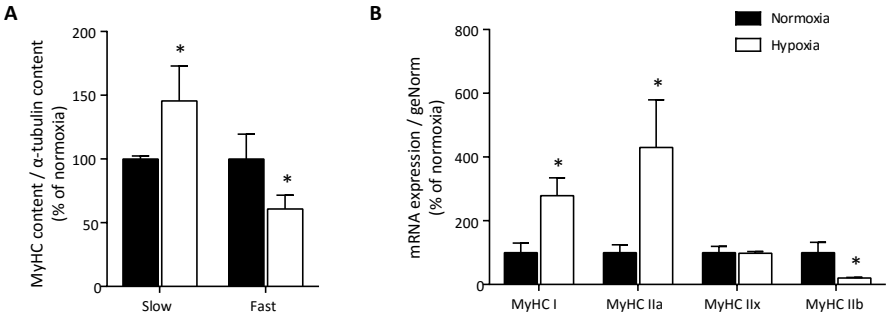

Figure 2 | Hypoxia (4% O_2) exposure for three days promotes expression of oxidative myosin heavy chain (MyHC) isoforms in myotubes. A, protein content of slow type I and fast type II MyHC isoforms and **B**, gene expression of MyHC isoforms. Mean + SD. Experiments were performed in triplicate; $^{*}p < 0.05$ compared to normoxic control.

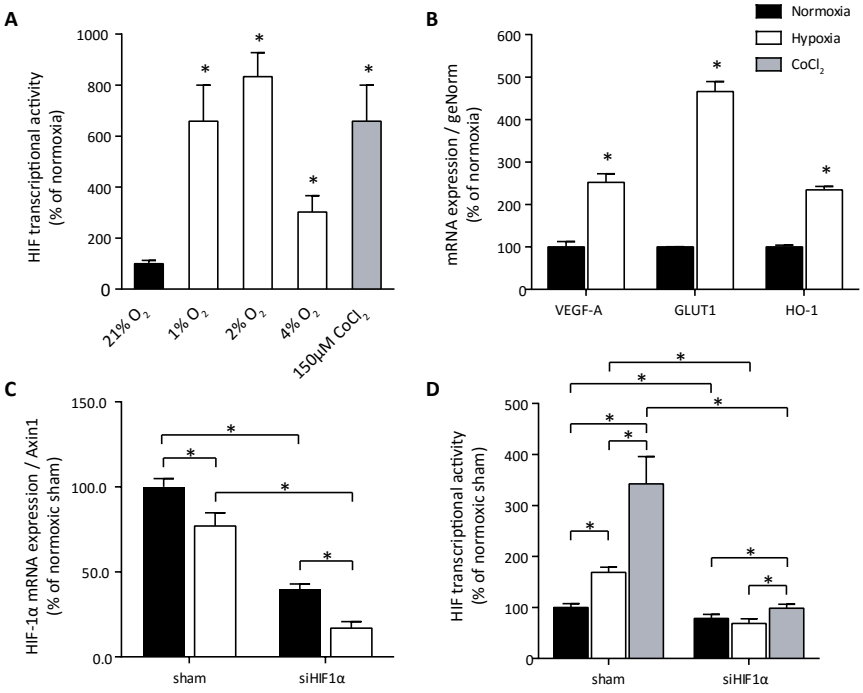

Figure 3 | Exposure of myotubes to 4% oxygen stimulates HIF transcriptional activity, which can be inhibited by knockdown of HIF-1α gene expression. A, dose-dependency of the HIF luciferase reporter in myotubes exposed to several oxygen concentrations for one day; **B**, expression levels of HIF-1α-regulated genes in myotubes exposed to 4% O_2 for three days; **C**, HIF-1α expression after knockdown with HIF-1α siRNA in myotubes exposed to 4% O_2 for three days, and **D**, HIF transcriptional activity by luciferase reporter assay after treatment with sham siRNA (sham) or HIF-1α siRNA (siHIF1α) and exposure to hypoxia (4% O_2) or $CoCl_2$ for three days. Mean + SD; VEGF-A, vascular endothelial growth factor A; GLUT1, glucose transporter 1; HO-1, heme oxygenase 1. Experiments were performed in triplicate; $^{*}p < 0.05$ compared to normoxic control or for the comparison indicated by the horizontal line.

Differential regulation of oxidative phenotype components is HIF-1α-dependent

To assess the role of HIF-1α in the hypoxia-induced changes of muscle oxidative phenotype, levels of markers of oxidative phenotype were determined in myotubes transiently transfected with the HIF-1α siRNA. Knockdown of HIF-1α gene expression resulted in significant preservation of the protein content of the OXPHOS complex V subunit (Figure 4A). A similar but less pronounced effect was observed for OXPHOS genes (data not shown), which corroborates that impairment of oxidative phenotype occurs at the transcriptional level. Gene expression levels of the transcription factors PPARα, PPARδ, and ERRα and their coregulators PGC-1α and PGC-1β were significantly reduced by hypoxia, however HIF-1α knockdown could only restore levels of PPARδ and PGC-1α (Figure 4B). Moreover, HIF-1α knockdown in hypoxia restored PPAR transcriptional activity to normoxic levels (Figure 4C). Together, these data suggest that PPARδ or PGC-1α could be the mediator in hypoxia-induced impairment of PPAR transcriptional activity.

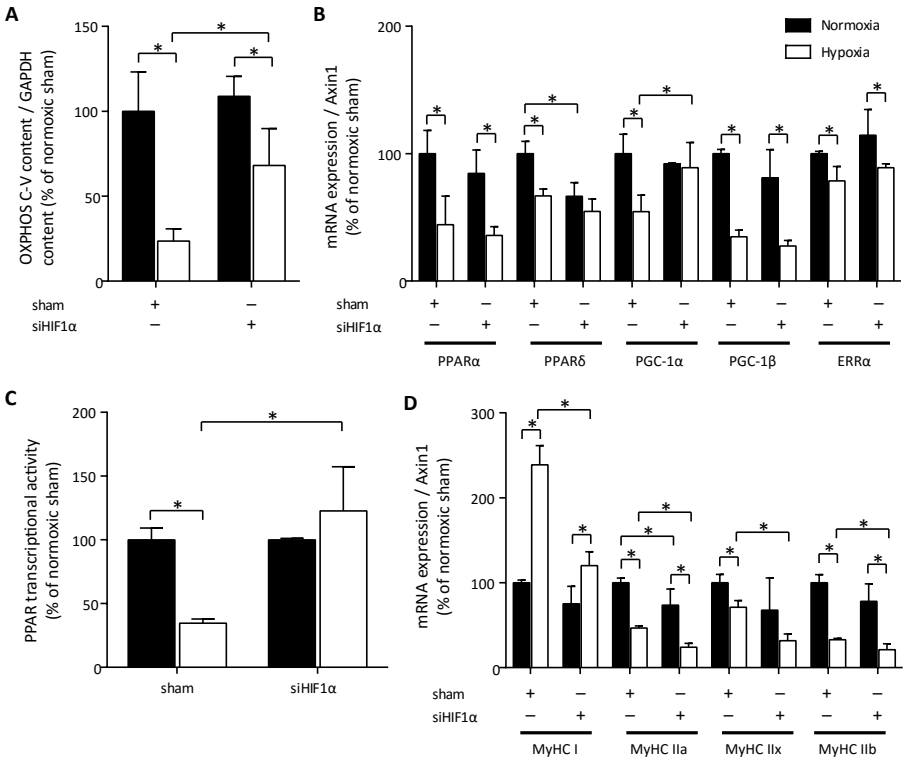

Figure 4 | HIF-1α knockdown results in sparing of oxidative capacity and blunted stimulation of oxidative myosin heavy chain components during exposure to hypoxia for three days. Myotubes were treated with sham siRNA (sham) or HIF-1α siRNA (siHIF1α), followed by measurement of **A**, protein content of OXPHOS complex V subunit ATP synthase subunit alpha; **B**, gene expression levels of several regulators of mitochondrial biogenesis and oxidative capacity; **C**, PPAR transcriptional activity by luciferase reporter assay and **D**, gene expression levels of myosin heavy chain isoforms. Mean + SD. Experiments were performed in triplicate; * $p < 0.05$ compared to normoxic control or for the comparison indicated by the horizontal line

Transient knockdown of HIF-1α expression resulted in attenuation or even abrogation of hypoxia-stimulated MyHC type I gene expression, but did not significantly affect the expression of the MyHC type II isoforms (Figure 4D).

Hypoxia-associated attenuation of PPAR transcriptional activity is mediated through PGC-1α

To assess whether synthetic stimulation could abolish the effect of hypoxia on PPAR transcriptional activity and identify PPARδ or PGC-1α as the key factor, we investigated the influence of ligand-dependent PPARδ activation and PPARδ/PGC-1α overexpression on PPAR transcriptional activity under hypoxic conditions. PPAR luciferase reporter activity was reduced by hypoxia to a similar extent in the absence and presence of GW501516, a specific PPARδ ligand (Figure 5A). However, by adding the PPARδ ligand PPAR transcriptional activity in hypoxia could be normalized to levels similar to basal PPAR transcriptional activity in normoxia.

Because myotubes are refractive to lipid-based transfection with plasmids, undifferentiated myoblasts were transfected with the PPAR luciferase reporter plasmid in combination with overexpression plasmids encoding either PPARδ, PPARα or PGC-1α. In myoblasts, PPAR transcriptional activity was markedly reduced after 2 days of exposure to hypoxia. Overexpression of PGC-1α radically increased PPAR transcriptional activity 14-fold and this was not attenuated by hypoxia (Figure 5B). Overexpression of PPARδ resulted in a modest 4-fold induction of PPAR transcriptional activity, but this effect was reduced by 25% under hypoxic conditions. PPARα overexpression stimulated PPAR transcriptional activity 17-fold, with a hypoxia-associated reduction of this effect by 18%. Overexpression of PGC-1α did not modify the expression levels of PPARα and PPARδ (Figure 5C). Together with the reduced sensitivity of the PPAR luciferase reporter to hypoxia in the presence of PGC-1α overexpression, this identifies PGC-1α as the likely mediator of hypoxia-associated attenuation of PPAR transcriptional activity and muscle oxidative phenotype.

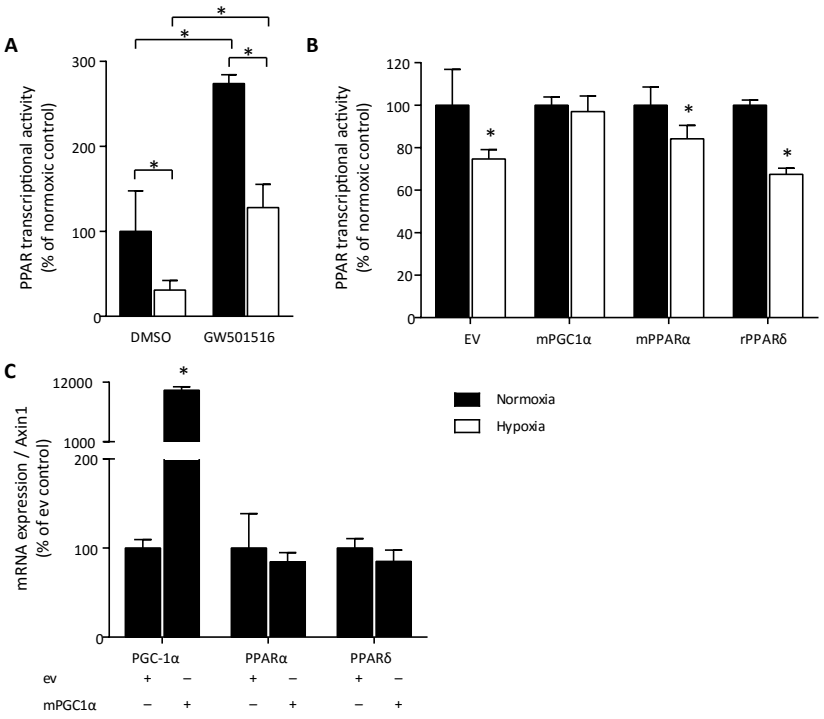

Figure 5 | Attenuation of PPAR transcriptional activity by hypoxia is mediated through suppression of PGC-1α expression. A, PPAR transcriptional activity in myotubes stimulated for two days with PPARδ agonist GW501516 (100 μM) or vehicle control (DMSO) during exposure to hypoxia; **B**, PPAR transcriptional activity in myoblasts transiently transfected with overexpression plasmids for murine PGC-1α (mPGC1α), PPARα (mPPARα) and rat PPARδ (rPPARδ) or empty vector (EV) after two days in normoxia or hypoxia. Activity is normalized to corresponding normoxic conditions, and **C**, gene expression of PGC-1α, PPARα and PPARδ in myoblasts in the presence (mPGC1α) or absence (EV) of mPGC1α overexpression for two days. Expression levels are normalized to respective EV controls. Experiments were performed in triplicate; $^{*}p < 0.05$ compared to normoxic control or for the comparison indicated by the horizontal line.

DISCUSSION

In this study we showed that hypoxia differentially regulates muscle oxidative phenotype by directly downregulating oxidative capacity through HIF-1α and PGC-1α and simultaneously stimulating oxidative myosin heavy chain type I levels, also in a HIF-1α-dependent manner. This suggests a segregation of the regulation of oxidative metabolism and structural muscle proteins under hypoxic conditions.

HIF-1 activity is progressively stimulated by decreasing oxygen concentrations and was found to be an essential mediator of oxygen homeostasis (37). It has been shown that HIF-1α stimulates muscle glycolytic phenotype (26) and HIF-1α knockout modestly improves muscle oxidative phenotype (27). However, these experiments were performed *in vivo* and do not provide insight into the direct regulation of muscle oxidative phenotype by HIF-1α. Therefore, we assessed the role of HIF-1α in downregulation of muscle oxidative phenotype by hypoxia. Indeed, we found significant stimulation of HIF transcriptional activity in our model of hypoxia-exposed myotubes. Our group recently showed that activation of NF-κB by TNF-α impairs muscle oxidative phenotype (32). However, using the same NF-κB responsive luciferase reporter construct we did not find increased activation of NF-κB by hypoxia in C2C12 myotubes (data not shown). Further experiments were therefore focused on modulation of HIF-1α.

PPARα, PPARδ, PGC-1α, PGC-1β and ERRα are important regulators of oxidative capacity. Hypoxia generally reduced the gene expression levels of all these markers. In addition, hypoxia markedly decreased PPAR transcriptional activity. The PPAR reporter we used is responsive to agonists for PPARα, PPARδ and PPARγ (33) and might thus be indirectly affected by PGC-1α and PGC-1β via coactivation of these PPARs (47). Restoration of both PPAR transcriptional activity and gene expression levels of PPARδ and PGC-1α by HIF-1α knockdown suggests that HIF-1α mediates the reduced PPAR transcriptional activity via either PPARδ or PGC-1α. However, only overexpression of PGC-1α could prevent hypoxia-associated depression of PPAR transcriptional activity with no associated changes in PPARδ gene expression. It should be noted that the overexpression studies were performed in myoblasts rather than in myotubes, because of the technical limitation of myotubes to be transfected with expression plasmids using lipid-based techniques. However, also in untransfected myoblasts PGC-1α expression was reduced by hypoxia (data not shown).

A central role for PGC-1α in hypoxia-induced impairment of oxidative capacity is further supported by the observation that HIF-1α knockdown could successfully restore OXPHOS subunit V content and OXPHOS gene expression. Regulation of OXPHOS expression levels is mediated largely through PGC-1α (28) and whole-body PGC-1α knockout experiments in mice have shown that skeletal muscle expression of OXPHOS genes is markedly blunted in the absence of PGC-1α (2).

A potential mechanism by which PGC-1α expression is negatively modulated by hypoxia is via histone deacetylases (HDACs). Ramjiawan *et al.* showed in hypoxic cardiomyocytes that histone 3 lysine 9 (H3K9) acetylation was significantly reduced in the PGC-1α promoter region, which resulted in reduced PGC-1α expression (31). Blocking HDAC activity abolished this hypoxia-induced loss of PGC-1α. Seo *et al.* showed that HDAC4, -5 and -7 promote HIF-1α transactivation under hypoxic conditions (38), whereas HDAC inhibitors inhibit HIF-1α activity (30). We previously showed that skeletal muscle of patients with COPD, a disease associated with hypoxia, is characterized by a

decreased gene expression of PGC-1α and OXPHOS protein content (44), which is in line with the results from the current study. Interestingly, in a different study, HDAC4 protein content was shown to be increased in the quadriceps muscle of patients with COPD compared to healthy controls (24). Moreover, a systems biology approach comparing muscle biopsies from patients with COPD and muscle tissue from mice exposed to chronic hypoxia, identified hypoxia as a key factor in the muscle abnormalities in COPD, associated with increased HDAC expression (43).

It is of interest that supplementation of the muscle cells under hypoxia with the selective PPARδ agonist GW501516 restored PPAR transcriptional activity to normoxic levels. Although decreased PGC-1α turned out to be most important for attenuation of PPAR transcriptional activity under hypoxic conditions, PPARδ seems a promising target for therapeutic intervention.

In contrast to what we expected, hypoxia induced rather than inhibited the expression of the oxidative myosin heavy chain (MyHC) type I gene and protein. Moreover, HIF-1α knockdown experiments showed that MyHC type I induction was HIF-1α-dependent, unlike the changes in gene expression levels of the other MyHC genes.

A role for PGC-1α in the hypoxia-associated increase of MyHC type I expression is unlikely, because muscle-specific PGC-1α knockout mice present with a fiber-type shift towards glycolytic rather than oxidative fibers (15). Moreover, transgenic mice that overexpress PGC-1α in the muscle are characterized by an increased proportion of type I fibers (25).

Interestingly, in cardiomyocytes a similar response of MyHC type I (also known as β-myosin in the heart) to hypoxia was observed (23). To our knowledge, only one paper reports on myosin heavy chain composition in C2C12 cells in relation to HIF-1α, showing that HIF-1α overexpression stimulated the expression of MyHC IIb and reduced MyHC I (26), although increased HIF-1α transcriptional activity was not confirmed in this study. However, these cells were still in a differentiating phase, whereas our C2C12 cells were fully differentiated when exposed to hypoxia. Ishihara *et al.* showed that the effect of hypoxia on fiber-type composition was indeed dependent on the developmental stage of the rats exposed to hypoxia (19). Nevertheless, the hypoxia-associated increase of oxidative MyHC isoforms that we found seems counterintuitive, because the type I fibers rely primarily on oxidative energy metabolism for muscle contraction. Possibly, the absence of contraction and extramuscular factors such as nerve stimulation or hormones, results in uncoupling of the regulation of MyHC profile and oxidative capacity.

CONCLUSION

Our results indicate that hypoxia could explain the loss of oxidative capacity as observed in the muscles of for example patients with COPD or CHF. However, the frequently co-occurring I-to-II fiber-type shift is possibly caused or overruled by factors other than direct hypoxia.

Our data furthermore suggests that the PPAR/PGC-1α pathway would be an interesting target for pharmacological modulation to treat disease-related loss of oxidative capacity. An intervention study by Broekhuizen *et al.* indeed showed a significant improvement of exercise capacity in COPD patients who received nutritional supplementation with PPAR-activating poly-unsaturated fatty acids (PUFAs) in addition to the effect of exercise training (7). Although no information was available on changes in skeletal muscle oxidative capacity, it can be speculated that the PUFA-induced improvement in exercise capacity was mediated by an improved muscle oxidative capacity. Further studies should focus on the effect of PUFA supplementation on muscle oxidative capacity under hypoxic conditions to explore PUFA supplementation as a therapy for hypoxia-associated loss of muscle oxidative phenotype.

ACKNOWLEDGMENTS

This project was supported by The Netherlands Asthma Foundation Award #3.2.05.038 and by the Transnational University Limburg (tTUL). These funders had no role in study design, in data collection, analysis and interpretation, in manuscript preparation, or in the decision to publish.

REFERENCES

1. Abdelmalki A, Fimbel S, Mayet-Sornay MH, Sempore B, and Favier R. Aerobic capacity and skeletal muscle properties of normoxic and hypoxic rats in response to training. Pflugers Arch 431: 671-679, 1996.
2. Arany Z, He H, Lin J, Hoyer K, Handschin C, Toka O, Ahmad F, Matsui T, Chin S, Wu PH, Rybkin, II, Shelton JM, Manieri M, Cinti S, Schoen FJ, Bassel-Duby R, Rosenzweig A, Ingwall JS, and Spiegelman BM. Transcriptional coactivator PGC-1 alpha controls the energy state and contractile function of cardiac muscle. Cell Metab 1: 259-271, 2005.
3. Bastin J, Aubey F, Rotig A, Munnich A, and Djouadi F. Activation of peroxisome proliferator-activated receptor pathway stimulates the mitochondrial respiratory chain and can correct deficiencies in patients' cells lacking its components. J Clin Endocrinol Metab 93: 1433-1441, 2008.
4. Bigard AX, Sanchez H, Birot O, and Serrurier B. Myosin heavy chain composition of skeletal muscles in young rats growing under hypobaric hypoxia conditions. J Appl Physiol (1985) 88: 479-486, 2000.
5. Boutellier U, Howald H, di Prampero PE, Giezendanner D, and Cerretelli P. Human muscle adaptations to chronic hypoxia. Prog Clin Biol Res 136: 273-285, 1983.
6. Brandt JM, Djouadi F, and Kelly DP. Fatty acids activate transcription of the muscle carnitine palmitoyltransferase I gene in cardiac myocytes via the peroxisome proliferator-activated receptor alpha. J Biol Chem 273: 23786-23792, 1998.
7. Broekhuizen R, Wouters EF, Creutzberg EC, Weling-Scheepers CA, and Schols AM. Polyunsaturated fatty acids improve exercise capacity in chronic obstructive pulmonary disease. Thorax 60: 376-382, 2005.
8. De Palma S, Ripamonti M, Vigano A, Moriggi M, Capitanio D, Samaja M, Milano G, Cerretelli P, Wait R, and Gelfi C. Metabolic modulation induced by chronic hypoxia in rats using a comparative proteomic analysis of skeletal muscle tissue. J Proteome Res 6: 1974-1984, 2007.
9. de Theije C, Costes F, Langen RC, Pison C, and Gosker HR. Hypoxia and muscle maintenance regulation: implications for chronic respiratory disease. Curr Opin Clin Nutr Metab Care 14: 548-553, 2011.
10. Faucher M, Guillot C, Marqueste T, Kipson N, Mayet-Sornay MH, Desplanches D, Jammes Y, and Badier M. Matched adaptations of electrophysiological, physiological, and histological properties of skeletal muscles in response to chronic hypoxia. Pflugers Arch 450: 45-52, 2005.
11. Flicek P, Amode MR, Barrell D, Beal K, Billis K, Brent S, Carvalho-Silva D, Clapham P, Coates G, Fitzgerald S, Gil L, Giron CG, Gordon L, Hourlier T, Hunt S, Johnson N, Juettemann T, Kahari AK, Keenan S, Kulesha E, Martin FJ, Maurel T, McLaren WM, Murphy DN, Nag R, Overduin B, Pignatelli M, Pritchard B, Pritchard E, Riat HS, Ruffier M, Sheppard D, Taylor K, Thormann A, Trevanion SJ, Vullo A, Wilder SP, Wilson M, Zadissa A, Aken BL, Birney E, Cunningham F, Harrow J, Herrero J, Hubbard TJ, Kinsella R, Muffato M, Parker A, Spudich G, Yates A, Zerbino DR, and Searle SM. Ensembl 2014. Nucleic Acids Res 42: D749-755, 2014.
12. Gosker HR, Lencer NH, Franssen FM, van der Vusse GJ, Wouters EF, and Schols AM. Striking similarities in systemic factors contributing to decreased exercise capacity in patients with severe chronic heart failure or COPD. Chest 123: 1416-1424, 2003.
13. Gosker HR, Wouters EF, van der Vusse GJ, and Schols AM. Skeletal muscle dysfunction in chronic obstructive pulmonary disease and chronic heart failure: underlying mechanisms and therapy perspectives. Am J Clin Nutr 71: 1033-1047, 2000.
14. Green HJ, Sutton JR, Cymerman A, Young PM, and Houston CS. Operation Everest II: adaptations in human skeletal muscle. J Appl Physiol (1985) 66: 2454-2461, 1989.
15. Handschin C, Chin S, Li P, Liu F, Maratos-Flier E, Lebrasseur NK, Yan Z, and Spiegelman BM. Skeletal muscle fiber-type switching, exercise intolerance, and myopathy in PGC-1alpha muscle-specific knock-out animals. J Biol Chem 282: 30014-30021, 2007.
16. Hoppeler H, and Desplanches D. Muscle structural modifications in hypoxia. Int J Sports Med 13 Suppl 1: S166-168, 1992.
17. Hoppeler H, Kleinert E, Schlegel C, Claassen H, Howald H, Kayar SR, and Cerretelli P. Morphological adaptations of human skeletal muscle to chronic hypoxia. Int J Sports Med 11 Suppl 1: S3-9, 1990.
18. Howald H, Pette D, Simoneau JA, Uber A, Hoppeler H, and Cerretelli P. Effect of chronic hypoxia on muscle enzyme activities. Int J Sports Med 11 Suppl 1: S10-14, 1990.
19. Ishihara A, Itoh K, Oishi Y, Itoh M, Hirofuji C, and Hayashi H. Effects of hypobaric hypoxia on histochemical fibre-type composition and myosin heavy chain isoform component in the rat soleus muscle. Pflugers Arch 429: 601-606, 1995.
20. Itoh K, Moritani T, Ishida K, Hirofuji C, Taguchi S, and Itoh M. Hypoxia-induced fibre type transformation in rat hindlimb muscles. Histochemical and electro-mechanical changes. European journal of applied physiology and occupational physiology 60: 331-336, 1990.
21. Katz SD, Maskin C, Jondeau G, Cocke T, Berkowitz R, and LeJemtel T. Near-maximal fractional oxygen extraction by active skeletal muscle in patients with chronic heart failure. J Appl Physiol (1985) 88: 2138-2142, 2000.
22. Kim JW, Tchernyshyov I, Semenza GL, and Dang CV. HIF-1-mediated expression of pyruvate dehydrogenase kinase: a metabolic switch required for cellular adaptation to hypoxia. Cell Metab 3: 177-185, 2006.
23. Krishnan J, Suter M, Windak R, Krebs T, Felley A, Montessuit C, Tokarska-Schlattner M, Aasum E, Bogdanova A, Perriard E, Perriard JC, Larsen T, Pedrazzini T, and Krek W. Activation of a HIF1alpha-PPARgamma axis underlies the integration of glycolytic and lipid anabolic pathways in pathologic cardiac hypertrophy. Cell Metab 9: 512-524, 2009.
24. Lewis A, Riddoch-Contreras J, Natanek SA, Donaldson A, Man WD, Moxham J, Hopkinson NS, Polkey MI, and Kemp PR. Downregulation of the serum response factor/miR-1 axis in the quadriceps of patients with COPD. Thorax 67: 26-34, 2012.
25. Lin J, Wu H, Tarr PT, Zhang CY, Wu Z, Boss O, Michael LF, Puigserver P, Isotani E, Olson EN, Lowell BB, Bassel-Duby R, and

Spiegelman BM. Transcriptional co-activator PGC-1 alpha drives the formation of slow-twitch muscle fibres. Nature 418: 797-801, 2002.
26. Lunde IG, Anton SL, Bruusgaard JC, Rana ZA, Ellefsen S, and Gundersen K. Hypoxia inducible factor 1 links fast-patterned muscle activity and fast muscle phenotype in rats. J Physiol 589: 1443-1454, 2011.
27. Mason SD, Howlett RA, Kim MJ, Olfert IM, Hogan MC, McNulty W, Hickey RP, Wagner PD, Kahn CR, Giordano FJ, and Johnson RS. Loss of skeletal muscle HIF-1alpha results in altered exercise endurance. PLoS Biol 2: e288, 2004.
28. Mootha VK, Handschin C, Arlow D, Xie X, St Pierre J, Sihag S, Yang W, Altshuler D, Puigserver P, Patterson N, Willy PJ, Schulman IG, Heyman RA, Lander ES, and Spiegelman BM. Erralpha and Gabpa/b specify PGC-1alpha-dependent oxidative phosphorylation gene expression that is altered in diabetic muscle. Proc Natl Acad Sci U S A 101: 6570-6575, 2004.
29. Papandreou I, Cairns RA, Fontana L, Lim AL, and Denko NC. HIF-1 mediates adaptation to hypoxia by actively downregulating mitochondrial oxygen consumption. Cell Metab 3: 187-197, 2006.
30. Qian DZ, Kachhap SK, Collis SJ, Verheul HM, Carducci MA, Atadja P, and Pili R. Class II histone deacetylases are associated with VHL-independent regulation of hypoxia-inducible factor 1 alpha. Cancer research 66: 8814-8821, 2006.
31. Ramjiawan A, Bagchi RA, Blant A, Albak L, Cavasin MA, Horn TR, McKinsey TA, and Czubryt MP. Roles of histone deacetylation and AMP kinase in regulation of cardiomyocyte PGC-1alpha gene expression in hypoxia. Am J Physiol Cell Physiol 304: C1064-1072, 2013.
32. Remels AH, Gosker HR, Schrauwen P, Hommelberg PP, Sliwinski P, Polkey M, Galdiz J, Wouters EF, Langen RC, and Schols AM. TNF-alpha impairs regulation of muscle oxidative phenotype: implications for cachexia? FASEB J 24: 5052-5062, 2010.
33. Remels AH, Langen RC, Gosker HR, Russell AP, Spaapen F, Voncken JW, Schrauwen P, and Schols AM. PPARgamma inhibits NF-kappaB-dependent transcriptional activation in skeletal muscle. Am J Physiol Endocrinol Metab 297: E174-183, 2009.
34. Remels AH, Schrauwen P, Broekhuizen R, Willems J, Kersten S, Gosker HR, and Schols AM. Peroxisome proliferator-activated receptor expression is reduced in skeletal muscle in COPD. Eur Respir J 30: 245-252, 2007.
35. Rupec RA, and Baeuerle PA. The genomic response of tumor cells to hypoxia and reoxygenation. Differential activation of transcription factors AP-1 and NF-kappa B. Eur J Biochem 234: 632-640, 1995.
36. Schreiber SN, Emter R, Hock MB, Knutti D, Cardenas J, Podvinec M, Oakeley EJ, and Kralli A. The estrogen-related receptor alpha (ERRalpha) functions in PPARgamma coactivator 1alpha (PGC-1alpha)-induced mitochondrial biogenesis. Proc Natl Acad Sci U S A 101: 6472-6477, 2004.
37. Semenza GL. HIF-1: mediator of physiological and pathophysiological responses to hypoxia. J Appl Physiol (1985) 88: 1474-1480, 2000.
38. Seo HW, Kim EJ, Na H, and Lee MO. Transcriptional activation of hypoxia-inducible factor-1alpha by HDAC4 and HDAC5 involves differential recruitment of p300 and FIH-1. FEBS letters 583: 55-60, 2009.
39. Shibata T, Giaccia AJ, and Brown JM. Development of a hypoxia-responsive vector for tumor-specific gene therapy. Gene Ther 7: 493-498, 2000.
40. Sillau AH, and Banchero N. Effects of hypoxia on capillary density and fiber composition in rat skeletal muscle. Pflugers Arch 370: 227-232, 1977.
41. Takahashi H, Asano K, and Nakayama H. Effect of endurance training under hypoxic condition on oxidative enzyme activity in rat skeletal muscle. Appl Human Sci 15: 111-114, 1996.
42. Takahashi H, Kikuchi K, and Nakayama H. Effect of chronic hypoxia on oxidative enzyme activity in rat skeletal muscle. Ann Physiol Anthropol 12: 363-369, 1993.
43. Turan N, Kalko S, Stincone A, Clarke K, Sabah A, Howlett K, Curnow SJ, Rodriguez DA, Cascante M, O'Neill L, Egginton S, Roca J, and Falciani F. A systems biology approach identifies molecular networks defining skeletal muscle abnormalities in chronic obstructive pulmonary disease. PLoS Comput Biol 7: e1002129, 2011.
44. van den Borst B, Slot IG, Hellwig VA, Vosse BA, Kelders MC, Barreiro E, Schols AM, and Gosker HR. Loss of quadriceps muscle oxidative phenotype and decreased endurance in patients with mild-to-moderate COPD. J Appl Physiol (1985) 114: 1319-1328, 2013.
45. Vandesompele J, De Preter K, Pattyn F, Poppe B, Van Roy N, De Paepe A, and Speleman F. Accurate normalization of real-time quantitative RT-PCR data by geometric averaging of multiple internal control genes. Genome Biol 3: RESEARCH0034, 2002.
46. Vescovo G, Ravara B, Gobbo V, Angelini A, and Dalla Libera L. Skeletal muscle fibres synthesis in heart failure: role of PGC-1alpha, calcineurin and GH. Int J Cardiol 104: 298-306, 2005.
47. Viswakarma N, Jia Y, Bai L, Vluggens A, Borensztajn J, Xu J, and Reddy JK. Coactivators in PPAR-Regulated Gene Expression. PPAR Res 2010: 2010.
48. Webster KA. Evolution of the coordinate regulation of glycolytic enzyme genes by hypoxia. J Exp Biol 206: 2911-2922, 2003.
49. Wu Z, Puigserver P, Andersson U, Zhang C, Adelmant G, Mootha V, Troy A, Cinti S, Lowell B, Scarpulla RC, and Spiegelman BM. Mechanisms controlling mitochondrial biogenesis and respiration through the thermogenic coactivator PGC-1. Cell 98: 115-124, 1999.

Chapter 3

Alterations in skeletal muscle oxidative phenotype in mice exposed to three weeks of normobaric hypoxia

Ilse G.M. Slot, Annemie M.W.J. Schols, Chiel C. de Theije, Frank J.M. Snepvangers, Harry R. Gosker

Journal of Cellular Physiology, 2015. Epub ahead of print

ABSTRACT

Skeletal muscle of patients with chronic respiratory failure is prone to loss of muscle mass and oxidative phenotype. Tissue hypoxia has been associated with cachexia and emphysema in humans. Experimental research on the role of hypoxia in loss of muscle oxidative phenotype however has yielded inconsistent results. Animal studies are frequently performed in young animals, which may hinder translation to generally older aged patients. Therefore in this study we tested the hypothesis that hypoxia induces loss of skeletal muscle oxidative phenotype in a model of aged (52 weeks) mice exposed to three weeks of hypoxia. Additional groups of young (4 weeks) and adult (12 weeks) mice were included to examine age effects. To verify hypoxia-induced cachexia, fat pad and muscle weights as well as muscle fiber cross-sectional areas were determined. Muscle oxidative phenotype was assessed by expression and activity of markers of mitochondrial metabolism and fiber-type distribution. A profound loss of muscle and fat was indeed accompanied by a slightly lower expression of markers of muscle oxidative capacity in the aged hypoxic mice. In contrast, hypoxia-associated changes of fiber-type composition were more prominent in the young mice. The differential response of the muscle of young, adult, and aged mice to hypoxia suggests that age matters and that the aged mouse is a better model for translation of findings to elderly patients with chronic respiratory disease. Furthermore, the findings warrant further mechanistic research into putative accelerating effects of hypoxia-induced loss of oxidative phenotype on the cachexia process in chronic respiratory disease.

INTRODUCTION

Skeletal muscle of patients with chronic obstructive pulmonary disease (COPD) is often characterized by low muscle mass (49), a reduced proportion of type I oxidative fibers and a diminished oxidative capacity (14, 21). In advanced disease stages hypoxia, a condition of inadequate oxygen content in a tissue, has been proposed as a driver of both phenotypic characteristics (12, 21, 62). Indeed the prevalence of weight loss and muscle atrophy is high in various respiratory disorders that are hallmarked by hypoxia, including acute exacerbations of COPD (10, 39), idiopathic pulmonary arterial hypertension (4), and acute respiratory distress syndrome (ARDS) (25), and hypoxia has been associated with reduced muscle mass (53). For the loss of muscle oxidative phenotype (Oxphen), a role for hypoxia is supported by observations of reduced proportions of oxidative type I fibers, decreased aerobic metabolism and impaired oxidative capacity in skeletal muscle of patients with respiratory failure (RF) (36, 37, 69). Furthermore, Filley *et al.* suggested already in 1968 that tissue hypoxia is responsible for cachexia in patients with end stage emphysema (16). Emphysema has also been associated with a more pronounced type I to II (oxidative to glycolytic) fiber-type shift in skeletal muscle (20). Moreover, hypoxemia often develops or worsens with acute exacerbations (38), and patients suffering an acute exacerbation have been shown to have decreased expression of subunits of mitochondrial cytochrome *c* oxidase and ATP synthase in the *vastus lateralis* muscle (10). The first report of an association between hypoxia and type I fiber proportion in human studies was probably by Jakobsson *et al.*, who showed an association between low type I proportion and low arterial oxygen pressure in patients with RF (36). Moreover, Wuyam *et al.* reported impaired oxidative capacity in patients with RF (69). A few years later, Jakobsson *et al.* also described decreased oxidative enzyme activities in quadriceps muscle of advanced COPD patients (37) which were partly restored by long-term oxygen therapy (35).

Previous studies involving healthy volunteers as well as experimental animal models gave inconsistent results with regard to hypoxia-associated loss of muscle oxidative phenotype. Human studies involved participants of mountaineering expeditions that were sampled before and after the expedition (8, 29) and showed decreased activity of mitochondrial enzymes after hypoxia exposure. However, mountaineering expeditions are heavily confounded by strenuous physical activity (27-29). To control for confounders related to these expeditions, such as low temperature, dietary imbalance and extreme exercise, Green *et al.* studied participants who were placed in a hypobaric chamber (23). Enzyme activities of citrate synthase, succinate dehydrogenase and hexokinase were repressed, but glycolytic enzymes other than hexokinase did not change and no fiber-type shift was observed (23). Many animal studies were performed in rats (1, 6, 11, 15, 26, 33, 56, 60, 61). Some of these studies report a fiber-type shift towards fast fibers (6, 15, 26, 31, 33, 34, 56, 59), whereas in others no change of fiber-type composition is observed (1, 61). In general, hypoxia appears to reduce oxidative enzyme activities (1, 11, 60), although Takahashi *et al.* did not observe reduced oxidative enzyme activity by hypoxia (59). However, some of the reported changes in fiber-type composition and oxidative enzyme activities by hypoxia have been suggested to be confounded by hypoxia-associated anorexia (1).

Many of the animal studies have been conducted under hypobaric hypoxia (6, 31, 33, 34), whereas normobaric hypoxia would be most appropriate from a physiological and pathological perspective. Also, most of these studies have been conducted in rats, whereas mouse models are nowadays more suitable because of the availability of research tools that can be applied (e.g. antibodies, transgenes). Animal models for COPD are indeed primarily mouse models, but surprisingly until recently this did not yet include a well-established hypoxia model (45). Moreover, as COPD mainly affects the elderly, using older animals would be most appropriate or at least preclude age-related variation in the investigated topic. To our knowledge however, old animals are rarely studied to model disease factors of COPD, except for a recent report by Van den Borst *et al.* investigating effects of hypoxia on adipose tissue inflammation and metabolism (63). Indeed, the abovementioned animal studies were conducted in animals of different ages (juvenile and still developing to barely full-grown), with age-dependent outcomes (32). We recently investigated the direct effect of hypoxia on muscle oxidative phenotype *in vitro* (57). In line with our hypothesis, markers of oxidative capacity were significantly reduced by hypoxia, but unexpectedly hypoxia stimulated expression of the oxidative type I myosin heavy chain (MyHC). *In vitro* cultured myotubes probably reflect the developmental stage of muscle in juvenile animals, further illustrating that age should be considered in animal models of COPD.

We therefore decided to conduct a methodological study on the effect of *normobaric* hypoxia on muscle oxidative phenotype in *aged mice* (52 weeks of age). We hypothesized that hypoxia induces loss of oxidative phenotype. In addition, we verified hypoxia-associated loss of muscle and fat mass and we determined protein oxidation levels. For comparison, also very young (4 weeks old, still growing) and adult (12 weeks old, limited muscle growth) mice were included.

MATERIALS AND METHODS

Experimental procedure

A total of 76 male C57BL/6J mice (Charles River Laboratories, Wilmington, MA) at the age of 4 weeks (young), 12 weeks (adult) and 52 weeks (aged) were randomly divided over groups that were subsequently exposed to hypoxia (8% oxygen, *n* = 10 for 4 weeks and 52 weeks, *n* = 8 for 12 weeks) or ambient air (normoxia, *n* = 8 per age group) for 21 days. Because decreased food intake is associated with hypoxia exposure and may act as a confounding factor in interpreting hypoxia-associated changes, an additional group of mice exposed to normoxia (*n* = 8 per age group) was pair-fed to match the food intake of the hypoxic mice. Seven mice were excluded because of infection (1 in 4 weeks hypoxic group, 2 in each of 4 weeks normoxic and 52 weeks normoxic and hypoxic groups). Baseline characteristics but not the primary outcome (Oxphen) of only the 52-week old normoxic and hypoxic but not pair-fed mice have been previously reported (63).

Mice were housed in experimental chambers at 21°C with a 12-h dark/light cycle and received standard chow (V1534–000 ssniff R/M-H, ssniff Spezialdiäten, Soest, Germany) and water *ad libitum*. For the hypoxia experiments, oxygen was replaced by nitrogen by the ProOx P110 oxygen controller (BioSpherix, Lacona, NY) in a stepwise manner to create normobaric oxygen levels of 12% (day 1), 10% (day 2), and finally 8% (60.8 mmHg) on day 3 and the remainder of the experiment. Three to four mice were housed per cage. Daily food intake was determined per cage. On day 21, mice were anesthetized with isoflurane gas, the abdominal cavity was opened, and aortic blood was collected into a heparin-coated 1-ml syringe (Becton Dickinson, Breda, The Netherlands). Oxygen levels and pH were measured immediately using the ABL 510 Blood Gas Analyzer (Radiometer; Diamond Diagnostics, Holliston, MA) and blood cell count was determined with the Coulter Ac T Diff Hematology Analyzer (Beckman Coulter, Woerden, The Netherlands).

Plasma was stored at –80°C until further analyses. Lower limb skeletal muscles (gastrocnemius, tibialis anterior, soleus (SOL), extensor digitorum longus (EDL), and plantaris), were dissected and weighed. One of each muscle was embedded in Tissue-Tek (Sakura Finetek Europe, Zoeterwoude, The Netherlands) and frozen in melting isopentane precooled in liquid nitrogen and stored at −80°C for histology. The other muscle was snap-frozen in liquid nitrogen and stored at –80°C for molecular analyses. The protocol was approved by the Committee for Animal Care and Use of Maastricht University (project 2009-151).

Immunohistochemistry

Muscle cryosections (7µm) with fibers in transverse orientation were incubated with primary anti-myosin heavy chain (MyHC) I, anti-MyHC IIa (both Developmental Studies Hybridoma Bank (DSHB), University of Iowa, USA), and anti-laminin (Sigma, Zwijndrecht, The Netherlands) followed by secondary antibodies labeled with Alexa Fluor 555, Alexa Fluor 488 and Alexa Fluor 350 (Invitrogen, Breda, The Netherlands). Stained sections were microscopically photographed at 200× magnification (Nikon Eclipse E800; Nikon Instruments Europe, Amsterdam, The Netherlands). In a blinded fashion, fiber types were classified based on their MyHC isotype content (fiber type I and IIa positive for MyHC isotype I and IIa, respectively; hybrid type I/IIa positive for

both MyHC isotypes I and IIa; types IIb and IIx together remain unstained) and fiber cross-sectional area was measured with Lucia 4.82 software (Laboratory Imaging, Czech Republic) based on laminin staining of the basement membrane (66). The number of fibers analyzed per fiber type is listed in Supplemental Table 1.

Enzyme activity assays and immunoblotting

One soleus and one EDL muscle were each homogenized in 240µl ice-cold SET buffer (250mM sucrose, 2mM EDTA, 10mM Tris, pH 7.4) using a Mini-BeadBeater (BioSpec Products Inc., Bartlesville, Oklahoma, USA) and incubated on ice for 10 minutes. Samples were spun for 5 minutes at maximum speed (20817×g) in a cooled centrifuge and supernatant was collected. Pellets were snap-frozen in liquid nitrogen and stored at –80°C for later analysis. Supernatants were divided into three aliquots. To the first aliquot aqueous BSA solution was added to a final concentration of 1% (v/v) and snap-frozen to be stored at –80°C until analysis of enzymatic activity. The second aliquot was supplemented with 4× sample buffer (250mM Tris-HCl pH6.8, 8% (w/v) sodium dodecyl sulfate, 40% (v/v) glycerol, 0.4M dithiothreitol, 0.02% (w/v) bromophenol blue) and samples were snap-frozen and stored until analysis by Western blot. The third aliquot of lysate was used to determine the protein concentration with the bicinchoninic acid assay (Pierce, Thermo Fisher Scientific, Breda, The Netherlands) according to manufacturer's instructions.

Citrate synthase (CS, EC 2.3.3.1), 3-hydroxyacyl-CoA dehydrogenase (HADH, EC 1.1.1.35), cytochrome *c* oxidase (COX, EC 1.9.3.1) and phosphofructokinase (PFK, EC 2.7.1.11) activities were assayed spectrophotometrically (Multiskan Spectrum; Thermo Labsystems, Breda, The Netherlands) as previously described (5, 18, 41, 55). Absolute CS, HADH, COX and PFK activities were normalized to total protein.

For immunoblotting, 10µg of unboiled protein in sample buffer was separated by electrophoresis in a gradient gel (4-12% Bis-Tris XT gel, Criterion, Bio-Rad, Veenendaal, The Netherlands) with XT MOPS running buffer (Bio-Rad). Samples from the same age group and the same muscle were run together on the same gel. Proteins were transferred to a 0.45µm nitrocellulose membrane (Protran, Schleicher and Schuell, 's-Hertogenbosch, The Netherlands) in transfer buffer (25mM Tris, 192mM glycine, 20% (v/v) methanol). After transfer, proteins were visualized using Ponceau S staining solution (Sigma-Aldrich, St. Louis, MO, USA). Membranes were subsequently blocked from nonspecific protein binding with blocking solution, which contains 5% (w/v) non-fat dry milk (Campina, Eindhoven, The Netherlands) in Tris-buffered saline with Tween20 (TBST; 25mM Tris, 137mM NaCl, 2.7mM KCl, 0.05% (v/v) Tween20, pH 7.4), for one hour at room temperature, followed by incubation in primary antibody solution overnight at 4°C (mouse anti-Total OXPHOS Rodent WB Antibody Cocktail (MS604-300, Abcam, Cambridge, UK; the cocktail contains 5 mAbs, one each against CI subunit NDUFB8, CII-30kDa, CIII-Core protein 2, CIV subunit I and CV alpha subunit) or rabbit anti-PGC-1α antibody (#516557, Calbiochem, Nottingham, United Kingdom) diluted 1:1000 in blocking solution). The next day, membranes were incubated in secondary antibody solution (peroxidase-labeled horse anti-mouse IgG or goat anti-rabbit IgG (PI-2000 and PI-1000, respectively; Vector Laboratories, Burlingame, CA, USA) diluted 1:5000 in blocking solution) for one hour at room temperature before incubation with enhanced chemiluminescence substrate (Pierce SuperSignal West PICO Chemiluminescent

Substrate; Thermo Fisher Scientific). Protein bands were detected using LAS-3000 Luminescent Image Analyzer (Fujifilm, Tokyo, Japan). Bands were quantified using AIDA Image Analyzer software (Fujifilm) and corrected for loading differences by the Ponceau S staining intensity.

Protein oxidation was detected with the Oxyblot kit according to the manufacturer's instructions (Chemicon International, Temecula, CA). Briefly, carbonyl groups in the protein side chains were derivatized to 2,4-dinitrophenylhydrazone (DNP) and immunoblotted according to the procedure described above. In addition, for each animal an underivatized sample was included, for which the derivatized sample was corrected in the analysis. After analysis of oxidation, the blot was reprobed for GAPDH (rabbit anti-GAPDH, #2118; Cell Signaling Technology, Leiden, The Netherlands; procedure as described above) to correct for differences in protein loading.

Gene expression analysis

RNA was extracted from muscle tissue leftovers from cryosectioning using the RNeasy Fibrous Tissue kit (Qiagen, Venlo, The Netherlands) according to the supplier's protocol. Samples were homogenized using a Mini-BeadBeater (BioSpec Products Inc.). After elution, RNA concentration was determined using a spectrophotometer (NanoDrop ND-1000, Isogen Lifescience, IJsselstein, The Netherlands) and integrity verified for a selection of samples by gel electrophoresis and on a Bioanalyzer (Agilent Technologies, Amstelveen, The Netherlands). Approximately 500ng of RNA was reverse transcribed to cDNA with random hexamer primers according to the supplier's protocol (Transcriptor First Strand cDNA Synthesis kit, Roche Diagnostics, Woerden, The Netherlands). RT-qPCR primers were designed based on Ensembl transcript sequences and ordered from Sigma Genosys (Zwijndrecht, The Netherlands). Primer sequences are listed in Table 1. RT-qPCR reactions contained SensiMix SYBR Hi-ROX Kit (Quantace-Bioline, London, UK) with 300nM primers and were run in 384-well MicroAmp Optical 384-Well Reaction Plate (Applied Biosystems, Nieuwerkerk a/d IJssel, The Netherlands) on a 7900HT Fast Real-Time PCR System (Applied Biosystems). Standard curves, prepared from pooled cDNA, and melt curves were analyzed to verify efficiency and specificity of amplification. Seven reference genes (*18s*, *Axin1*, *B2m*, *Canx*, *Ppia*, *Rplp0*, and *Tuba1a*) were measured and stability of expression was assessed by visual inspection of expression differences between the study groups and a stability assessment by geNorm (65). Eventually, six reference genes (all but *Rplp0*) were used to calculate a geNorm factor, which was used to normalize expression levels of the target genes.

Statistics

Comparisons between the groups were made using Kruskal-Wallis non-parametric ANOVA (*post hoc* Mann-Whitney U with Bonferroni correction), which is most appropriate for the current group sizes. Extreme outliers were removed from the analysis. To test the effect of age in the hypoxic group, per age group the values of the hypoxic animals were expressed as a percentage of those of the normoxic animals and compared as said above. Correlations were tested using the Pearson correlation coefficient. Analyses were performed using IBM SPSS Statistics 22.0 (IBM Corp., Armonk, NY). A p-value < 0.05 was considered statistically significant.

Table 1 | Primer sequences used for RT-qPCR

Symbol	Name	Ensembl ID	Forward primer (5'→3')	Reverse primer (5'→3')	Amplicon size (bp)
Axin1	Axin 1	ENSMUSG00000024182	AGTGGATCATTGAGGGAGAGA	GCCCCAGGACGCTCGAT	124
B2m	Beta-2-microglobulin	ENSMUSG00000060802	CTTTCTGGTGCTTGTCTCACTGA	GTATGTTCGGCTTCCCATTCTC	104
Canx	Calnexin	ENSMUSG00000020368	GCAGCGACCTATGATTGACAACC	GCTCCAAACCAATAGCACTGAAAGG	170
Cox5a	Cytochrome c oxidase subunit Va	ENSMUSG00000000088	TGCGAGCATGTAGACCGTTAAAT	GAGGTCCTGCTTTGTCCTTAACA	77
Cyc1	Cytochrome c-1	ENSMUSG00000022551	GCATTCGGAGGGGTTTCCAG	CCGCATGAACATCTCCCCA	176
Esrra	Estrogen-related receptor alpha	ENSMUSG00000024955	GGCGGACGGCAGAAGTACAAA	GCGACACCAGAGCGTTCAC	130
Gabpa	GA binding protein alpha; nuclear respiratory factor 2 alpha	ENSMUSG00000008976	TGCTGCACTGGAAGGCTACA	TTACCCAAACCACCCAATGC	104
mt-Co2	Cytochrome c oxidase subunit II	ENSMUSG00000064354	CCATCCCAGGCCGACTAA	ATTTCAGAGCATTGGCCATAGAA	76
Myh1	Myosin heavy chain 1 (type IIx isoform)	ENSMUSG00000056328	GACAAACTGCAATCAAAGG	TTGGTCACTTTCCTGCACTT	231
Myh2	Myosin heavy chain 2 (type IIa isoform)	ENSMUSG00000033196	CGATGATCTTGCCAGTAATG	ATAACTGAGATACCAGCG	221
Myh4	Myosin heavy chain 4 (type IIb isoform)	ENSMUSG00000057003	AGGGCGGCGGTGGAA	TGGGAATGAGGCATCTGACAA	141
Myh7	Myosin heavy chain 7 (type I isoform)	ENSMUSG00000053093	CAGATCGGGAGAATCAGTCCAT	AGCAAAATATTGGATGACCCTCTTA	89
Ndufb3	NADH dehydrogenase (ubiquinone) 1 beta subcomplex 3	ENSMUSG00000026032	ACAGACAGTGGAAAATTGAAGGG	GCCCATGTATCTCCAAGCCT	110

Table 1 (continued) | Primer sequences used for RT-qPCR

Symbol	Name	Ensembl ID	Forward primer (5'→3')	Reverse primer (5'→3')	Amplicon size (bp)
Nrf1	Nuclear respiratory factor 1	ENSMUSG00000058440	AGCCACATTGGCTGATGCTT	GGTCATTTCACCGCCCTGTA	124
Ppara	Peroxisome proliferator-activated receptor alpha	ENSMUSG00000022383	ACTACGGAGTTCACGCATGTG	TTGTCGTACACCAGCTTCAGC	76
Ppard	Peroxisome proliferator-activated receptor delta	ENSMUSG00000002250	AGGCCCGGAGCATCCTCA	TGGATGACAAAGGGTGCGTTG	55
Pparg	Peroxisome proliferator-activated receptor gamma	ENSMUSG00000000440	CGGAAGCCCTTTGGTGACTT	TGGGCTTCACGTTCAGCAAG	148
Ppargc1a	Peroxisome proliferator-activated receptor gamma coactivator 1 alpha	ENSMUSG00000029167	CAACAATGAGCCTGCGAACA	CTTCATCCACGGGGAGACTG	104
Ppargc1b	Peroxisome proliferator-activated receptor gamma coactivator 1 beta	ENSMUSG00000033871	ACCCTGAGAAAGCGCAATGA	CCCAGATGAGGGAAGGGACT	120
Ppia	Peptidyl-prolyl cis-trans isomerase A; Cyclophilin A	ENSMUSG00000071866	TTCCTCCTTTCACAGAATTATTCCA	CCGCCAGTGCCATTATGG	75
Rn18s	18S ribosomal RNA	*RefSeq NR_003278.1	AGTTAGCATGCCAGAGTCTCG	TGCATGGCCGTTCTTAGTTG	76
Rplp0	Large ribosomal protein P0	ENSMUSG00000067274	GGACCCGAGAAGACCTCCTT	GCACATCACTCAGAATTTCAATGG	85
Sdhb	Succinate dehydrogenase complex, subunit B	ENSMUSG00000009863	AATTTGCCATTTACCGATGGGA	AGCATCCAACACCATAGGTCC	104
Tfam	Mitochondrial transcription factor A	ENSMUSG00000003923	CCGGCAGAGACGGTTAAAAA	TCATCCTTTGCCTCCTGGAA	129
Tuba1a	Tubulin, alpha 1A	ENSMUSG00000072235	CGTAGACCTGGAACCCACGGT	TGCCTGTGATGAGCTGCTCA	86

*no existing Ensembl ID-

RESULTS

Arterial blood gas and hematological adaptations

The arterial blood of hypoxic mice of all ages showed increased acidosis, hypoxemia, and polycythemia (Table 2, Table 3, Table 4).

Body weight

Hypoxia significantly reduced body weight of aged mice (Figure 1A). In response to the initiation of the experiment, hypoxic mice showed a reduced food intake (Figure 1B). However, after approximately 9 days, food intake was normalized to that of normoxic animals and body weight loss after 21 days of hypoxia was significantly stronger in the hypoxic than in the pair-fed aged mice ($p = 0.002$; Figure 1A). Together, these data reveal a food intake-independent effect of hypoxia on body weight.

Fat pad and muscle weights and muscle fiber cross-sectional area

Hypoxia-associated body weight loss was reflected by hypoxia-induced reductions of fat pad (Figure 1C) and muscle weights (Figure 1D); this loss was only partly dependent on the reduced food intake.

Table 2 | Arterial blood gas analysis and hematological adaptations in aged (52 week old) mice.

	Normoxia	Pair-fed	Hypoxia
Arterial blood gas analysis			
pH	7.28 (7.25, 7.30)	7.35 (7.30, 7.37)*	7.10 (7.06, 7.16)$^{*,\#}$
PaO_2, mmHg	129.5 (120.4, 139.1)	133.7 (128.6, 136.5)	33.8 (33.3, 34.4)$^{*,\#}$
$PaCO_2$, mmHg	36.2 (28.1, 41.0)	29.0 (28.3, 34.3)	35.5 (31.3, 37.6)
HCO_3^-, mM	16.3 (13.2, 18.4)	16.5 (16.1, 18.1)	10.4 (9.4, 12.0)$^{*,\#}$
SaO_2, %	101 (100, 101)	102 (101, 102)	24 (19, 27)$^{*,\#}$
Base excess, mEq L^{-1}	−9.9 (−11.7, −7.6)	−7.2 (−8.5, −7.0)	−22.6 (−24.0, −17.7)$^{*,\#}$
Hematological adaptations			
Hematocrit, %	0.46 (0.44, 0.47)	0.45 (0.44, 0.47)	0.76 (0.74, 0.78)$^{*,\#}$
Hemoglobin, mM	9.0 (8.6, 9.5)	8.7 (8.2, 9.3)	14.5 (14.2, 14.7)$^{*,\#}$
Erythrocytes, $\times 10^6$	10.0 (9.4, 10.0)	9.7 (9.5, 10.2)	13.5 (13.3, 13.8)$^{*,\#}$
MCV, fL	45.8 (45.7, 46.1)	46.3 (45.8, 46.9)	55.3 (54.7, 58.4)$^{*,\#}$
MCH, pg	0.91 (0.89, 0.92)	0.89 (0.88, 0.91)	1.08 (1.02, 1.10)$^{*,\#}$
MCHC, g dl^{-1}	20.0 (19.3, 20.2)	19.1 (18.5, 19.7)	19.1 (18.3, 19.6)
*p*50(a)	29.6 (28.7, 30.9)	27.6 (26.8, 29.0)	50.8 (49.9, 51.6)$^{*,\#}$
Spleen (g)	80.6 (66.1, 90.3)	82.7 (77.6, 92.6)	215.1 (159.7, 238.9)$^{*,\#}$

Values are median (25th percentile, 75th percentile). MCV, mean corpuscular volume; MCH, mean corpuscular hemoglobin; MCHC, mean corpuscular hemoglobin concentration. Blood gas data were available for 6 normoxic, 7 pair-fed and 6 hypoxic mice. Level of significance: * $p < 0.05$ compared to normoxic mice, $^{\#}$ $p < 0.05$ compared to pair-fed mice. Data partly overlap with our previous study (63).

Whereas soleus showed a discrepancy between muscle weight and fiber cross-sectional area in the aged mice (Figure 1D and 1E), EDL mean fiber cross-sectional area (Figure 1F) closely resembled the changes in EDL muscle weight (Figure 1D). The fibers in the EDL seemed most affected by hypoxia, with no additional effect of reduced food intake. In the soleus, food intake appears to have a larger role in atrophy, although changes between pair-fed and normoxia are not significant, except for type I/IIa and IIx/b fibers. Overall, hypoxia thus affected muscle fiber cross-sectional area in both a food intake-dependent and -independent manner.

Muscle fiber-type composition and fiber-specific myosin heavy chain (MyHC) expression in skeletal muscle

Hypoxia increased soleus hybrid type I/IIa fiber proportion (Figure 2A). On the level of gene expression, the hypoxic aged mice showed decreased MyHC type IIb in the soleus (Figure 2C) and increased MyHC type I in the EDL (Figure 2D).

Table 3 | Arterial blood gas analysis and hematological adaptations in young (4 week old) mice.

	Normoxia	Pair-fed	Hypoxia
Arterial blood gas analysis			
pH	7.31 (7.26, 7.34)	7.31 (7.26, 7.33)	7.16 (7.09, 7.19)$^{*,\#}$
PaO_2, mmHg	134.9 (132.1, 150.6)	135.6 (131.1, 138.4)	41.9 (37.8, 43.1)$^{*,\#}$
$PaCO_2$, mmHg	23.3 (22.5, 32.3)	30.5 (26.4, 33.0)	28.0 (23.7, 29.0)
HCO_3^-, mM	12.4 (11.2, 13.9)	14.9 (12.9, 16.3)	8.6 (7.6, 10.4)$^{*,\#}$
SaO_2, %	101 (101, 102)	101 (100, 101)	33 (27, 37)$^{*,\#}$
Base excess, mEq L^{-1}	−12.5 (−13.3, −11.3)	−10.2 (−11.7, −8.6)	−21.8 (−25.7, −18.0)$^{*,\#}$
Hematological adaptations			
Hematocrit, %	0.36 (0.35, 0.36)	0.37 (0.36, 0.39)	0.64 (0.61, 0.65)$^{*,\#}$
Hemoglobin, mM	7.9 (7.8, 8.0)	8.4 (8.0, 8.8)	13.8 (13.1, 13.9)$^{*,\#}$
Erythrocytes, $\times 10^6$	8.6 (8.4, 8.8)	9.0 (8.7, 9.3)	13.1 (12.7, 13.3)$^{*,\#}$
MCV, fL	41.3 (41.0, 41.6)	41.4 (41.1, 42.0)	48.2 (47.8, 49.3)$^{*,\#}$
MCH, pg	0.92 (0.91, 0.92)	0.93 (0.91, 0.94)	1.03 (1.02, 1.04)$^{*,\#}$
MCHC, g dl^{-1}	22.3 (21.9, 22.4)	22.3 (22.1, 22.4)	21.3 (21.2, 21.6)$^{*,\#}$
*p*50(a)	28.3 (27.4, 30.2)	28.7 (28.0, 30.1)	53.3 (49.7, 56.6)$^{*,\#}$
Spleen (g)	69.1 (67.5, 71.9)	51.8 (50.2, 57.3)*	73.2 (63.5, 86.1)$^{\#}$

Values are median (25th percentile, 75th percentile). MCV, mean corpuscular volume; MCH, mean corpuscular hemoglobin; MCHC, mean corpuscular hemoglobin concentration. Blood gas data were available for 6 normoxic, 8 pair-fed and 8 hypoxic mice. Level of significance: $^{*}p < 0.05$ compared to normoxic mice, $^{\#}p < 0.05$ compared to pair-fed mice.

Metabolic enzyme activities in skeletal muscle

Phosphofructokinase (PFK) activity was significantly increased by hypoxia in the soleus (Figure 3A) and EDL (Figure 3B) of aged mice. The aged hypoxic mice showed a slight reduction of citrate synthase (CS) activity in the EDL (Figure 3B) but no change in cytochrome *c* oxidase (COX) activity (Figure 3A and Figure 3B). Changes in 3-hydroxyacyl-CoA dehydrogenase (HAD) activity were non-significant.

Protein and gene expression levels of mitochondrial components

To assess whether reduced citrate synthase activity was associated with a reduced mitochondrial content, we measured protein content of five subunits of the oxidative phosphorylation (OXPHOS) chain. There was generally no sign of repressed content of these subunits in soleus (Figure 3C; a representative blot is included in Supplemental Figure 1), nor in EDL (Figure 3D) of aged hypoxic mice. In contrast, gene expression levels of some OXPHOS subunits were repressed (Figure 3E and Figure 3F). These changes were sometimes partly caused by the reduced food intake.

Table 4 | Arterial blood gas analysis and hematological adaptations in adult (12 week old) mice.

	Normoxia	Pair-fed	Hypoxia
Arterial blood gas analysis			
pH	7.38 (7.34, 7.39)	7.31 (7.29, 7.36)*	7.17 (7.14, 7.19)$^{*,\#}$
PaO_2, mmHg	139.5 (132.6, 143.7)	138.9 (132.7, 142.0)	35.9 (34.1, 37.6)$^{*,\#}$
$PaCO_2$, mmHg	27.6 (26.4, 29.6)	28.2 (27.2, 31.2)	30.6 (27.7, 32.4)
HCO_3^-, mM	15.3 (15.0, 16.5)	14.2 (13.8, 15.1)	10.5 (9.9, 11.6)$^{*,\#}$
SaO_2, %	101 (101, 102)	101 (101, 101)	27 (23, 29)$^{*,\#}$
Base excess, mEq L^{-1}	−7.9 (−8.0, −6.7)	−10.2 (−10.8, −9.6)*	−18.1 (−20.7, −17.4)$^{*,\#}$
Hematological adaptations			
Hematocrit, %	0.38 (0.36, 0.42)	0.39 (0.38, 0.50)	0.71 (0.64, 0.77)$^{*,\#}$
Hemoglobin, mM	8.2 (7.8, 8.6)	8.8 (8.6, 10.3)*	14.2 (13.5, 14.6)$^{*,\#}$
Erythrocytes, $\times 10^6$	9.1 (8.9, 9.4)	10.4 (9.5, 11.0)	14.0 (13.5, 14.2)$^{*,\#}$
MCV, fL	40.5 (40.4, 45.1)	40.4 (40.0, 45.7)	50.1 (47.1, 54.5)$^{*,\#}$
MCH, pg	0.88 (0.87, 0.91)	0.91 (0.89, 0.95)	1.01 (0.99, 1.04)$^{*,\#}$
MCHC, g dl^{-1}	21.5 (20.2, 21.8)	22.3 (20.8, 22.6)	20.1 (19.1, 21.3)
*p*50(a)	26.7 (26.3, 28.1)	28.5 (27.0, 29.1)*	51.5 (49.6, 53.2)$^{*,\#}$
Spleen (g)	72.9 (66.5, 74.6)	61.4 (58.8, 66.8)	135.2 (128.7, 194.1)$^{*,\#}$

Values are median (25th percentile, 75th percentile). MCV, mean corpuscular volume; MCH, mean corpuscular hemoglobin; MCHC, mean corpuscular hemoglobin concentration. Blood gas data were available for 7 normoxic, 7 pair-fed and 8 hypoxic mice. Level of significance: * $p < 0.05$ compared to normoxic mice, $^{\#}$ $p < 0.05$ compared to pair-fed mice.

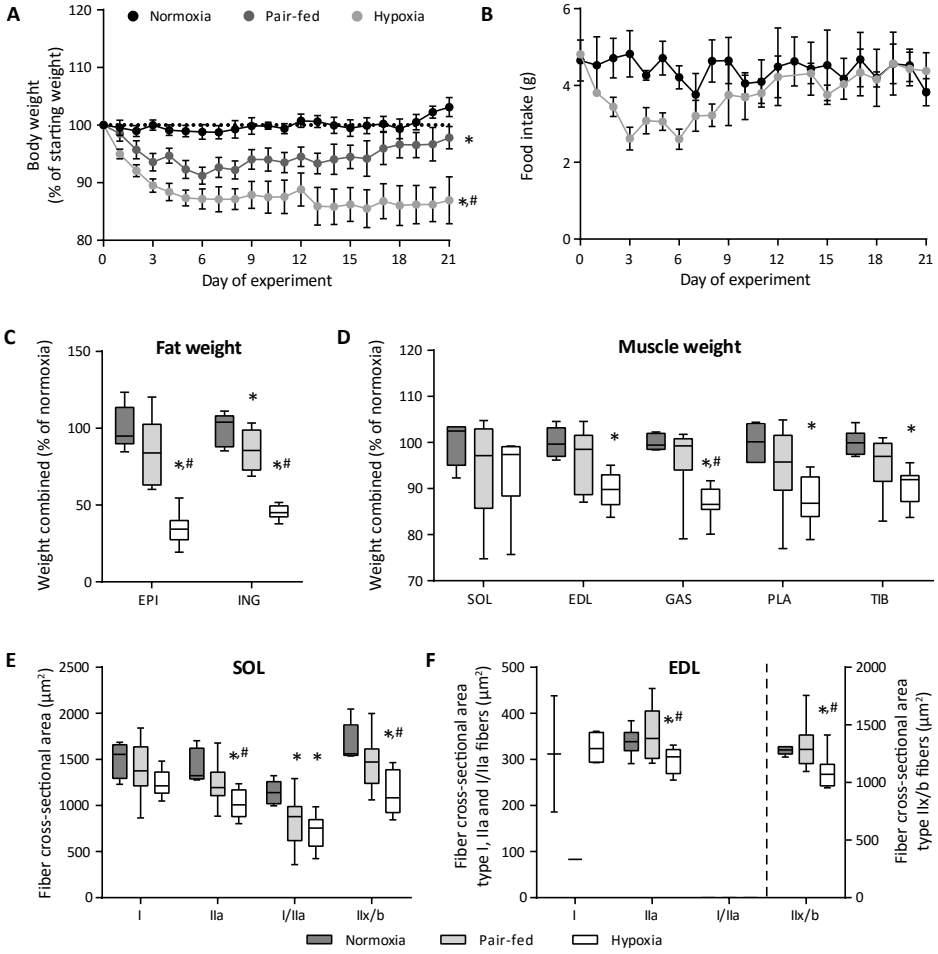

Figure 1 | Aged mice exposed to hypoxia develop cachexia, which is only partly explained by reduced food intake. A, Body weight as percentage of starting weight (mean ± SD). Significance indicated for comparison on day 21. **B**, Food intake was determined per cage and averaged over the number of mice in the cage (mean ± SD). **C**, Paired fat weight of both fat pads per animal. EPI, epididymal fat pad; ING, inguinal fat pad. **D**, Paired muscle weight of both muscles per animal. SOL, soleus; EDL, extensor digitorum longus; GAS, gastrocnemius; PLA, plantaris; TIB, tibialis anterior. **E-F**, Fiber-type specific cross-sectional areas in the soleus (**E**) and EDL (**F**). Number of animals per group: normoxic $n = 6$, pair-fed $n = 8$, hypoxic $n = 8$, except in panel **C**: normoxic $n = 5$. Box plots indicate median and interquartile range, whiskers indicate minimum and maximum. Level of significance: $^{*}p < 0.05$ compared to normoxic mice, $^{\#}p < 0.05$ compared to pair-fed mice. Data in panels A-D partly overlap with our previous study (63).

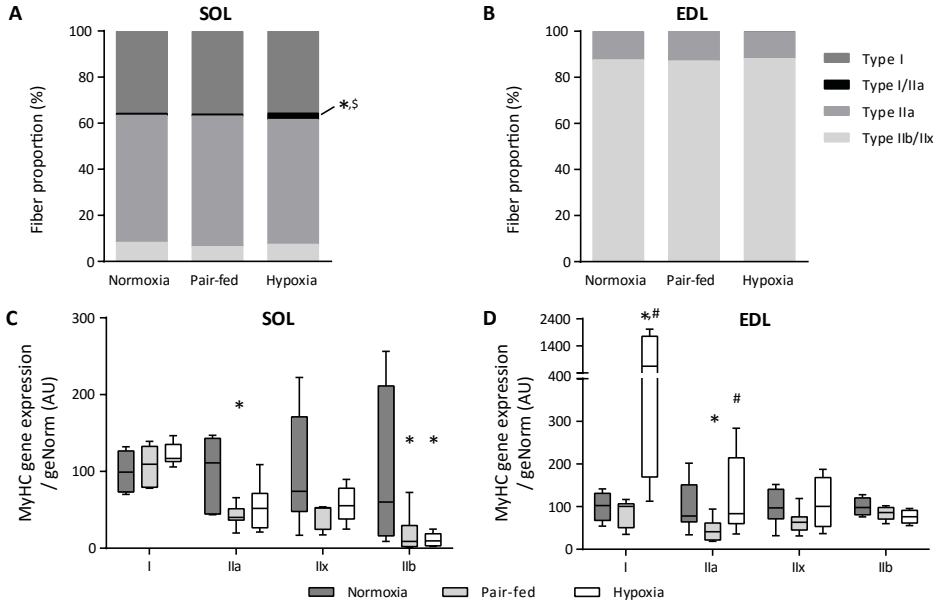

Figure 2 | In aged mice, hypoxia increases type I/IIa hybrid fiber proportion. A-B, Fiber-type composition in the soleus (**A**) and EDL (**B**). **C-D**, Myosin heavy chain gene expression levels in the soleus (**C**) and EDL (**D**). Number of animals per group: normoxic $n = 6$, pair-fed $n = 8$, hypoxic $n = 8$, except in panel **A**: normoxic $n = 5$, panel **C**: pair-fed $n = 7$. Box plots indicate median and interquartile range, whiskers indicate minimum and maximum. Level of significance: $^{*}p < 0.05$ compared to normoxic mice, $^{\#}p < 0.05$ compared to pair-fed mice.

Figure 3 | In aged mice, oxidative capacity is mildly affected by hypoxia. A-B, Metabolic enzyme activity in the soleus (**A**) and EDL (**B**). **C-D**, Protein content of labile subunits of OXPHOS complexes in the soleus (**C**) and EDL (**D**). **E-F**, Gene expression of subunits of OXPHOS complexes in the soleus (**E**) and EDL (**F**). **G and I**, Gene expression of regulators of oxidative metabolism in the soleus (**G**) and EDL (**I**). **H and J**, Protein content of PGC-1α in the soleus (**H**) and EDL (**J**). CS, citrate synthase; HAD, 3-hydroxyacyl-CoA dehydrogenase; COX, cytochrome *c* oxidase; PFK, phosphofructokinase. NDUFB3, OXPHOS complex I; SDHB, OXPHOS complex II; CYC1, OXPHOS complex III; COX-Va, OXPHOS complex IV, nuclear encoded; COX-II, OXPHOS complex IV, mitochondrially encoded; PGC-1, PPAR gamma coactivator 1; PPAR, peroxisome proliferator-activated receptor; ERRα, estrogen-related receptor α; NRF, nuclear respiratory factor; Tfam, mitochondrial transcription factor A. Number of animals per group: normoxic $n = 6$, pair-fed $n = 8$, hypoxic n= 8, except in panel **B**, **D** and **J**: normoxic $n = 5$, panel **B**, **E** and **G**: pair-fed $n = 7$. Box plots indicate median and interquartile range, whiskers indicate minimum and maximum. Level of significance: $^{*}p < 0.05$ compared to normoxic mice, $^{\#}p < 0.05$ compared to pair-fed mice.

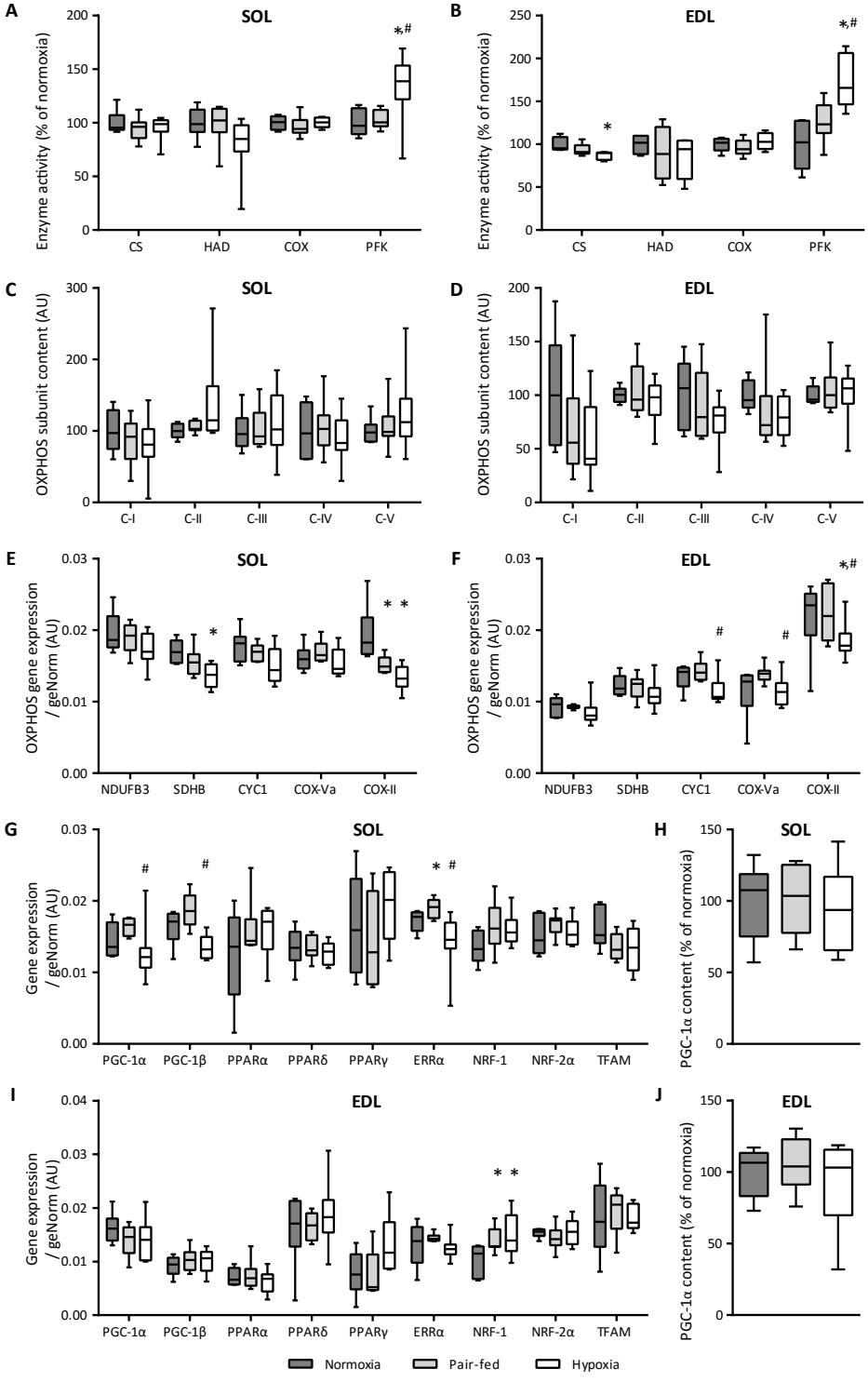
A
SOL
Enzyme activity (% of normoxia)
CS
HAD
COX
PFK
B
EDL
C
SOL
OXPHOS subunit content (AU)
C-I
C-II
C-III
C-IV
C-V
D
EDL
E
SOL
OXPHOS gene expression / geNorm (AU)
NDUFB3
SDHB
CYC1
COX-Va
COX-II
F
EDL
G
SOL
Gene expression / geNorm (AU)
PGC-1α
PGC-1β
PPARα
PPARδ
PPARγ
ERRα
NRF-1
NRF-2α
TFAM
H
SOL
PGC-1α content (% of normoxia)
I
EDL
J
EDL
Normoxia
Pair-fed
Hypoxia

Expression of key regulators of muscle oxidative phenotype in skeletal muscle

Because gene expression of some of the OXPHOS subunits was repressed by hypoxia, we measured gene expression levels of important regulators of oxidative phenotype. Expression of PGC-1α, PGC-1β and ERRα was reduced by hypoxia, but mainly in the soleus of aged mice (Figure 3G). We could however not detect differences in PGC-1α content (Figure 3H).

Age-dependent differences in hypoxia effects on body and muscle composition

Age-related differences of hypoxia-associated changes were observed on body weight, fiber-type composition and OXPHOS gene expression. In response to hypoxia, the aged mice lost body weight, which was still significantly decreased at day 21 compared to the normoxic as well as the pair-fed animals (Figure 1A). In contrast, the body weight of the adult hypoxic mice had recovered by the end of the experiment (Figure 4A). The hypoxic young mice had significantly lower body weights by the end of the experiment, but this was not different compared to pair-fed mice (Figure 5A). In the young mice, reduced body weight appeared to be related to a food-dependent stagnation of growth rather than weight loss as was observed in the aged animals.

Hypoxic mice of all ages showed an increased proportion of hybrid type I/IIa fibers in the soleus (Figure 2, Figure 6 and Figure 7), but in addition the young mice showed a significant decrease of the type IIa fiber proportion (Figure 6A). Furthermore, MyHC type I gene expression was increased in the soleus of young hypoxic mice (Figure 6C). In summary, hypoxia appears to cause a change in soleus fiber-type distribution in mice of all ages, although a direction can only be discerned in the young mice: the increased hybrid type I/IIa and decreased type II proportions combined with the increased gene expression levels of type I MyHC appear to indicate a fiber shift from type IIa fibers towards hybrid type I/IIa fibers. The more apparent fiber-type changes in the young mice were in contrast to the hypoxia-associated repression of OXPHOS subunit gene expression, which was generally strongest in the aged hypoxic mice (Figure 3, Figure 8 and Figure 9).

Protein oxidation of muscle proteins

To assess whether oxidative stress was increased in the muscle after exposure to hypoxia, we measured protein carbonylation in the soleus and EDL (Figure 10). There were no significant differences, except for the EDL of 4-week old mice, where oxidation was significantly lower with pair-feeding and hypoxia. Protein carbonylation in the EDL of 4-week old mice correlated significantly with COX activity (Figure 10C).

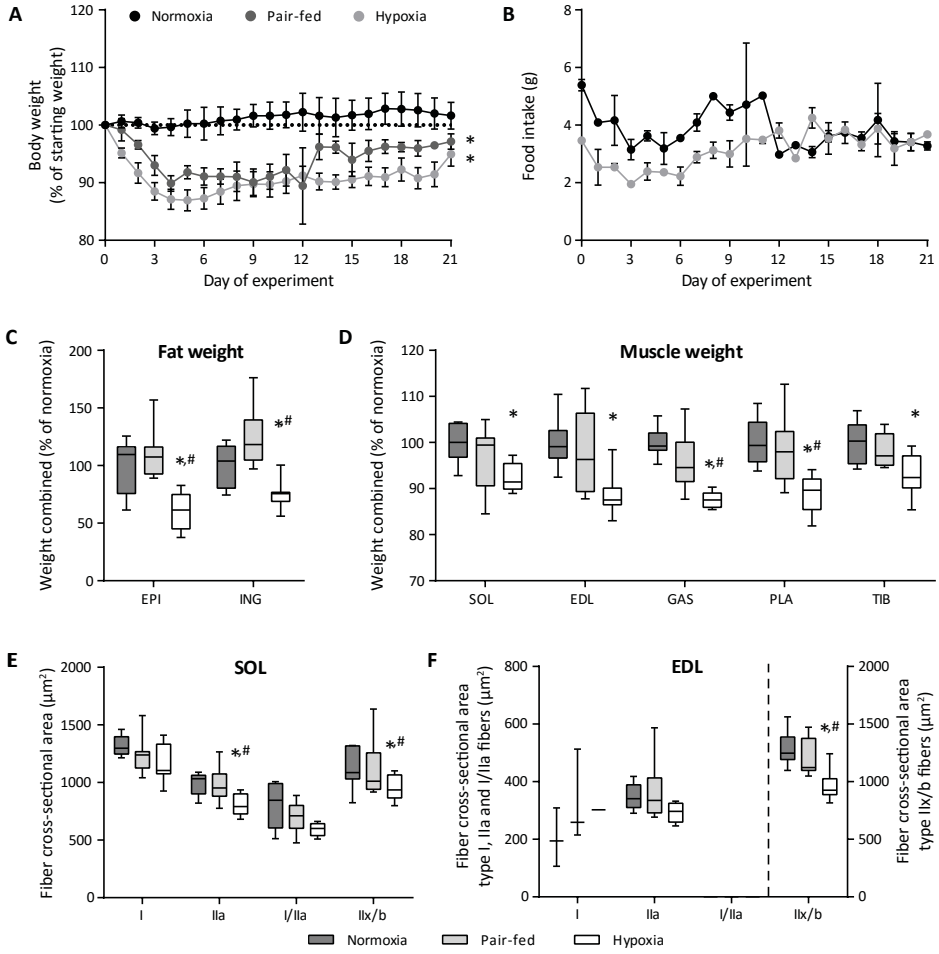

Figure 4 | Adult mice exposed to hypoxia develop cachexia, which is only partly explained by reduced food intake. A, Body weight as percentage of starting weight (mean ± SD). Significance indicated for comparison on day 21. **B**, Food intake was determined per cage and averaged over the number of mice in the cage (mean ± SD). Note that half of the adult pair-fed mice were accidentally deprived of food on day 11 and consequently had lower body weight on day 12. On day 12 extra food was provided to compensate; this is reflected by the steep weight gain on day 13. **C**, Paired fat weight of both fat pads per animal. EPI, epididymal fat pad; ING, inguinal fat pad. **D**, Paired muscle weight of both muscles per animal. SOL, soleus; EDL, extensor digitorum longus; GAS, gastrocnemius; PLA, plantaris; TIB, tibialis anterior. **E-F**, Fiber-type specific cross-sectional areas in the soleus (**E**) and EDL (**F**). Number of animals per group: normoxic $n = 8$, pair-fed $n = 8$, hypoxic $n = 8$, except in panel **E** and **F**: normoxic $n = 7$, panel **E**: pair-fed $n = 7$. Box plots indicate median and interquartile range, whiskers indicate minimum and maximum. Level of significance: * $p < 0.05$ compared to normoxic mice, $^{\#}$ $p < 0.05$ compared to pair-fed mice.

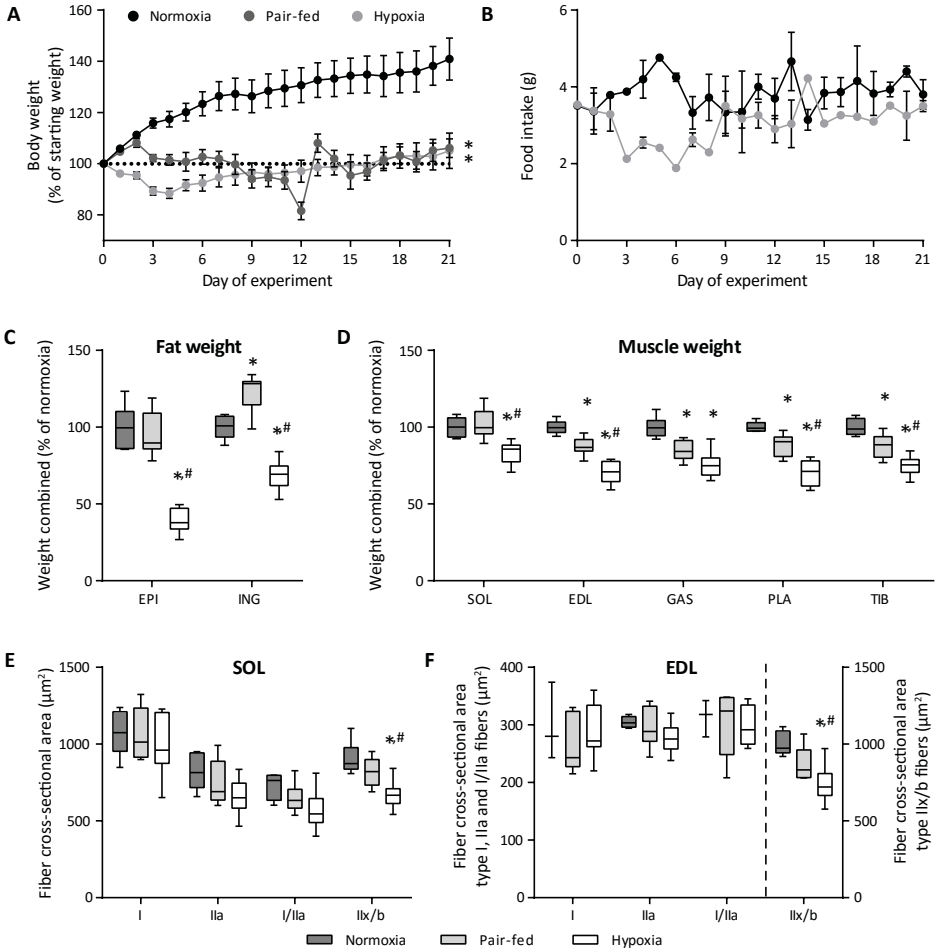

Figure 5 | Young mice exposed to hypoxia show growth stagnation due to hypofagia, but also experience food intake-independent loss of fat and muscle weight. A, Body weight as percentage of starting weight (mean ± SD). Significance indicated for comparison on day 21. **B**, Food intake was determined per cage and averaged over the number of mice in the cage (mean ± SD). Note that all young pair-fed mice were accidentally deprived of food on day 11 and consequently had lower body weight on day 12. On day 12 extra food was provided to compensate; this is reflected by the steep weight gain on day 13. **C**, Paired fat weight of both fat pads per animal. EPI, epididymal fat pad; ING, inguinal fat pad. **D**, Paired muscle weight of both muscles per animal. ESOL, soleus; EDL, extensor digitorum longus; GAS, gastrocnemius; PLA, plantaris; TIB, tibialis anterior. **E-F**, Fiber-type specific cross-sectional areas in the soleus (**E**) and EDL (**F**). Number of animals per group: normoxic $n = 6$, pair-fed $n = 8$, hypoxic $n = 9$, except in panel **A** and **F**: hypoxic $n = 8$, panel **E**: pair-fed $n = 7$, panel **F**: normoxic $n = 5$. Box plots indicate median and interquartile range, whiskers indicate minimum and maximum. Level of significance: $^{*}p < 0.05$ compared to normoxic mice, $^{\#}p < 0.05$ compared to pair-fed mice.

DISCUSSION

In this study we show that three weeks of hypoxia only mildly attenuates muscle oxidative phenotype in mice, whereas muscle weight and fat weight are clearly decreased in a hypoxia-dependent manner. Moreover, hypoxia-associated changes were age-dependent: altered fiber-type composition was most prominent in young mice, whereas aged mice specifically show hypoxia-associated reductions of mitochondrial regulators and components.

In the current study we aimed to establish the effect of hypoxia on muscle oxidative phenotype in aged mice to be able to translate these findings to patients with COPD and chronic respiratory failure, which predominates in the older population. Hence, we mainly focused on 52-week old mice in this study. Ishihara *et al.* indeed showed that the age of rats exposed to hypoxia affects how hypoxia impacts muscle fiber-type composition (32). Limb muscles of rats undergo a postnatal shift from glycolytic to oxidative fiber types (67). Hypoxia exposure during this developmental period supposedly inhibits this shift and results in a smaller proportion of oxidative fibers in hypoxic young rats (32). However, Wigston *et al.* showed that murine postnatal development of the muscle does not include a shift in fiber type towards oxidative fibers (67). Therefore, an inhibition of such developmental shift by hypoxia is not to be expected in mice. Nevertheless, we found an effect of age on the hypoxia response, because changes in fiber-type composition were more prominent, albeit still modest, in the youngest mice. This is potentially related to a higher adaptive plasticity of muscle

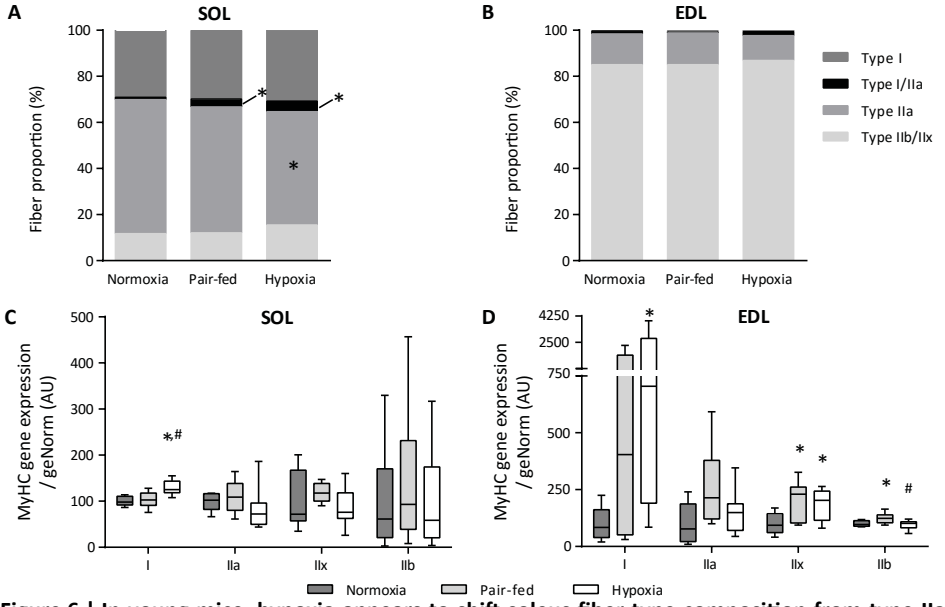

Figure 6 | In young mice, hypoxia appears to shift soleus fiber-type composition from type IIa to type I/IIa hybrid fibers. A-B, Fiber-type composition in the soleus (**A**) and EDL (**B**). **C-D**, Myosin heavy chain gene expression levels in the soleus (**C**) and EDL (**D**). Number of animals per group: normoxic *n* = 6, pair-fed *n* = 8, hypoxic *n* = 9, except in panel **A**: pair-fed *n* = 7, panel **B**: normoxic *n* = 5 and hypoxic *n* = 8. Box plots indicate median and interquartile range, whiskers indicate minimum and maximum. Level of significance: $^{*}p < 0.05$ compared to normoxic mice, $^{\#}p < 0.05$ compared to pair-fed mice.

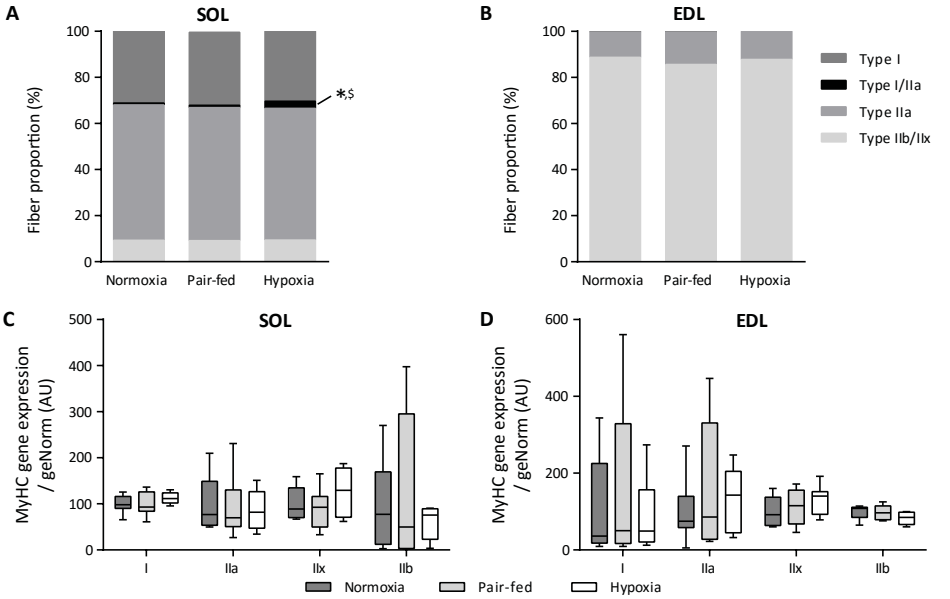

Figure 7 | In adult mice, hypoxia increases type I/IIa hybrid fiber proportion. A-B, Fiber-type composition in the soleus (**A**) and EDL (**B**). **C-D**, Myosin heavy chain gene expression levels in the soleus (**C**) and EDL (**D**). Number of animals per group: normoxic $n = 8$, pair-fed $n = 8$, hypoxic $n = 8$, except for panel **A** and **B**: normoxic $n = 7$, panel **-**: pair-fed $n = 7$. Box plots indicate median and interquartile range, whiskers indicate minimum and maximum. Level of significance: $^{*}p < 0.05$ compared to normoxic mice, $^{\#}p < 0.05$ compared to pair-fed mice.

Figure 8 | In young mice, oxidative capacity is only mildly affected by hypoxia. A-B, Metabolic enzyme activity in the soleus (**A**) and EDL (**B**). **C-D**, Protein content of labile subunits of OXPHOS complexes in the soleus (**C**) and EDL (**D**). **E-F**, Gene expression of subunits of OXPHOS complexes in the soleus (**E**) and EDL (**F**). **G and I**, Gene expression of regulators of oxidative metabolism in the soleus (**G**) and EDL (**I**). **H and J**, Protein content of PGC-1α in the soleus (**H**) and EDL (**J**). CS, citrate synthase; HAD, 3-hydroxyacyl-CoA dehydrogenase; COX, cytochrome *c* oxidase; PFK, phosphofructokinase. NDUFB3, OXPHOS complex I; SDHB, OXPHOS complex II; CYC1, OXPHOS complex III; COX-Va, OXPHOS complex IV, nuclear encoded; COX-II, OXPHOS complex IV, mitochondrially encoded; PGC-1, PPAR gamma coactivator 1; PPAR, peroxisome proliferator-activated receptor; ERRα, estrogen-related receptor α; NRF, nuclear respiratory factor; Tfam, mitochondrial transcription factor A. Number of animals per group: normoxic $n = 6$, pair-fed $n = 8$, hypoxic $n = 9$. Box plots indicate median and interquartile range, whiskers indicate minimum and maximum. Level of significance: $^{*}p < 0.05$ compared to normoxic mice, $^{\#}p < 0.05$ compared to pair-fed mice.

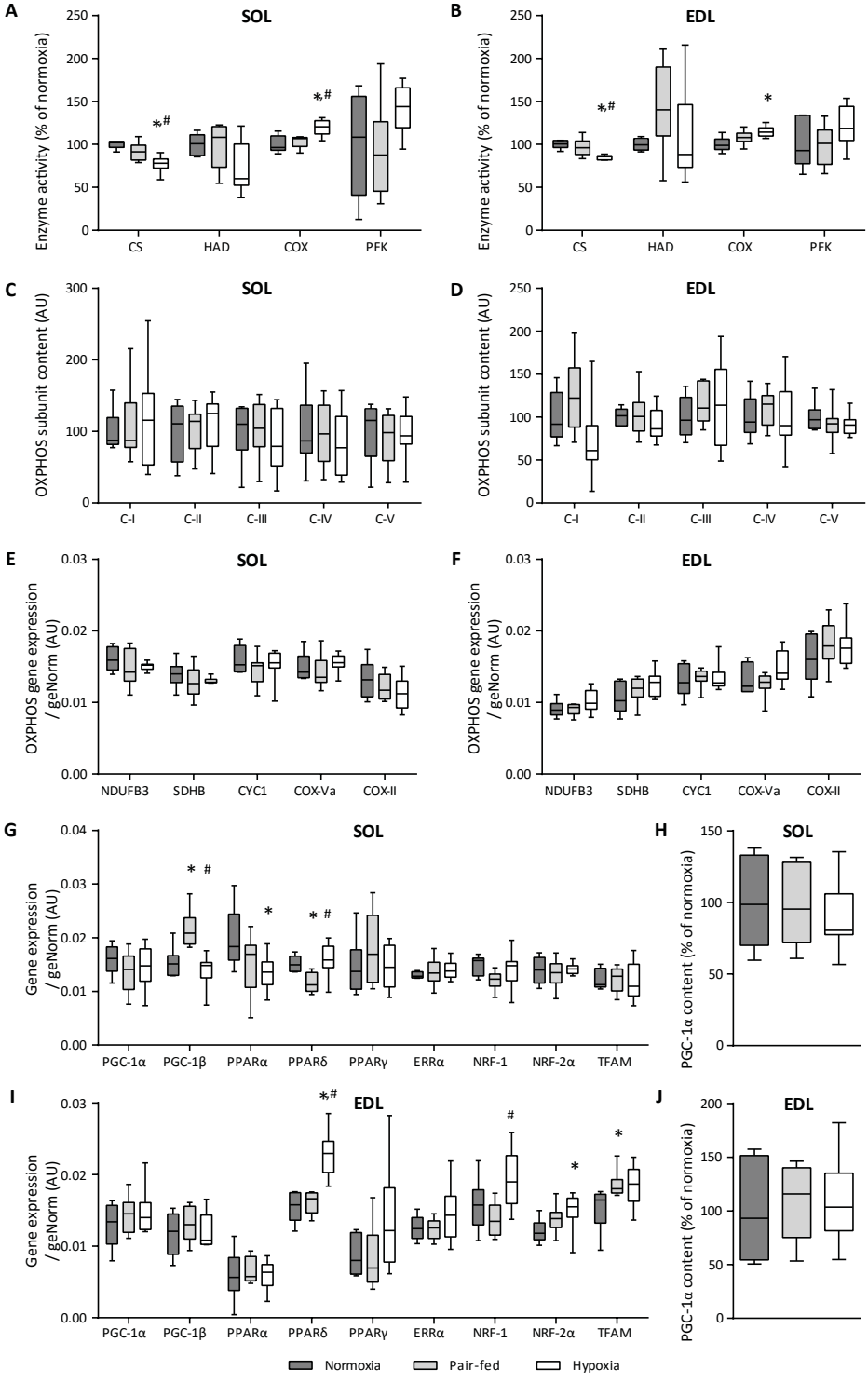
A
SOL
Enzyme activity (% of normoxia)
CS
HAD
COX
PFK
B
EDL
C
SOL
OXPHOS subunit content (AU)
C-I
C-II
C-III
C-IV
C-V
D
EDL
E
SOL
OXPHOS gene expression / geNorm (AU)
NDUFB3
SDHB
CYC1
COX-Va
COX-II
F
EDL
G
SOL
Gene expression / geNorm (AU)
PGC-1α
PGC-1β
PPARα
PPARδ
PPARγ
ERRα
NRF-1
NRF-2α
TFAM
H
SOL
PGC-1α content (% of normoxia)
I
EDL
J
EDL
Normoxia
Pair-fed
Hypoxia

in young compared to old mice, analogous to what has been observed in response to electrical stimulation (42) and denervation (46).

Interestingly, the young mice exposed to hypoxia appear to shift towards type I/IIa fibers in the soleus, with a concomitant reduction of the proportion of type IIa fibers, suggesting co-expression of MyHC I in IIa fibers. It should be noted that the proportion of type I/IIa fibers is still small (median 4.2%, interquartile range [1.85; 6.34]). An increase of MyHC I expression is however in line with our recent *in vitro* findings, where hypoxia exposure of C2C12 myotubes stimulated the expression of type I MyHC gene and protein (57). In soleus muscle of mice, it has been shown that type IIa fibers have a higher oxidative potential than type I fibers (7). Moreover, Gouspillou *et al.* recently reported on variations in rodent and human muscle fiber types: whereas mouse type IIa fibers have a higher mitochondrial content than type I, in human muscle type I is more enriched in mitochondria than type IIa (22). Therefore, a shift from type IIa fibers to type I/IIa fibers and/or type IIx/b fibers in mouse could be adaptive to decrease oxidative phenotype in the muscle in response to reduced oxygen supply. This would be analogous to a type I to II fiber-type shift in the skeletal muscle of COPD patients, where fibers also shift towards less oxidative types. The finding that fiber-type changes appear more prominent in the young mice suggests that hypoxia mainly affects developing muscle fibers and could implicate that hypoxia-associated fiber-type changes occur during the muscle regeneration phase in patients with COPD.

Although the changes in fiber-type composition are associated with decreased citrate synthase activity, no change in protein expression levels of OXPHOS subunits was apparent. In contrast, patients with mild to moderate COPD were shown to have decreased content of several OXPHOS subunits in the quadriceps muscle (64). Possibly, the changes in the hypoxic mice are modest due to the relative short period of hypoxia exposure. Expression of PGC-1α, PGC-1β and ERRα, which are important regulators of mitochondrial biogenesis (3, 54, 68), was repressed in the aged mice. This is in line with the reduced gene expression of OXPHOS subunits in soleus of the aged mice and could indicate that changes were still under way. In line with results in patients with chronic respiratory failure, we found that cytochrome *c* oxidase (COX) activity was significantly increased in the young hypoxic mice. In the patients, COX activity inversely correlates with arterial oxygen pressure (52). Altogether, hypoxia-associated changes of muscle

Figure 9 | In adult mice, oxidative capacity is marginally affected by hypoxia. A-B, Metabolic enzyme activity in the soleus (**A**) and EDL (**B**). **C-D**, Protein content of labile subunits of OXPHOS complexes in the soleus (**C**) and EDL (**D**). **E-F**, Gene expression of subunits of OXPHOS complexes in the soleus (**E**) and EDL (**F**). **G and I**, Gene expression of regulators of oxidative metabolism in the soleus (**G**) and EDL (**I**). **H and J**, Protein content of PGC-1α in the soleus (**H**) and EDL (**J**). CS, citrate synthase; HAD, 3-hydroxyacyl-CoA dehydrogenase; COX, cytochrome *c* oxidase; PFK, phosphofructokinase. NDUFB3, OXPHOS complex I; SDHB, OXPHOS complex II; CYC1, OXPHOS complex III; COX-Va, OXPHOS complex IV, nuclear encoded; COX-II, OXPHOS complex IV, mitochondrially encoded; PGC-1, PPAR gamma coactivator 1; PPAR, peroxisome proliferator-activated receptor; ERRα, estrogen-related receptor α; NRF, nuclear respiratory factor; Tfam, mitochondrial transcription factor A. Number of animals per group: normoxic $n = 8$, pair-fed $n = 8$, hypoxic $n = 8$. Box plots indicate median and interquartile range, whiskers indicate minimum and maximum. Level of significance: $^{*}p < 0.05$ compared to normoxic mice, $^{\#}p < 0.05$ compared to pair-fed mice.

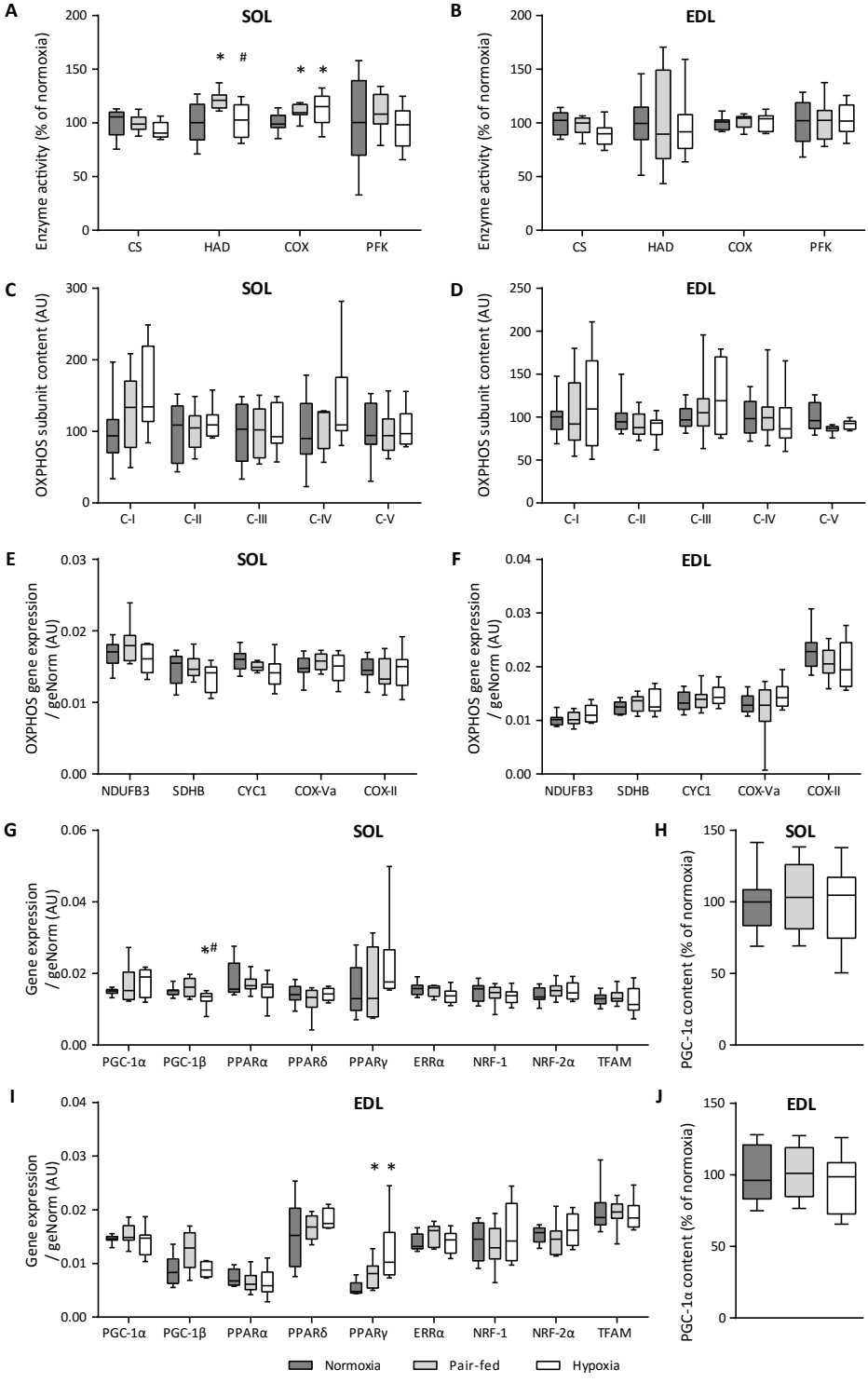
A
SOL
Enzyme activity (% of normoxia)
CS
HAD
COX
PFK
B
EDL
C
SOL
OXPHOS subunit content (AU)
C-I
C-II
C-III
C-IV
C-V
D
EDL
E
SOL
OXPHOS gene expression / geNorm (AU)
NDUFB3
SDHB
CYC1
COX-Va
COX-II
F
EDL
G
SOL
Gene expression / geNorm (AU)
PGC-1α
PGC-1β
PPARα
PPARδ
PPARγ
ERRα
NRF-1
NRF-2α
TFAM
H
SOL
PGC-1α content (% of normoxia)
I
EDL
J
EDL
Normoxia
Pair-fed
Hypoxia

Oxphen appear subtle in the mice, which is in line with the modest response of HIF-1 signaling in response to hypoxia in human skeletal muscle (43) as well as our recent finding that hypoxia-associated changes of OXPHOS and MyHCI gene expression *in vitro* were HIF-dependent (57).

Hypoxia stimulated fiber atrophy in both soleus and EDL. Again, age appeared to affect the hypoxia effect, as the strongest decrease of cross-sectional area appeared to occur in the aged mice, but this difference between age groups was not significant (data not shown). Especially the type II fibers were prone to atrophy. This is in line with skeletal muscle of patients with COPD, where atrophy is most pronounced in type II fibers (19). A sensitivity of glycolytic fibers for hypoxia-associated atrophy has been reported before (13). Hypoxia has been shown to induce expression of myostatin (MSTN) (24). Moreover, MSTN expression is positively correlated to MyHC type IIb content (9). These two observations may explain why type II fibers are more prone to hypoxia-associated fiber atrophy. Interestingly, Hayot *et al.* showed increased MSTN expression in chronic hypoxemic COPD patients as well (24).

The difference in muscle weight between normoxic and hypoxic animals was largest in the young mice. Possibly this is the result of retarded growth rather than increased weight loss. This suggestion is indeed supported by the body weight response, which shows growth retardation rather than weight loss in both pair-fed and hypoxic young mice; the similar body weights in pair-fed and hypoxic mice indicate that growth retardation occurred mainly due to reduced food intake and not due to hypoxia *per se*. In the adult mice, reduced food intake was also the main reason for loss of body weight. However, in the aged mice hypoxia had an additive effect to reduced food intake on the body weight loss, which suggests that aged mice are more susceptible to hypoxia-associated weight loss. Interestingly, weights of the epididymal and inguinal fat depots in the hypoxic mice were significantly reduced compared to those of both pair-fed and normoxic mice. This suggests that fat weight is lost in the hypoxic animals independent of the reduced food intake. Possibly, this is an indication of an altered metabolic rate under influence of hypoxia. Indeed, we recently reported increased expression of oxidative metabolic markers and lipolysis genes in the fat depots in hypoxia-exposed aged mice (63). The increased lipolysis could result in more circulating fatty acids that in turn stimulate expression of oxidative type I MyHC in the muscle, possibly through PPARδ which has been shown to shift MyHC content to slower isoforms (44). Moreover, chronic administration of arachidonic acid to aged rats has been shown to increase the number of MyHCI-positive cells and increase the relative content of MyHCIIx while reducing MyHCIIb content (30).

We found that muscle of aged mice was most affected by hypoxia both in terms of markers of oxidative capacity and fiber cross-sectional area. We expected that muscle of young mice would be characterized by a stronger adaptive plasticity, because increasing age has been shown to reduce the amplitude of adaptations in response to stresses such as limb ischemia, chronic electrical stimulation and disuse caused by denervation (42, 46, 50, 51). For example, attenuated hypoxia-associated induction of VEGF expression has been shown in aged rabbits (50). This was associated with reduced HIF-1 activity (50) and is suggested to explain the impairment of angiogenesis in response to ischemia in old compared to young mice and rabbits (51). This could imply that young mice adapt better to hypoxic conditions by improving capillarization and therefore can maintain

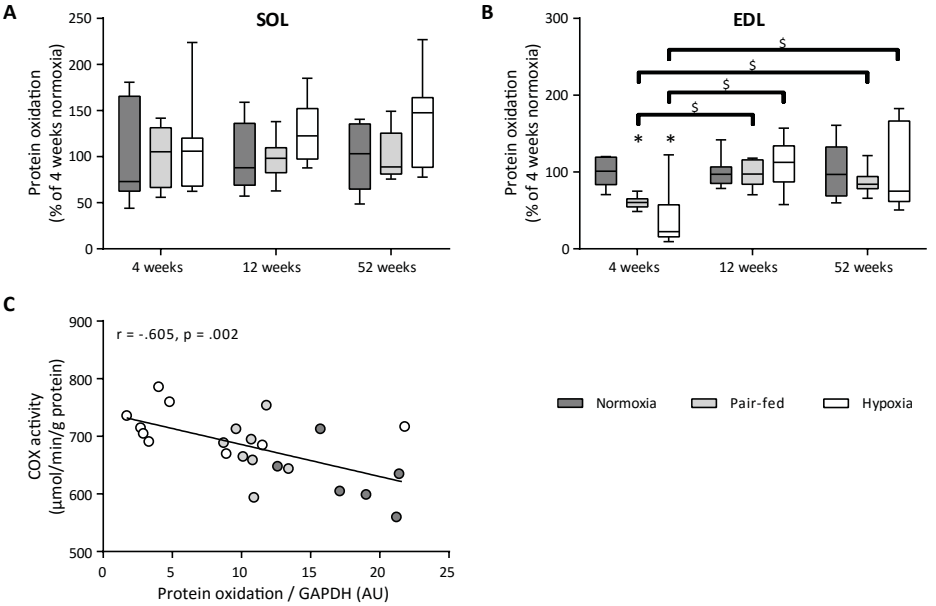

Figure 10 | Protein oxidation is only affected by hypoxia in the EDL of young mice. Protein carbonylation measured by Oxyblot in soleus (**A**) and EDL (**B**) lysates. **C**, Correlation of protein oxidation with cytochrome *c* oxidase (COX) activity in the EDL of 4-week old mice. Number of animals per group: panel **A** 4 weeks normoxic *n* = 6, pair-fed *n* = 8, hypoxic *n* = 8; 12 weeks normoxic *n* = 8, pair-fed *n* = 7, hypoxic *n* = 8; 52 weeks normoxic *n* = 6, pair-fed *n* = 8, hypoxic *n* = 7; panel **B** 4 weeks normoxic *n* = 6, pair-fed *n* = 8, hypoxic *n* = 9; 12 weeks normoxic *n* = 8, pair-fed *n* = 7, hypoxic *n* = 8; 52 weeks normoxic *n* = 5, pair-fed *n* = 7, hypoxic *n* = 8; panel **C** 4 weeks normoxic *n* = 6, pair-fed *n* = 8, hypoxic *n* = 9. Box plots indicate median and interquartile range, whiskers indicate minimum and maximum. Level of significance: $^{*}p < 0.05$ compared to normoxic mice of that particular age, $^{\$}p < 0.05$ compared to 4-week old mice in that particular condition.

Oxphen status. An impaired capillary adaptability in the aged mice could thus underlie the more pronounced loss of muscle Oxphen observed in these mice.

Another explanation for the stronger effects of hypoxia in the aged mice is accumulation of oxidative stress-derived damage during their life. Postmitotic cells have been shown to be more prone to accumulate oxidative damage (48). This damage could make the cells more sensitive to hypoxia or less effective in compensation of hypoxia-associated stress. Moreover, it has been shown that oxidatively modified proteins are prone to degradation (47, 58), which could explain the increased fiber atrophy in hypoxic aged mice. However, we could not detect a significant difference between the levels of skeletal muscle protein carbonylation in the normoxic mice of the three age groups. Unexpectedly though, the young mice showed a decreased level of protein carbonylation in the EDL muscle with pair-feeding and hypoxia, in contrast to the adult and aged pair-fed and hypoxic mice in which protein carbonylation was unchanged. The protein carbonylation in the young mice correlated with COX activity, which was increased in the 4-week old mice after hypoxia exposure. Fukuda *et al.* have reported that hypoxia stimulates the HIF-dependent replacement of COX IV isoform 1 (COX IV-1) with COX IV isoform 2 (COX IV-2) to optimize efficiency of respiration at lower oxygen concentrations

(17). COX containing the COX IV-2 isoform has been shown to be more active under hypoxic conditions than COX with the COX IV-1 isoform, but also to produce less H_2O_2 in hypoxia (17). A change in the composition of the COX protein complex could thus explain both increased COX activity and lower protein carbonylation. Future research will have to prove whether the replacement of COX IV-1 with COX IV-2 occurs in mouse muscle *in vivo* and can account for the decrease in protein carbonylation as observed in this study. However, in mouse sternohyoid muscle (40) and heart (2), 2-3 weeks of hypoxia has previously been shown to increase protein carbonylation. It is unclear whether our results diverge from the literature due to a difference in muscle type (skeletal muscle *vs.* respiratory muscle and heart), as reports on protein carbonylation in skeletal muscle after chronic hypoxia are missing. Alternatively, increased hypoxia-associated oxidative stress is resolved during the three weeks of exposure. Previous work from our group showed that muscle atrophy already is ongoing at 4 days into the experiment (13). Therefore, we are unable to disprove that a transient increase of carbonylated protein underlies muscle atrophy in our model.

The differential response of the muscle of young, adult, and aged mice to hypoxia suggests that age does matter and that the aged mouse is indeed a better model for translation of findings to elderly patients with chronic respiratory disease. In addition to the role of hypoxia in the cachectic processes of muscle and fat weight loss, we now also show that hypoxia can reduce expression of markers of mitochondrial metabolism and shift oxidative fiber types to less oxidative types. Hypoxia-associated effects on Oxphen are subtle, but compared to the clinical situation of patients with COPD, loss of Oxphen in this model occurred in a relatively short time period.

REFERENCES

1. Abdelmalki A, Fimbel S, Mayet-Sornay MH, Sempore B, and Favier R. Aerobic capacity and skeletal muscle properties of normoxic and hypoxic rats in response to training. Pflugers Arch 431: 671-679, 1996.
2. Ashmore T, Fernandez BO, Branco-Price C, West JA, Cowburn AS, Heather LC, Griffin JL, Johnson RS, Feelisch M, and Murray AJ. Dietary nitrate increases arginine availability and protects mitochondrial complex I and energetics in the hypoxic rat heart. J Physiol 592: 4715-4731, 2014.
3. Bastin J, Aubey F, Rotig A, Munnich A, and Djouadi F. Activation of peroxisome proliferator-activated receptor pathway stimulates the mitochondrial respiratory chain and can correct deficiencies in patients' cells lacking its components. J Clin Endocrinol Metab 93: 1433-1441, 2008.
4. Batt J, Ahmed SS, Correa J, Bain A, and Granton J. Skeletal muscle dysfunction in idiopathic pulmonary arterial hypertension. Am J Respir Cell Mol Biol 50: 74-86, 2014.
5. Bergmeyer HU, Gawehn K, and Grassl M. 3-Hydroxyacyl-CoA dehydrogenase. In: Methods of enzymatic analysis, edited by Bergmeyer HU. Weinheim; Germany: Verlag Chemie GmbH, 1974, p. 474.
6. Bigard AX, Sanchez H, Birot O, and Serrurier B. Myosin heavy chain composition of skeletal muscles in young rats growing under hypobaric hypoxia conditions. J Appl Physiol (1985) 88: 479-486, 2000.
7. Bloemberg D, and Quadrilatero J. Rapid determination of myosin heavy chain expression in rat, mouse, and human skeletal muscle using multicolor immunofluorescence analysis. PLoS One 7: e35273, 2012.
8. Boutellier U, Howald H, di Prampero PE, Giezendanner D, and Cerretelli P. Human muscle adaptations to chronic hypoxia. Prog Clin Biol Res 136: 273-285, 1983.
9. Carlson CJ, Booth FW, and Gordon SE. Skeletal muscle myostatin mRNA expression is fiber-type specific and increases during hindlimb unloading. Am J Physiol 277: R601-606, 1999.
10. Crul T, Testelmans D, Spruit MA, Troosters T, Gosselink R, Geeraerts I, Decramer M, and Gayan-Ramirez G. Gene expression profiling in vastus lateralis muscle during an acute exacerbation of COPD. Cell Physiol Biochem 25: 491-500, 2010.
11. De Palma S, Ripamonti M, Vigano A, Moriggi M, Capitanio D, Samaja M, Milano G, Cerretelli P, Wait R, and Gelfi C. Metabolic modulation induced by chronic hypoxia in rats using a comparative proteomic analysis of skeletal muscle tissue. J Proteome Res 6: 1974-1984, 2007.
12. de Theije C, Costes F, Langen RC, Pison C, and Gosker HR. Hypoxia and muscle maintenance regulation: implications for chronic respiratory disease. Curr Opin Clin Nutr Metab Care 14: 548-553, 2011.
13. de Theije CC, Langen RC, Lamers WH, Gosker HR, Schols AM, and Kohler SE. Differential sensitivity of oxidative and glycolytic muscles to hypoxia-induced muscle atrophy. J Appl Physiol (1985) 118: 200-211, 2015.
14. Decramer M, De Benedetto F, Del Ponte A, and Marinari S. Systemic effects of COPD. Respir Med 99 Suppl B: S3-10, 2005.
15. Faucher M, Guillot C, Marqueste T, Kipson N, Mayet-Sornay MH, Desplanches D, Jammes Y, and Badier M. Matched adaptations of electrophysiological, physiological, and histological properties of skeletal muscles in response to chronic hypoxia. Pflugers Arch 450: 45-52, 2005.
16. Filley GF, Beckwitt HJ, Reeves JT, and Mitchell RS. Chronic obstructive bronchopulmonary disease. II. Oxygen transport in two clinical types. Am J Med 44: 26-38, 1968.
17. Fukuda R, Zhang H, Kim JW, Shimoda L, Dang CV, and Semenza GL. HIF-1 regulates cytochrome oxidase subunits to optimize efficiency of respiration in hypoxic cells. Cell 129: 111-122, 2007.
18. Gohil K, Edwards RHT, and Jones DA. Analysis of muscle mitochondrial function with techniques applicable to needle biopsy samples. Clin Physiol 1: 195-207, 1981.
19. Gosker HR, Engelen MP, van Mameren H, van Dijk PJ, van der Vusse GJ, Wouters EF, and Schols AM. Muscle fiber type IIX atrophy is involved in the loss of fat-free mass in chronic obstructive pulmonary disease. Am J Clin Nutr 76: 113-119, 2002.
20. Gosker HR, van Mameren H, van Dijk PJ, Engelen MP, van der Vusse GJ, Wouters EF, and Schols AM. Skeletal muscle fibre-type shifting and metabolic profile in patients with chronic obstructive pulmonary disease. Eur Respir J 19: 617-625, 2002.
21. Gosker HR, Wouters EF, van der Vusse GJ, and Schols AM. Skeletal muscle dysfunction in chronic obstructive pulmonary disease and chronic heart failure: underlying mechanisms and therapy perspectives. Am J Clin Nutr 71: 1033-1047, 2000.
22. Gouspillou G, Sgarioto N, Norris B, Barbat-Artigas S, Aubertin-Leheudre M, Morais JA, Burelle Y, Taivassalo T, and Hepple RT. The relationship between muscle fiber type-specific PGC-1alpha content and mitochondrial content varies between rodent models and humans. PLoS One 9: e103044, 2014.
23. Green HJ, Sutton JR, Cymerman A, Young PM, and Houston CS. Operation Everest II: adaptations in human skeletal muscle. J Appl Physiol (1985) 66: 2454-2461, 1989.
24. Hayot M, Rodriguez J, Vernus B, Carnac G, Jean E, Allen D, Goret L, Obert P, Candau R, and Bonnieu A. Myostatin up-regulation is associated with the skeletal muscle response to hypoxic stimuli. Mol Cell Endocrinol 332: 38-47, 2011.
25. Herridge MS, Cheung AM, Tansey CM, Matte-Martyn A, Diaz-Granados N, Al-Saidi F, Cooper AB, Guest CB, Mazer CD, Mehta S, Stewart TE, Barr A, Cook D, Slutsky AS, and Canadian Critical Care Trials G. One-year outcomes in survivors of the acute respiratory distress syndrome. N Engl J Med 348: 683-693, 2003.
26. Hirofuji C, Ishihara A, Itoh K, Itoh M, Taguchi S, and Takeuchi-Hayashi H. Fibre type composition of the soleus muscle in hypoxia-acclimatised rats. J Anat 181 (Pt 2): 327-333, 1992.
27. Hoppeler H, and Desplanches D. Muscle structural modifications in hypoxia. Int J Sports Med 13 Suppl 1: S166-168, 1992.
28. Hoppeler H, Kleinert E, Schlegel C, Claassen H, Howald H, Kayar SR, and Cerretelli P. Morphological adaptations of human skeletal muscle to chronic hypoxia. Int J Sports Med 11 Suppl 1: S3-9, 1990.
29. Howald H, Pette D, Simoneau JA, Uber A, Hoppeler H, and Cerretelli P. Effect of chronic hypoxia on muscle enzyme

activities. Int J Sports Med 11 Suppl 1: S10-14, 1990.
30. Inoue T, Hashimoto M, Katakura M, Tanabe Y, Al Mamun A, Matsuzaki K, Otani H, and Shido O. Effects of chronic administration of arachidonic acid on lipid profiles and morphology in the skeletal muscles of aged rats. Prostaglandins Leukot Essent Fatty Acids 91: 119-127, 2014.
31. Ishihara A, Itho K, Itoh M, Hirofuji C, and Hayashi H. Hypobaric-hypoxic exposure and histochemical responses of soleus muscle fibers in the rat. Acta Histochem 96: 74-80, 1994.
32. Ishihara A, Itoh K, Oishi Y, Itoh M, Hirofuji C, and Hayashi H. Effects of hypobaric hypoxia on histochemical fibre-type composition and myosin heavy chain isoform component in the rat soleus muscle. Pflugers Arch 429: 601-606, 1995.
33. Itoh K, Moritani T, Ishida K, Hirofuji C, Taguchi S, and Itoh M. Hypoxia-induced fibre type transformation in rat hindlimb muscles. Histochemical and electro-mechanical changes. Eur J Appl Physiol Occup Physiol 60: 331-336, 1990.
34. Itoh M, Itoh K, Taguchi S, Hirofuji C, Takeuchi H, and Ishihara A. Effect of hypobaric hypoxia on fiber type composition of the soleus muscle in the developing rat. Aviat Space Environ Med 63: 583-587, 1992.
35. Jakobsson P, and Jorfeldt L. Long-term oxygen therapy may improve skeletal muscle metabolism in advanced chronic obstructive pulmonary disease patients with chronic hypoxaemia. Respir Med 89: 471-476, 1995.
36. Jakobsson P, Jorfeldt L, and Brundin A. Skeletal muscle metabolites and fibre types in patients with advanced chronic obstructive pulmonary disease (COPD), with and without chronic respiratory failure. Eur Respir J 3: 192-196, 1990.
37. Jakobsson P, Jorfeldt L, and Henriksson J. Metabolic enzyme activity in the quadriceps femoris muscle in patients with severe chronic obstructive pulmonary disease. Am J Respir Crit Care Med 151: 374-377, 1995.
38. Lainscak M, Gosker HR, and Schols AM. Chronic obstructive pulmonary disease patient journey: hospitalizations as window of opportunity for extra-pulmonary intervention. Curr Opin Clin Nutr Metab Care 16: 278-283, 2013.
39. Lainscak M, von Haehling S, Doehner W, Sarc I, Jeric T, Ziherl K, Kosnik M, Anker SD, and Suskovic S. Body mass index and prognosis in patients hospitalized with acute exacerbation of chronic obstructive pulmonary disease. J Cachexia Sarcopenia Muscle 2: 81-86, 2011.
40. Lewis P, Sheehan D, Soares R, Varela Coelho A, and O'Halloran KD. Chronic sustained hypoxia-induced redox remodeling causes contractile dysfunction in mouse sternohyoid muscle. Front Physiol 6: 122, 2015.
41. Ling KH, Paetkau V, Marcus F, and Lardy HA. Phosphofructokinase: I. Skeletal Muscle. In: Methods EnzymolAcademic Press, 1966, p. 425-429.
42. Ljubicic V, Joseph AM, Adhihetty PJ, Huang JH, Saleem A, Uguccioni G, and Hood DA. Molecular basis for an attenuated mitochondrial adaptive plasticity in aged skeletal muscle. Aging (Albany NY) 1: 818-830, 2009.
43. Lundby C, Calbet JA, and Robach P. The response of human skeletal muscle tissue to hypoxia. Cell Mol Life Sci 66: 3615-3623, 2009.
44. Lunde IG, Ekmark M, Rana ZA, Buonanno A, and Gundersen K. PPARdelta expression is influenced by muscle activity and induces slow muscle properties in adult rat muscles after somatic gene transfer. J Physiol 582: 1277-1287, 2007.
45. Marcelino MY, Fuoco NL, de Faria CA, Kozma Rde L, Marques LF, and Ribeiro-Paes JT. Animal models in chronic obstructive pulmonary disease-an overview. Exp Lung Res 40: 259-271, 2014.
46. O'Leary MF, Vainshtein A, Iqbal S, Ostojic O, and Hood DA. Adaptive plasticity of autophagic proteins to denervation in aging skeletal muscle. Am J Physiol Cell Physiol 304: C422-430, 2013.
47. Powers SK, Kavazis AN, and McClung JM. Oxidative stress and disuse muscle atrophy. J Appl Physiol (1985) 102: 2389-2397, 2007.
48. Radak Z, Taylor AW, Ohno H, and Goto S. Adaptation to exercise-induced oxidative stress: from muscle to brain. Exerc Immunol Rev 7: 90-107, 2001.
49. Remels AH, Gosker HR, Langen RC, and Schols AM. The mechanisms of cachexia underlying muscle dysfunction in COPD. J Appl Physiol (1985) 114: 1253-1262, 2013.
50. Rivard A, Berthou-Soulie L, Principe N, Kearney M, Curry C, Branellec D, Semenza GL, and Isner JM. Age-dependent defect in vascular endothelial growth factor expression is associated with reduced hypoxia-inducible factor 1 activity. J Biol Chem 275: 29643-29647, 2000.
51. Rivard A, Fabre JE, Silver M, Chen D, Murohara T, Kearney M, Magner M, Asahara T, and Isner JM. Age-dependent impairment of angiogenesis. Circulation 99: 111-120, 1999.
52. Sauleda J, Garcia-Palmer F, Wiesner RJ, Tarraga S, Harting I, Tomas P, Gomez C, Saus C, Palou A, and Agusti AG. Cytochrome oxidase activity and mitochondrial gene expression in skeletal muscle of patients with chronic obstructive pulmonary disease. Am J Respir Crit Care Med 157: 1413-1417, 1998.
53. Schols A, Mostert R, Soeters P, Greve LH, and Wouters EF. Inventory of nutritional status in patients with COPD. Chest 96: 247-249, 1989.
54. Schreiber SN, Emter R, Hock MB, Knutti D, Cardenas J, Podvinec M, Oakeley EJ, and Kralli A. The estrogen-related receptor alpha (ERRalpha) functions in PPARgamma coactivator 1alpha (PGC-1alpha)-induced mitochondrial biogenesis. Proc Natl Acad Sci U S A 101: 6472-6477, 2004.
55. Shepherd D, and Garland PB. Citrate synthase from rat liver. In: Methods EnzymolAcademic Press, 1969, p. 11-16.
56. Sillau AH, and Banchero N. Effects of hypoxia on capillary density and fiber composition in rat skeletal muscle. Pflugers Arch 370: 227-232, 1977.
57. Slot IG, Schols AM, Vosse BA, Kelders MC, and Gosker HR. Hypoxia differentially regulates muscle oxidative fiber type and metabolism in a HIF-1alpha-dependent manner. Cell Signal 26: 1837-1845, 2014.
58. Smuder AJ, Kavazis AN, Hudson MB, Nelson WB, and Powers SK. Oxidation enhances myofibrillar protein degradation via calpain and caspase-3. Free Radic Biol Med 49: 1152-1160, 2010.

59. Takahashi H, Asano K, and Nakayama H. Effect of endurance training under hypoxic condition on oxidative enzyme activity in rat skeletal muscle. Appl Human Sci 15: 111-114, 1996.
60. Takahashi H, Kikuchi K, and Nakayama H. Effect of chronic hypoxia on oxidative enzyme activity in rat skeletal muscle. Ann Physiol Anthropol 12: 363-369, 1993.
61. Takahashi H, Kikuchi K, and Nakayama H. Effect of chronic hypoxia on skeletal muscle fiber type in adult male rats. The Annals of physiological anthropology = Seiri Jinruigaku Kenkyukai kaishi 11: 625-630, 1992.
62. Turan N, Kalko S, Stincone A, Clarke K, Sabah A, Howlett K, Curnow SJ, Rodriguez DA, Cascante M, O'Neill L, Egginton S, Roca J, and Falciani F. A systems biology approach identifies molecular networks defining skeletal muscle abnormalities in chronic obstructive pulmonary disease. PLoS Comput Biol 7: e1002129, 2011.
63. van den Borst B, Schols AM, de Theije C, Boots AW, Kohler SE, Goossens GH, and Gosker HR. Characterization of the inflammatory and metabolic profile of adipose tissue in a mouse model of chronic hypoxia. J Appl Physiol (1985) 114: 1619-1628, 2013.
64. van den Borst B, Slot IG, Hellwig VA, Vosse BA, Kelders MC, Barreiro E, Schols AM, and Gosker HR. Loss of quadriceps muscle oxidative phenotype and decreased endurance in patients with mild-to-moderate COPD. J Appl Physiol (1985) 114: 1319-1328, 2013.
65. Vandesompele J, De Preter K, Pattyn F, Poppe B, Van Roy N, De Paepe A, and Speleman F. Accurate normalization of real-time quantitative RT-PCR data by geometric averaging of multiple internal control genes. Genome Biol 3: RESEARCH0034, 2002.
66. Verdijk LB, Koopman R, Schaart G, Meijer K, Savelberg HH, and van Loon LJ. Satellite cell content is specifically reduced in type II skeletal muscle fibers in the elderly. Am J Physiol Endocrinol Metab 292: E151-157, 2007.
67. Wigston DJ, and English AW. Fiber-type proportions in mammalian soleus muscle during postnatal development. J Neurobiol 23: 61-70, 1992.
68. Wu Z, Puigserver P, Andersson U, Zhang C, Adelmant G, Mootha V, Troy A, Cinti S, Lowell B, Scarpulla RC, and Spiegelman BM. Mechanisms controlling mitochondrial biogenesis and respiration through the thermogenic coactivator PGC-1. Cell 98: 115-124, 1999.
69. Wuyam B, Payen JF, Levy P, Bensaidane H, Reutenauer H, Le Bas JF, and Benabid AL. Metabolism and aerobic capacity of skeletal muscle in chronic respiratory failure related to chronic obstructive pulmonary disease. Eur Respir J 5: 157-162, 1992.

SUPPLEMENTAL MATERIALS

Table S1 | Number of fibers analyzed per fiber type.

	Normoxia	Pair-fed	Hypoxia
4 weeks			
Soleus, n	6	7	9
Type I	131.0 (79.5, 189.5)	130.0 (105.0, 185.0)	128.0 (96.0, 158.0)
Type IIa	269.0 (170.0, 329.3)	241.0 (203.0, 285.0)	191.0 (152.5, 250.5)
Type IIb/IIx	49.0 (23.0, 89.8)	54.0 (44.0, 67.0)	66.0 (41.5, 71.0)
Type I/IIa	3.0 (0.0, 8.8)	17.0 (12.0, 22.0)	16.0 (6.0, 32.5)
Total	477.5 (263.5, 601.0)	444.0 (356.0, 531.0)	395.0 (318.0, 503.5)
EDL, n	5	8	8
Type I	1.0 (0.0, 2.0)	1.0 (0.0, 6.0)	3.5 (2.0, 6.8)
Type IIa	54.0 (38.5, 74.5)	74.5 (50.8, 102.5)	74.5 (25.3, 106.5)
Type IIb/IIx	367.0 (255.5, 472.5)	419.0 (354.5, 640.3)	583.5 (392.0, 649.3)
Type I/IIa	2.0 (0.0, 9.5)	1.5 (0.0, 7.8)	8.5 (0.5, 22.5)
Total	453.0 (301.5, 536.5)	519.0 (406.8, 748.3)	677.0 (439.8, 782.8)
12 weeks			
Soleus, n	7	7	8
Type I	109.0 (99.0, 129.0)	136.0 (90.0, 152.0)	120.0 (84.0, 135.0)
Type IIa	213.0 (196.0, 269.0)	223.0 (169.0, 267.0)	214.5 (156.8, 280.5)
Type IIb/IIx	29.0 (11.0, 53.0)	36.0 (13.0, 57.0)	30.5 (26.0, 43.8)
Type I/IIa	2.0 (1.0, 4.0)	3.0 (2.0, 6.0)	12.0 (2.8, 21.5)
Total	372.0 (316.0, 469.0)	399.0 (259.0, 488.0)	396.0 (267.5, 458.0)
EDL, n	7	8	8
Type I	0.0 (0.0, 2.0)	0.0 (0.0, 5.0)	0.0 (0.0, 0.0)
Type IIa	31.0 (13.0, 45.0)	61.0 (31.3, 68.3)	75.5 (26.0, 87.8)
Type IIb/IIx	304.0 (207.0, 366.0)	295.0 (237.0, 479.3)	408.5 (284.8, 488.3)
Type I/IIa	0.0 (0.0, 0.0)	0.0 (0.0, 0.0)	0.0 (0.0, 0.0)
Total	316.0 (232.0, 411.0)	334.0 (297.3, 547.5)	484.0 (318.5, 572.5)
52 weeks			
Soleus, n	5	8	8
Type I	107.0 (101.0, 143.5)	134.0 (127.3, 150.3)	113.0 (96.5, 146.0)
Type IIa	213.0 (129.0, 236.0)	227.5 (163.0, 270.0)	173.0 (133.8, 236.5)
Type IIb/IIx	21.0 (20.5, 40.5)	26.0 (13.3, 34.5)	24.0 (19.8, 37.8)
Type I/IIa	2.0 (1.5, 5.5)	1.5 (0.3, 8.3)	7.0 (4.3, 13.5)
Total	341.0 (257.0, 421.5)	390.5 (311.3, 440.0)	302.0 (275.8, 426.3)

Table S1 (continued) | Number of fibers analyzed per fiber type.

	Normoxia	Pair-fed	Hypoxia
EDL, n	6	8	8
Type I	0.0 (0.0, 1.3)	0.0 (0.0, 0.0)	0.5 (0.0, 1.8)
Type IIa	47.0 (37.3, 60.3)	44.0 (38.0, 70.3)	57.0 (46.5, 64.8)
Type IIb/IIx	349.5 (278.3, 396.8)	299.0 (244.8, 440.8)	393.0 (379.8, 419.8)
Type I/IIa	0.0 (0.0, 0.0)	0.0 (0.0, 0.0)	0.0 (0.0, 0.0)
Total	395.5 (324.5, 451.8)	345.5 (283.3, 493.3)	449.0 (428.0, 485.5)

Values are median (25th percentile, 75th percentile).

Table S2 | Muscle and fat pad weight loss in hypoxic relative to normoxic mice.

	Young (n = 9)	Adult (n = 8)	Aged (n = 8)
Muscles			
Soleus, %	−14 (−23, −12)	−9 (−11, −6)*	−4 (−13, −2)*
EDL, %	−30 (−36, −23)	−13 (−14, −11)*	−10 (−13, −7)*
Gastrocnemius, %	−25 (−31, −20)	−12 (−14, −11)*	−13 (−15, −10)*
Plantaris, %	−29 (−38, −22)	−10 (−15, −8)*	−13 (−16, −7)*
Tibialis, %	−25 (−29, −21)	−8 (−10, −3)*	−8 (−13, −7)*
Fat pads			
Epididymal	−62 (−66, −53)	−39 (−55, −25)*	−66 (−73, −60)$^{\#}$
Inguinal	−31 (−38, −25)	−25 (−31, −23)	−55 (−58, −51)$^{*,\#}$

Values are median (25th percentile, 75th percentile). Data were available for 9 young, 8 adult and 8 aged hypoxic mice. Level of significance: $^{*}p < 0.05$ compared to 4 weeks, $^{\#}p < 0.05$ compared to 12 weeks.

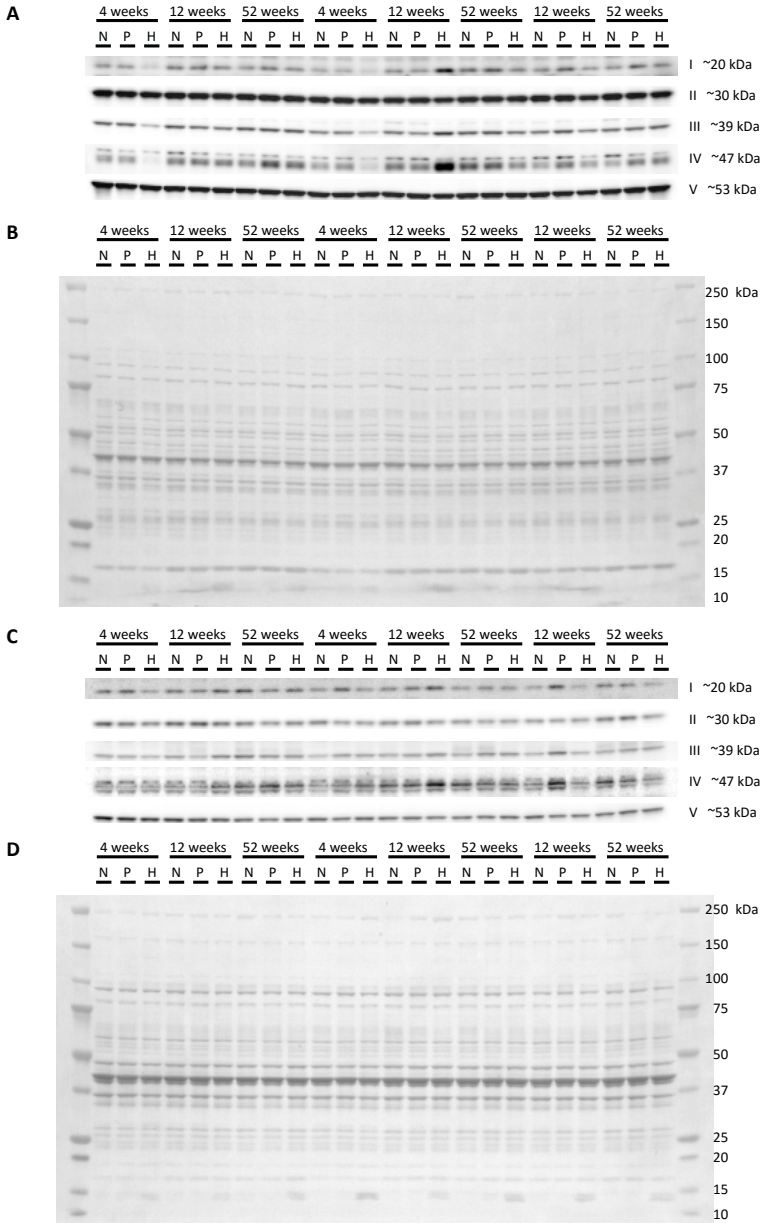

Figure S1 | Representative Western blots of subunits of the five OXPHOS complexes. A, Representative Western blot of the five OXPHOS subunits in soleus. All bands are from the same blot and were reorganized to respect the ascending order of the five subunits. COX-I (complex IV) is a highly hydrophobic protein that consequently appears as a broad band on the gel. **B**, Ponceau S stain that was used to normalize the blot depicted in **A**. **C**, Representative Western blot of the five OXPHOS subunits in EDL. All bands are from the same blot and were reorganized to respect the ascending order of the five subunits. **D**, Ponceau S stain that was used to normalize the blot depicted in **C**. N, normoxia; P, pair-fed; H, hypoxia.

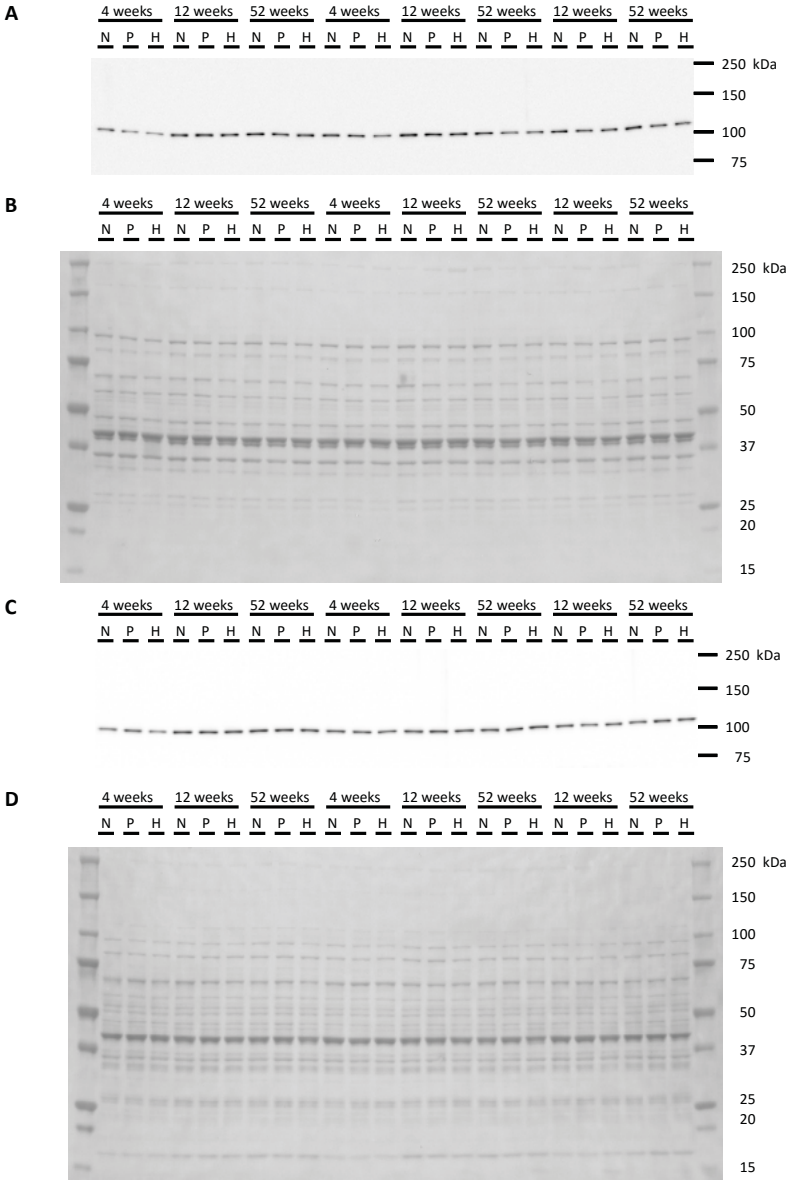

Figure S2 | Representative Western blots of PGC-1α. A, Representative Western blot of PGC-1α in soleus. **B**, Ponceau S stain that was used to normalize the blot depicted in **A**. **C**, Representative Western blot of PGC-1α in EDL. **D**, Ponceau S stain that was used to normalize the blot depicted in **C**. N, normoxia; P, pair-fed; H, hypoxia.

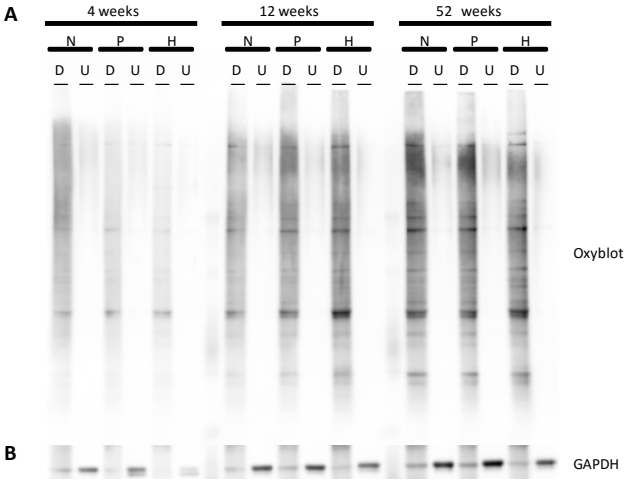

Figure S3 | Western blot depicting protein oxidation by Oxyblot. A, Protein oxidation in soleus. **B**, Western blot of GAPDH. The bands in the untreated control lanes were used for normalization of the blot depicted in **A**. N, normoxia; P, pair-fed; H, hypoxia; D, derivatized side chains; U, untreated control.

Chapter 4

Loss of quadriceps muscle oxidative phenotype and decreased endurance in patients with mild-to-moderate COPD

Bram van den Borst, Ilse G.M. Slot, Valéry A.C.V. Hellwig, Bettine A.H. Vosse, Marco C.J.M. Kelders, Esther Barreiro, Annemie M.W.J. Schols, Harry R. Gosker

Journal of Applied Physiology (1985), 2013. 114(9): p. 1319-28

ABSTRACT

Being well-established in advanced chronic obstructive pulmonary disease (COPD), skeletal muscle dysfunction and its underlying pathology have been scarcely investigated in patients with mild-to-moderate airflow obstruction. We hypothesized that a loss of oxidative phenotype (Oxphen) associated with decreased endurance is present in the skeletal muscle of patients with mild-to-moderate COPD. In quadriceps muscle biopsies from 29 patients with COPD (forced expiratory volume in 1 s [FEV_1] 58 ± 16%pred, body mass index [BMI] 26 ± 4 kg/m^2) and 15 controls (BMI 25 ± 3 kg/m^2) we assessed fiber-type distribution, fiber cross-sectional areas (CSA), oxidative and glycolytic gene expression, OXPHOS protein levels, metabolic enzyme activity, and levels of oxidative stress markers. Quadriceps function was assessed by isokinetic dynamometry, body composition by dual-energy X-ray absorptiometry, exercise capacity by an incremental load test, and physical activity level by accelerometry. Compared with controls, patients had comparable fat-free mass index, quadriceps strength, and fiber CSA, but quadriceps endurance was decreased by 29% ($p = 0.002$). Patients with COPD had a clear loss of muscle Oxphen: a fiber type I-to-II shift, decreased levels of OXPHOS complexes IV and V subunits (47% and 31%, respectively; $p < 0.05$), a decreased ratio of 3-hydroxyacyl-CoA dehydrogenase/phosphofructokinase (PFK) enzyme activities (38%, $p < 0.05$), and decreased peroxisome proliferator-activated receptor-γ coactivator-1α (40%; $p < 0.001$) *vs.* increased PFK (67%; $p < 0.001$) gene expression levels. Within the patient group, markers of Oxphen were significantly positively correlated with quadriceps endurance and inversely with the increase in plasma lactate relative to work rate during the incremental test. Levels of protein carbonylation, tyrosine nitration, and malondialdehyde protein adducts were comparable between patients and controls. However, among patients, oxidative stress levels were significantly inversely correlated with markers of Oxphen and quadriceps endurance. Reduced muscle endurance associated with underlying loss of muscle Oxphen is already present in patients with mild-to-moderate COPD without muscle wasting.

INTRODUCTION

Skeletal muscle dysfunction is a hallmark of advanced chronic obstructive pulmonary disease (COPD) and significantly contributes to decreased exercise capacity and poor quality of life (1, 5). Peripheral skeletal muscle wasting and a loss of oxidative phenotype (Oxphen) are the two major myopathological findings recognized in patients with advanced COPD, being associated with decreased muscle strength (9) and endurance (2), respectively. Important to note is that studies investigating skeletal muscle dysfunction and its underlying pathology in COPD have been performed almost exclusively in patients with GOLD stages 3–4 with significant muscle wasting. In the INTERCOM trial, Van Wetering *et al.* (43) recently showed that patients with mild-to-moderate COPD (mean forced expiratory volume in 1 s [FEV_1] 60% of predicted) responded well to a lifestyle intervention program in terms of improvement in cycle endurance capacity and health status. Muscle strength and muscle mass of that study group were within the normal range, but no information was available regarding peripheral muscle endurance and markers of skeletal muscle Oxphen.

Loss of peripheral muscle Oxphen in advanced COPD includes a I-to-II fiber type shift and reduced activities of enzymes involved in oxidative energy metabolism (2, 15, 37). In addition, Remels *et al.* (33) previously showed that key Oxphen regulators (peroxisome proliferator-activated receptors [PPARs], PPAR-γ coactivator-1α [PGC-1α], and mitochondrial transcription factor A [Tfam]) were reduced in muscles of patients with advanced COPD. Moreover, loss of muscle Oxphen may render the muscle more susceptible to oxidative stress (21, 22, 31). Oxidative stress is believed to be an important player in skeletal muscle wasting and dysfunction in COPD (6, 10). However, data on muscle Oxphen and oxidative stress in patients with COPD and milder degrees of airflow obstruction are scarce.

In the current study we compared markers of Oxphen measured in biopsies of quadriceps muscle from patients with mild-to-moderate COPD and from healthy controls matched for age, sex, and body mass index (BMI). In addition, we explored associations between muscle metabolic profile and quadriceps function, exercise capacity, physical activity level, and skeletal muscle oxidative stress. We hypothesized that a loss of Oxphen, associated with decreased endurance, is already present in skeletal muscle of patients with mild-to-moderate COPD.

METHODS

Subjects and study design

The study population comprised 29 patients with clinically stable mild-to-moderate COPD and 15 healthy controls. Patients were recruited from the outpatient clinic of the Maastricht University Medical Center+ (MUMC+, Maastricht, The Netherlands) and via advertisements in local newspapers. Patients were excluded if they were on long-term oxygen therapy, used oral prednisolone, or had an acute exacerbation of symptoms with hospital admission in the previous 8 wk and rehabilitation in the previous 6 mo. Patients with a known comorbidity that could potentially interfere with study outcome parameters were carefully excluded. These included diabetes, recent cardiovascular event, inflammatory bowel disease, obstructive sleep apnea, thyroid disease, and cancer. Healthy controls were recruited via advertising in local newspapers. The absence of these diseases in the healthy subjects was verified through history-taking by a physician and pulmonary function tests to verify the absence of airflow limitation. Care was taken to select a group of healthy controls with similar age, BMI, and sex distribution as the patients with COPD regardless of their daily physical activity level. Written, informed consent was obtained from all subjects and the ethical review board of the MUMC+ approved the study (08-2-059). The trial was registered at http://www.trialregister.nl as NTR1402.

On day 1, body composition and quadriceps function were assessed as described below, and subjects started wearing an accelerometer for 6 days to objectively quantify physical activity level. On day 7, the accelerometry data were retrieved, quadriceps tissue samples were obtained, pulmonary function was assessed, and an incremental load test was performed.

Pulmonary function, smoking status, and exercise capacity

Pulmonary function testing included forced spirometry and single-breath diffusion capacity measurement (Masterlab, Jaeger, Würzburg, Germany). Instruments were calibrated twice a day. All values obtained were expressed as a percentage of reference values (32). Smoking status was based on self-report, and those who had smoked or were current smokers were designated as ever-smokers. All subjects performed an incremental load cycling test to determine peak oxygen uptake ($\dot{V}O_2$ peak) and peak load (W peak) as previously described (12). Arterial punctures of the radial artery at rest and at $\dot{V}O_2$ peak were available from 19 patients with COPD and 11 healthy subjects. Arterial blood gas analyses and lactate concentrations were determined (Blood gas analyzer 865; Chiron Diagnostics, Emeryville, CA).

Anthropometry and body composition

Height in meters and weight in kilograms were assessed on a standard scale. BMI was calculated as weight/height^2. Whole-body dual-energy X-ray absorptiometry was performed to assess body composition as described (42). Fat-free mass index (FFMI) was calculated as fat-free mass/height^2. The prevalence of muscle depletion was explored by applying the criteria described by Schols *et al.* (38) (FFMI <16 kg/m^2 for men and FFMI <15 kg/m^2 for women).

Quadriceps endurance and strength

Isokinetic muscle endurance and strength of the dominant knee extensor (quadriceps muscle) were measured using a dynamometer (Biodex System; Biodex, Shirley, NY). Subjects were seated upright on the chair of the dynamometer with the back supported. Subjects were secured with straps at the level of the chest, pelvis, and thigh. The hip joint was at an angle between 90 and 100° of flexion during testing. The test consisted of 30 sequential volitional maximal contractions at an angular velocity of 90°/s, during which the subject was strongly encouraged. Maximal isokinetic strength was defined as the highest peak torque (in N·m) in this series of 30. To determine isokinetic quadriceps endurance, the proportional decline in peak torques (relative to the highest peak torque) per repetition (%N·m/rep) was used as determined by linear regression, as described previously (11). We used this slope as a measure of quadriceps endurance (*i.e.*, a slope closer to zero indicates a better endurance). Valid quadriceps endurance measures were available for 24 patients with COPD and 13 healthy controls.

Daily physical activity

Physical activity (PA) was measured using a dual-axis GT1M accelerometer (ActiGraph; Fort Walton Beach, FL) for 6 consecutive days (4 week days and 2 weekend days). Subjects were instructed to wear the accelerometer during the time they were not asleep, except when showering or bathing (46). The accelerometer was firmly attached to an elastic belt worn at the waist. The accelerometer registers PA in counts, which are the summation of the accelerations measured during a specified time interval (epoch), which was set at 1 min. Counts represent the intensity of activity in that epoch. Non-wear time was defined as 60 consecutive counts of 0 in which up to two epochs <100 counts were allowed (41). Only days with ≥10 h of wear time were accepted as valid days (41). The total amount of PA was expressed as the total counts divided by the total wear time (counts/min). Cutoff points for sedentary lifestyle and combined moderate-to-vigorous PA (MVPA) intensity levels were defined as <100, 100–759, and ≥760 counts/min, respectively (20, 41). The time spent in each category of intensity was presented as a percentage of total wear time. Furthermore, we analyzed the number, duration, and intensity of MVPA bouts (≥10 consecutive min spent in MVPA) (19). The classification of MVPA bouts was motivated by the PA recommendations of the Centers for Disease Control and Prevention, the American College of Sports Medicine (26), and the British Association of Sport and Exercise Sciences (24), which call for MVPA to be accumulated in bouts of ≥10 min to achieve health benefits. Moreover, these recommendations call for at least 150 min/wk of bouted MVPA. We investigated whether the participants in our study complied with these recommendations, accounting for the number of valid accelerometry days.

Skeletal muscle biopsy

Biopsies of the quadriceps muscle (*vastus lateralis*) from the dominant leg were obtained using a needle biopsy technique (8). Muscle tissue was frozen in melting isopentane precooled in liquid nitrogen and stored at −80°C for histological purposes. Another specimen was snap-frozen in liquid nitrogen and stored at −80°C for gene and protein expression analyses and for enzyme activity assays.

Fiber size and composition analysis

Serial cryosections (5 µm) with fibers in transverse orientation were cut from OCT-embedded muscle biopsies on a cryostat microtome (Leica CM 1900; Meyer Instruments) at −20°C and mounted on SuperFrost microscope slides (Menzel-Glüser, Braunschweig, Germany) to be stored at −80°C until further analyses. For immunohistochemistry, sections were incubated with primary antimyosin heavy chain (MyHC)-I [Developmental Studies Hybridoma Bank (DSHB), University of Iowa, Ames, IA], anti-MyHC-IIa (DSHB), and anti-laminin (Sigma, Zwijndrecht, The Netherlands) followed by secondary antibodies labeled with Alexa Fluor 555, Alexa Fluor 488, and Alexa Fluor 350 (Invitrogen, Breda, The Netherlands). Fiber typing was aided by means of myosin ATPase-activity staining with acidic preincubation at pH 4.40 (25). Immunofluorescence-stained and ATPase-stained sections were microscopically photographed at 10× magnification. In a blinded fashion, fibers were classified primarily on the basis of immunofluorescence, with ATPase-stained sections used to confirm type I/IIa and type IIa/IIx hybrid fiber types. Fiber cross-sectional area was measured with Lucia 4.82 software (Laboratory Imaging, Prague, Czech Republic) on the basis of laminin staining of the basement membrane (45).

RNA extraction and RT-qPCR analysis

Muscle tissue (10–30 mg) was homogenized in denaturation solution (ToTALLY RNA Kit; Ambion, Foster City, CA) using a Polytron PT 1600 E (Kinematica, Littau/Luzern, Germany) and was RNA-extracted according to the supplier's protocol followed by genomic DNA removal and cleanup with the RNeasy Mini Kit with RNase-free DNase (Qiagen, Venlo, The Netherlands). After elution, RNA concentration was determined using a spectrophotometer (NanoDrop ND-1000; Isogen Lifescience, IJsselstein, The Netherlands) and integrity was verified for a selection of samples by gel electrophoresis and on a bioanalyzer (Agilent Technologies, Amstelveen, The Netherlands). RNA (400 ng) was reverse transcribed to cDNA with anchored oligo(dT) primers according to the supplier's protocol (Transcriptor First Strand cDNA Synthesis Kit; Roche Diagnostics, Woerden, The Netherlands). RT-qPCR primers were designed on the basis of Ensembl transcript sequences or selected from literature (3, 44) and ordered from Sigma Genosys (Zwijndrecht, The Netherlands). The genes encoding PGC-1α, PGC-1β, PGC-related coactivator (PRC), PPAR-α, Tfam, Nuclear Respiratory Factor (NRF)-1, NRF-2α, MyHC-I, muscle phosphofructokinase (PFKM), MyHC-IIa, and MyHC-IIx were the target genes. RT-qPCR reactions contained SensiMix SYBR Hi-ROX Kit (Quantace-Bioline, London, UK) with 300 nM primers and were run in a 384-well MicroAmp Optical 384-Well Reaction Plate (Applied Biosystems, Nieuwerkerk a/d IJssel, The Netherlands) on a 7900HT Fast Real-Time PCR System (Applied Biosystems). Standard curves prepared from pooled cDNA and melt curves were analyzed to verify efficiency and specificity of amplification. Twelve reference genes (*ALAS1*, *ACTB*, *B2M*, *PPIA*, *GAPDH*, *GUSB*, *HMBS*, *HPRT1*, *RPL13A*, *RPLP0*, *UBC*, *YWHAZ*) were measured and stability of expression was assessed by visual inspection of expression differences between the study groups and a stability assessment by geNorm (44). Eventually, nine reference genes (all except *ACTB*, *GAPDH*, and *UBC*) were used to calculate a geNorm factor, which was used to normalize expression levels of the target genes.

Immunoblotting of OXPHOS subunits and oxidative stress markers

Tissue (10–20 mg) was crushed in liquid nitrogen and homogenized in 400 µl of IP lysis buffer (50 mM Tris, 150 mM NaCl, 10% glycerol, 0.5% Nonidet P40, 1 mM EDTA, 1 mM Na_3VO_4, 5 mM NaF, 10 mM β-glycerophosphate, 1 mM $Na_4O_7P_2$, 1 mM dithiothreitol, 10 µg/ml leupeptin, 1% aprotenin, 1 mM PMSF, pH 7.4) with a Polytron PT 1600 E (Kinematica). After homogenization, samples were incubated for 15 min on a rotating wheel at 4°C and spun for 30 min at maximum speed (20,817 × *g*) in a centrifuge cooled to 4°C. Supernatant was aliquoted, snap-frozen, and stored without sample buffer at −80°C until analysis.

Protein concentration in lysates was determined using the bicinchoninic acid assay (Pierce; Thermo Fisher Scientific, Breda, The Netherlands). For Western blot analysis, aliquots were supplemented with 4× sample buffer [250 mM Tris-HCl pH 6.8, 8% (wt/vol) sodium dodecyl sulfate, 40% (vol/vol) glycerol, 0.4 M dithiothreitol, 0.02% (wt/vol) bromophenol blue] and kept on ice. Per sample, 5 µg unboiled protein was separated on gel (4–12% Bis-Tris XT gel; Criterion, Bio-Rad Laboratories, Hercules, CA) with XT MOPS running buffer (Bio-Rad). One sample was loaded on all gels to facilitate gel-gel comparisons. Proteins were transferred to a 0.45-µm nitrocellulose membrane (Protran; Schleicher and Schuell, 's-Hertogenbosch, The Netherlands) in transfer buffer [25 mM Tris, 192 mM glycine, 20% (vol/vol) methanol] by electrophoresis. After transfer, membranes were blocked from nonspecific protein binding with blocking solution, which contains 5% (wt/vol) nonfat dry milk (Campina, Eindhoven, The Netherlands) in Tris-buffered saline with Tween20 [TBST; 25 mM Tris, 137 mM NaCl, 2.7 mM KCl, 0.05% (vol/vol) Tween20, pH 7.4], for 1 h at room temperature, followed by incubation in primary antibody solution overnight at 4°C [mouse anti-Total OXPHOS Rodent WB Antibody Cocktail (MS604–300; Abcam, Cambridge, UK) diluted 1:1,000 in blocking solution or rabbit anti-GAPDH (#2118; Cell Signaling Technology, Leiden, The Netherlands) diluted 1:5,000 in TBST]. Membranes were incubated in secondary antibody solution [peroxidase-labeled horse anti-mouse IgG or goat anti-rabbit IgG (PI-2000 and PI-1000, respectively; Vector Laboratories, Burlingame, CA] diluted 1:5,000 in blocking solution) for 1 h at room temperature before incubation with enhanced chemiluminescence substrate (Pierce SuperSignal West PICO Chemiluminescent Substrate; Thermo Fisher Scientific). Protein bands were detected using Super RX films (Fujifilm, Düsseldorf, Germany) and scanned on a GS-800 densitometer (Bio-Rad). Bands were quantified using Quantity One software (v4.6.2; Bio-Rad), with GAPDH as loading control (GAPDH levels were not different between patients with COPD and controls).

Protein content of oxidative stress markers was identified using specific primary antibodies for protein carbonylation (anti-2,4-DNP moiety antibody, Oxyblot kit; Chemicon International, Temecula, CA), total protein nitration (anti-3-nitrotyrosine antibody, Invitrogen, Eugene, OR), and total malondialdehyde (MDA)-protein adducts (anti-MDA antibody; Academy Biomedical, Houston, TX). For protein carbonylation, carbonyl groups in the protein side chains were first derivatized to 2,4-dinitrophenylhydrazone (DNP) using the Oxyblot kit (Chemicon) according to the manufacturer's instructions. Briefly, 15 µg of protein was used per derivatization reaction; proteins were then denatured by addition of 12% SDS. The samples were subsequently derivatized by adding 10 µl of 1× 2, 4-dinitrophenylhydrazine solution and incubated for 20 min. Finally, 7.5 µl of neutralization solution and 2-mercaptoethanol were added to the sample

mixture. Immunoblotting was similar as described above with some minor differences: polyvinylidene difluoride (PVDF) membranes were used, which were scanned with the Molecular Imager Chemidoc XRS System (Bio-Rad) and bands were quantified using the software Image Lab version 2.0.1 (Bio-Rad). Values of total reactive carbonyl groups, total protein tyrosine nitration, and total MDA-protein adducts in a given sample were calculated by addition of optical densities (arbitrary units) of individual protein bands in each case. Final optical densities obtained in each specific group of subjects corresponded to the mean values of the different samples (lanes) of each antigen studied. Actin (anti-alpha-sarcomeric actin antibody, clone 5C**5**; Sigma-Aldrich, St. Louis, MO) was used as the loading control for all the oxidative stress markers (10, 34).

Enzyme activity assays

Tissue (15–30 mg) was crushed in liquid nitrogen and homogenized in 350 µl SET buffer (250 mM sucrose, 2 mM EDTA, 10 mM Tris, pH 7.4) with a Polytron PT 1600 E (Kinematica). After homogenization, samples were incubated for 10 min on a rotating wheel at 4°C and spun for 5 min at maximum speed (20,817 × *g*) in a centrifuge cooled to 4°C. An aliquot of supernatant was stored for protein determination. To the remaining supernatant, 5× aqueous BSA solution was added to a final BSA concentration of 1% (vol/vol) and samples were aliquoted, snap-frozen, and stored at −80°C until analysis. Protein concentration in SET lysate aliquots without BSA was determined using the bicinchoninic acid assay (Pierce). Citrate synthase (CS, EC 2.3.3.1), 3-hydroxyacyl-CoA dehydrogenase (HADH, EC 1.1.1.35) and PFK (EC 2.7.1.11) activities were assayed spectrophotometrically (Multiskan Spectrum; Thermo Labsystems, Breda, The Netherlands) as previously described (7, 18, 39). Absolute CS, HADH, and PFK activities were normalized to total protein.

Statistics

Differences between patients with COPD and controls were tested using Student's *t*-tests, Mann-Whitney-U tests, or χ^2 tests as appropriate. Correlations were tested using the Pearson correlation coefficient or the Spearman ρ in case of non-normally distributed data. Analyses were performed using PASW Statistics 17.0 (SPSS, Chicago, IL). A p value < 0.05 was considered statistically significant.

RESULTS

The control subjects were matched to the patients with COPD on the basis of age, sex, and BMI (Table 1). FEV_1 was between 30 and 50% of the predicted value in 13 patients (45%), between 50–70% of predicted value in 11 patients (38%), and >70% of predicted value in 5 patients (17%). $\dot{V}O_2$ peak and W peak were significantly decreased in the patients with COPD (Table 1). FEV_1 (% of predicted) was strongly correlated with $\dot{V}O_2$ peak (% of predicted) in the total population ($r = 0.83$, $p < 0.001$), within the group of patients with COPD ($r = 0.78$, $p < 0.001$), and within the controls ($r = 0.53$, $p = 0.044$).

Table 1 | Main characteristics of healthy controls and patients with COPD

	Controls (*n* = 15)	Patients (*n* = 29)
Demographics		
Age, yr	65 (6)	65 (6)
Sex, % men	60	55
Ever-smoker, %	53	100†
BMI, kg/m^2	24.9 (3.3)	25.5 (3.6)
Pulmonary function		
FEV_1, %pred	113 (15)	58 (16)†
FVC, %pred	120 (17)	104 (22)*
FEV_1/FVC, %	74 (5)	45 (11)
DLCO, %pred	95 (19)	53 (18)†
Incremental load test		
Peak VO_2, %pred	123 (8)	72 (4)†
Peak WR, %pred	133 (7)	61 (4)†
ΔBorg dyspnea score	3.4 (0.8)	3.6 (0.4)
ΔBorg leg fatigue score	2.7 (0.6)	2.3 (0.4)
ΔPaO_2, kPa	1.04 (0.53)	−0.38 (0.31)*
ΔLactate/WR (mmol/L/W)	0.039 (0.003)	0.035 (0.003)

BMI, body mass index; DLCO, diffusion capacity of the lungs for carbon monoxide; FEV_1, forced expiratory volume in 1 s; FVC, forced vital capacity; WR, work rate. * $p < 0.05$, † $p < 0.001$.

Quadriceps muscle endurance and markers of oxidative phenotype

Quadriceps muscle endurance was significantly lower in the patients with COPD (Figure 1A). The mean decline in peak torque per repetition was −1.67 ± 0.09% N·m/rep in patients with COPD *vs.* −1.18 ± 0.10% N·m/rep in the controls ($p = 0.002$). Patients had a lower proportion of type I fibers and a higher proportion of type IIa, type IIa/IIx, and IIx fibers than controls, indicative of a I-to-II fiber type shift (Figure 1, B–D). The mean mRNA expression levels of the key regulator of oxidative metabolism PGC-1α and of the structural marker of oxidative fibers, MyHC-I, were significantly decreased in the patients with COPD compared with controls, and reached borderline significance for Tfam (Figure 1E). Other (co-)transcription factors implicated in driving oxidative gene expression (PPAR-α, PGC-1β, PRC, NRF-1, and NRF-2α) were not differentially expressed

between the patient and control groups. Gene expression levels of the key glycolytic enzyme PFKM and of the structural markers of glycolytic fibers (*i.e.*, MyHC-IIa and MyHC-IIx) were significantly higher in patients with COPD (Figure 1F). Congruently, mean OXPHOS subunit protein levels were all lower in patients with COPD than in controls, reaching statistical significance for those of complexes IV and V (Figure 1, F and G). The mean differences in HADH, CS, and PFK enzyme activity were not statistically significant (Figure 1H), yet the ratio HADH/PFK was significantly lower in patients with COPD. The ratio CS/PFK reached borderline significance (Figure 1I).

Quadriceps strength, muscle mass, and fiber cross-sectional area

Neither FFMI nor quadriceps peak torque were significantly different between the patients with COPD and controls (Figure 2, A and B). The prevalence of muscle wasting was not different between patients with COPD and controls (20.7% *vs.* 13.3%, respectively; $p = 0.70$). Congruently, there were no differences in muscle fiber CSA (Figure 2C).

Daily living physical activity level

From all the subjects, 5.5 ± 0.9 valid accelerometry days were available with a mean of 14 ± 1 h of wear time per day. Total PA was significantly lower in patients with COPD than controls, and patients spent more time in sedentary behavior and less time in MVPA (Table 2). Also, patients had fewer MVPA bouts, which were shorter and less intense than the MVPA bouts of controls (Table 2). Total PA (counts/min) was positively correlated with FEV_1 (% of predicted) in the entire study population ($r = 0.58$, $p < 0.001$) and also within the group of patients with COPD ($r = 0.55$, $p = 0.002$) but not in the controls ($r = -0.06$, $p = 0.82$). Within the group of patients with COPD, FEV_1 (% of predicted) was negatively correlated with time spent in sedentary PA ($r = -0.54$, $p = 0.002$) and positively correlated with time spent in MVPA ($r = 0.61$, $p < 0.001$), number of MVPA bouts per day ($r = 0.46$, $p = 0.013$), and with time spent in MVPA bouts ($r = 0.41$, $p = 0.039$). Only 31% of the patients fulfilled the criteria of 150 min/wk of bouted MVPA time *vs.* 80% of the controls ($p = 0.004$). Within the patient group, those who fulfilled

Figure 1 | Quadriceps muscle endurance, fiber type distribution, gene expression, OXPHOS protein expression, and enzyme activity. A, quadriceps endurance as assessed by isokinetic dynamometry. The *p* value denotes the statistical significance of the difference in slopes between patients with COPD and healthy controls. **B**, quadriceps muscle fiber type distribution as determined by fluorescent immunohistochemistry and ATPase staining. **C**, box plot of fiber type IIa/IIx proportion. Boxes represent 25th and 75th percentiles; whiskers represent 10th and 90th percentiles. **D**, box plot of fiber type IIx proportion. Boxes represent 25th and 75th percentiles; whiskers represent 10th and 90th percentiles. **E**, quadriceps muscle mRNA expression of peroxisome proliferator-activated receptor (PPAR)-γ; coactivator-1α (PGC-1α); myosin heavy chain (MyHC) I, IIa, and IIx; mitochondrial transcription factor (Tfam); PPAR-α; PGC-1β; nuclear respiratory factor (NRF)-1; NRF-2α; PGC-related coactivator (PRC); and phosphofructokinase muscle (PFKM) as determined by RT-qPCR. **F**, representative Western Blot of the five OXPHOS protein subunits and GAPDH from three healthy controls and three patients with COPD. All bands are from the same blot and were reorganized for illustrative purposes because patients and controls were randomized over the blot and to respect the ascending order of the five subunits. **G**, levels of the five OXPHOS protein subunits as determined by Western Blot. **H**, 3-hydroxyacyl-CoA dehydrogenase (HADH), citrate synthase (CS), and phosphofructokinase (PFK) enzyme activities. **I**, ratios between HADH/PFK and CS/PFK. $^{*}p < 0.05$; $^{**}p < 0.01$; $^{***}p < 0.001$.

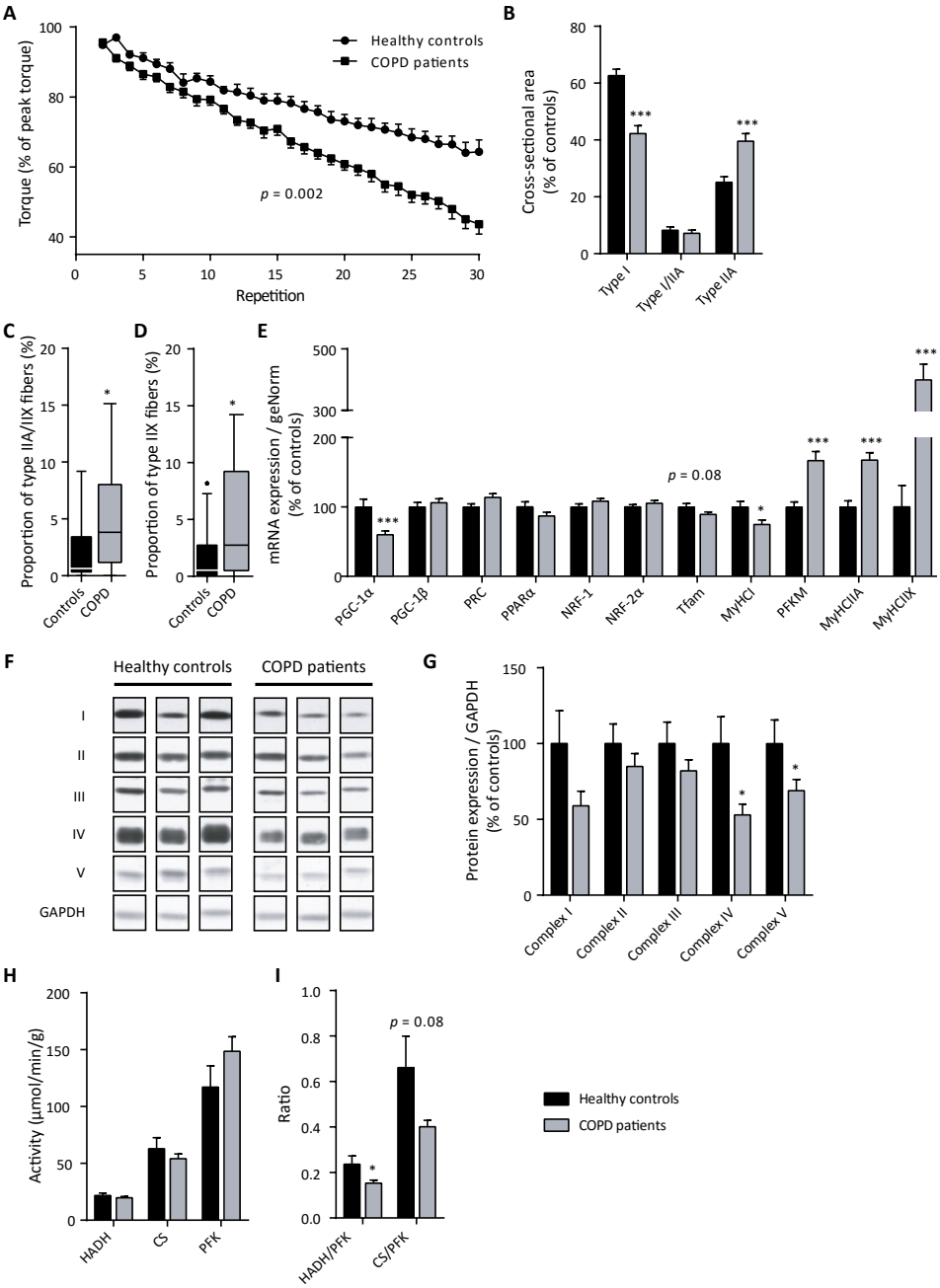
A
Torque (% of peak torque)
Repetition
Healthy controls
COPD patients
p = 0.002
B
Cross-sectional area (% of controls)
Type I
Type I/IIA
Type IIA
C
Proportion of type IIA/IIX fibers (%)
Controls
COPD
D
Proportion of type IIX fibers (%)
Controls
COPD
E
mRNA expression / geNorm (% of controls)
p = 0.08
PGC-1α
PGC-1β
PRC
PPARα
NRF-1
NRF-2α
Tfam
MyHCI
PFKM
MyHCIIA
MyHCIIX
F
Healthy controls
COPD patients
I
II
III
IV
V
GAPDH
G
Protein expression / GAPDH (% of controls)
Complex I
Complex II
Complex III
Complex IV
Complex V
H
Activity (µmol/min/g)
HADH
CS
PFK
I
Ratio
p = 0.08
HADH/PFK
CS/PFK
Healthy controls
COPD patients

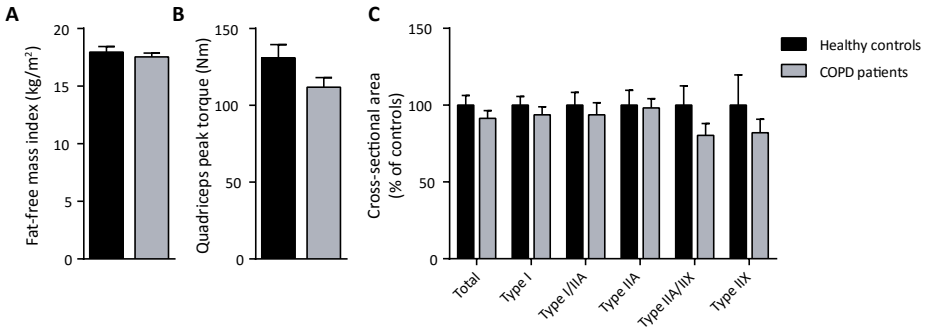

Figure 2 | Fat-free mass index, quadriceps strength, and fiber cross-sectional area. A, fat-free mass index as determined by whole-body dual-energy X-ray absorptiometry; $p > 0.05$. **B**, quadriceps peak torque as determined by isokinetic dynamometry; $p > 0.05$. **C**, quadriceps muscle fiber cross-sectional areas presented for total fibers and per fiber type; all $p > 0.05$.

these criteria had a significantly higher FEV_1 compared with patients who did not fulfill these criteria (67 ± 5% *vs.* 54 ± 3% of predicted; $p = 0.049$).

Associations with quadriceps Oxphen in patients with COPD

In the group of patients with COPD, quadriceps endurance was significantly, positively correlated with MyHC-I gene expression and PGC-1α gene expression, and showed a trend toward a positive correlation with type I fiber proportion (Figure 3, A–C). In line with this finding, type IIx fiber proportion was negatively correlated with quadriceps endurance ($\rho = -0.434$, $p = 0.038$). Moreover, type I fiber proportion was negatively correlated with the increase in lactate relative to work rate (Figure 3D).

No significant correlations were found between markers of Oxphen and quadriceps peak torque, pulmonary function, exercise capacity, total PA, time spent in sedentary PA or MVPA, or any of the MVPA bout-related variables (data not shown).

Table 2 | Accelerometry data from patients with COPD and controls

	Controls ($n = 15$)	Patients ($n = 29$)
Total activity, counts/min	360 (134)	220 (101)‡
Time spent in sedentary PA, % of total wear time	60.5 (6.6)	67.4 (9.4)†
Time spent in lifestyle PA, % of total wear time	25.5 (4.6)	24.3 (6.5)
Time spent in MVPA, % of total wear time	13.8 (5.3)	8.6 (5.3)†
Total number of MVPA bouts	12 (8–18)	5 (3–11)†
Number of MVPA bouts per day	2.0 (1.3–2.0)	1.0 (0.6–2.2)*
Time spent in MVPA bouts, min	267 (108–494)	68 (38–204)†
Mean MVPA bout duration, min	22.1 (9.4)	14.7 (3.7)†
Mean intensity of MVPA bouts, counts[a]	2700 (605)	1913 (498)‡
Compliance with MVPA recommendation, %[b]	80	31†

MVPA, moderate-to-vigorous physical activity; PA, physical activity; [a] Weighted for individual MVPA bout duration; [b] At least 150 min/wk of bouted MVPA time; * $p < 0.05$; † $p < 0.01$; ‡ $p < 0.001$.

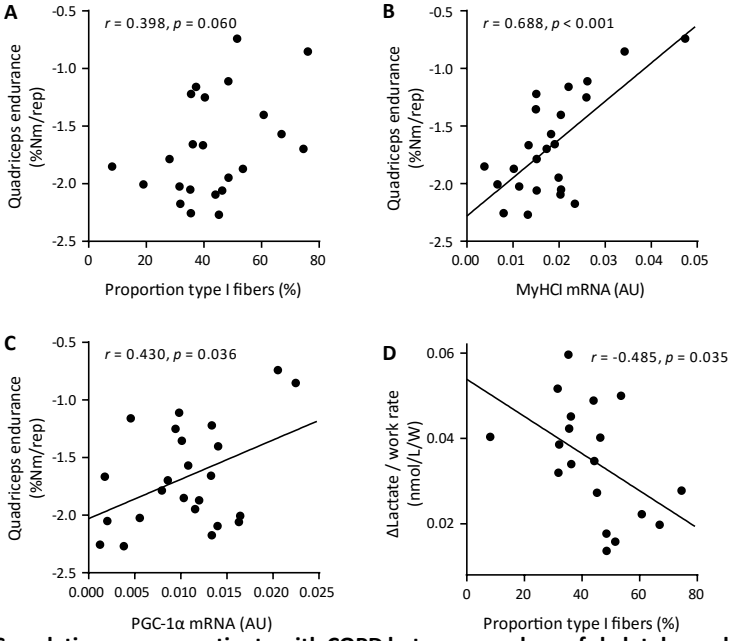

Figure 3 | Correlations among patients with COPD between markers of skeletal muscle oxidative phenotype and quadriceps endurance, and the rise in blood lactate relative to work rate during an incremental cycling test. A, correlation between the proportion of type I fibers and quadriceps endurance. **B**, correlation between myosin heavy chain I mRNA expression and quadriceps endurance. **C**, correlation between PGC-1α mRNA expression and quadriceps endurance. **D**, correlation between the proportion of type I fibers and the rise in blood lactate relative to work rate during an incremental cycling test.

Skeletal muscle oxidative stress

The levels of protein carbonylation, tyrosine nitration, and MDA-protein adducts were not different between patients and controls (Figure 4). Among the patients with COPD, we found inverse correlations between protein carbonylation and type I fiber proportion, MyHC-I gene expression, and quadriceps endurance, and a positive correlation between protein carbonylation level and MyHC-IIa expression (Figure 5). In line with this finding, protein carbonylation was positively correlated with type IIx fiber proportion (ρ = 0.429, p = 0.023). Additionally, tyrosine nitration was inversely correlated with quadriceps endurance (r = −0.422, p = 0.040), and MDA-protein adducts were inversely associated with MyHC-I gene expression (r = −0.384, p = 0.044). Markers of oxidative stress were not correlated with FFMI or fiber CSA among patients with COPD, and no correlations were found between oxidative stress markers and markers of Oxphen in the healthy subjects (data not shown).

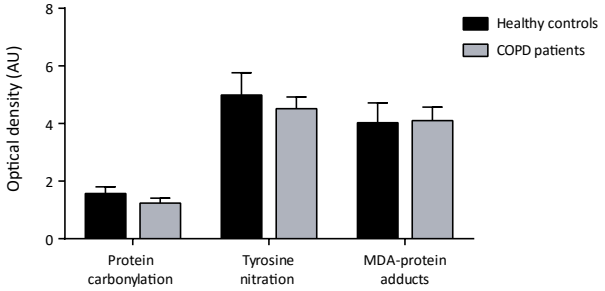

Figure 4 | Levels of skeletal muscle oxidative stress. The levels of protein carbonylation, tyrosine nitration, and MDA-protein adducts were not different between patients with COPD and controls; all $p > 0.05$.

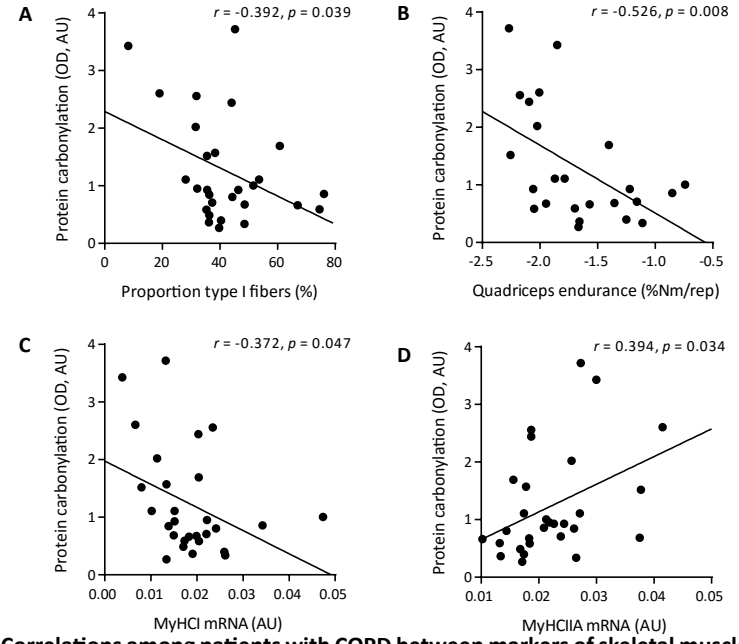

Figure 5 | Correlations among patients with COPD between markers of skeletal muscle oxidative phenotype, quadriceps endurance, and level of protein carbonylation. Correlations between the level of protein carbonylation and proportion type I fibers (**A**), quadriceps endurance (**B**), myosin heavy chain mRNA expression (**C**), and myosin heavy chain IIa mRNA expression (**D**).

DISCUSSION

Whereas previous studies have clearly shown skeletal muscle dysfunction in patients with advanced COPD, the main novelty of the current study is that we identified a loss of quadriceps Oxphen and decreased quadriceps endurance in patients with mild-to-moderate COPD. Interestingly, these abnormalities existed even in the absence of significant muscle wasting. Also, we found consistent, inverse correlations between markers of Oxphen and oxidative stress among the patients with COPD. Note that our study was of cross-sectional nature and did not allow for longitudinal inferences. However, linking the various cross-sectional studies across COPD severity stages, the available data suggest that the loss of skeletal muscle endurance and skeletal muscle Oxphen already occur in patients with mild-to-moderate COPD and progress with declining lung function, and suggest a potential involvement of oxidative stress.

We assessed a large panel of markers of skeletal muscle Oxphen and found that many were significantly decreased in our patients with mild-to-moderate COPD compared with well-matched controls. More specifically, the loss of Oxphen in our group of patients with COPD was characterized by a decreased proportion of type I fibers, decreased gene expression of PGC-1α and MyHC-I, decreased protein expression of subunits of OXPHOS complexes IV and V, and decreased HADH/PFK enzyme activity. The mean differences in proportions of type I, IIa, and IIx fibers between our patients with mild-to-moderate COPD and matched healthy controls were 20%, 15%, and 4%, respectively. For comparison, pooled analyses from a meta-analysis in patients with advanced COPD showed these differences to be 22%, 7%, and 13%, respectively (15). These combined data suggest that a decrease in slow-oxidative type I fiber proportion already occurs in the early stages of COPD, and that a further shift from fast-oxidative type IIa to fast-glycolytic type IIx fibers continues in advanced COPD toward even more dependence on glycolytic metabolism. It should be acknowledged that decreased expression of subunits of the key respiratory chain complexes does not necessarily indicate decreased cytochrome *c* oxidase (COX) activity or overall lower mitochondrial respiration. Several other studies have assessed COX activity in muscle biopsies of patients with COPD and showed contrasting results. For example, reduced skeletal muscle COX activity has been reported in patients with moderate COPD by some authors (14, 16, 23), whereas others reported even higher COX activity in patients with moderate-to-severe COPD (30, 36). Between-study differences remain unexplained; therefore, these data provide further indication for studying mitochondrial respiration in more detail in different COPD disease stages, including the early stages.

We found that markers of oxidative phenotype were significantly correlated with quadriceps endurance, implying that the magnitude of loss of oxidative phenotype reached the level of clinical importance in terms of quadriceps endurance. Similar findings were previously reported in a population of patients with advanced COPD with significant muscle wasting (2). Our data show that these abnormalities are already present in early COPD even in the absence of muscle wasting. In a recent study by Saey *et al.* (35), the change in lactate/work rate during a constant work rate test was significantly higher in patients with COPD and muscle wasting (mean FEV_1 45% of predicted) compared with controls. This coincided with a decreased proportion of type I fibers and increased type IIa fibers, and a wide array of increased glycolytic markers. The authors argued that increased glycolysis underlies the increased change in lactate/work rate. Although this

seems plausible, no correlations between the change in lactate/work rate and metabolic markers were presented by Saey *et al.* (35). We did, however, find that the proportion of type I fibers was associated with an increased change in lactate/work rate during an incremental load test in patients with COPD without muscle wasting.

PGC-1α is considered the major regulator of skeletal muscle oxidative metabolism. Indeed, its expression is known to be significantly induced upon aerobic exercise, which subsequently orchestrates oxidative gene expression to prepare the muscle for a next bout of exercise (28). Puente-Maestu *et al.* (29) have recently shown that moderate-intensity exercise increased skeletal muscle PGC-1α gene expression in patients with COPD (FEV_1 50% of predicted) with normal FFMI. Because we found that PGC-1α gene expression was decreased by 40% in our group of patients, this would suggest that the muscle oxidative machinery fails, at least in part, at the regulatory level. The downstream target of PGC-1α, Tfam, tended to be decreased expressed as well. Expression levels of other co-transcription factors implicated in the regulation of Tfam expression (e.g., PGC-1β, PRC, NRF-1, and NRF-2α) were not differentially expressed between patients with COPD and controls.

Physical inactivity, or deconditioning, has been proposed to contribute to skeletal muscle dysfunction in COPD (47). We used accelerometry to assess both quantitative and qualitative daily living physical activity, and studied the relations with muscle Oxphen. We did not specifically select the healthy subjects on the basis of sedentary behavior, so the finding that our patients with COPD were on average 39% less physically active compared with the controls was not surprising. In addition, we found that our group of patients engaged in less MVPA bouts and that these bouts were shorter and less intense than those of controls. The level and intensity of physical activity was positively correlated with FEV_1 within the group of patients with COPD, which is consistent with previous reports (13, 17, 40). Interestingly, however, we could not identify any relation between markers of Oxphen and total physical activity level nor its intensity in our group of patients. Although we did not select our healthy controls on the basis of sedentary behavior, our data do not support the presumption that physical inactivity is the principal determinant of impaired skeletal muscle Oxphen in mild-to-moderate COPD. Still, the fact that no association between loss of Oxphen and physical inactivity was found does not exclude the possibility that physical activity plays a role in the multifactorial pathways involved in loss of Oxphen.

Whereas basal levels of skeletal muscle oxidative stress were comparable between our patients and controls, we found that markers of muscle oxidative stress were significantly associated with the loss in muscle Oxphen among patients with COPD, but were not related to muscle mass. Oxidative stress has been suggested to render the muscle susceptible to atrophy because damaged (oxidized) proteins are prone to be degraded. However, this concept has recently been challenged because no differences in basal skeletal muscle oxidative stress levels were found between patients with advanced COPD with and without muscle wasting (10). Enhanced mitochondrial production of reactive oxygen species (ROS) has been observed in patients with moderate-to-severe COPD, which has been proposed to be linked to the proportional increase in type II fibers (27). Recently, it has also been demonstrated that OXPHOS complex III is the main site of ROS production within peripheral muscles of patients with COPD, who exhibited similar clinical features as those recruited in the current investigation (31). Furthermore,

compared with type I fiber mitochondria, type II fiber mitochondria exhibit enhanced ROS production, as was shown in rats (4). Taken together, the associations encountered between protein oxidation levels and the slow-to-fast phenotype shift among patients with mild-to-moderate COPD may be partly explained by mitochondrial dysfunction and enhanced ROS production.

In peripheral skeletal muscle of emphysematous hamsters, decreased citrate synthase activity and increased lipid peroxidation have been reported, which were not related to decreased body weight, muscle mass, or physical activity level (21, 22). In line with these findings, in a rat model of emphysema, Zhang *et al.* (48) reported no change in muscle mass but showed increased skeletal muscle lipofuscin inclusions (a marker of oxidative stress), which was correlated with decreased muscle endurance. Collectively, the available data suggest a relation between oxidative stress and the loss of oxidative capacity in COPD-related muscle dysfunction and it can be speculated that loss of Oxphen, through enhanced oxidative stress, may eventually augment muscle wasting as well.

In conclusion, this study shows evidence for a loss of muscle Oxphen and decreased quadriceps endurance in patients with mild-to-moderate COPD without overt loss of muscle mass. Our results indicate that timely intervention strategies aimed at improving muscle Oxphen in early COPD may improve or prevent a further loss in quadriceps endurance.

ACKNOWLEDGMENTS

This study was performed within the framework of Project T1–201 of the Dutch Top Institute Pharma. Partners in the project include Maastricht University Medical Center+, University Medical Center Utrecht, University Medical Center Groningen, AstraZeneca, Nycomed, GlaxoSmithKline, and Danone Research. The partners had no role in the interpretation of the data or the writing of the manuscript. All the partners approved the manuscript. None of the authors have a conflict of interest. We thank Kathleen Daenen and Monica Vila-Ubach for their technical support.

REFERENCES

1. Skeletal muscle dysfunction in chronic obstructive pulmonary disease. A statement of the American Thoracic Society and European Respiratory Society. Am J Respir Crit Care Med 159: S1-40, 1999.
2. Allaire J, Maltais F, Doyon JF, Noel M, LeBlanc P, Carrier G, Simard C, and Jobin J. Peripheral muscle endurance and the oxidative profile of the quadriceps in patients with COPD. Thorax 59: 673-678, 2004.
3. Allen D, Winters E, Kenna PF, Humphries P, and Farrar GJ. Reference gene selection for real-time rtPCR in human epidermal keratinocytes. J Dermatol Sci 49: 217-225, 2008.
4. Anderson EJ, and Neufer PD. Type II skeletal myofibers possess unique properties that potentiate mitochondrial H(2)O(2) generation. Am J Physiol Cell Physiol 290: C844-851, 2006.
5. Barnes PJ, and Celli BR. Systemic manifestations and comorbidities of COPD. Eur Respir J 33: 1165-1185, 2009.
6. Barreiro E, Gea J, Corominas JM, and Hussain SN. Nitric oxide synthases and protein oxidation in the quadriceps femoris of patients with chronic obstructive pulmonary disease. Am J Respir Cell Mol Biol 29: 771-778, 2003.
7. Bergmeyer HU, Gawehn K, and Grassl M. 3-Hydroxyacyl-CoA dehydrogenase. In: Methods of enzymatic analysis, edited by Bergmeyer HU. Weinheim; Germany: Verlag Chemie GmbH, 1974, p. 474.
8. Bergström J. Muscle electrolytes in man. Determination by neutron activation analysis on needle biopsy specimens. A study on normal subjects, kidney patients, and patients with chronic diarrhea. Scand J Clin Lab Invest 14: 1–110, 1962.
9. Bernard S, LeBlanc P, Whittom F, Carrier G, Jobin J, Belleau R, and Maltais F. Peripheral muscle weakness in patients with chronic obstructive pulmonary disease. Am J Respir Crit Care Med 158: 629-634, 1998.
10. Fermoselle C, Rabinovich R, Ausin P, Puig-Vilanova E, Coronell C, Sanchez F, Roca J, Gea J, and Barreiro E. Does oxidative stress modulate limb muscle atrophy in severe COPD patients? Eur Respir J 40: 851-862, 2012.
11. Franssen FM, Broekhuizen R, Janssen PP, Wouters EF, and Schols AM. Limb muscle dysfunction in COPD: effects of muscle wasting and exercise training. Med Sci Sports Exerc 37: 2-9, 2005.
12. Franssen FM, Sauerwein HP, Ackermans MT, Rutten EP, Wouters EF, and Schols AM. Increased postabsorptive and exercise-induced whole-body glucose production in patients with chronic obstructive pulmonary disease. Metabolism 60: 957-964, 2011.
13. Garcia-Rio F, Lores V, Mediano O, Rojo B, Hernanz A, Lopez-Collazo E, and Alvarez-Sala R. Daily physical activity in patients with chronic obstructive pulmonary disease is mainly associated with dynamic hyperinflation. Am J Respir Crit Care Med 180: 506-512, 2009.
14. Gosker HR, van Mameren H, van Dijk PJ, Engelen MP, van der Vusse GJ, Wouters EF, and Schols AM. Skeletal muscle fibre-type shifting and metabolic profile in patients with chronic obstructive pulmonary disease. Eur Respir J 19: 617-625, 2002.
15. Gosker HR, Zeegers MP, Wouters EF, and Schols AM. Muscle fibre type shifting in the vastus lateralis of patients with COPD is associated with disease severity: a systematic review and meta-analysis. Thorax 62: 944-949, 2007.
16. Green HJ, Bombardier E, Burnett M, Iqbal S, D'Arsigny CL, O'Donnell DE, Ouyang J, and Webb KA. Organization of metabolic pathways in vastus lateralis of patients with chronic obstructive pulmonary disease. Am J Physiol Regul Integr Comp Physiol 295: R935-941, 2008.
17. Jehn M, Schmidt-Trucksass A, Meyer A, Schindler C, Tamm M, and Stolz D. Association of daily physical activity volume and intensity with COPD severity. Respir Med 105: 1846-1852, 2011.
18. Ling KH, Paetkau V, Marcus F, and Lardy HA. Phosphofructokinase: I. Skeletal Muscle. In: Methods EnzymolAcademic Press, 1966, p. 425-429.
19. Masse LC, Fuemmeler BF, Anderson CB, Matthews CE, Trost SG, Catellier DJ, and Treuth M. Accelerometer data reduction: a comparison of four reduction algorithms on select outcome variables. Med Sci Sports Exerc 37: S544-554, 2005.
20. Matthew CE. Calibration of accelerometer output for adults. Med Sci Sports Exerc 37: S512-522, 2005.
21. Mattson JP, and Poole DC. Pulmonary emphysema decreases hamster skeletal muscle oxidative enzyme capacity. J Appl Physiol (1985) 85: 210-214, 1998.
22. Mattson JP, Sun J, Murray DM, and Poole DC. Lipid peroxidation in the skeletal muscle of hamsters with emphysema. Pathophysiology 8: 215-221, 2002.
23. Naimi AI, Bourbeau J, Perrault H, Baril J, Wright-Paradis C, Rossi A, Taivassalo T, Sheel AW, Rabol R, Dela F, and Boushel R. Altered mitochondrial regulation in quadriceps muscles of patients with COPD. Clin Physiol Funct Imaging 31: 124-131, 2011.
24. O'Donovan G, Blazevich AJ, Boreham C, Cooper AR, Crank H, Ekelund U, Fox KR, Gately P, Giles-Corti B, Gill JM, Hamer M, McDermott I, Murphy M, Mutrie N, Reilly JJ, Saxton JM, and Stamatakis E. The ABC of Physical Activity for Health: a consensus statement from the British Association of Sport and Exercise Sciences. J Sports Sci 28: 573-591, 2010.
25. Ogilvie RW, and Feeback DL. A metachromatic dye-ATPase method for the simultaneous identification of skeletal muscle fiber types I, IIA, IIB and IIC. Stain Technol 65: 231-241, 1990.
26. Pate RR, Pratt M, Blair SN, Haskell WL, Macera CA, Bouchard C, Buchner D, Ettinger W, Heath GW, King AC, and et al. Physical activity and public health. A recommendation from the Centers for Disease Control and Prevention and the American College of Sports Medicine. JAMA 273: 402-407, 1995.
27. Picard M, Godin R, Sinnreich M, Baril J, Bourbeau J, Perrault H, Taivassalo T, and Burelle Y. The mitochondrial phenotype of peripheral muscle in chronic obstructive pulmonary disease: disuse or dysfunction? Am J Respir Crit Care Med 178: 1040-1047, 2008.
28. Pilegaard H, Saltin B, and Neufer PD. Exercise induces transient transcriptional activation of the PGC-1alpha gene in human skeletal muscle. J Physiol 546: 851-858, 2003.

29. Puente-Maestu L, Lazaro A, Tejedor A, Camano S, Fuentes M, Cuervo M, Navarro BO, and Agusti A. Effects of exercise on mitochondrial DNA content in skeletal muscle of patients with COPD. Thorax 66: 121-127, 2011.
30. Puente-Maestu L, Perez-Parra J, Godoy R, Moreno N, Tejedor A, Gonzalez-Aragoneses F, Bravo JL, Alvarez FV, Camano S, and Agusti A. Abnormal mitochondrial function in locomotor and respiratory muscles of COPD patients. Eur Respir J 33: 1045-1052, 2009.
31. Puente-Maestu L, Tejedor A, Lazaro A, de Miguel J, Alvarez-Sala L, Gonzalez-Aragoneses F, Simon C, and Agusti A. Site of mitochondrial reactive oxygen species production in skeletal muscle of chronic obstructive pulmonary disease and its relationship with exercise oxidative stress. Am J Respir Cell Mol Biol 47: 358-362, 2012.
32. Quanjer PH, Tammeling GJ, Cotes JE, Pedersen OF, Peslin R, and Yernault JC. Lung volumes and forced ventilatory flows. Report Working Party Standardization of Lung Function Tests, European Community for Steel and Coal. Official Statement of the European Respiratory Society. Eur Respir J Suppl 16: 5-40, 1993.
33. Remels AH, Schrauwen P, Broekhuizen R, Willems J, Kersten S, Gosker HR, and Schols AM. Peroxisome proliferator-activated receptor expression is reduced in skeletal muscle in COPD. Eur Respir J 30: 245-252, 2007.
34. Rodriguez DA, Kalko S, Puig-Vilanova E, Perez-Olabarria M, Falciani F, Gea J, Cascante M, Barreiro E, and Roca J. Muscle and blood redox status after exercise training in severe COPD patients. Free Radic Biol Med 52: 88-94, 2012.
35. Saey D, Lemire BB, Gagnon P, Bombardier E, Tupling AR, Debigare R, Cote CH, and Maltais F. Quadriceps metabolism during constant workrate cycling exercise in chronic obstructive pulmonary disease. J Appl Physiol (1985) 110: 116-124, 2011.
36. Sauleda J, Garcia-Palmer F, Wiesner RJ, Tarraga S, Harting I, Tomas P, Gomez C, Saus C, Palou A, and Agusti AG. Cytochrome oxidase activity and mitochondrial gene expression in skeletal muscle of patients with chronic obstructive pulmonary disease. Am J Respir Crit Care Med 157: 1413-1417, 1998.
37. Schols AM, and Gosker HR. The pathophysiology of cachexia in chronic obstructive pulmonary disease. Curr Opin Support Palliat Care 3: 282-287, 2009.
38. Schols AM, Soeters PB, Dingemans AM, Mostert R, Frantzen PJ, and Wouters EF. Prevalence and characteristics of nutritional depletion in patients with stable COPD eligible for pulmonary rehabilitation. Am Rev Respir Dis 147: 1151-1156, 1993.
39. Shepherd D, and Garland PB. Citrate synthase from rat liver. In: Methods EnzymolAcademic Press, 1969, p. 11-16.
40. Steele BG, Holt L, Belza B, Ferris S, Lakshminaryan S, and Buchner DM. Quantitating physical activity in COPD using a triaxial accelerometer. Chest 117: 1359-1367, 2000.
41. Troiano RP, Berrigan D, Dodd KW, Masse LC, Tilert T, and McDowell M. Physical activity in the United States measured by accelerometer. Med Sci Sports Exerc 40: 181-188, 2008.
42. van den Borst B, Gosker HR, Wesseling G, de Jager W, Hellwig VA, Snepvangers FJ, and Schols AM. Low-grade adipose tissue inflammation in patients with mild-to-moderate chronic obstructive pulmonary disease. Am J Clin Nutr 94: 1504-1512, 2011.
43. van Wetering CR, Hoogendoorn M, Mol SJ, Rutten-van Molken MP, and Schols AM. Short- and long-term efficacy of a community-based COPD management programme in less advanced COPD: a randomised controlled trial. Thorax 65: 7-13, 2010.
44. Vandesompele J, De Preter K, Pattyn F, Poppe B, Van Roy N, De Paepe A, and Speleman F. Accurate normalization of real-time quantitative RT-PCR data by geometric averaging of multiple internal control genes. Genome Biol 3: RESEARCH0034, 2002.
45. Verdijk LB, Koopman R, Schaart G, Meijer K, Savelberg HH, and van Loon LJ. Satellite cell content is specifically reduced in type II skeletal muscle fibers in the elderly. Am J Physiol Endocrinol Metab 292: E151-157, 2007.
46. Wagenmakers R, van den Akker-Scheek I, Groothoff JW, Zijlstra W, Bulstra SK, Kootstra JW, Wendel-Vos GC, van Raaij JJ, and Stevens M. Reliability and validity of the short questionnaire to assess health-enhancing physical activity (SQUASH) in patients after total hip arthroplasty. BMC Musculoskelet Disord 9: 141, 2008.
47. Wagner PD. Skeletal muscles in chronic obstructive pulmonary disease: deconditioning, or myopathy? Respirology 11: 681-686, 2006.
48. Zhang XL, Pang BS, Hou XL, Wang J, and Wang C. Oxidative stress and peripheral skeletal muscle dysfunction in rats with emphysema. Chin Med J (Engl) 123: 40-44, 2010.

Chapter 5

The muscle oxidative regulatory response to acute exercise is not impaired in less advanced COPD despite a decreased oxidative phenotype

Ilse G.M. Slot, Bram van den Borst, Valéry A.C.V. Hellwig, Esther Barreiro, Annemie M.W.J. Schols, Harry R. Gosker

PLoS One, 2014. 9(2): p. e90150

ABSTRACT

Already in an early disease stage, patients with chronic obstructive pulmonary disease (COPD) are confronted with impaired skeletal muscle function and physical performance due to a loss of oxidative type I muscle fibers and oxidative capacity (*i.e.* oxidative phenotype; Oxphen). Physical activity is a well-known stimulus of muscle Oxphen and crucial for its maintenance. We hypothesized that a blunted response of Oxphen genes to an acute bout of exercise could contribute to decreased Oxphen in COPD. For this, 28 patients with less advanced COPD (age 65±7 yrs, FEV_1 59±16% predicted) and 15 age- and gender-matched healthy controls performed an incremental cycle ergometry test. The Oxphen response to exercise was determined by the measurement of gene expression levels of Oxphen markers in pre and 4h-post exercise quadriceps biopsies. Because exercise-induced hypoxia and oxidative stress may interfere with Oxphen response, oxygen saturation and oxidative stress markers were assessed as well. Regardless of oxygen desaturation and absolute exercise intensities, the Oxphen regulatory response to exercise was comparable between COPD patients and controls with no evidence of increased oxidative stress. In conclusion, the muscle Oxphen regulatory response to acute exercise is not blunted in less advanced COPD, regardless of exercise-induced hypoxia. Hence, this study provides further rationale for incorporation of exercise training as integrated part of disease management to prevent or slow down loss of muscle Oxphen and related functional impairment in COPD.

INTRODUCTION

Loss of skeletal muscle oxidative phenotype (Oxphen) is prevalent in chronic obstructive pulmonary disease (COPD) (13, 24, 25). It includes a proportional shift from slow-oxidative type I muscle fibers towards the fast-glycolytic type II fibers, associated with a reduced capacity of oxidative metabolism and in advanced disease also mitochondrial dysfunction (1). Loss of muscle Oxphen is related to functional impairments, such as a reduction in muscle endurance (1), whole body exercise capacity, and mechanical efficiency (19), and it has been proposed as a driver of cardiovascular and metabolic risk (42) and cachexia (36). Loss of muscle Oxphen is most prominent in severe COPD, but we recently showed that the process is already ongoing in patients with less advanced COPD (43). Hence, this earlier stage of the disease is of particular importance to gain mechanistic insight into the onset of Oxphen loss in COPD.

Exercise is an important stimulus for maintenance of muscle Oxphen. Because patients with COPD are physically less active (30), it is tempting to attribute Oxphen loss in these patients to disuse. However, several recent reports could not show such an association between physical activity level and Oxphen (14, 28, 43). Physiologically, muscle Oxphen is progressively stimulated and maintained by repeated bouts of exercise through induction of among others peroxisome proliferator-activated receptor (PPAR) coactivator-1α (PGC-1α), PPAR-α and -δ, and mitochondrial transcription factor A (TFAM) (23, 33). We hypothesized that the response of Oxphen regulation to acute bouts of exercise is blunted in COPD, which could contribute to a loss of muscle Oxphen irrespective of physical activity level. To test this hypothesis we compared Oxphen markers and their regulators in muscle biopsies obtained before and after an acute bout of exercise, between less advanced COPD patients and healthy controls who were matched for age and body mass index (BMI).

Hypoxia is known to increase muscle glycolytic capacity relative to oxidative capacity (17, 26). In humans, hypoxic exposure also induces loss of muscle oxidative capacity by reducing mitochondrial volume (reviewed in (16)). Exercise-induced oxygen desaturation even occurs in some patients with less advanced COPD, potentially reflecting or leading to hypoxia in the exercising muscle. Experimental research in mice has shown that exposure to acute hypoxia can also induce oxidative stress in skeletal muscle mitochondria (22). Indeed, elevated levels of oxidative stress markers have been shown in muscles of COPD patients with chronic hypoxemia (18). Moreover, enhanced exercise-induced oxidative stress has frequently been observed in muscle of patients with severe COPD (27), particularly in the wasted subgroup (6). Interestingly, in severe patients, oxidative stress is inversely associated with muscle endurance (10) and *in vitro* permeabilized muscle fibers of patients with severe COPD produce significantly more reactive oxygen species than those of healthy controls (31). This is possibly related to a fiber-type shift, since studies in rats have shown that mitochondria within type II fibers release significantly more H_2O_2 than those within oxidative fibers (5). As such, oxygen desaturation and/or muscle oxidative stress could mediate an anticipated blunted Oxphen response in COPD. A secondary objective was therefore to determine the involvement of exercise-induced oxygen desaturation and oxidative stress in the response to an acute exercise bout.

METHODS

Ethics statement

Written informed consent was obtained from all subjects and the ethical review board of the Maastricht University Medical Center+ approved the study (08-2-059). The study was registered at www.trialregister.nl as NTR1402.

Patient characteristics

The study population included 28 clinically stable mild to moderate COPD patients (FEV_1 59±16% predicted; Pa,O_2 9.3±1.0 kPa) and 15 healthy controls. Recruitment of patients and controls and exclusion criteria were previously described (43). Briefly, patients were recruited from the outpatient clinic of Maastricht University Medical Center+ (MUMC+, Maastricht, The Netherlands) and via advertisements in local newspapers. Exclusion criteria were long-term oxygen therapy, oral corticosteroid use, acute exacerbation requiring hospital admission in the past eight weeks, rehabilitation in the past six months and known co-morbidities potentially interfering with study outcome parameters. Healthy controls were recruited via advertising in local newspapers and absence of co-morbidities and airflow limitation was verified through history-taking by a physician, and pulmonary function tests. Healthy controls were matched to COPD patients on age, BMI and sex distribution. Study subjects were carefully characterized regarding body composition, lung function, smoking status and daily physical activity level, as reported previously (43). The protocol used to determine quadriceps function on a dynamometer was previously described (43). Briefly, under strong encouragement, subjects performed thirty sequential volitional maximal contractions at an angular velocity of 90°/s. Isokinetic quadriceps endurance was determined as proportional decline in peak torques (relative to the highest peak torque) per repetition (%/rep).

Experimental protocol

To study the response of Oxphen regulators and oxidative stress to acute exercise, subjects performed an incremental load cycle ergometry test. Quadriceps muscle biopsies were obtained directly before and 4 h after the exercise test for Oxphen and oxidative stress analyses to obtain a maximal response of metabolic and oxidative stress-related genes after exercise. During the entire exercise test, oxygen saturation was measured by means of traditional finger pulse oximetry, as well as using a portable continuous-wave near-infrared spectroscopy (NIRS) system to examine oxygen saturation locally at the muscular level. Arterial punctures were performed before exercise and at maximal exertion for gas and lactate analyses.

Acute exercise protocol

All subjects performed an incremental load cycle ergometry test. The rationale for this protocol was to invoke a rapid exercise response in terms of Oxphen regulation particularly in the quadriceps muscle (see below). Peak oxygen uptake ($V'O_2peak$) and peak work load were determined as previously described (11). Anaerobic threshold was determined from ergospirometry data using the v-slope method (7). Arterial punctures of the radial artery at rest and at $V'O_2peak$ were available from *n* = 19 COPD patients and *n* = 11 healthy subjects. Arterial blood gas and lactate concentrations were analyzed on a Chiron blood gas analyzer 865 (Chiron Diagnostics, Emeryville, CA).

Arterial and peripheral muscle oxygenation

Arterial oxygen saturation was continuously monitored using a finger pulse oximeter. By *post hoc* stratification the patients were divided into those who desaturated during exercise (Sp,O_2 fall ≥ 4%; $COPD_D$, n = 13) and those who did not (Sp,O_2 fall < 4%; $COPD_{ND}$, n = 15) according to ATS criteria (4). Quadriceps muscle oxygenation was measured using the PortaMon portable continuous-wave near-infrared spectrophotometer (NIRS, Artinis Medical Systems, Zetten, The Netherlands). The probe was attached with Velcro straps on the *vastus lateralis* of the non-biopsied leg approximately 10 cm proximally from the knee joint, and covered with a black cloth to eliminate environmental light. Measurements started 3 minutes before exercise while the subject was still at rest and continued for 2–5 minutes after the exercise test until the signal had stabilized. Baseline values were established during 3 minutes of unloaded cycling before the incremental exercise test. Tissue oxygenation was measured continuously. Traces were analyzed with OxySoft Software (v2.1.2; Artinis Medical Systems). The tissue saturation index (TSI) was calculated using spatial resolved spectroscopy using the equation below, with $[O_2Hb]$ and [HHb] representing concentrations of oxygenated and deoxygenated hemoglobin/myoglobin.

$$TSI = 100\times \frac{[O_2Hb]}{[O_2Hb]+[HHb]}$$

Values were reported as change from baseline (Δ). Using mono-exponential curve fitting, the time constant of muscle reoxygenation (tau, τ) was determined from the slope of the TSI curve during the reoxygenation phase. Twelve subjects (4 $COPD_{ND}$, 4 $COPD_D$ patients, and 4 healthy controls) were excluded from further NIRS analyses mainly because their skin fold at the site of the NIRS measurement was greater than 3 cm (which is the operational limit for the NIRS probe), or because the signal was poor or did not show a clear drop in TSI.

Muscle biopsy and analyses

Biopsies were obtained at rest and 4 h after the exercise test from quadriceps muscle (*vastus lateralis*) of the dominant leg from two separate incisions approximately 2 cm apart using the needle biopsy technique (9). The interval between the exercise test and the second biopsy was chosen after careful study of the literature to obtain a maximal response of metabolic genes after exercise (e.g., (32, 45)). Muscle tissue was frozen in melting isopentane precooled in liquid nitrogen and stored in aliquots at −80°C for histology and molecular analyses.

Techniques for sample preparation for analyses of fiber-type composition, gene expression, oxidative stress markers, metabolic enzyme activity as well as the corresponding analyses have been previously described (43). Briefly, fiber-type composition was determined on 5 µm serial cryosections using antibodies against myosin heavy chain (MyHC) I, MyHC IIa (both from Developmental Studies Hybridoma Bank, University of Iowa, USA), and laminin (Sigma, Zwijndrecht, the Netherlands). Fiber-type classification was aided by myosin ATPase-activity staining with acidic pre-incubation at pH 4.40 (29). For qRT-PCR, RNA was extracted from 10–30 mg muscle tissue using the ToTALLY RNA™ Kit (Ambion Ltd., Foster City, CA, USA) according to the supplier's protocol, followed by genomic DNA removal with the RNeasy Mini Kit with RNase-free DNase (Qiagen, Venlo, The Netherlands). 400 ng RNA was reverse transcribed to

cDNA with anchored oligo(dT) primers according to the supplier's protocol (Transcriptor First Strand cDNA Synthesis kit, Roche Diagnostics, Woerden, The Netherlands). qRT-PCR primers were designed based on Ensembl transcript sequences or selected from literature (2, 44) and ordered from Sigma Genosys (Zwijndrecht, the Netherlands), with primer details shown in Table 1 and Table 2. Using these analyses, regulators and markers of oxidative and glycolytic metabolism as well as oxidative stress were assessed. Contents of antioxidant enzymes were determined with the western blot protocol using anti-catalase antibody (Calbiochem, San Diego, CA, USA) and anti-manganese superoxide dismutase and anti-Cu/Zn superoxide dismutase antibodies (Santa Cruz Biotechnology, CA, USA). Protein content of oxidative stress markers were identified using antibodies for protein carbonylation (anti-2,4-DNP moiety antibody, Oxyblot kit, Chemicon International Inc., Temecula, CA, USA), total protein nitration (anti-3-nitrotyrosine antibody, Invitrogen, Eugene, OR, USA), and total malondialdehyde (MDA)-protein adducts (anti-MDA antibody, Academy Biomedical Company Inc., Houston, TX, USA). For protein carbonylation, carbonyl groups in the protein side chains were first derivatized to 2,4-dinitrophenylhydrazone (DNP) using the Oxyblot kit (Chemicon International Inc., Temecula, CA, USA) according to the manufacturer's instructions. Exercise responses of gene expression and oxidative stress product variables were summarized with fold inductions, which were calculated by dividing post-exercise values by baseline values. Contents of representative subunits of oxidative phosphorylation (OXPHOS) complexes were determined by western blot using an anti-total OXPHOS antibody cocktail (MS604-300, Abcam, Cambridge, UK) with GAPDH (anti-GAPDH, #2118, Cell Signaling Technology, Leiden, The Netherlands) as a loading control. Metabolic activities for citrate synthase (CS, EC 2.3.3.1) and 3-hydroxyacyl-CoA dehydrogenase (HADH, EC 1.1.1.35) were assayed spectrophotometrically (Multiskan Spectrum; Thermo Labsystems, Breda, The Netherlands) as previously described (8, 20, 38). Absolute CS and HADH activities were normalized to total protein.

Statistics

The assumptions of normality and homogeneity of variances were checked for all experimental groups with the Shapiro-Wilk test and Levene's test. Three different sets of statistical comparisons were made. First, baseline comparisons between the COPD patients and controls were tested using independent Student's *t* test or Mann-Whitney test as appropriate. Comparisons between $COPD_{ND}$, $COPD_{D}$ and control groups were made using one-way ANOVA (*post hoc* Gabriel), Welch's ANOVA (*post hoc* Games-Howell) or Kruskal-Wallis non-parametric ANOVA (*post hoc* Mann-Whitney U with Bonferroni correction) as appropriate. Discontinuous variables were tested using Fisher's Exact test. These same tests were subsequently employed to analyze differences in exercise-induced response of skeletal muscle metabolic genes and oxidative stress markers between the groups (expressed as fold inductions), whereas paired Student's *t* test or Wilcoxon signed-rank test were performed to analyze such changes within each study group. Correlations were tested using Pearson's correlation coefficient, or Spearman's ρ in case of non-normally distributed data. Analyses were performed using IBM SPSS Statistics 20.0 (IBM Corp., Armonk, NY). A p-value < 0.05 was considered statistically significant.

Table 1 | qRT PCR primer details for reference genes

Symbol	Name	Ensembl ID	Forward primer (5'→3')	Reverse primer (5'→3')	Amplicon size (bp)
ALAS1	5-Aminolevulinate synthase 1	ENSG00000023330	CTGCAAAGATCTGACCCCTC	CCTCATCCACGAAGGTGATT	136
ACTB	Beta-actin	ENSG00000075624	AAGCCACCCCACTTCTCTCTAA	AATGCTATCACCTCCCCTGTGT	73
B2M	Beta-2-microglobulin	ENSG00000166710	CTGTGCTCGCGCTACTCTCTCTT	TGAGTAAACCTGAATCTTTGGAGTACGC	71
PPIA	Peptidyl-prolyl cis-trans isomerase A; Cyclophilin A	ENSG00000196262	CATCTGCACTGCCAAGACTGA	TTCATGCCTTCTTTCACTTTGC	72
GAPDH	Glyceraldehyde-3-phosphate dehydrogenase	ENST00000229239	GCACCACCAACTGCTTAGCA	TGGCAGTGATGGCATGGA	96
GUSB	Beta-glucuronidase	ENSG00000169919	CTCATTTGGAATTTTGCCGATT	CCGAGTGAAGATCCCCTTTTTA	81
HMBS	Hydroxymethyl-bilane synthase	ENSG00000256269	GGCAATGCGGCTGCAA	GGGTACCCACGCGAATCAC	64
HPRT1	Hypoxanthine phosphoribosyl-transferase 1	ENSG00000165704	TGACACTGGCAAAACAATGCA	GGTCCTTTTCACCAGCAAGCT	94
RPL13A	Ribosomal protein 13A	ENSG00000142541	CCTGGAGGAGAAGAGGAAAGAGA	TTGAGGACCTCTGTGTATTTGTCAA	126
RPLP0	Large ribosomal protein P0	ENSG00000089157	TCTACAACCCTGAAGTGCTTGATATC	GCAGACAGACACTGGCAACATT	90
UBC	Ubiquitin C	ENSG00000150991	ATTTGGGTCGCAGTTCTTG	TGCCTTGACATTCTCGATGGT	133
YWHAZ	Tyrosine 3-monooxygenase/ tryptophan 5-mono-oxygenase activation protein, zeta polypeptide	ENSG00000164924	ACTTTTGGTACATTGTGGCTTCAA	CCGCCAGGACAAACCAGTAT	94

Table 2 | qRT PCR primer details for genes of interest

Symbol	Name	Ensembl ID	Forward primer (5'→3')	Reverse primer (5'→3')	Amplicon size (bp)
COX4I1	Cytochrome c oxidase subunit IV isoform 1	ENSG00000131143	CCATGGATGAGAAAGTCGAGT	CGTTCGAGCCCCTGTTCA	75
CS	Citrate synthase	ENSG00000062485	GATGTGTCAGATGAGAAGTTACGAGACT	TGGCCATAGCCTGGAACAA	77
ESRRA	Estrogen-related receptor	ENSG00000173153	GCGGCTGGAGCGAGAGGAG	CTCGGCATCTTCGATGTGCAC	82
GABPA	GA binding protein alpha; nuclear respiratory factor 2 alpha	ENSG00000154727	CTCACCTGGGAACAGAACAGGAA	ACCCAAGAAATGCAGTCTCGAGC	102
HADHA	3 hydroxyacyl-CoA dehydrogenase/3 ketoacyl-CoA thiolase/ enoyl-CoA hydratase alpha	ENSG00000084754	TGGCTTCCCGCCTTGTC	TGGAGCCGGTCCACTATCTTC	78
HIF1A	Hypoxia inducible factor 1 alpha	ENSG00000100644	TGAACATAAAGTCTGCAACATGGA	TGAGGTTGGTTACTGTTGGTATCATATA	82
HK2	Hexokinase II	ENSG00000159399	GTAAATACAGTGGATCTCAATCTTCGGG	CAAGGATTTGAGATGATTCGCTATTCA	61
HMOX1	Heme oxygenase-1	ENSG00000100292	CACCCAGGCAGAGAATGCTGAGTTC	GCCGCTTCACATAGCGCTGCA	278
NRF1	Nuclear respiratory factor 1	ENSG00000106459	ACGTGGCCAGACACAGTCACC	TGGTCACCTCCGCCTGAGTTT	83
PFKM	PFK muscle	ENSG00000152556	CCTGCCCCTCATGGAATGT	GGGCTTCGTCAAATTTCTTCTC	77
PPARGC1A	Peroxisome proliferator-activated receptor gamma coactivator 1 alpha	ENSG00000109819	GACCAGTGCTACCTGAGAGAGACTT	GCTCGGCTCGGATTTCCT	97

Table 2 (continued) | qRT PCR primer details for genes of interest

Symbol	Name	Ensembl ID	Forward primer (5'→3')	Reverse primer (5'→3')	Amplicon size (bp)
PPARGC1B	Peroxisome proliferator-activated receptor gamma coactivator 1 beta	ENSG00000155846	GGCGCTTTGAAGTGTTTGGTG	TGATGAAGCCGTACTTCTCGCCT	81
PPARA	Peroxisome proliferator-activated receptor alpha	ENSG00000186951	CAGAACAAGGAGGCGGAGGTC	AGGTCCAAGTTTGCGAAGC	116
PPARD	Peroxisome proliferator-activated receptor delta	ENSG00000112033	TGACCAAAAAGAAGGCCCGC	GTCGTGGATCACAAAGGGCG	71
PPRC1	Peroxisome proliferator-activated receptor gamma coactivator-related 1	ENSG00000148840	GCCCTTTGATCTCTGCTTTGGG	AAGTCTTCCCGGTTGGAGTCAAG	81
SLC2A1	Glucose transporter (GLUT) 1	ENSG00000117394	TCTGGGCTGCCGGGTTCTAG	TTTGCAGGCTCCCACAGGC	81
SOD2	Mitochondrial superoxide dismutase 2; MnSOD	ENSG00000112096	TGGACAAACCTCAGCCCTAACG	TGATGGCTTCCAGCAACTCCC	60
TFAM	Mitochondrial transcription factor A	ENSG00000108064	GAAAGATTCCAAGAAGCTAAGGGTGATT	TCCAGTTTTCCTTTACAGTCTTCAGCTTTT	67
VEGFA	Vascular endothelial growth factor A	ENSG00000112715	CCAGGCCCTCGTCATTG	AAGGAGGAGGGCAGAATCAT	186

RESULTS

Pulmonary and anthropometric characteristics

Characteristics of the study subjects are summarized in Table 3. COPD patients had moderate airflow obstruction (FEV_1 59±16). Compared to healthy controls, the COPD patients had a lower resting arterial oxygen saturation (Sp,O_2 96 (95, 97) *vs.* 98 (98, 100)%) and daily physical activity level (214 (129, 300) *vs.* 328 (276, 489) counts/min). $COPD_D$ patients did not differ from $COPD_{ND}$ patients in terms of pulmonary function indices, but had a lower BMI.

Oxidative phenotype in quadriceps muscle

At baseline, as reported previously (43) and listed in Table 4, Oxphen markers were lower in COPD patients than in controls, which was reflected by lower type I and higher type II fiber proportions, and reduced content of some subunits of the oxidative phosphorylation complexes. Oxphen markers were not different between patients who did or did not desaturate during exercise (Table 4). Moreover, quadriceps endurance was reduced in this COPD cohort (decline in peak torque −1.74 (−2.04, −1.28) in COPD *vs.* −1.09 (−1.57, −0.91)%/repetition in healthy controls), but it was not different between $COPD_D$ and $COPD_{ND}$ patients (−1.86 (−2.02, −1.35) in $COPD_D$ *vs.* −1.61 (−2.14, −1.25)%/repetition in $COPD_{ND}$).

Cycle ergometry performance

Data from the cycle ergometry test are listed in Table 5. As expected, peak work rate was lower in COPD patients than in controls (72 (56, 96) *vs.* 156 (134, 255) Watt). No differences were found between $COPD_D$ and $COPD_{ND}$ patients.

Exercise-induced metabolic gene expression

The acute exercise clearly evoked an upregulation of genes known to be exercise-responsive, including PGC-1α-related co-activator PRC, glycolysis-involved hexokinase II and the master regulator of the hypoxic response, HIF-1α (Figure 1). The COPD patients did not respond differently to exercise than controls regarding expression of genes associated with muscle oxidative metabolism, nor of genes involved in glycolytic metabolism or hypoxia signaling. We also did not observe a different response in $COPD_D$ patients compared to $COPD_{ND}$ patients.

Exercise response of oxidative stress markers

At baseline, oxidative stress-induced protein modification levels such as carbonylation, tyrosine nitration and MDA adducts were not different between COPD patients and controls (43), nor between $COPD_D$ and $COPD_{ND}$ patients (data not shown). After exercise, gene expression levels of heme oxygenase-1 (HO-1) and manganese superoxide dismutase (MnSOD) were increased in both COPD patients and healthy controls (Figure 2A). An exercise response of the antioxidant enzymes was not detected at the protein level as manganese and copper/zinc superoxide dismutase and catalase protein content remained unchanged (Figure 2B). No differential response was shown between $COPD_D$ and $COPD_{ND}$ patients.

The increases in HO-1 and MnSOD gene expression did not correlate with exercise-induced oxidative stress-derived products; only MDA-protein adducts were slightly increased (Figure 2C) in $COPD_{ND}$ patients.

Table 3 | Main characteristics of subjects

	Healthy controls	COPD	$COPD_{ND}$	$COPD_{D}$
N (M / F)	15 (9 / 6)	28 (16 / 12)	15 (9 / 6)	13 (7 / 6)
Age, y	65 ± 6	65 ± 7	66 ± 7	65 ± 6
Height, cm	170 ± 11	169 ± 9	168 ± 7	169 ± 11
Weight, kg	72 ± 12	71 ± 10	74 ± 10	67 ± 10
BMI, kg/m	24.9 ± 3.3	25.1 ± 2.8	26.4 ± 2.5	23.5 ± 2.3 $^{\#}$
FFMI, kg/m	18.0 ± 1.9	17.5 ± 1.8	18.0 ± 2.0	16.9 ± 1.5
Smoking status current / former / never	1 / 7 / 7	10 / 18 / 0 **	7 / 8 / 0 **	3 / 10 / 0 *
FEV_1, % predicted	113 ± 15	59 ± 16 ***	61 ± 13 ***	56 ± 19 ***
FVC, % predicted	120 ± 17	104 ± 22 *	98 ± 20 *	110 ± 24
DL,CO, % predicted	95 ± 19	51 ± 16 ***	55 ± 16 ***	47 ± 16 ***
Sp,O_2 at rest, %	98 (98, 100)	96 (95, 97) ***	97 (96, 97) ***	95 (94, 98) ***
Pa,O_2 at rest, kPa	12.1 ± 1.1	9.3 ± 1.0 ***	9.5 ± 0.8 ***	9.1 ± 1.2 ***
Pa,CO_2 at rest, kPa	5.3 ± 0.2	5.2 ± 0.5	5.1 ± 0.5	5.2 ± 0.4
Daily physical activity, counts/min	328 (276, 489)	214 (129, 300) **	208 (140, 278) **	220 (108, 366)

Values are expressed as mean ± SD or median (25th percentile, 75th percentile). Abbreviations: BMI, body mass index; FFMI, fat-free mass index; FEV_1, forced expiratory volume in one second; FVC, forced vital capacity; DL,CO, diffusion capacity of the lungs for carbon monoxide; Sp,O_2, oxygen saturation measured via pulse oximetry. Significance of difference compared to controls: $^{*}p < 0.05$, $^{**}p < 0.01$, $^{***}p \leq 0.001$. Level of significance $COPD_D$ *vs.* $COPD_{ND}$ patients: $^{\#}p < 0.05$.

Table 4 | Main characteristics of *vastus lateralis* muscle fibers

	Healthy controls	COPD	$COPD_{ND}$	$COPD_{D}$
Type I proportion, %	62.7 (55.3, 68.3)	39.7 (35.3, 48.6) ***	40.3 (35.5, 62.3) *	39.7 (29.8, 47.4) ***
Type I/IIa proportion, %	8.1 (4.6, 11.0)	5.6 (2.2, 9.5)	5.3 (3.5, 9.0)	6.4 (1.2, 12.7)
Type IIa proportion, %	25.5 (16.8, 32.4)	40.5 (25.9, 48.9) **	32.0 (24.5, 46.1) *	45.4 (39.7, 55.2) ***
Type IIa/IIx proportion, %	1.0 (0.3, 3.4)	3.6 (1.1, 8.1)	4.3 (1.0, 9.4)	3.6 (0.7, 7.4)
Type IIx proportion, %	0.5 (0.0, 2.7)	2.3 (0.5, 9.4) *	2.2 (0.2, 8.8)	3.2 (0.6, 11.0)
Type I fiber CSA, µm2	8703 ± 1858	8154 ± 2460	8524 ± 2655	7756 ± 2268
Type I/IIa fiber CSA, µm2	6540 ± 2048	6073 ± 2742	6274 ± 2810	5838 ± 2766
Type IIa fiber CSA, µm2	7107 ± 2580	7016 ± 2309	7030 ± 2533	7001 ± 2144
Type IIa/IIx fiber CSA, µm2	7214 ± 3139	5760 ± 2795	6082 ± 3124	5341 ± 2396
Type IIx fiber CSA, µm2	4694 ± 2613	3792 ± 2032	4375 ± 2192	3257 ± 1799
CS activity, µmol/min/g protein	63 ± 37	54 ± 22	52 ± 24	56 ± 21
HADH activity, µmol/min/g protein	22 ± 9	19 ± 7	19 ± 7	19 ± 6
OXPHOS complex I subunit content, AU	2.0 (1.2, 3.9)	1.5 (0.8, 2.1)	1.6 (1.0, 1.9)	1.2 (0.3, 2.4)
OXPHOS complex II subunit content, AU	2.8 (1.7, 4.3)	2.2 (1.5, 3.6)	2.3 (1.6, 2.5)	2.2 (1.2, 4.2)
OXPHOS complex III subunit content, AU	1.5 (0.7, 2.0)	1.2 (0.8, 1.7)	1.2 (0.9, 1.4)	1.4 (0.7, 1.8)
OXPHOS complex IV subunit content, AU	4.1 (2.8, 8.1)	2.4 (1.1, 3.6) *	2.9 (1.3, 4.1)	1.9 (0.6, 3.3) *
OXPHOS complex V subunit content, AU	0.7 (0.4, 1.1)	0.5 (0.3, 0.7) *	0.5 (0.3, 0.8)	0.6 (0.3, 0.7)

Values are expressed as mean ± SD or median (25th percentile, 75th percentile). Abbreviations: CSA, cross-sectional area; CS, citrate synthase; HADH, 3 hydroxyacyl-CoA dehydrogenase; OXPHOS, oxidative phosphorylation; AU, arbitrary units. Significance of difference compared to controls: $^{*}p < 0.05$, $^{**}p < 0.01$, $^{***}p \leq 0.001$.

Table 5 | Results from the maximal cycle ergometry test

	Healthy controls	COPD	$COPD_{ND}$	$COPD_{D}$
Total exercise time, min	10.0 (8.8, 10.6)	7.4 (5.5, 9.4) **	7.5 (5.5, 8.9) *	7.0 (5.7, 9.7) *
Peak work load, Watt	156 (134, 255)	72 (56, 96) ***	76 (66, 100) ***	66 (53, 96) ***
Work load, % predicted	133 (106, 152)	60 (44, 71) ***	65 (48, 73) ***	57 (37, 69) ***
$V'o_2$peak, ml/min	1852 (1680, 2785)	1130 (1025, 1406) ***	1162 (1075, 1434) ***	1084 (901, 1358) ***
$V'o_2$peak, % predicted	120 (102, 155)	74 (55, 84) ***	78 (66, 88) ***	64 (51, 74) ***
V'e,peak, % MVV	66 (61, 80)	85 (81, 94) ***	82 (77, 94) **	89 (82, 94) **
HRpeak, % HR predicted	100 (97, 106)	78 (68, 89) ***	77 (66, 89) **	78 (71, 92) **
$ATV'o_2$, ml/min	1061 (862, 1395)	736 (607, 873) ***	776 (601, 875) **	727 (605, 889) **
Sp,o_2 at $V'o_2$peak, %	97 (97, 99)	92 (87, 95) ***	94 (93, 96) ***	87 (85, 90) $^{***,\#\#\#}$
$\Delta Sp,o_2$, %	−1.0 (−2.0, 0.0)	−4.0 (−8.0, −2.3) ***	−3.0 (−4.0, 0.0)	−8.0 (−10.0, −6.5) $^{***,\#\#\#}$
$\Delta Sa,o_2$, %	0.0 (0.0, 1.0)	−1.0 (−4.0, 0.0) *	−1.0 (−1.8, 1.5)	−4.0 (−10.0, −3.0) $^{**,\#\#}$

Values are expressed as median (25th percentile, 75th percentile). Abbreviations: $V'O_2$, oxygen uptake; V'E, minute ventilation; MVV, maximal voluntary ventilation, calculated as $FEV_1 \times 37.5$; HR, heart rate; HR predicted calculated as (220 − age); $ATV'O_2$, $V'O_2$ at anaerobic threshold; Sp,O_2, oxygen saturation measured via pulse oximetry; Sa,O_2, arterial oxygen saturation. Level of significance of difference *vs.* controls: $^{*}p < 0.05$, $^{**}p < 0.01$, $^{***}p \leq 0.001$. Level of significance of difference $COPD_D$ *vs.* $COPD_{ND}$ patients: $^{\#\#}p < 0.01$, $^{\#\#\#}p \leq 0.001$.

Leg muscle desaturation

Although by definition $COPD_D$ patients had significantly reduced end-exercise systemic saturation compared to $COPD_{ND}$ patients and controls, no differences were detected in quadriceps tissue desaturation or time constant of recovery of muscle oxygen saturation among the groups (Table 6). Also, no association was found between systemic and local muscle desaturation (Figure 3). To assess whether the Oxphen response was influenced by muscle oxygen saturation, we tested correlations between Oxphen markers and ΔTSI in the combined group of COPD patients and controls, but did not find significant associations. In addition, we stratified the COPD patients based on the median value of ΔTSI to high (≤−9.1%) and low muscle desaturation (>−9.1%) groups, due to lack of a reference value for muscle desaturation. The response of Oxphen markers was not different between the two groups.

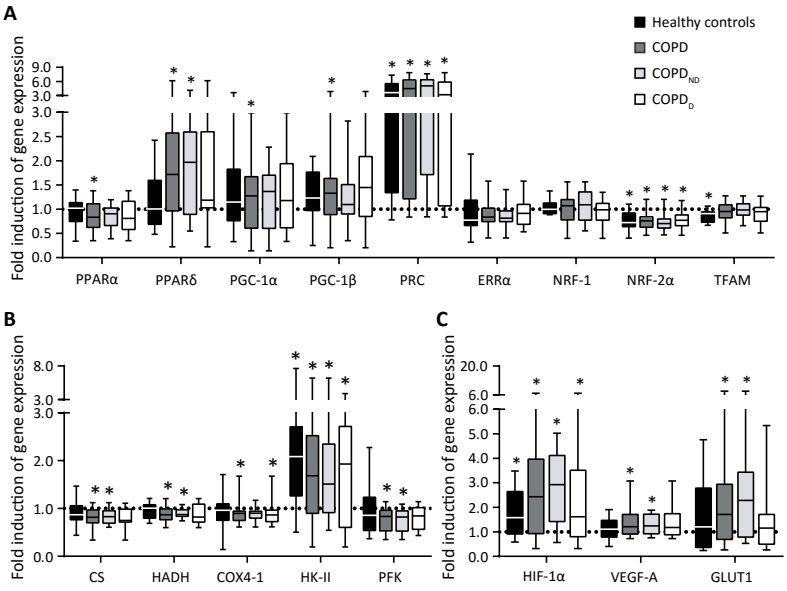

Figure 1 | Gene expression responses to exercise are not significantly different between COPD patients and healthy controls, regardless of desaturation status. A, Gene expression inductions (post/pre) for regulators of Oxphen. PPAR, peroxisome proliferator-activated receptor; PGC, PPAR gamma co-activator; PRC, PGC-1-related co-activator; ERRα, estrogen-related receptor α; NRF, nuclear respiratory factor; TFAM, mitochondrial transcription factor A. **B**, Gene expression inductions for metabolic enzymes involved in citric acid cycle, β-oxidation and glycolysis. CS, citrate synthase; HADH, 3-hydroxyacyl-CoA dehydrogenase; COX4-1, cytochrome c oxidase subunit IV isoform 1; HK-II, hexokinase II; PFK, phosphofructokinase muscle isoform. **C**, Gene expression inductions of hypoxia-associated targets. HIF-1α, hypoxia-inducible factor 1 alpha; VEGF-A, vascular endothelial growth factor A; GLUT1, glucose transporter 1. Whiskers indicate minimum and maximum values. Level of significance: * p <0.05 for post *vs.* pre.

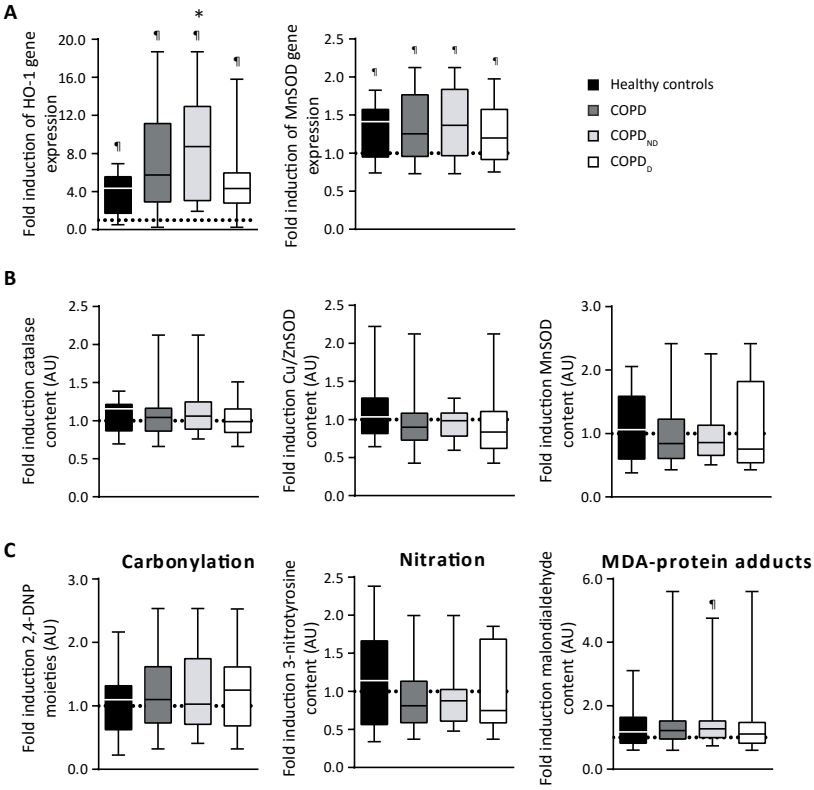

Figure 2 | Oxidative stress in quadriceps muscle is only mildly increased in non-desaturating COPD patients; both patients and healthy controls show significant induction of antioxidant genes after exercise. A, Box plots of the response of heme oxygenase-1 (HO-1) and manganese superoxide dismutase (MnSOD) genes to exercise presented as fold induction (post/pre). **B**, Box plot of the exercise-induced fold inductions of catalase, Cu/ZnSOD and MnSOD content. **C**, Box plot of the exercise-induced fold inductions of protein carbonylation, tyrosine nitration and malondialdehyde (MDA)-protein adducts. Whiskers indicate minimum and maximum values. AU, arbitrary units. Level of significance: $^{*}p < 0.05$ for post *vs.* pre.

Table 6 | Quadriceps desaturation during cycle ergometry

	Healthy controls	COPD	$COPD_{ND}$	$COPD_{D}$
ΔTSI, %	−13 (−24, −7)	−9 (−14, −6)	−6 (−14, −5)	−9 (−13, −8)
τ, s	24 (17, 26)	25 (18, 40)	28 (18, 46)	24 (18, 37)

Values are expressed as median (25th percentile, 75th percentile). Abbreviations: TSI, tissue saturation index; τ, time constant of recovery of muscle oxygen saturation.

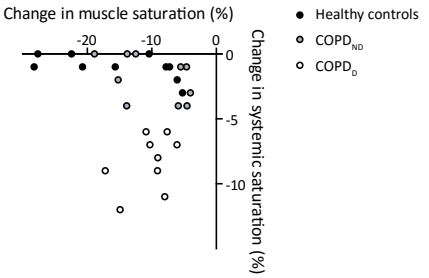

Figure 3 | Change in quadriceps muscle saturation during exercise is not associated with systemic desaturation. Reliable muscle saturation data was available for 11 $COPD_{ND}$, 9 $COPD_{D}$ patients and 11 healthy controls.

DISCUSSION

The mechanisms leading to loss of muscle Oxphen in COPD thus far remain unclear. We recently showed that the Oxphen loss is not limited to advanced disease but also ongoing in earlier phases of the disease, even in absence of muscle wasting. Potential determinants such as disease-associated persistent systemic inflammation and chronic hypoxia are less likely to be causally involved in this stage. As exercise is a potent Oxphen stimulant we hypothesized that a blunted regulatory Oxphen response to exercise would occur in less advanced COPD, resulting from either exercise-induced hypoxia or oxidative stress, or both. However, we did not demonstrate such a blunted response in quadriceps muscle, regardless of co-occurring oxygen desaturation. Also exercise-induced oxidative stress was not aggravated in these patients with less advanced COPD compared to controls. Moreover, as the COPD patients exercised at an intensity significantly lower than that of healthy controls, it could be argued that, adjusted for absolute intensity, the exercise response was even larger in the patients as compared to the controls. In line, after a constant load test at 80% peak capacity in COPD patients and healthy controls, Steiner *et al.* also did not find significantly different exercise-induced changes in absolute magnitude of the muscle metabolites ATP, inosine monophosphate, phosphocreatine and lactate, despite marked differences in workload between COPD patients and controls (39).

Exercise intensity and response

One explanation for the comparable exercise responses in the COPD patients and healthy controls could be that the induction of Oxphen is not linearly related to exercise intensity but rather determined by a threshold that has to be exceeded to invoke a maximal response. The fact that in our study the anaerobic threshold was reached in all healthy controls and almost all COPD patients would be supportive of this hypothesis. Congruently, in healthy individuals only exercise above the lactate threshold has been shown to significantly induce muscle PGC-1α gene expression (34, 41). In COPD patients, however, exercise both below and above the lactate threshold increased PGC-1α gene expression, although the induction was stronger with the latter (34). Puente-Maestu *et al.* found increased induction of PGC-1α mRNA in muscle of COPD patients compared to healthy controls after a 45-minutes exercise test at 65% of $V'O_2peak$ (34). Whereas the COPD patients in our study had significantly increased PGC-1α gene expression after exercise compared to baseline, the induction in healthy controls only showed a trend to significance. However, we did not observe a significant difference in the magnitude of the exercise-associated induction between the patients and controls. Puente-Maestu *et al.* found an association of PGC-1α mRNA induction with the amount of ROS that

was estimated to be produced during the exercise test (34). In our study there was no evidence of increased oxidative stress in the quadriceps muscle of COPD patients, which together with the lack of a differential response of PGC-1α mRNA with exercise, is in line with the findings by Puente-Maestu.

Regulatory gene responses to exercise

Transient induction of PGC-1α gene expression by exercise is well-described (*i.e.* (33)). Remarkably, in addition to a mild induction of PGC-1α gene expression, we found a strong induction of PRC, a PGC-1-related coactivator involved in mitochondrial respiratory function. Induction of PRC with exercise has been described before in healthy individuals (37), but this is to our knowledge the first time that this marker has been measured in COPD patients in response to acute exercise.

Exercise-induced elevation of HIF-1α gene expression has been proposed to be an important factor in the regulation of adaptive gene responses to exercise (3, 21). In addition to HIF-1α, we found increased expression of some of its target genes, such as VEGF-A, HK-II and GLUT1. The inductions of these genes and PGC-1α and PRC support that there is an ongoing exercise response in the muscle. It is thought that induction of the HIF-1α gene with exercise does not depend on hypoxia *per se*, but may result in increased capillarization and increased glycolytic flux within the mitochondria (21). Inductions of HIF-1α gene expression have been found to blunt with training (21), and the seemingly stronger inductions of HIF-1α gene expression and its target genes in COPD patients compared to controls could be a reflection of the on average lower physical activity level of the patients.

Exercise-associated hypoxia

In contrast to what we expected, exercise-induced desaturation did not blunt the Oxphen response in COPD patients. This could indicate that acute local hypoxia does not hamper the Oxphen response. Another explanation for the comparable exercise responses between the $COPD_{ND}$ and $COPD_{D}$ subgroups is that "systemic" oxygen desaturation as measured by finger pulse oximetry does not reflect oxygen desaturation locally in the exercising limb muscle. To define exercise-induced oxygen desaturation, we used the criterion by the American Thoracic Society (ATS), which specifies that the drop in saturation during exercise should be ≥4% (4). It has also been suggested that desaturation is only clinically relevant when saturation drops below 90% (40), which applied to 12 patients in the current study. However, the outcomes did not change when we used this alternative criterion (results not shown). Indeed, we did not find an association between systemic and skeletal muscle desaturation. The mismatch between systemic and muscle desaturation could be explained by an increased oxygen extraction rate from the systemic circulation to maintain oxygen tension in the muscle but resulting in decreased arterial oxygen saturation in some patients. Nevertheless, we found no significant difference in exercise-induced muscle oxygen desaturation levels among the groups, including the healthy controls, and no associations of muscle desaturation with markers of the Oxphen response.

Exercise-associated oxidative stress response

Previous research in advanced COPD demonstrated an increased resting and exercise-induced oxidative stress response. We also investigated relevant oxidative stress markers in this study to see if a similar enhancement is seen in less advanced COPD, in particular in desaturating patients. No striking differences were observed between COPD patients, subgroups and healthy controls. In contrast Puente-Maestu *et al.* recently described increased exercise-induced oxidative stress in mild to moderate COPD patients, who, similar to those in our study, had a slight loss of muscle Oxphen (35). However, differences in the intensity of exercise (15 minutes constant work rate at ~65% Wmax *vs.* incremental exercise until exhaustion) and the timing of the muscle biopsy after the exercise test (1 h *vs.* 4 h) hamper comparison between our study and theirs.

Although we did not find increased oxidative stress-derived products after exercise, gene expression levels of the antioxidants MnSOD and HO-1 were increased, which is a normal response to exercise (15, 32). The induction of MnSOD and HO-1 gene expression could indicate that the stimulation of the antioxidant system by exercise is not blunted in COPD patients and increased formation of reactive oxygen species by exercise is well-balanced by the antioxidant system (12).

Limitations of the study

A limitation of this study is that only one biopsy was taken after the exercise bout. The timing of the single post biopsy was chosen after careful review of the literature focusing on Oxphen gene expression after exercise, but no inferences can be made regarding differences in the temporal pattern of gene expression changes between COPD patients and controls.

An important constraint of the near-infrared spectroscopy (NIRS) technique is the limited optical penetration depth. As such, subcutaneous fat disturbs or even obstructs the quadriceps NIRS measurement. Therefore, subjects with a large skin fold at the site of the NIRS probe were excluded from the NIRS measurement in our study. We explicitly report this methodological issue as it often seems to be overlooked in the existing literature.

CONCLUSION

Taken together, the data in this study suggest that patients with less advanced COPD do not have a blunted muscle oxidative regulatory response to acute exercise, regardless of exercise-induced systemic desaturation. This observation, together with a normal oxidative stress response, further supports that incorporation of exercise training as integrated part of COPD management already in early disease could have a pivotal role to prevent or slow down loss of muscle Oxphen and related functional impairment. Further research is needed to investigate if the muscle oxidative regulatory response is blunted in more severe disease stages (*i.e.* chronic respiratory failure) and disentangle potential contributing factors that may require additional modulation to optimize exercise training in these stages.

ACKNOWLEDGMENTS

We thank Kathleen Daenen and Monica Vila-Ubach for their technical support.

REFERENCES

1. Allaire J, Maltais F, Doyon JF, Noel M, LeBlanc P, Carrier G, Simard C, and Jobin J. Peripheral muscle endurance and the oxidative profile of the quadriceps in patients with COPD. Thorax 59: 673-678, 2004.
2. Allen D, Winters E, Kenna PF, Humphries P, and Farrar GJ. Reference gene selection for real-time rtPCR in human epidermal keratinocytes. J Dermatol Sci 49: 217-225, 2008.
3. Ameln H, Gustafsson T, Sundberg CJ, Okamoto K, Jansson E, Poellinger L, and Makino Y. Physiological activation of hypoxia inducible factor-1 in human skeletal muscle. FASEB J 19: 1009-1011, 2005.
4. American Thoracic S, and American College of Chest P. ATS/ACCP Statement on cardiopulmonary exercise testing. Am J Respir Crit Care Med 167: 211-277, 2003.
5. Anderson EJ, and Neufer PD. Type II skeletal myofibers possess unique properties that potentiate mitochondrial H(2)O(2) generation. Am J Physiol Cell Physiol 290: C844-851, 2006.
6. Barreiro E, Rabinovich R, Marin-Corral J, Barbera JA, Gea J, and Roca J. Chronic endurance exercise induces quadriceps nitrosative stress in patients with severe COPD. Thorax 64: 13-19, 2009.
7. Beaver WL, Wasserman K, and Whipp BJ. A new method for detecting anaerobic threshold by gas exchange. J Appl Physiol (1985) 60: 2020-2027, 1986.
8. Bergmeyer HU, Gawehn K, and Grassl M. 3-Hydroxyacyl-CoA dehydrogenase. In: Methods of enzymatic analysis, edited by Bergmeyer HU. Weinheim; Germany: Verlag Chemie GmbH, 1974, p. 474.
9. Bergström J. Muscle electrolytes in man. Determination by neutron activation analysis on needle biopsy specimens. A study on normal subjects, kidney patients, and patients with chronic diarrhea. Scand J Clin Lab Invest 14: 1–110, 1962.
10. Couillard A, Maltais F, Saey D, Debigare R, Michaud A, Koechlin C, LeBlanc P, and Prefaut C. Exercise-induced quadriceps oxidative stress and peripheral muscle dysfunction in patients with chronic obstructive pulmonary disease. Am J Respir Crit Care Med 167: 1664-1669, 2003.
11. Franssen FM, Broekhuizen R, Janssen PP, Wouters EF, and Schols AM. Limb muscle dysfunction in COPD: effects of muscle wasting and exercise training. Med Sci Sports Exerc 37: 2-9, 2005.
12. Gosker HR, Bast A, Haenen GR, Fischer MA, van der Vusse GJ, Wouters EF, and Schols AM. Altered antioxidant status in peripheral skeletal muscle of patients with COPD. Respir Med 99: 118-125, 2005.
13. Gosker HR, Zeegers MP, Wouters EF, and Schols AM. Muscle fibre type shifting in the vastus lateralis of patients with COPD is associated with disease severity: a systematic review and meta-analysis. Thorax 62: 944-949, 2007.
14. Gouzi F, Maury J, Molinari N, Pomies P, Mercier J, Prefaut C, and Hayot M. Reference values for vastus lateralis fiber size and type in healthy subjects over 40 years old: a systematic review and metaanalysis. J Appl Physiol (1985) 115: 346-354, 2013.
15. Hollander J, Fiebig R, Gore M, Ookawara T, Ohno H, and Ji LL. Superoxide dismutase gene expression is activated by a single bout of exercise in rat skeletal muscle. Pflugers Arch 442: 426-434, 2001.
16. Hoppeler H, Vogt M, Weibel ER, and Fluck M. Response of skeletal muscle mitochondria to hypoxia. Exp Physiol 88: 109-119, 2003.
17. Itoh K, Itoh M, Ishihara A, Hirofuji C, and Hayashi H. Influence of 12 weeks of hypobaric hypoxia on fibre type composition of the rat soleus muscle. Acta Physiol Scand 154: 417-418, 1995.
18. Koechlin C, Maltais F, Saey D, Michaud A, LeBlanc P, Hayot M, and Prefaut C. Hypoxaemia enhances peripheral muscle oxidative stress in chronic obstructive pulmonary disease. Thorax 60: 834-841, 2005.
19. Layec G, Haseler LJ, Hoff J, and Richardson RS. Evidence that a higher ATP cost of muscular contraction contributes to the lower mechanical efficiency associated with COPD: preliminary findings. Am J Physiol Regul Integr Comp Physiol 300: R1142-1147, 2011.
20. Ling KH, Paetkau V, Marcus F, and Lardy HA. Phosphofructokinase: I. Skeletal Muscle. In: Methods EnzymolAcademic Press, 1966, p. 425-429.
21. Lundby C, Gassmann M, and Pilegaard H. Regular endurance training reduces the exercise induced HIF-1alpha and HIF-2alpha mRNA expression in human skeletal muscle in normoxic conditions. Eur J Appl Physiol 96: 363-369, 2006.
22. Magalhaes J, Ascensao A, Soares JM, Ferreira R, Neuparth MJ, Marques F, and Duarte JA. Acute and severe hypobaric hypoxia increases oxidative stress and impairs mitochondrial function in mouse skeletal muscle. J Appl Physiol (1985) 99: 1247-1253, 2005.
23. Mahoney DJ, Parise G, Melov S, Safdar A, and Tarnopolsky MA. Analysis of global mRNA expression in human skeletal muscle during recovery from endurance exercise. FASEB J 19: 1498-1500, 2005.
24. Maltais F, LeBlanc P, Whittom F, Simard C, Marquis K, Belanger M, Breton MJ, and Jobin J. Oxidative enzyme activities of the vastus lateralis muscle and the functional status in patients with COPD. Thorax 55: 848-853, 2000.
25. Maltais F, Sullivan MJ, LeBlanc P, Duscha BD, Schachat FH, Simard C, Blank JM, and Jobin J. Altered expression of myosin heavy chain in the vastus lateralis muscle in patients with COPD. Eur Respir J 13: 850-854, 1999.
26. Mason SD, Howlett RA, Kim MJ, Olfert IM, Hogan MC, McNulty W, Hickey RP, Wagner PD, Kahn CR, Giordano FJ, and Johnson RS. Loss of skeletal muscle HIF-1alpha results in altered exercise endurance. PLoS Biol 2: e288, 2004.
27. Mercken EM, Gosker HR, Rutten EP, Wouters EF, Bast A, Hageman GJ, and Schols AM. Systemic and pulmonary oxidative stress after single-leg exercise in COPD. Chest 136: 1291-1300, 2009.
28. Natanek SA, Gosker HR, Slot IG, Marsh GS, Hopkinson NS, Man WD, Tal-Singer R, Moxham J, Kemp PR, Schols AM, and Polkey MI. Heterogeneity of quadriceps muscle phenotype in chronic obstructive pulmonary disease (Copd); implications for stratified medicine? Muscle Nerve 48: 488-497, 2013.

29. Ogilvie RW, and Feeback DL. A metachromatic dye-ATPase method for the simultaneous identification of skeletal muscle fiber types I, IIA, IIB and IIC. Stain Technol 65: 231-241, 1990.
30. Park SK, Richardson CR, Holleman RG, and Larson JL. Physical activity in people with COPD, using the National Health and Nutrition Evaluation Survey dataset (2003-2006). Heart & lung : the journal of critical care 42: 235-240, 2013.
31. Picard M, Godin R, Sinnreich M, Baril J, Bourbeau J, Perrault H, Taivassalo T, and Burelle Y. The mitochondrial phenotype of peripheral muscle in chronic obstructive pulmonary disease: disuse or dysfunction? Am J Respir Crit Care Med 178: 1040-1047, 2008.
32. Pilegaard H, Ordway GA, Saltin B, and Neufer PD. Transcriptional regulation of gene expression in human skeletal muscle during recovery from exercise. Am J Physiol Endocrinol Metab 279: E806-814, 2000.
33. Pilegaard H, Saltin B, and Neufer PD. Exercise induces transient transcriptional activation of the PGC-1alpha gene in human skeletal muscle. J Physiol 546: 851-858, 2003.
34. Puente-Maestu L, Lazaro A, Tejedor A, Camano S, Fuentes M, Cuervo M, Navarro BO, and Agusti A. Effects of exercise on mitochondrial DNA content in skeletal muscle of patients with COPD. Thorax 66: 121-127, 2011.
35. Puente-Maestu L, Tejedor A, Lazaro A, de Miguel J, Alvarez-Sala L, Gonzalez-Aragoneses F, Simon C, and Agusti A. Site of mitochondrial reactive oxygen species production in skeletal muscle of chronic obstructive pulmonary disease and its relationship with exercise oxidative stress. Am J Respir Cell Mol Biol 47: 358-362, 2012.
36. Remels AH, Gosker HR, Langen RC, and Schols AM. The mechanisms of cachexia underlying muscle dysfunction in COPD. J Appl Physiol (1985) 114: 1253-1262, 2013.
37. Russell AP, Hesselink MK, Lo SK, and Schrauwen P. Regulation of metabolic transcriptional co-activators and transcription factors with acute exercise. FASEB J 19: 986-988, 2005.
38. Shepherd D, and Garland PB. Citrate synthase from rat liver. In: Methods EnzymolAcademic Press, 1969, p. 11-16.
39. Steiner MC, Evans R, Deacon SJ, Singh SJ, Patel P, Fox J, Greenhaff PL, and Morgan MD. Adenine nucleotide loss in the skeletal muscles during exercise in chronic obstructive pulmonary disease. Thorax 60: 932-936, 2005.
40. Stoller JK, Panos RJ, Krachman S, Doherty DE, Make B, and Long-term Oxygen Treatment Trial Research G. Oxygen therapy for patients with COPD: current evidence and the long-term oxygen treatment trial. Chest 138: 179-187, 2010.
41. Tobina T, Yoshioka K, Hirata A, Mori S, Kiyonaga A, and Tanaka H. Peroxisomal proliferator-activated receptor gamma co-activator-1 alpha gene expression increases above the lactate threshold in human skeletal muscle. J Sports Med Phys Fitness 51: 683-688, 2011.
42. van den Borst B, Gosker HR, and Schols AM. Central fat and peripheral muscle: partners in crime in chronic obstructive pulmonary disease. Am J Respir Crit Care Med 187: 8-13, 2013.
43. van den Borst B, Slot IG, Hellwig VA, Vosse BA, Kelders MC, Barreiro E, Schols AM, and Gosker HR. Loss of quadriceps muscle oxidative phenotype and decreased endurance in patients with mild-to-moderate COPD. J Appl Physiol (1985) 114: 1319-1328, 2013.
44. Vandesompele J, De Preter K, Pattyn F, Poppe B, Van Roy N, De Paepe A, and Speleman F. Accurate normalization of real-time quantitative RT-PCR data by geometric averaging of multiple internal control genes. Genome Biol 3: RESEARCH0034, 2002.
45. Yang Y, Creer A, Jemiolo B, and Trappe S. Time course of myogenic and metabolic gene expression in response to acute exercise in human skeletal muscle. J Appl Physiol (1985) 98: 1745-1752, 2005.

Chapter 6

Summary and general discussion

INTRODUCTION

Chronic obstructive pulmonary disease (COPD) is a lung disease with multiple systemic manifestations that increase disease burden, including skeletal muscle weakness (41, 74). Skeletal muscle of patients with COPD is often characterized by wasting and a loss of oxidative phenotype (Oxphen), which includes a reduced proportion of oxidative muscle fiber types and mitochondrial capacity (26, 28). Since 2001, severity of COPD is classified by the Global Initiative for Chronic Obstructive Lung Disease (GOLD) staging according to the degree of airflow limitation or obstruction measured using pulmonary function tests (Table 1) (1). However, original GOLD staging is incomplete, because airflow limitation is not the only factor that determines severity as other factors (e.g. overweight/obesity, comorbidities, and physical fitness) influence symptoms and quality of life as well. Since 2011 the GOLD stages are therefore replaced by GOLD grades that include symptoms and exacerbations (Table 2) (2).

The two main lung pathologies included in COPD are chronic bronchitis and emphysema. Chronic bronchitis involves chronic inflammation of the lining of the airways resulting in fibrosis and increased resistance, whereas emphysema involves damage of the alveolar walls and consequent impaired gas exchange. Depending on these two subtypes, patients may experience various degrees and frequencies of oxygen desaturation which could result in tissue hypoxia and tissue dysfunction, for example during exercise (exertional desaturation) (72), during the night (nocturnal desaturation) (38), short-term during disease exacerbations or chronically due to severely impaired lung function, such as in the case of chronic respiratory failure (37). Respiratory failure according to GOLD is defined by an arterial partial pressure of O_2 (PaO_2) < 8.0 kPa (60 mmHg) with or without arterial partial pressure of CO_2 ($PaCO_2$) > 6.7 kPa (50 mmHg) breathing ambient air (2).

Table 1 | Classification of COPD severity according to the Global Initiative for Chronic Obstructive Lung Disease (GOLD) 2001 guidelines

GOLD stage		Criteria	Symptoms
I	Mild COPD	FEV_1/FVC < 70%; FEV_1 ≥ 80% predicted	Sometimes chronic cough and sputum production
II	Moderate COPD	FEV_1/FVC < 70%; FEV_1 50-79% predicted	Shortness of breath typically developing on exertion
III	Severe COPD	FEV_1/FVC < 70%; FEV_1 30-49% predicted	Greater shortness of breath, reduced exercise capacity, repeated exacerbations which have an impact on patients' quality of life
IV	Very severe COPD	FEV_1/FVC < 70%; FEV_1 < 30% predicted, or < 50% predicted in the presence of chronic respiratory failure	Quality of life very impaired, exacerbations may be life-threatening

FEV_1: forced expiratory volume in 1 second. FVC: forced vital capacity. Respiratory failure: PaO_2 < 8.0 kPa (60 mmHg) and/or SaO_2 < 90% with or without $PaCO_2$ > 6.7 kPa (50 mmHg) when breathing room air.

Table 2 | Classification of COPD severity according to the updated Global Initiative for Chronic Obstructive Lung Disease (GOLD) 2011 guidelines

GOLD grade		Criteria
A	Low risk, low symptom burden	Low symptom burden (mMRC of 0-1 OR CAT score < 10) AND FEV_1 of 50% or greater (old GOLD 1-2) AND low exacerbation rate (0-1/year)
B	Low risk, higher symptom burden	Higher symptom burden (mMRC of 2 or more OR CAT of 10 or more) AND FEV_1 of 50% or greater (old GOLD 1-2) AND low exacerbation rate (0-1/year)
C	High risk, low symptom burden	Low symptom burden (mMRC of 0-1 OR CAT score < 10) AND FEV_1 < 50% (old GOLD 3-4) AND/OR high exacerbation rate (2 or more/year)
D	High risk, higher symptom burden	Higher symptom burden (mMRC of 2 or more OR CAT of 10 or more) AND FEV_1 < 50% (old GOLD 3-4) AND/ OR high exacerbation rate (2 or more/year)

FEV_1: forced expiratory volume in 1 second. FVC: forced vital capacity. Symptom burden is measured by the modified Medical Research Council questionnaire (mMRC) or the COPD assessment test (CAT).

Although no clear relationship has been shown between muscle abnormalities and disease severity based on airflow limitation, skeletal muscle dysfunction has been shown to be a predictor of morbidity and mortality, independent of lung function impairment measured as FEV_1 (69). Indeed, we showed in a large cohort that the COPD population is heterogeneous and that muscle dysfunction is not related to FEV_1 (49). However, a weak association was found between diffusion capacity for carbon monoxide (DLCO) in the lung and skeletal muscle type I fiber proportion (49). It was previously described that loss of Oxphen is more prominent in patients with emphysema, who are characterized by a lower DLCO (27). Figure 1 shows the relationship of DLCO with type I fiber proportion in the combined group of COPD patients (Figure 1A) or healthy subjects (Figure 1C) from our previous study (49) and the study described in **Chapter 4**. Moreover, type I fiber proportion was significantly associated with arterial oxygen tension (PaO_2) in the COPD patients (Figure 1B). This relationship has been reported before for patients with advanced COPD by Jakobsson *et al.* (35) and implicates involvement of hypoxemia in the reduced type I proportion that is observed in lower-limb muscle of COPD patients.

The definition of hypoxemia is arterial oxygen tension or partial pressure of oxygen (PaO_2) below normal. Normal PaO_2 for an adult breathing room air at sea level is 80-100 mmHg (40), so hypoxemia would be PaO_2 < 80 mmHg. The degree of hypoxemia determines the propensity for tissue hypoxia. Therefore, hypoxemia is classified as being mild (60-79 mmHg), moderate (45-59 mmHg), or severe (<45 mmHg) (40). In the absence of other oxygenation problems, mild hypoxemia is unlikely to result in tissue hypoxia, because SaO_2 remains over 90%. Moderate hypoxemia could result in hypoxia when compensating mechanisms are insufficient to maintain oxygenation, for example due to cardiovascular disease. Severe hypoxemia presents a critical condition that will likely result in tissue hypoxia and needs to be dealt with (40). The American Thoracic Society (ATS) recommends oxygen therapy if a patient has 'severe hypoxemia', which is defined as a resting $PaO_2 \leq 55$ mmHg (7.3 kPa) or $SpO_2 \leq 88\%$ (58). The Dutch Society

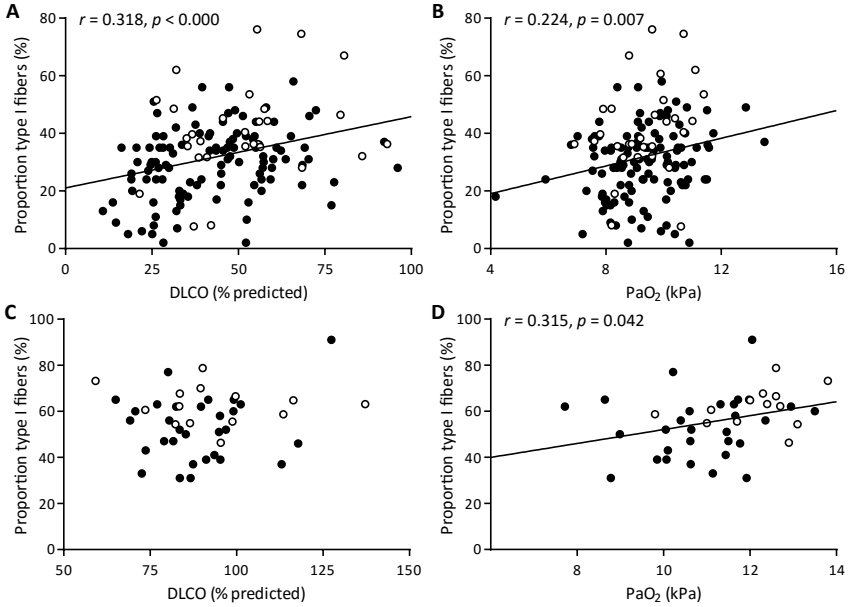

Figure 1 | Relationships of DLCO and PaO_2 with type I fiber proportion. Data are combined from two studies ((49) (black dots) and Chapter 4 (white dots)) for patients with COPD (**A**, **B**) and healthy controls (**C**, **D**). Correlations were tested using Pearson's correlation coefficient. DLCO, diffusion capacity of the lungs for carbon monoxide; PaO_2, partial pressure of oxygen in arterial blood.

of Physicians for Lung Diseases and Tuberculosis (NVALT) recommends oxygen therapy when the patient has persistent hypoxemia (PaO_2 < 7.3 kPa (55 mmHg)) or a combination of PaO_2 of 7.3-8.0 kPa (55-60 mmHg) and peripheral oedema, right atrial enlargement (P pulmonale on the ECG) or hematocrit >55 % (3). As was shown by Engelen *et al.*, many COPD patients have a PaO_2 lower than that of healthy physically active and inactive age-matched controls (19).

ONSET OF LOSS OF SKELETAL MUSCLE OXIDATIVE PHENOTYPE IN COPD

Many factors related to COPD are potentially involved in the loss of muscle Oxphen, so to resolve underlying mechanisms it would be helpful to know in what stage of the disease loss of Oxphen is initiated. In **Chapter 4** we showed that loss of skeletal muscle Oxphen is already present in patients with mild to moderate COPD (GOLD 2-3), although these patients did not yet show overt muscle atrophy. A recent study by Gagnon *et al.* showed that patients with GOLD 1 COPD are not yet characterized by decreased endurance and loss of Oxphen, which was determined based on fiber-type distribution and citrate synthase and hydroxyacyl dehydrogenase activities (21). However, they did find that gene expression of pro-angiogenic factors was depressed in COPD, despite normal capillarization, which indicates that regulation of angiogenesis is disturbed already in mild COPD. With regard to the loss of Oxphen, it would therefore be interesting to investigate Oxphen regulators, such as PGC-1α, in patients with GOLD I COPD.

In **Chapter 4** we also showed that the reduced proportion of type I muscle fibers correlated with quadriceps endurance, which implies that the loss of Oxphen is of clinical relevance as it indeed affects quadriceps endurance. Reduced physical activity levels have been associated with lower mitochondrial capacity in healthy subjects (16) and have been hypothesized to explain loss of Oxphen in patients with COPD as well (75). Gagnon *et al.* found reduced physical activity already in patients with GOLD 1 COPD (21), which suggests that reduced physical activity could be a factor involved in initiation of loss of Oxphen. However, no relationships were found between markers of Oxphen and total physical activity level or intensity of physical activity in the patients in the study described in **Chapter 4** (GOLD 2-3) or in our previous study of a large COPD cohort of 114 patients (GOLD 3-4) (49). Nevertheless, these studies are of cross-sectional nature, so a role for physical activity cannot be completely ruled out until a longitudinal study has been performed.

EXERTIONAL DESATURATION AND OXPHEN RESPONSE TO EXERCISE

Previous findings of a relationship between type I fiber proportion and PaO_2 (35) strengthen the hypothesis that hypoxia is involved in the loss of Oxphen. Because exercise is a physiological stimulant of Oxphen and patients with COPD often suffer from exercise-induced oxygen desaturation (72), in **Chapter 5** we focused on the role of exertional oxygen desaturation on the response of Oxphen to acute exercise. We hypothesized that the response of Oxphen regulators was blunted due to oxygen desaturation. The patients were pre-stratified according to arterial oxygen desaturation during exercise to study the effect of exercise desaturation on Oxphen and oxidative stress response to exercise. Although the patients exercised at a significantly lower intensity, we did not demonstrate a blunted response of Oxphen regulators, regardless of co-occurring oxygen desaturation. In addition to systemic oxygen desaturation, we measured oxygen desaturation in the muscle using near-infrared spectroscopy (NIRS). We did not find an association between systemic and muscle oxygen desaturation. Also, muscle desaturation was not different between healthy controls and patients, although healthy controls appeared to desaturate more than patients (not significant). Possibly this is related to the higher exercise intensity of the controls. Moreover, stratification according to muscle desaturation did not yield significant differences in the response of Oxphen regulators in patients and controls. A possible explanation for the difference between systemic and muscle oxygen saturation is that the working muscle demands increased oxygen extraction from the systemic circulation to maintain oxygen tension in the muscle, which results in a decreased arterial oxygen saturation when it is not sufficiently compensated for by gas exchange in the lung. Although our results do not support a role for exertional desaturation in the loss of skeletal muscle Oxphen in this disease stage, further research is warranted to investigate the impact of muscle desaturation in a larger group of patients and controls and to verify that processes downstream of gene transcription (e.g. protein translation, synthesis and breakdown) in response to exercise are not altered in skeletal muscle of patients with COPD.

OXIDATIVE STRESS

The switch in muscle fiber-type composition could possibly result in increased oxidative stress, because it has been shown in rats that mitochondria within type II fibers release significantly more H_2O_2 than those within oxidative fibers (4). Increased oxidative stress has been shown in muscle of patients with severe COPD (44), especially in patients with wasted muscle (6). Moreover, an association has been found between oxidative stress and endurance (12). Indeed, in **Chapter 4** we found a negative correlation of type I fiber proportion and markers of oxidative stress. However, these oxidative stress markers did not differ between patients and controls. Also, patients did not have a stronger response of oxidative stress markers after the acute exercise test, although gene expression of oxidative-stress enzymes (MnSOD, HO-1) was increased (**Chapter 5**). Possibly this indicates that stimulation of the antioxidant system by exercise is not blunted in mild to moderate COPD and increased reactive oxygen species (ROS) formation is adequately tackled by the antioxidant system in this disease stage. This is in line with a previous report of an increased muscle total antioxidant capacity in patients with severe COPD (25). However, total antioxidant capacity is reported to be reduced in patients with wasted muscle, who accordingly have increased levels of oxidative stress markers in muscle (73). Moreover, it was shown that muscle-wasted patients have depressed mitochondrial function (60). Interestingly, Rabinovich *et al.* found that reduced mitochondrial function was associated with lower arterial oxygen concentration (PaO_2) (60), whereas Sauleda *et al.* and Puente-Maestu *et al.* reported an association of reduced PaO_2 with increased cytochrome *c* oxidase (COX) activity in skeletal muscle of COPD patients (56, 65). However, two other groups showed decreased COX activity in skeletal muscle of patients with COPD (27, 47). It is unclear how these differences can be explained, unless COX activity depends on PaO_2: the patients in the studies with elevated COX activity (56, 65) had lower PaO_2 than those in the study by Gosker *et al.* (27). The patients with mild to moderate COPD characterized in this thesis (**Chapter 4** and **5**) had a mean PaO_2 similar to those in the study by Gosker *et al.* and did not have different COX activity compared to healthy controls (Figure 2). The *in vivo* activity of COX is regulated by several mechanisms, including phosphorylation (subunits I, IV and Va), allosteric regulation by ATP and ADP (subunit IV), and transcriptionally through specific isoform expression (subunit IV, VIa, VIb, VIIa and VIII) (32). It has been shown that hypoxia stimulates the HIF-dependent replacement of COX IV isoform 1 (COX IV-1) with COX IV isoform 2 (COX IV-2) to optimize efficiency of respiration at lower oxygen concentrations (20). COX containing the COX IV-2 isoform has been shown to be approximately 2-fold more active than COX with the COX IV-1 isoform (33). However, it has been shown in neural cells that the replacement of COX IV-1 with COX IV-2 results in abolition of the allosteric inhibition of COX by ATP, which results in increased COX activity independently of cellular energy level and concomitantly increased production of ROS (31). Indeed, evidence is accumulating that COX dysfunction is associated with increased mitochondrial ROS production in multiple diseases (67). Possibly, a gradual replacement of the COX IV-1 isoform with COX IV-2 with lower PaO_2 explains the increased COX activity in skeletal muscle of patients with COPD as reported by Sauleda and Puente-Maestu (56, 65). Therefore, it would be interesting to assess protein content of COX IV-1 and COX IV-2 in patients with COPD that have higher COX activity compared to those with lower COX activity and healthy controls.

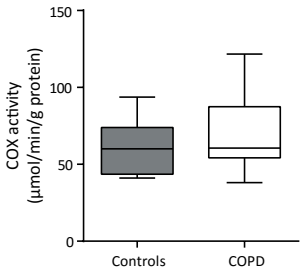

Figure 2 | COX activity in quadriceps muscle of patients with mild to moderate COPD. Cytochrome *c* oxidase (COX, EC 1.9.3.1) was assayed spectrophotometrically as previously described (24). Boxes indicate median and interquartile range; whiskers indicate minimum and maximum values.

MODELS APPLIED TO INVESTIGATE MUSCLE OXPHEN LOSS DUE TO HYPOXIA

To investigate the hypothesis that hypoxia is involved in the loss of muscle Oxphen in COPD, it is valuable to have a study group of patients with hypoxemia. Despite our effort, we did not manage to include a sufficient number of severely hypoxemic patients in our study. Severely hypoxemic patients are hard to find, because upon diagnosis of severe hypoxemia they receive oxygen therapy. However, mild or moderate hypoxia could affect muscle as well and especially in patients with COPD, in which endothelial dysfunction and cardiovascular disease are prevalent (17, 46), mild or moderate hypoxemia might be associated with tissue hypoxia.

To study hypoxia-associated loss of Oxphen in muscle *in vivo* and without the confounders such as inactivity and medication that are present in patients with COPD, we used a model of mice exposed to chronic hypoxia. In addition, we used an *in vitro* model of C2C12 myotubes to assess the effect of hypoxia on skeletal muscle *per se* and involvement of regulators such as the PPARs and HIF-1α, and to modulate expression of these regulators. Together, both the *in vitro* and the *in vivo* mouse study support that hypoxia can decrease oxidative capacity while at the same time it can stimulate myosin heavy chain (MyHC) type I (**Chapter 2** and **3**). In **Chapter 2** we found that gene expression of oxidative phosphorylation (OXPHOS) genes as well as regulators including PPARα, PPARδ, ERRα, PGC-1α and PGC-1β and PPAR transcriptional activity were depressed under hypoxic conditions. Depression of PPAR activity was HIF-1α-dependent and occurred through PGC-1α. On the other hand, expression and content of MyHC type I was induced by hypoxia in a HIF-1α-dependent manner. The finding of increased MyHC type I mRNA by hypoxia was confirmed in the mouse model, although changes were more subtle in the mouse than in the *in vitro* experiments. The finding of increased MyHC type I is interesting, because patients with COPD show reduced expression of MyHC type I. However, the C2C12 cells are of murine origin and in contrast to human muscle fibers, rodent fibers expressing MyHC type I are less oxidative than fibers expressing MyHC type IIa (29). Therefore, these results should be confirmed in cultured human myotubes to verify if hypoxia specifically stimulates expression of MyHC type I, or if it promotes expression of a less oxidative MyHC gene in general.

A possible mechanism through which hypoxia affects expression of Oxphen modulators is through microRNAs (miRNAs). Previously, El Azzouzi *et al.* showed in cardiac muscle that the miRNA cluster miR-199a/214 targets PPARδ to stimulate glycolytic metabolism (18). Expression of miR-199a/214 is regulated by Twist1 (18), which is a hypoxia-sensitive transcription factor (78). To investigate if this pathway was involved in loss of Oxphen in C2C12 myotubes as well, we tried to measure *Twist1* expression,

but could not detect its mRNA using qPCR. Even so, expression of miR-214 was slightly induced by hypoxia in the myotubes (Figure 3). PGC-1α is a predicted target of miR-214. However, because *Twist1* is not expressed in the myotubes, a different hypoxia-sensitive pathway is expected to regulate miR-214 in the myotubes. Further research is needed to implicate miR-214 in the repression of PGC-1α gene expression and to elucidate the pathways that are involved.

Expression of the myosin heavy chain genes is also affected by certain miRNAs, so in addition to miR-199a/214 we measured expression of muscle-specific microRNAs, of which some are known to regulate MyHC expression. miR-208b was significantly induced by hypoxia (Figure 3). miR-208b is encoded in the MyHC type I gene (also known as cardiac β-MyHC), and it has been shown in heart to inhibit expression of α-MyHC and to increase the β-MyHC proportion (43). However, because miR-208b is expressed together with MyHC type I, it is unclear whether miR-208b expression is intentionally increased by hypoxia or increased as a consequence of stimulated transcription of MyHC type I. Moreover, it is not yet clear whether miR-208b can inhibit expression of fast MyHC in skeletal muscle, because α-MyHC is cardiac specific. Strikingly, quadriceps muscle of patients with COPD showed a trend of increased expression of miR-208 (39). In contrast, miR-499 expression was not different (39). Based on this observation, it seems unlikely that miR-208b is involved in a fiber shift of type I to type II fibers in COPD.

Hypoxia significantly upregulated expression of miR-133a and miR-206. Described functions of these miRNAs are related to muscle differentiation (11, 42), but our experiments were performed in already differentiated myotubes. Moreover, miR-486 has a role in differentiation, but is also involved in muscle hypertrophy (30). Further research is needed to investigate the meaning of hypoxia-associated upregulation of these miRNAs as well as their role in the hypoxia-associated changes of MyHC type I and PGC-1α expression. Expression of miR-133 and miR-206 has been measured in quadriceps muscle of patients with COPD, but was not different compared to controls (39). Lewis *et al.* showed that miR-1 expression was associated with type I fiber proportion in quadriceps of COPD patients (39). However, our *in vitro* data show no change of miR-1 expression after 24 or 48 hours of exposure to hypoxia. Therefore, miR-1 does not appear to be involved in the acute response of PGC-1α and MyHC type I gene expression to hypoxia.

In the mouse experiment, mice at the age of 4 weeks, 12 weeks and 52 weeks were exposed to hypoxia for 3 weeks (**Chapter 3**). Hypoxic exposure significantly reduced body, muscle and fat pad weights, independent of reduced food intake. However, hypoxia-associated repression of oxidative capacity was much more subtle. Mitochondrial regulators were repressed stronger in the oldest mice, whereas fiber-type changes and muscle atrophy were most prominent in the youngest mice. Although gene expression of regulators of oxidative capacity and OXPHOS subunits were depressed by hypoxia, no changes were detectable at the protein level for OXPHOS.

The subtle changes of skeletal muscle Oxphen in the mouse study contrast the prominent hypoxia-associated reductions of the expression of oxidative capacity-related genes and proteins in the *in vitro* study. Possibly there is an adaptive effect ongoing in the mice. Hypoxia exposure lasted for 3 weeks, which gives the tissue ample time to adapt and optimize oxygen delivery, for example through increased vascularization. Such adaptive processes are impossible in a cell culture environment with only myotubes

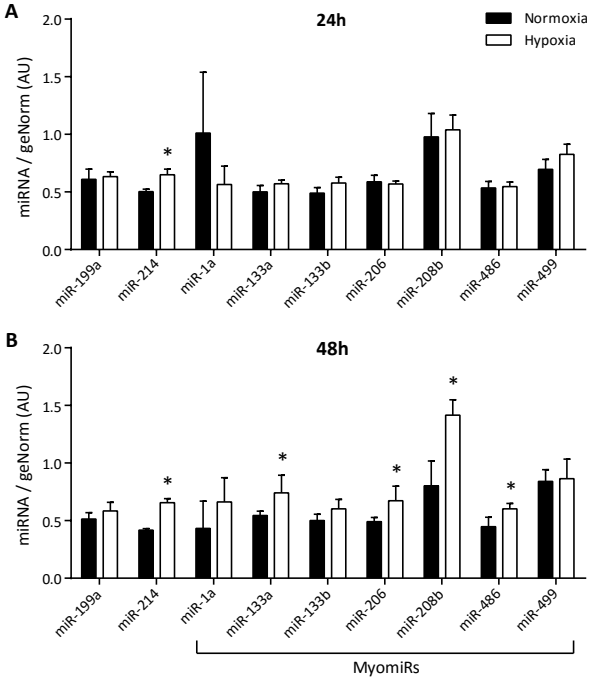

Figure 3 | microRNA expression in five-day differentiated myotubes after hypoxia. Myotubes were exposed to 4% oxygen for 24h (**A**) or 48h (**B**). Expression of the miRNAs of interest was corrected for reference RNAs RNU1a and RNU6 using geNorm. Differences between normoxic and hypoxic condition were analysed using Mann-Whitney test. $^{*}p < 0.05$; mean + SD.

and myoblasts. Alternatively, 3 weeks could be too short to mediate large changes in muscle Oxphen: patients with COPD are exposed to hypoxia for years and have a more pronounced loss of Oxphen. However, the mice in the *in vivo* study where otherwise healthy, so the more pronounced loss of Oxphen in COPD patients could very well be accelerated by underlying conditions such as impaired capillarization (17, 36, 46) or systemic inflammation (22, 53). A period of 3 weeks is interesting, however, when we consider that patients with COPD experience periods of disease exacerbations that are characterized by hypoxia (37). Indeed, Crul *et al.* showed that patients have decreased expression of genes related to oxidative phosphorylation and the mitochondrial respiratory chain during an exacerbation (13). Regardless, it would be interesting to explore in future studies what happens with markers of Oxphen after a longer period of hypoxic exposure.

Limitations of our hypoxia models

For the *in vitro* experiments, myotubes were kept in normoxic (21% O_2) and hypoxic (4% O_2) incubators. Because we could not determine intracellular oxygen concentration or the extracellular oxygen concentration near the muscle cell in the dish, we did an optimization experiment to verify hypoxic (HIF) signaling in the cells. We chose 4% O_2 for further experiments because morphological differences and cell viability were least affected, which is essential because we want to study loss of Oxphen and not muscle atrophy.

To investigate the integrated responses to hypoxia at the level of the whole organism, we studied a mouse model of chronic hypoxia. Although a more complete view is obtained regarding the primary and secondary effects of hypoxia on muscle Oxphen, it should be appreciated that in patients with COPD hypoxia may develop downstream of the lung, for example due to reduced oxygen diffusion over the alveolar–capillary barrier in the lung or impaired muscle capillarization, which is different from a reduced oxygen tension in the inspired air. To study the sole effect of hypoxia on muscle, an *in vitro* model is preferred. However, the *in vivo* situation adds extramuscular factors that may influence muscle Oxphen and occur in patients as well.

PERSPECTIVES FOR IMPROVING OXPHEN IN COPD

The most obvious treatment for severe hypoxemia is oxygen therapy. In the past, Payen *et al.* showed in hypoxemic patients with COPD that skeletal muscle oxidative metabolism can be acutely improved with oxygen supplementation (52). However, muscle oxidative capacity was still lower in patients with oxygen supplementation compared to healthy controls, which suggests that structural muscle abnormalities, possibly loss of Oxphen, underlie the reduced exercise capacity in COPD. Jakobsson *et al.* showed that long-term oxygen therapy structurally improved oxidative capacity in hypoxemic patients, whereas that in hypoxemic patients without oxygen therapy further deteriorated in time (34). However, these studies concern patients with advanced COPD and severe hypoxemia, whereas in **Chapter 4** we showed that patients without mild to moderate hypoxemia already show loss of Oxphen. These patients do not qualify for oxygen therapy. There are nevertheless alternative approaches, both established and new, that could be employed to boost Oxphen in COPD, which will be discussed below.

Chapter 5 showed that patients with mild to moderate COPD have a normal induction of Oxphen regulators in response to exercise. Together with the result from **Chapter 2** that PPAR activity could be induced by a PPARδ agonist even under hypoxic conditions. Indeed, intervention studies have shown that exercise capacity of patients with COPD can be improved by exercise training (10, 57, 62). Although we do not yet have evidence of a normal Oxphen response in patients with advanced COPD, our results support that the incorporation of exercise training as integrated part of COPD management already in earlier stages of the disease could have a pivotal role to prevent or slow down loss of muscle Oxphen and related functional impairment. Moreover, Gagnon *et al.* propose rehabilitation already in GOLD 1 COPD, because these mild patients already have decreased physical activity levels (21).

Furthermore, pharmacological or nutritional modulation of the PPAR/PGC-1 pathway to improve training outcome should be investigated. Polyunsaturated fatty acids (PUFAs) are physiological stimulators of the PPARs. An intervention study by Broekhuizen *et al.* indeed showed significant improvement of exercise capacity in COPD patients who received nutritional supplementation with PUFAs, in addition to the effect of exercise training (9). Although no information was available on changes in skeletal muscle oxidative capacity, it can be speculated that the PUFA-induced improvement in exercise capacity was mediated by an improved muscle oxidative capacity. Alternatively, PPARs could be activated by synthetic ligands, such as GW501516 which specifically binds to PPARδ and has been shown to improve exercise capacity in mice (48). The drug was tested in clinical trials, but long-term rodent studies showed that GW501516 caused

cancers (23, 51) and this led to termination of drug development. The World Anti-Doping Agency advised athletes against the use of GW501516, which is still available on the black market as Endurobol (77). Possibly, GW501516 might still be of interest for patients with COPD, who already have decreased life expectancy and whose quality of life could be improved by supplementation with GW501516 during rehabilitation.

Another interesting target for pharmacological modulation is 5'-adenosine monophosphate-activated protein kinase (AMPK). Natanek *et al.* showed that the phosphorylated state of this protein was decreased in patients with COPD who are characterized by a fiber-type shift (50). The AMPK activator 5-aminoimidazole-4-carboxamide-1-β-D-ribofuranoside (AICAR) has successfully been used in animal models to stimulate exercise capacity (48). Clinical trials have been done to test the applicability of AICAR in treating diabetes because animal studies have shown increased glucose uptake after AICAR treatment (45, 64). The results from human studies are however inconclusive in regard to modulation of glucose uptake (5, 7, 8, 14). AMPK phosphorylation was not changed after AICAR treatment in these studies (5, 7, 14) and there are no clues yet whether AICAR can improve endurance or Oxphen in humans.

Resveratrol is a polyphenolic compound that is present in grapes, red wine, nuts and berries. Resveratrol has been shown to modulate AMPK via Sirtuin 1 (SIRT1) (55). With AMPK, SIRT1 is involved in regulation of cellular energy homeostasis and mitochondrial biogenesis (63). In obese humans, resveratrol has been shown to increase PGC-1α protein in skeletal muscle (70). Therefore, resveratrol would appear an interesting compound to improve skeletal muscle Oxphen in patients with COPD. Resveratrol has also been shown to have anti-inflammatory effects, some of which are mediated through inhibition of cyclooxygenase-2 (68). In rats exposed to cigarette smoke and LPS to model COPD, supplementation with resveratrol and AICAR lowered serum and muscle TNF-α and improved mitochondrial abnormalities in skeletal muscle (59). Resveratrol has been used in clinical trials related to inflammation, obesity and cardiovascular diseases, but results are not as convincing as those of animal studies (15, 54, 79).

Finally, a compound that has recently been shown to improve endurance is SR9009, which is a Rev-erbα agonist (66). Rev-erbα is a nuclear receptor that regulates circadian rhythm and mitochondrial biogenesis (71, 76). Clinical trials with SR9009 are underway, but animal studies prove promising (66, 76). Although several promising drugs to improve skeletal muscle Oxphen exist, incorporation of aerobic exercise is still advised, because effects elicited by contracting muscle are more comprehensive and beneficial to health than those obtained by taking the pharmacological agents alone (61).

Overall, from the results described in this thesis it can be concluded that hypoxia indeed decreases several markers of skeletal muscle oxidative metabolism. However, differences between the mouse model and the clinical situation of a patient with COPD include a plethora of factors that possibly modify the effects of hypoxia on muscle Oxphen. From the *in vivo* study, it appears that hypoxia only subtly affects muscle Oxphen. However, hypoxia could act as a modifier of other disease-related factors such as inflammation, medication and inactivity. To obtain a more translationally applicable model, it would be relevant to investigate the interaction of hypoxia with other factors defining COPD.

REFERENCES

1. Global Initiative for Chronic Obstructive Lung Disease www.goldcopd.org. [1 Feb, 2015].
2. Global Initiative for Chronic Obstructive Lung Disease (GOLD). Global strategy for the diagnosis, management and prevention of chronic pulmonary disease, 2015. http://www.goldcopd.org/uploads/users/files/GOLD_Report_2015.pdf. [1 Feb, 2015].
3. Richtlijn Diagnostiek en behandeling van COPD, 2010. Nederlandse Vereniging van Artsen voor Longziekten en Tuberculose. http://www.nvalt.nl/uploads/Mn/U9/MnU99pqRBYK7a_zStHhumA/Richtlijn-Diagnostiek-en-behandeling-van-COPD-maart-2010.pdf. [1 Feb, 2015].
4. Anderson EJ, and Neufer PD. Type II skeletal myofibers possess unique properties that potentiate mitochondrial H(2)O(2) generation. Am J Physiol Cell Physiol 290: C844-851, 2006.
5. Babraj JA, Mustard K, Sutherland C, Towler MC, Chen S, Smith K, Green K, Leese G, Hardie DG, Rennie MJ, and Cuthbertson DJ. Blunting of AICAR-induced human skeletal muscle glucose uptake in type 2 diabetes is dependent on age rather than diabetic status. Am J Physiol Endocrinol Metab 296: E1042-1048, 2009.
6. Barreiro E, Rabinovich R, Marin-Corral J, Barbera JA, Gea J, and Roca J. Chronic endurance exercise induces quadriceps nitrosative stress in patients with severe COPD. Thorax 64: 13-19, 2009.
7. Boon H, Bosselaar M, Praet SF, Blaak EE, Saris WH, Wagenmakers AJ, McGee SL, Tack CJ, Smits P, Hargreaves M, and van Loon LJ. Intravenous AICAR administration reduces hepatic glucose output and inhibits whole body lipolysis in type 2 diabetic patients. Diabetologia 51: 1893-1900, 2008.
8. Bosselaar M, Boon H, van Loon LJ, van den Broek PH, Smits P, and Tack CJ. Intra-arterial AICA-riboside administration induces NO-dependent vasodilation in vivo in human skeletal muscle. Am J Physiol Endocrinol Metab 297: E759-766, 2009.
9. Broekhuizen R, Wouters EF, Creutzberg EC, Weling-Scheepers CA, and Schols AM. Polyunsaturated fatty acids improve exercise capacity in chronic obstructive pulmonary disease. Thorax 60: 376-382, 2005.
10. Cambach W, Wagenaar RC, Koelman TW, van Keimpema AR, and Kemper HC. The long-term effects of pulmonary rehabilitation in patients with asthma and chronic obstructive pulmonary disease: a research synthesis. Arch Phys Med Rehabil 80: 103-111, 1999.
11. Chen JF, Mandel EM, Thomson JM, Wu Q, Callis TE, Hammond SM, Conlon FL, and Wang DZ. The role of microRNA-1 and microRNA-133 in skeletal muscle proliferation and differentiation. Nat Genet 38: 228-233, 2006.
12. Couillard A, Maltais F, Saey D, Debigare R, Michaud A, Koechlin C, LeBlanc P, and Prefaut C. Exercise-induced quadriceps oxidative stress and peripheral muscle dysfunction in patients with chronic obstructive pulmonary disease. Am J Respir Crit Care Med 167: 1664-1669, 2003.
13. Crul T, Testelmans D, Spruit MA, Troosters T, Gosselink R, Geeraerts I, Decramer M, and Gayan-Ramirez G. Gene expression profiling in vastus lateralis muscle during an acute exacerbation of COPD. Cell Physiol Biochem 25: 491-500, 2010.
14. Cuthbertson DJ, Babraj JA, Mustard KJ, Towler MC, Green KA, Wackerhage H, Leese GP, Baar K, Thomason-Hughes M, Sutherland C, Hardie DG, and Rennie MJ. 5-aminoimidazole-4-carboxamide 1-beta-D-ribofuranoside acutely stimulates skeletal muscle 2-deoxyglucose uptake in healthy men. Diabetes 56: 2078-2084, 2007.
15. de Ligt M, Timmers S, and Schrauwen P. Resveratrol and obesity: Can resveratrol relieve metabolic disturbances? Biochim Biophys Acta 2014.
16. den Hoed M, Hesselink MK, van Kranenburg GP, and Westerterp KR. Habitual physical activity in daily life correlates positively with markers for mitochondrial capacity. J Appl Physiol (1985) 105: 561-568, 2008.
17. Eickhoff P, Valipour A, Kiss D, Schreder M, Cekici L, Geyer K, Kohansal R, and Burghuber OC. Determinants of Systemic Vascular Function in Patients with Stable Chronic Obstructive Pulmonary Disease. Am J Respir Crit Care Med 178: 1211-1218, 2008.
18. el Azzouzi H, Leptidis S, Dirkx E, Hoeks J, van Bree B, Brand K, McClellan EA, Poels E, Sluimer JC, van den Hoogenhof MM, Armand AS, Yin X, Langley S, Bourajjaj M, Olieslagers S, Krishnan J, Vooijs M, Kurihara H, Stubbs A, Pinto YM, Krek W, Mayr M, da Costa Martins PA, Schrauwen P, and De Windt LJ. The hypoxia-inducible microRNA cluster miR-199a~214 targets myocardial PPARdelta and impairs mitochondrial fatty acid oxidation. Cell metabolism 18: 341-354, 2013.
19. Engelen MP, Schols AM, Does JD, Gosker HR, Deutz NE, and Wouters EF. Exercise-induced lactate increase in relation to muscle substrates in patients with chronic obstructive pulmonary disease. Am J Respir Crit Care Med 162: 1697-1704, 2000.
20. Fukuda R, Zhang H, Kim JW, Shimoda L, Dang CV, and Semenza GL. HIF-1 regulates cytochrome oxidase subunits to optimize efficiency of respiration in hypoxic cells. Cell 129: 111-122, 2007.
21. Gagnon P, Lemire BB, Dube A, Saey D, Porlier A, Croteau M, Provencher S, Debigare R, and Maltais F. Preserved function and reduced angiogenesis potential of the quadriceps in patients with mild COPD. Respir Res 15: 4, 2014.
22. Gan WQ, Man SF, Senthilselvan A, and Sin DD. Association between chronic obstructive pulmonary disease and systemic inflammation: a systematic review and a meta-analysis. Thorax 59: 574-580, 2004.
23. Geiger LE, Dunsford WS, Lewis DJ, Brennan C, Liu KC, and Newsholme SJ. Rat carcinogenicity study with GW501516, a PPAR delta agonist. The Toxicologist 108: 185, 2009.
24. Gohil K, Edwards RHT, and Jones DA. Analysis of muscle mitochondrial function with techniques applicable to needle biopsy samples. Clin Physiol 1: 195-207, 1981.
25. Gosker HR, Bast A, Haenen GR, Fischer MA, van der Vusse GJ, Wouters EF, and Schols AM. Altered antioxidant status in peripheral skeletal muscle of patients with COPD. Respir Med 99: 118-125, 2005.

26. Gosker HR, Lencer NH, Franssen FM, van der Vusse GJ, Wouters EF, and Schols AM. Striking similarities in systemic factors contributing to decreased exercise capacity in patients with severe chronic heart failure or COPD. Chest 123: 1416-1424, 2003.
27. Gosker HR, van Mameren H, van Dijk PJ, Engelen MP, van der Vusse GJ, Wouters EF, and Schols AM. Skeletal muscle fibre-type shifting and metabolic profile in patients with chronic obstructive pulmonary disease. Eur Respir J 19: 617-625, 2002.
28. Gosker HR, Wouters EF, van der Vusse GJ, and Schols AM. Skeletal muscle dysfunction in chronic obstructive pulmonary disease and chronic heart failure: underlying mechanisms and therapy perspectives. Am J Clin Nutr 71: 1033-1047, 2000.
29. Gouspillou G, Sgarioto N, Norris B, Barbat-Artigas S, Aubertin-Leheudre M, Morais JA, Burelle Y, Taivassalo T, and Hepple RT. The relationship between muscle fiber type-specific PGC-1alpha content and mitochondrial content varies between rodent models and humans. PLoS One 9: e103044, 2014.
30. Hitachi K, Nakatani M, and Tsuchida K. Myostatin signaling regulates Akt activity via the regulation of miR-486 expression. Int J Biochem Cell Biol 47: 93-103, 2014.
31. Horvat S, Beyer C, and Arnold S. Effect of hypoxia on the transcription pattern of subunit isoforms and the kinetics of cytochrome c oxidase in cortical astrocytes and cerebellar neurons. J Neurochem 99: 937-951, 2006.
32. Huttemann M, Helling S, Sanderson TH, Sinkler C, Samavati L, Mahapatra G, Varughese A, Lu G, Liu J, Ramzan R, Vogt S, Grossman LI, Doan JW, Marcus K, and Lee I. Regulation of mitochondrial respiration and apoptosis through cell signaling: cytochrome c oxidase and cytochrome c in ischemia/reperfusion injury and inflammation. Biochim Biophys Acta 1817: 598-609, 2012.
33. Huttemann M, Lee I, Gao X, Pecina P, Pecinova A, Liu J, Aras S, Sommer N, Sanderson TH, Tost M, Neff F, Aguilar-Pimentel JA, Becker L, Naton B, Rathkolb B, Rozman J, Favor J, Hans W, Prehn C, Puk O, Schrewe A, Sun M, Hofler H, Adamski J, Bekeredjian R, Graw J, Adler T, Busch DH, Klingenspor M, Klopstock T, Ollert M, Wolf E, Fuchs H, Gailus-Durner V, Hrabe de Angelis M, Weissmann N, Doan JW, Bassett DJ, and Grossman LI. Cytochrome c oxidase subunit 4 isoform 2-knockout mice show reduced enzyme activity, airway hyporeactivity, and lung pathology. FASEB J 26: 3916-3930, 2012.
34. Jakobsson P, and Jorfeldt L. Long-term oxygen therapy may improve skeletal muscle metabolism in advanced chronic obstructive pulmonary disease patients with chronic hypoxaemia. Respir Med 89: 471-476, 1995.
35. Jakobsson P, Jorfeldt L, and Brundin A. Skeletal muscle metabolites and fibre types in patients with advanced chronic obstructive pulmonary disease (COPD), with and without chronic respiratory failure. Eur Respir J 3: 192-196, 1990.
36. Jobin J, Maltais F, Doyon JF, LeBlanc P, Simard PM, Simard AA, and Simard C. Chronic obstructive pulmonary disease: capillarity and fiber-type characteristics of skeletal muscle. J Cardiopulm Rehabil 18: 432-437, 1998.
37. Kent BD, Mitchell PD, and McNicholas WT. Hypoxemia in patients with COPD: cause, effects, and disease progression. Int J Chron Obstruct Pulmon Dis 6: 199-208, 2011.
38. Lacasse Y, Series F, Vujovic-Zotovic N, Goldstein R, Bourbeau J, Lecours R, Aaron SD, and Maltais F. Evaluating nocturnal oxygen desaturation in COPD--revised. Respir Med 105: 1331-1337, 2011.
39. Lewis A, Riddoch-Contreras J, Natanek SA, Donaldson A, Man WD, Moxham J, Hopkinson NS, Polkey MI, and Kemp PR. Downregulation of the serum response factor/miR-1 axis in the quadriceps of patients with COPD. Thorax 67: 26-34, 2012.
40. Malley WJ. Clinical Blood Gases: Assessment & Intervention. Elsevier Health Sciences, 2013.
41. Maltais F, Decramer M, Casaburi R, Barreiro E, Burelle Y, Debigare R, Dekhuijzen PN, Franssen F, Gayan-Ramirez G, Gea J, Gosker HR, Gosselink R, Hayot M, Hussain SN, Janssens W, Polkey MI, Roca J, Saey D, Schols AM, Spruit MA, Steiner M, Taivassalo T, Troosters T, Vogiatzis I, Wagner PD, and COPD AEAHCoLMDi. An official American Thoracic Society/European Respiratory Society statement: update on limb muscle dysfunction in chronic obstructive pulmonary disease. Am J Respir Crit Care Med 189: e15-62, 2014.
42. McCarthy JJ. MicroRNA-206: the skeletal muscle-specific myomiR. Biochim Biophys Acta 1779: 682-691, 2008.
43. McCarthy JJ, Esser KA, Peterson CA, and Dupont-Versteegden EE. Evidence of MyomiR network regulation of beta-myosin heavy chain gene expression during skeletal muscle atrophy. Physiol Genomics 39: 219-226, 2009.
44. Mercken EM, Gosker HR, Rutten EP, Wouters EF, Bast A, Hageman GJ, and Schols AM. Systemic and pulmonary oxidative stress after single-leg exercise in COPD. Chest 136: 1291-1300, 2009.
45. Merrill GF, Kurth EJ, Hardie DG, and Winder WW. AICA riboside increases AMP-activated protein kinase, fatty acid oxidation, and glucose uptake in rat muscle. Am J Physiol 273: E1107-1112, 1997.
46. Moro L, Pedone C, Scarlata S, Malafarina V, Fimognari F, and Antonelli-Incalzi R. Endothelial dysfunction in chronic obstructive pulmonary disease. Angiology 59: 357-364, 2008.
47. Naimi AI, Bourbeau J, Perrault H, Baril J, Wright-Paradis C, Rossi A, Taivassalo T, Sheel AW, Rabol R, Dela F, and Boushel R. Altered mitochondrial regulation in quadriceps muscles of patients with COPD. Clin Physiol Funct Imaging 31: 124-131, 2011.
48. Narkar VA, Downes M, Yu RT, Embler E, Wang Y-X, Banayo E, Mihaylova MM, Nelson MC, Zou Y, Juguilon H, Kang H, Shaw RJ, and Evans RM. AMPK and PPARδ Agonists Are Exercise Mimetics. Cell 134: 405-415, 2008.
49. Natanek SA, Gosker HR, Slot IG, Marsh GS, Hopkinson NS, Man WD, Tal-Singer R, Moxham J, Kemp PR, Schols AM, and Polkey MI. Heterogeneity of quadriceps muscle phenotype in chronic obstructive pulmonary disease (Copd); implications for stratified medicine? Muscle Nerve 48: 488-497, 2013.
50. Natanek SA, Gosker HR, Slot IG, Marsh GS, Hopkinson NS, Moxham J, Kemp PR, Schols AM, and Polkey MI. Pathways associated with reduced quadriceps oxidative fibres and endurance in COPD. Eur Respir J 41: 1275-1283, 2013.
51. Newsholme SJ, Dunsford WS, Brodie T, Brennan C, Brown M, and Geiger LE. Mouse carcinogenicity study with GW501516, a PPAR delta agonist. The Toxicologist 108: 185, 2009.

52. Payen JF, Wuyam B, Levy P, Reutenauer H, Stieglitz P, Paramelle B, and Le Bas JF. Muscular metabolism during oxygen supplementation in patients with chronic hypoxemia. Am Rev Respir Dis 147: 592-598, 1993.
53. Pinto-Plata VM, Mullerova H, Toso JF, Feudjo-Tepie M, Soriano JB, Vessey RS, and Celli BR. C-reactive protein in patients with COPD, control smokers and non-smokers. Thorax 61: 23-28, 2006.
54. Poulsen MM, Fjeldborg K, Ornstrup MJ, Kjaer TN, Nohr MK, and Pedersen SB. Resveratrol and inflammation: Challenges in translating pre-clinical findings to improved patient outcomes. Biochim Biophys Acta 2015.
55. Price NL, Gomes AP, Ling AJ, Duarte FV, Martin-Montalvo A, North BJ, Agarwal B, Ye L, Ramadori G, Teodoro JS, Hubbard BP, Varela AT, Davis JG, Varamini B, Hafner A, Moaddel R, Rolo AP, Coppari R, Palmeira CM, de Cabo R, Baur JA, and Sinclair DA. SIRT1 is required for AMPK activation and the beneficial effects of resveratrol on mitochondrial function. Cell metabolism 15: 675-690, 2012.
56. Puente-Maestu L, Perez-Parra J, Godoy R, Moreno N, Tejedor A, Gonzalez-Aragoneses F, Bravo JL, Alvarez FV, Camano S, and Agusti A. Abnormal mitochondrial function in locomotor and respiratory muscles of COPD patients. Eur Respir J 33: 1045-1052, 2009.
57. Puente-Maestu L, Tena T, Trascasa C, Perez-Parra J, Godoy R, Garcia MJ, and Stringer WW. Training improves muscle oxidative capacity and oxygenation recovery kinetics in patients with chronic obstructive pulmonary disease. Eur J Appl Physiol 88: 580-587, 2003.
58. Qaseem A, Wilt TJ, Weinberger SE, Hanania NA, Criner G, van der Molen T, Marciniuk DD, Denberg T, Schunemann H, Wedzicha W, MacDonald R, Shekelle P, American College of P, American College of Chest P, American Thoracic S, and European Respiratory S. Diagnosis and management of stable chronic obstructive pulmonary disease: a clinical practice guideline update from the American College of Physicians, American College of Chest Physicians, American Thoracic Society, and European Respiratory Society. Ann Intern Med 155: 179-191, 2011.
59. Qi Y, Shang JY, Ma LJ, Sun BB, Hu XG, Liu B, and Zhang GJ. Inhibition of AMPK expression in skeletal muscle by systemic inflammation in COPD rats. Respir Res 15: 156, 2014.
60. Rabinovich RA, Bastos R, Ardite E, Llinas L, Orozco-Levi M, Gea J, Vilaro J, Barbera JA, Rodriguez-Roisin R, Fernandez-Checa JC, and Roca J. Mitochondrial dysfunction in COPD patients with low body mass index. Eur Respir J 29: 643-650, 2007.
61. Richter EA, Kiens B, and Wojtaszewski JF. Can exercise mimetics substitute for exercise? Cell metabolism 8: 96-98, 2008.
62. Rochester CL. Exercise training in chronic obstructive pulmonary disease. J Rehabil Res Dev 40: 59-80, 2003.
63. Ruderman NB, Xu XJ, Nelson L, Cacicedo JM, Saha AK, Lan F, and Ido Y. AMPK and SIRT1: a long-standing partnership? Am J Physiol Endocrinol Metab 298: E751-760, 2010.
64. Sakoda H, Ogihara T, Anai M, Fujishiro M, Ono H, Onishi Y, Katagiri H, Abe M, Fukushima Y, Shojima N, Inukai K, Kikuchi M, Oka Y, and Asano T. Activation of AMPK is essential for AICAR-induced glucose uptake by skeletal muscle but not adipocytes. Am J Physiol Endocrinol Metab 282: E1239-1244, 2002.
65. Sauleda J, Garcia-Palmer F, Wiesner RJ, Tarraga S, Harting I, Tomas P, Gomez C, Saus C, Palou A, and Agusti AG. Cytochrome oxidase activity and mitochondrial gene expression in skeletal muscle of patients with chronic obstructive pulmonary disease. Am J Respir Crit Care Med 157: 1413-1417, 1998.
66. Solt LA, Wang Y, Banerjee S, Hughes T, Kojetin DJ, Lundasen T, Shin Y, Liu J, Cameron MD, Noel R, Yoo SH, Takahashi JS, Butler AA, Kamenecka TM, and Burris TP. Regulation of circadian behaviour and metabolism by synthetic REV-ERB agonists. Nature 485: 62-68, 2012.
67. Srinivasan S, and Avadhani NG. Cytochrome c oxidase dysfunction in oxidative stress. Free Radic Biol Med 53: 1252-1263, 2012.
68. Subbaramaiah K, Chung WJ, Michaluart P, Telang N, Tanabe T, Inoue H, Jang M, Pezzuto JM, and Dannenberg AJ. Resveratrol inhibits cyclooxygenase-2 transcription and activity in phorbol ester-treated human mammary epithelial cells. J Biol Chem 273: 21875-21882, 1998.
69. Swallow EB, Reyes D, Hopkinson NS, Man WD, Porcher R, Cetti EJ, Moore AJ, Moxham J, and Polkey MI. Quadriceps strength predicts mortality in patients with moderate to severe chronic obstructive pulmonary disease. Thorax 62: 115-120, 2007.
70. Timmers S, Konings E, Bilet L, Houtkooper RH, van de Weijer T, Goossens GH, Hoeks J, van der Krieken S, Ryu D, Kersten S, Moonen-Kornips E, Hesselink MK, Kunz I, Schrauwen-Hinderling VB, Blaak EE, Auwerx J, and Schrauwen P. Calorie restriction-like effects of 30 days of resveratrol supplementation on energy metabolism and metabolic profile in obese humans. Cell metabolism 14: 612-622, 2011.
71. Triqueneaux G, Thenot S, Kakizawa T, Antoch MP, Safi R, Takahashi JS, Delaunay F, and Laudet V. The orphan receptor Rev-erbalpha gene is a target of the circadian clock pacemaker. J Mol Endocrinol 33: 585-608, 2004.
72. van Gestel AJ, Clarenbach CF, Stowhas AC, Teschler S, Russi EW, Teschler H, and Kohler M. Prevalence and Prediction of Exercise-Induced Oxygen Desaturation in Patients with Chronic Obstructive Pulmonary Disease. Respiration 2012.
73. Van Helvoort HA, Heijdra YF, Thijs HM, Vina J, Wanten GJ, and Dekhuijzen PN. Exercise-induced systemic effects in muscle-wasted patients with COPD. Med Sci Sports Exerc 38: 1543-1552, 2006.
74. van Wetering CR, van Nooten FE, Mol SJ, Hoogendoorn M, Rutten-Van Molken MP, and Schols AM. Systemic impairment in relation to disease burden in patients with moderate COPD eligible for a lifestyle program. Findings from the INTERCOM trial. Int J Chron Obstruct Pulmon Dis 3: 443-451, 2008.
75. Wagner PD. Skeletal muscles in chronic obstructive pulmonary disease: deconditioning, or myopathy? Respirology 11: 681-686, 2006.
76. Woldt E, Sebti Y, Solt LA, Duhem C, Lancel S, Eeckhoute J, Hesselink MK, Paquet C, Delhaye S, Shin Y, Kamenecka TM, Schaart G, Lefebvre P, Neviere R, Burris TP, Schrauwen P, Staels B, and Duez H. Rev-erb-alpha modulates skeletal muscle

oxidative capacity by regulating mitochondrial biogenesis and autophagy. Nat Med 19: 1039-1046, 2013.
77. World Anti-Doping Agency. WADA issues alert on GW501516. https://www.wada-ama.org/en/media/news/2013-03/wada-issues-alert-on-gw501516: 2013.
78. Yang MH, Wu MZ, Chiou SH, Chen PM, Chang SY, Liu CJ, Teng SC, and Wu KJ. Direct regulation of TWIST by HIF-1 alpha promotes metastasis. Nat Cell Biol 10: 295-305, 2008.
79. Zordoky BN, Robertson IM, and Dyck JR. Preclinical and clinical evidence for the role of resveratrol in the treatment of cardiovascular diseases. Biochim Biophys Acta 2014.

Samenvatting

INTRODUCTION

COPD staat voor “Chronic Obstructive Pulmonary Disease” en is ni*et all*een een chronische longziekte maar wordt vaak ook gekenmerkt door meerdere systemische manifestaties die de ziektelast vergroten, waaronder skeletspierzwakte. De skeletspier van patiënten met ernstige COPD wordt vaak gekarakteriseerd door verlies van spiermassa en een verlies van het oxidatief fenotype. Onder verlies van oxidatief fenotype worden een verminderd aantal oxidatieve spiervezels en een verminderde capaciteit van het oxidatieve metabolisme in deze spiercellen verstaan. Het verlies van het oxidatief fenotype ligt ten grondslag aan een verminderd uithoudingsvermogen van de beenspieren, zoals wordt waargenomen bij patiënten met COPD. Mogelijke COPD-gerelateerde factoren die aan dit verlies ten grondslag kunnen liggen zijn systemische ontsteking, verlaagde zuurstofspanning (hypoxie), medicatie (glucocorticoïden), verminderde fysieke activiteit en ongezonde voedingsgewoonten. Echter, of en in welke mate elk van deze factoren daadwerkelijk bijdraagt is tot op heden nog onduidelijk. Dit proefschrift richt zich specifiek op de rol van hypoxie in het verlies van het oxidatief fenotype van de skeletspier. Daarbij is gekozen voor een translationele aanpak: het effect van chronische hypoxie op de spiercel op zichzelf is onderzocht (*in vitro*), alsook het effect van hypoxie op de spier in de context van een heel organisme. Tevens werd onderzocht of tijdelijke hypoxie tijdens inspanning een verstorende rol speelt in de natuurlijke stimulatie van het oxidatief fenotype in de COPD patiënt.

HYPOXIE-SENSOR HIF-1α MODULEERT HET OXIDATIEVE METABOLISME VIA DE REGULATOR PGC-1α

Afhankelijk van de ernst van de longaandoening kan in het spierweefsel van een COPD patiënt een verlaagde zuurstofspanning optreden. De functie van het spierweefsel, met name het zuurstofafhankelijke metabolisme, kan daardoor verstoord raken. In **Hoofdstuk 2** is daarom onderzocht of en via welk mechanisme chronische hypoxie de indicatoren van het oxidatief fenotype negatief reguleert in een *in vitro* model van spiercellen. Het oxidatief fenotype bestaat grofweg uit een structurele component, dit zijn de eiwitten die zorgen voor contractie van de spiercellen, en een metabole component bestaande uit de eiwitten die betrokken zijn bij de productie van energie. Uit dit experiment bleek dat de expressie van mitochondriële eiwitten die betrokken zijn bij energieproductie via oxidatieve fosforylering verlaagd is onder hypoxische omstandigheden. Dit gaat gepaard met een verlaagde expressie en activiteit van regulatoren van het oxidatieve metabolisme, waaronder de belangrijke regulator PGC-1α alsook transcriptiefactoren die het activeert, waaronder PPARα, PPARδ en ERRα. Er is verder aangetoond dat de verlaagde genexpressie van PGC-1α wordt gemedieerd door HIF-1α, een belangrijke regulator van de reactie op hypoxie.

In de mens is type I myosine een belangrijke component van het contractiele apparaat van de meest oxidatieve spiervezels. In patiënten met ernstige COPD is eerder aangetoond dat het aandeel spiervezels dat type I myosine tot expressie brengt gereduceerd is. Echter, de meest oxidatieve spiervezels van knaagdieren bevatten type IIa myosine in plaats van type I. In **Hoofdstuk 2** is ook aangetoond dat hypoxie de expressie van type I myosine stimuleert in de gekweekte muizenspiercellen. Dit effect wordt wederom gemedieerd door HIF-1α. Uit **Hoofdstuk 2** blijkt dus dat HIF-1α een belangrijke rol speelt in de hypoxie-afhankelijke verstoring van zowel de structurele

als de metabole component van het oxidatief fenotype in spiercellen, wat betekent dat hypoxie inderdaad het verlies van oxidatief fenotype in de beenspieren van COPD patiënten zou kunnen verklaren.

HYPOXIE MODULEERT HET OXIDATIEF SPIERFENOTYPE IN MUIZEN

In tegenstelling tot de spiercellen in een kweekschaaltje kunnen spiercellen in een organisme indirect beïnvloed worden door hypoxie, bijvoorbeeld via effecten op andere organen of weefsels. In **Hoofdstuk 3** wordt daarom het effect van chronische hypoxie (3 weken) op het oxidatief fenotype van skeletspier in een muismodel behandeld. Eerder werd in ratten aangetoond dat de leeftijd van de rat bij blootstelling aan hypoxie een belangrijke invloed heeft op de effecten van hypoxie op het oxidatief spierfenotype. De studie is daarom uitgevoerd in muizen in drie leeftijdsgroepen van 4 weken (in de groei), 12 weken (stabiel lichaamsgewicht) en 52 weken (middelbare leeftijd).

In overeenstemming met de *in vitro* resultaten wordt in **Hoofdstuk 3** aangetoond dat chronische hypoxieblootstelling ook *in vivo* in een verlaging van de genexpressie van indicatoren van het oxidatief metabolisme resulteert, zij het slechts subtiel. De hoeveelheid van de eiwitten betrokken bij oxidatieve fosforylering was echter niet aangedaan door hypoxie. In lijn met **Hoofdstuk 2** wordt in **Hoofdstuk 3** een verhoging van de expressie van type I myosine gevonden onder invloed van hypoxie. De negatieve effecten van chronische hypoxie op het oxidatief fenotype in skeletspier worden door beide studies bevestigd, alhoewel de resultaten van de *in vivo* studie wat genuanceerder zijn.

Een secundaire vraagstelling in **Hoofdstuk 3** is of de leeftijd van de muis bij blootstelling de effecten van chronische hypoxie beïnvloedt, zoals eerder aangetoond in ratten. Inderdaad blijkt leeftijd het effect van hypoxie te moduleren: de oude muizen vertonen een sterkere afname van gentranscripten voor eiwitten betrokken bij het oxidatief metabolisme en ondergaan ook een groter verlies van spier- en vetmassa onder invloed van hypoxie. De jongste muizen daarentegen vertoonden grotere veranderingen met betrekking tot vezeltype en spieratrofie. Bij het modelleren van componenten uit een ziekte die voorkomt in een populatie van middelbare tot hogere leeftijd, zoals het geval is bij COPD, lijkt het dus verstandig om de leeftijd van de muizen hierop aan te passen.

VERLIES VAN HET OXIDATIEF SPIERFENOTYPE TREEDT OP IN MILDERE STADIA VAN COPD

Hoewel h*et al* langer bekend is dat in patiënten met ernstige COPD een verlies van het oxidatief fenotype in skeletspier optreedt, zijn er nog relatief weinig studies gedaan naar spierafwijkingen in mildere stadia van de ziekte. In **Hoofdstuk 4** is daarom een groep patiënten met milde tot matige COPD bestudeerd. Hoewel deze patiënten nog geen significant spiermassaverlies vertonen, is er wel een verlaging van indicatoren van het oxidatief fenotype meetbaar. Onder andere de genexpressie van de regulator PGC-1α, die belangrijk is voor het oxidatieve metabolisme, is verlaagd. In **Hoofdstuk 2** werd al aangetoond dat in spiercellen *in vitro* PGC-1α expressie verlaagd werd onder hypoxische omstandigheden door de hypoxie-afhankelijke regulator HIF-1α. Mogelijk ligt dit mechanisme ook ten grondslag aan het verlaagde expressieniveau van PGC-1α in de

spier van de patiënten. Wel duidelijk is dat het verlies van oxidatief fenotype in de spier klinisch relevant is, omdat het gepaard gaat met een verminderd uithoudingsvermogen van die zelfde spier in deze patiëntengroep. Afwijkingen van het spiermetabolisme treden dus reeds op in een milder stadium van de ziekte, onafhankelijk van spiermassaverlies.

Patiënten met COPD zijn gemiddeld minder actief. Ook fysieke inactiviteit kan resulteren in een verlies van oxidatief fenotype van de spier. In **Hoofdstuk 2** is echter geen verband gevonden tussen indicatoren van het oxidatief fenotype en de totale fysieke activiteit van de COPD patiënten of de intensiteit van die activiteit. Een rol voor inactiviteit in het verlies van oxidatief fenotype kan echter niet worden uitgesloten, omdat onze studie transversaal en niet longitudinaal van opzet was.

DE REGULATOIRE RESPONS VAN OXIDATIEF FENOTYPE OP INSPANNING IS NORMAAL IN PATIËNTEN MET MILDE TOT MATIGE COPD

In gezonde personen zorgt inspanning voor verhoging van de genexpressie van PGC-1α en stimulatie van het oxidatief fenotype in de spier. De vraagt rijst in hoeverre een verlaagde zuurstofspanning in het bloed tijdens inspanning, een geregeld voorkomend symptoom bij COPD patiënten, een verstoring oplevert van de natuurlijke stimulatie van het oxidatief fenotype door inspanning. Daarom is in **Hoofdstuk 5** de inspanningsreactie van genen coderend voor eiwitten betrokken bij het oxidatief metabolisme in de beenspier bestudeerd in dezelfde groep milde tot matige COPD patiënten waarbij in **Hoofdstuk 4** reeds een verlies van oxidatief fenotype werd geconstateerd. Bij de helft van de patiënten werd tijdens de fietstest een verlaagde zuurstofspanning in het arteriële bloed gedetecteerd. De genen van indicatoren van het oxidatief fenotype, waaronder PGC-1α, reageerden in deze test echter niet anders in de patiënten dan in de controles, ondanks dat patiënten op een lagere intensiteit fietsten. Ook was er geen onderscheid in de respons van patiënten met inspanningsgeassocieerde verlaagde zuurstofspanning en patiënten met normale zuurstofspanning.

Naast de arteriële zuurstofspanning werd ook de zuurstofspanning in de spier gevolgd met behulp van infraroodspectroscopie (NIRS). In **Hoofdstuk 5** is aangetoond dat er geen significante verschillen zijn in de zuurstofspanning in de spier tussen patiënten en controles of tussen patiënten met normale en verlaagde arteriële zuurstofspanning tijdens de fietstest. Ook was er geen verband tussen de zuurstofspanning in de arteriën en die in de spier tijdens de fietstest. De respons van de genen van indicatoren van het oxidatief fenotype bleek ook niet verschillend in patiënten met een hoge of lage zuurstofspanning in de spier tijdens de fietstest. Op dit niveau van regulatie van het oxidatief fenotype vertonen de patiënten dus een normale reactie op inspanning. Er is echter niet onderzocht in hoeverre processen na deze initiële regulatie verstoord zijn in de patiënten. Een intacte respons van regulatoren van het oxidatief fenotype op inspanning impliceert dat patiënten met milde tot matige COPD baat kunnen hebben bij geregelde fysieke activiteit om het oxidatief fenotype van de beenspieren op pijl te houden.

GEEN VERHOOGDE OXIDATIEVE STRESS IN DE SPIER IN MILDERE STADIA VAN COPD

Uit eerder onderzoek is bekend dat glycolytische spiervezels, die minder afhankelijk zijn van zuurstof dan oxidatieve vezels, een grotere hoeveelheid oxidatieve stress veroorzaken. Oxidatieve stress ontstaat als de hoeveelheid schadelijke reactieve zuurstofverbindingen groter is dan de capaciteit van de cel om deze verbindingen op te ruimen. De reactieve zuurstofverbindingen ontstaan tijdens verschillende cellulaire processen, waaronder het mitochondrieel metabolisme. In **Hoofdstuk 4** is aangetoond dat er inderdaad een negatieve correlatie bestaat tussen het aandeel oxidatieve type I vezels en de aanwezigheid van producten van oxidatieve stress in de beenspieren van COPD patiënten. Hoewel de patiënten relatief minder oxidatieve vezels in de beenspier hebben, is de hoeveelheid oxidatieve stressproducten echter niet verschillend tussen patiënten en controles. Bovendien is In **Hoofdstuk 5** aangetoond dat ook tijdens de fietstest er geen verhoogde ophoping optreedt van oxidatieve stressproducten in de spier van patiënten vergeleken met controles, onafhankelijk van eventueel verlaagde arteriële zuurstofspanning tijdens de test. De patiënten vertoonden in vergelijking met de gezonde controles echter wel een verhoogde genexpressie van zogenaamde antioxidant enzymen betrokken bij de verdediging tegen oxidatieve stress. Uit deze resultaten blijkt dat zowel basale alsook inspanningsgeïnduceerde oxidatieve stress in deze mildere stadia van COPD nog niet verhoogd is in de spier, zoals eerder wel werd aangetoond voor patiënten met ernstige COPD.

HYPOXIE: IMPLICATIES VOOR COPD

In **Hoofdstuk 6** worden de resultaten van de studies zoals beschreven in dit proefschrift bediscussieerd. Hoewel er voorheen in de COPD patiënten geen duidelijk verband is aangetoond tussen spierafwijkingen en de ernst van de ziekte (gebaseerd op de mate van luchtwegobstructie), vonden wij in een gecombineerde analyse van de studie beschreven in **Hoofdstuk 4** en een eerdere studie wel enig verband tussen de mate waarin de long zuurstof kan opnemen (bepaald als DLCO) en het aandeel oxidatieve type I spiervezels in de quadriceps beenspier. Ook vonden wij in deze gecombineerde analyse voor de milde tot matige COPD patiënten een verband van het aandeel type I spiervezels met de arteriële zuurstofspanning, wat eerder al werd aangetoond in ernstige COPD. Dit wijst op een potentiële rol voor verlaagde zuurstofspanning in het bloed (hypoxemie) in het verlies van oxidatief fenotype zoals aangetoond in de beenspieren van COPD patiënten. Deze aanwijzingen worden onderbouwd door de bevindingen in de spiercellen *in vitro* en in het muismodel, waar indicatoren van het oxidatieve metabolisme negatief werden beïnvloed door hypoxie. Meer onderzoek naar de onderliggende moleculaire mechanismen zullen kunnen leiden tot de ontwikkeling van interventies om een verlies van het oxidatief fenotype van skeletspieren te voorkomen of af te zwakken en daarmee de kwaliteit van leven van de COPD patiënt te verbeteren.

Samengevat kan uit de resultaten zoals beschreven in dit proefschrift worden geconcludeerd dat hypoxie inderdaad verscheidene indicatoren van het oxidatief metabolisme van de skeletspier verlaagt. Niettemin zijn er vele factoren die verschillen tussen het muismodel en de klinische situatie van een COPD patiënt die mogelijk de effecten van hypoxie op het oxidatief spierfenotype beïnvloeden. Uit de *in vivo* studie blijkt dat chronische hypoxie op zichzelf slechts een milde aantasting van het oxidatief

fenotype van de spier oplevert. Echter, hypoxie kan de uitwerking van andere ziekte-gerelateerde factoren, zoals ontsteking, medicatie en fysieke inactiviteit, op het oxidatief fenotype beïnvloeden. Om een beter toepasbaar translationeel onderzoeksmodel te verkrijgen is het daarom relevant om de interacties van hypoxie met andere factoren die COPD definiëren te onderzoeken.

Valorisation addendum

WHAT IS THE PROBLEM AND HOW DO WE CONTRIBUTE?

Chronic obstructive pulmonary disease (COPD) is a lung disease characterized by irreversible obstruction of airflow in the lungs. The main risk factor for development of COPD is active smoking, but second-hand smoke, frequent lower respiratory infections, dust, chemical fumes, and air pollution in the workplace or the environment also contribute. In addition, there are genetic disorders that predispose to develop COPD. COPD is frequently diagnosed in people aged over 40 because disease development is slow. According to estimates by the World Health Organization, approximately 65 million people worldwide are affected by COPD. The 'global burden of disease' study indicates that in 2020 COPD will be the third leading cause of death and the fifth leading cause of years lost through early mortality or handicap. In The Netherlands 1 in 50 people are diagnosed with COPD. From people over 80 years of age, 1 in 6 people are affected.

COPD is not limited to the lung; systemic manifestations including skeletal muscle dysfunction seriously affect disease burden. Loss ovf skeletal muscle mass due to muscle fiber atrophy results in reduced muscular strength and is independently associated with increased morbidity and mortality. Furthermore, a reduced proportion of oxidative muscle fiber types and mitochondrial metabolism (loss of oxidative phenotype; Oxphen) in the limb muscle is associated with increased muscular fatigability and reduced exercise capacity. Moreover, patients are more susceptible to comorbidities such as the metabolic syndrome and cardiovascular disease. Interestingly, loss of Oxphen has been proposed to be associated with muscle wasting and to be a driver of cardiovascular and metabolic risk in COPD. Delaying or even reversing loss of Oxphen might therefore be a promising therapeutical approach, increasing quality of life and decreasing health care costs by reducing the amount of hospital admissions.

Skeletal muscle of a COPD patient is exposed to multiple deleterious factors, such as low-grade systemic inflammation, malnutrition, hypoxia, physical inactivity, corticosteroid medication, and oxidative and nitrosative stress. All these factors may be implicated in skeletal muscle dysfunction and their role in skeletal muscle wasting has been described before. However, their role in loss of Oxphen is not elaborately explored. In the research described in this thesis, we focused on the role of hypoxia in the loss of skeletal muscle Oxphen. We investigated the effect of chronic hypoxia on muscle cells directly (*in vitro*) and on muscle as a part of the mouse (*in vivo*). In addition, we investigated the effect of acute hypoxia as a consequence of exercise-induced systemic oxygen desaturation in COPD patients. The results reported in this thesis suggest that hypoxia *per se* can play a role in the loss of muscle Oxphen. Consequently, the research described in this thesis certainly has substantial societal impact, albeit not with immediate monetary value.

WHAT DO WE KNOW NOW?

One of the main findings of this research in relation to COPD was that patients with mild to moderate disease already have a loss of skeletal muscle Oxphen, while muscle weakness and atrophy are not (yet) present. Another main finding from the exercise study described in this thesis is that the initial regulatory gene expression response to exercise, which is a natural stimulant of muscle Oxphen, is intact in the skeletal muscle of mild to moderate COPD patients. This would implicate that patients already at an early disease stage would benefit from an intervention program that includes endurance training while pulmonary rehabilitation (PR) is currently mostly considered in more advanced disease. Early exercise intervention and counseling may also be more cost effective as in more advanced disease often a multidisciplinary PR approach is required, including not only exercise training but also nutritional counseling and psychosocial interventions. During early disease, patients are less symptomatic and exercise training is only moderately hampered by ventilatory impairment which may also from a metabolic perspective enhance intervention efficacy.

Findings from the *in vitro* research described in this thesis include that hypoxia attenuates the activity of PPAR transcription factors by reducing expression of their coactivator PGC-1α in a HIF-1α-dependent manner. PPARs and PGC-1α are important regulators of muscle oxidative phenotype and their expression has been shown to be decreased in skeletal muscle of COPD patients, even in mild to moderate COPD as shown in this thesis. The *in vitro* experiments showed that PPAR transcriptional activity could be boosted under hypoxic conditions using the PPARδ ligand GW501516. Furthermore, removing HIF-1α, which is a master regulator of the hypoxic response, under hypoxic conditions could restore PGC-1α gene expression and PPAR transcriptional activity. These findings indicate that nutritional or pharmacological interventions targeted at these regulatory molecules could help maintain or boost skeletal muscle oxidative phenotype in patients with COPD. These interventions could be combined with exercise training for a synergistic effect. Previously it has been shown that supplementation with poly-unsaturated acids in addition to exercise training indeed significantly improves exercise capacity of patients with advanced COPD (1). However, since no muscle biopsies were taken in that study, there is no information available regarding molecular changes in the muscle.

FOR WHOM IS IT OF INTEREST AND HOW SHOULD WE PROCEED?

The results from this thesis are of interest for primary health care physicians, chest physicians and physiotherapists to optimize COPD therapy and improve patients' quality of life. Particularly general practitioners (GPs) are in a position to recognize symptoms of COPD in an early stage and to contribute to counteract the loss of Oxphen already

in early COPD. Analyses by the American Thoracic Society and European Respiratory Society indicate that PR in advanced COPD is cost-effective: hospitalizations are of shorter duration and lower frequency in the years following PR. It stands to reason that earlier exercise intervention and potentially nutritional or pharmacological intervention can further improve patient health and reduce health care costs. However, there is still research to be done in this area. From our results it appears that the response to a single exercise bout is not abnormal in patients with mild to moderate COPD. Future research should uncover whether the training response downstream of the regulators' gene expression is also intact in these patients.

The results regarding nutritional and pharmacological intervention will eventually also be of interest for the nutrition and pharmaceutical industries that can develop medical nutrition and supplements for patients with COPD. However, this thesis only slightly touched upon the subject of pharmacological intervention and further experimentation both *in vitro* and *in vivo* is necessary before it is financially feasible to be pursued by commercial parties.

FEASIBILITY

A potential obstacle for early exercise/nutritional/pharmacological intervention to boost Oxphen is that patients that are not (yet) symptomatic will likely be less motivated to work to improve their health. Therefore, early implementation of (pre-emptive) intervention programs does not only depend on well-timed prescription by health care workers, but also on the intrinsic motivation of patients. Consequently, an effort should be made to increase patients' awareness of the benefits of early intervention.

SPREAD

To increase societal impact, a large spread is essential. Ultimately we would like the patients, especially those with mild to moderate disease, to benefit from our findings. A first place to start the spreading would therefore be the GP office. GPs see the patients first when they present with mild symptoms of what possibly is COPD. Therefore, GPs should be made aware that intervention by physical exercise programs at this stage could improve the outlook for patients by delaying or maybe even preventing progression of the disease. Secondly, pulmonologists should be informed on the potential benefits of early exercise/nutritional/pharmacological intervention for their patients. Information can be spread at conferences. Clinicians can relay this information to the patients. Thirdly, patients should be made aware of the importance and benefit of early exercise/nutritional/pharmacological intervention to boost their muscle Oxphen. This information can be relayed through patient groups, who also visit the national Lung Days, a yearly conference visited by researchers, clinicians and patient groups. In addition, patients to include in early exercise intervention trials should be recruited via

for example newspaper advertisements, so that patient recruitment is not biased by the willingness of clinicians to cooperate with patient inclusion. If the trials turn out to be beneficial for the patients, patients can then further spread the word to their doctors so these doctors will be convinced not just from the academic perspective, but also from the perspective of the patients, who are the ultimate beneficiaries.

REFERENCES

1. Broekhuizen R, Wouters EF, Creutzberg EC, Weling-Scheepers CA, and Schols AM. Polyunsaturated fatty acids improve exercise capacity in chronic obstructive pulmonary disease. Thorax 60: 376-382, 2005.
2. Nici L, Donner C, Wouters E, Zuwallack R, Ambrosino N, Bourbeau J, Carone M, Celli B, Engelen M, Fahy B, Garvey C, Goldstein R, Gosselink R, Lareau S, MacIntyre N, Maltais F, Morgan M, O'Donnell D, Prefault C, Reardon J, Rochester C, Schols A, Singh S, Troosters T, and Committee AEPRW. American Thoracic Society/European Respiratory Society statement on pulmonary rehabilitation. Am J Respir Crit Care Med 173: 1390-1413, 2006.

List of publications

Ilse G.M. Slot, Annemie M.W.J. Schols, Chiel C. de Theije, Frank J.M. Snepvangers and Harry R. Gosker, Alterations in Skeletal Muscle Oxidative Phenotype in Mice Exposed to Three Weeks of Normobaric Hypoxia. *J Cell Physiol, 2015. Epub ahead of print.*

Ilse G.M. Slot, Annemie M.W.J. Schols, Bettine A.H. Vosse, Marco C.J.M. Kelders and Harry R. Gosker, Hypoxia differentially regulates muscle oxidative fiber type and metabolism in a HIF-1alpha-dependent manner. *Cell Signal, 2014. 26(9): p. 1837-45.*

Ilse G. M. Slot*, Bram van den Borst*, Valéry A. C. V. Hellwig, Esther Barreiro, Annemie M. W. J. Schols and Harry R. Gosker, The muscle oxidative regulatory response to acute exercise is not impaired in less advanced COPD despite a decreased oxidative phenotype. *PLoS One, 2014. 9(2): p. e90150.*

Samantha A. Natanek, Harry R. Gosker, **Ilse G.M. Slot**, Gemma S. Marsh, Nicholas S. Hopkinson, William D.-C. Man, Ruth Tal-Singer, John Moxham, Paul R. Kemp, Annemie M.W.J. Schols and Michael I. Polkey, Heterogeneity of quadriceps muscle phenotype in chronic obstructive pulmonary disease (COPD); implications for stratified medicine? *Muscle Nerve, 2013. 48(4): p. 488-97.*

Samantha A. Natanek, Harry R. Gosker, **Ilse G.M. Slot**, Gemma S. Marsh, Nicholas S. Hopkinson, John Moxham, Paul R. Kemp, Annemie M.W.J. Schols and Michael I. Polkey, Pathways associated with reduced quadriceps oxidative fibres and endurance in COPD. *Eur Respir J, 2013. 41(6): p. 1275-83.*

Bram van den Borst*, **Ilse G. M. Slot***, Valéry A. C. V. Hellwig, Bettine A. H. Vosse, Marco C. J. M. Kelders, Esther Barreiro, Annemie M. W. J. Schols and Harry R. Gosker, Loss of quadriceps muscle oxidative phenotype and decreased endurance in patients with mild-to-moderate COPD. *J Appl Physiol (1985), 2013. 114(9): p. 1319-28.*

* equal contributor

List of abbreviations

LIST OF ABBREVIATIONS

ACTB	β-actin
ADP	adenosine diphosphate
AICAR	5-aminoimidazole-4-carboxamide-1-β-D-ribofuranoside
ALAS1	5-aminolevulinate synthase 1
AMP	adenosine monophosphate
AMPK	adenosine monophosphate-activated protein kinase
ANOVA	analysis of variance
ARDS	acute respiratory distress syndrome
ARNT	aryl hydrocarbon nuclear receptor
ATF2	activating transcription factor 2
ATP	adenosine triphosphate
ATS	American Thoracic Society
$ATVO_2$	oxygen uptake (VO_2) at anaerobic threshold
AU	arbitrary units
B2M	β2-microglobulin
β-gal	β-galactosidase
BMI	body mass index
BOLD	'global burden of disease' study
BSA	bovine serum albumin
C2C12	mouse skeletal muscle cell line
CaMK	Ca_2^+/calmodulin-dependent protein kinase
cAMP	cyclic adenosine monophosphate
Canx	calnexin
CAT	COPD assessment test
CBP	CREB binding protein
cDNA	complementary DNA
CHF	chronic heart failure
CMV	cytomegalovirus
Cn	calcineurin
COPD	chronic obstructive pulmonary disease
$COPD_D$	COPD patients that desaturated during exercise (SpO_2 fall ≥ 4%)
$COPD_{ND}$	COPD patients that did not desaturate during exercise (SpO_2 fall < 4%)
COX	cytochrome *c* oxidase
CP	Chuvash polycythemia
CRE	cAMP response element
CREB	cAMP response element-binding protein
CS	citrate synthase
CSA	cross-sectional area
CXCL	chemokine (C-X-C motif) ligand
CYC1	cytochrome *c*-1
DLCO	diffusion capacity of the lungs for carbon monoxide
DMEM	Dulbecco's Modified Eagle's Medium
DMSO	dimethyl sulfoxide
DNA	deoxyribonucleic acid
DNP	2,4-dinitrophenylhydrazone

DSHB	Developmental Studies Hybridoma Bank
DTT	dithiothreitol
EC	Enzyme Commission number
ECG	electrocardiogram
EDL	extensor digitorum longus
EDTA	ethylenediaminetetraacetic acid
eIF4E	eukaryotic translation initiation factor 4E
ENSG	Ensembl Gene annotation
ENST	Ensembl Transcript annotation
EPI	epididymal
ERR	estrogen-related receptor
ESRRA	estrogen-related receptor α
ETC	electron transport chain
EV	empty vector
FADH	flavin adenine dinucleotide
FBS	fetal bovine serum
FEV1	forced expiratory volume in 1 s
FFA	free fatty acids
FFMI	fat-free mass index
FIH-1	factor inhibiting HIF-1
FVC	forced vital capacity
GABPA	GA binding protein alpha
GAPDH	glyceraldehyde 3-phosphate dehydrogenase
GAS	gastrocnemius
GCN5	general control non-derepressible 5
gDNA	genomic DNA
GLUT	glucose transporter
GOLD	Global Initiative for Chronic Obstructive Lung Disease
GP	general practitioner
GSK-3β	glycogen-synthase kinase 3β
GUSB	β-glucuronidase
h	hour(s)
HAD/HADH(A)	3-hydroxyacyl-CoA dehydrogenase /3 ketoacyl- CoA thiolase/enoyl-CoA hydratase alpha
HAT	histone acetyltransferase
HBSS	Hank's Buffered Salt Solution
HCO_3^-	bicarbonate
HDAC	histone deacetylase
HHb	deoxygenated hemoglobin/myoglobin
HIF	hypoxia-inducible factor
HIV	human immunodeficiency virus
HK	hexokinase
HMBS	hydroxymethyl-bilane synthase
HMOX1	heme oxygenase-1
HO-1	heme oxygenase-1
HPRT1	hypoxanthine phosphoribosyl-transferase 1

HR	heart rate
HRE	hypoxia-responsive element
IGF-1	insulin-like growth factor 1
ING	inguinal
IP	immunoprecipitation
kDa	kilodalton
LPS	lipopolysaccharide
LTOT	long-term oxygen therapy
MAPK	mitogen-activated protein kinase
MCH	mean corpuscular hemoglobin
MCHC	mean corpuscular hemoglobin concentration
MCPT	muscle carnitine palmitoyltransferase
MCV	mean corpuscular volume
MDA	malondialdehyde
MEF2	myocyte enhancer factor-2
MHC	myosin heavy chain
min	minute(s)
miRNA	microRNA
mM	millimolar
µM	micromolar
µm	micrometer
mMRC	modified Medical Research Council questionnaire
MOPS	3-(N-morpholino)propansulfonic acid
mPGC1α	mouse PGC-1α
mPPARα	mouse PPARα
mRNA	messenger RNA
MSTN	myostatin
mtDNA	mitochondrial DNA
mTOR	mammalian target of rapamycin
MUMC+	Maastricht University Medical Center+
MVPA	moderate to vigorous physical activity
MVV	maximal voluntary ventilation
MyHC	myosin heavy chain
NAD^+	nicotinamide adenine dinucleotide, oxidized
NADH	nicotinamide adenine dinucleotide, reduced
nDNA	nuclear DNA
NDUFB	NADH dehydrogenase (ubiquinone) 1 beta
NFAT	nuclear factor of activated T-cells
NF-κB	nuclear factor kappa-light-chain-enhancer of activated B cells
NIRS	near-infrared spectroscopy
nM	nanomolar
NR	nuclear receptor
NRF	nuclear respiratory factor
NTR	Nederlands Trial Register
NVALT	Nederlandse Vereniging van Artsen voor Longziekten en Tuberculose (Dutch Society of Physicians for Lung Diseases and Tuberculosis)

O_2Hb	oxygenated hemoglobin/myoglobin
OCT	Optimal Cutting Temperature compound
ODDD	oxygen-dependent degradation domain
Oxphen	oxidative phenotype
OXPHOS	oxidative phosphorylation
PA	physical activity
PAS	protein domain first discovered in Per, Arnt and Sim proteins
PBS	phosphate-buffered saline
PCr	phosphocreatine
PCR	polymerase chain reaction
PDC	pyruvate dehydrogenase complex
PDK	pyruvate dehydrogenase kinase
PFK	phosphofructokinase
PFKM	phosphofructokinase, muscle isoform
PGC-1α/β	peroxisome proliferator-activated receptor γ, co-activator 1α/β
PHD	prolyl hydroxylase domain enzyme
PKA	protein kinase A
PLA	plantaris
PMSF	phenylmethylsulfonyl fluoride
PPARα/δ/γ	peroxisome proliferator-activated receptor α/δ/γ
PPARGC1A/B	peroxisome proliferator-activated receptor γ, co-activator 1α/β
PPIA	peptidyl-prolyl cis–trans isomerase A
PR	pulmonary rehabilitation
PRC or PPRC	PGC-1-related coactivator
PRMT1	protein arginine N-methyltransferase 1
PUFA	poly-unsaturated fatty acid
PVDF	polyvinylidene difluoride
RF	respiratory failure
RISC	RNA-induced silencing complex
RNA	ribonucleic acid
RNAi	RNA interference
RNU	small nuclear RNA
ROS	reactive oxygen species
RPL13A	ribosomal protein 13A
RPLP0	large ribosomal protein P0
rPPARδ	rat PPARδ
RT-PCR	reverse-transcription polymerase chain reaction
SD	standard deviation
SDHB	succinate dehydrogenase complex, subunit B
SDS	sodium dodecyl sulfate
SET	sucrose/EDTA/Tris buffer
siRNA	small interfering RNA
SIRT1	sirtuin 1
SLC2A1	glucose transporter (GLUT) 1
SOD	superoxide dismutase
SOL	soleus

SpO_2	arterial oxygen saturation
SRC-1/3	steroid receptor coactivator-1/3
SRF	serum response factor
TBS	Tris-buffered saline
TBST	Tris-buffered saline with Tween-20
TCA	tricarboxylic acid
TFAM	mitochondrial transcription factor A
TFB1M/TFB2M	mitochondrial transcription factor B1/2
TIB	tibialis anterior
TK	thymidine kinase
TNF-α	tumor necrosis factor α
TR	thyroid hormone receptor
TSI	tissue saturation index
Tuba1a	α-tubulin 1A
UBC	ubiquitin C
v/v	volume/volume (concentration)
VEGF	vascular endothelial growth factor
VHL	von Hippel-Lindau protein
VO2max	maximal oxygen consumption
w/v	weight/volume (concentration)
WB	western blot
WR	work rate
YWHAZ	tyrosine 3-monooxygenase/ tryptophan 5-mono-oxygenase activation protein, zeta polypeptide